PRINCIPLES OF PETROLEUM PROSPECTING

KINJI MAGARA
Professor of Petroleum Geology
Faculty of Earth Sciences, King Abdulaziz University, Jeddah, Saudi Arabia

Published by
Scientific Publishing Centre
King Abdulaziz University
P.O. Box 1540, Jeddah 21441, Saudi Arabia.

1st Edition 1407 A.H. (1986 A.D.)

Printed at King Abdulaziz University Press

Foreword

The Kingdom of Saudi Arabia, being one of the leading oil-producing countries in the world, needs qualified technical cadres in a wide range of petroleum disciplines. With a view to satisfying the demand for highly qualified petroleum geologists, the Department of Petroleum Geology at the Faculty of Earth Sciences, of King Abdulaziz University, started its formal curriculum for the undergraduate level in 1978, and soon after that, post graduate studies were offered by that department in 1981. Ever since, the staff members of the department have exerted strenuous efforts to develop their department through active teaching and research work.

So far, nearly thirty students have earned their B.Sc. in Applied Geology, or M.Sc. degrees, and most of them are currently working in the petroleum industry or in the various government agencies in the Kingdom. Furthermore, some of the M.Sc. graduates have already been accepted to pursue their higher studies abroad in order to obtain the Ph.D. degree as well.

In this respect, I am pleased to introduce this book "Principles of Petroleum Prospecting" written by Dr. Kinji Magara, as a prime textbook for one of the undergraduate geology courses, "411 Petroleum Geology". It describes the principles of petroleum exploration using both geological and geophysical concepts and techniques. Practical applications of various modern technologies, including computer applications, are likewise outlined in this book, which is written in simple language. Nevertheless, I believe that this work may effectively be used as a reference in other petroleum geology or general geology courses offered by other universities.

I hope that the publication of this book will promote the activities of the Department of Petroleum Geology, at King Abdulaziz University and will also contribute to the education of the science of petroleum geology in general.

Dr. Rida Mohammad Said Obaid
President
King Abdulaziz University, Jeddah

Preface

Advancement of science of petroleum geology in the last few decades has been quite significant. Following are some of these major advancements:

1. Applications of both organic geochemical and microscopic methods for source rock evaluation.
2. Application of concept of sediment diagenesis for reservoir development and destruction.
3. Application of seismic stratigraphy for exploration, backed by the improvements in seismic data processing.
4. Application of concept of primary hydrocarbon migration for exploration.
5. Application of the global tectonics concept for petroleum exploration.
6. Development of quantitative well-log-analysis methods.
7. Development of detection techniques of abnormally high fluid pressures.
8. Application of statistical and computer methods for predicting future oil/gas discoveries.

In addition to these recent progresses in petroleum geology, there are also many other basic concepts and techniques which must be taught for training a petroleum geologist. In other words, the subject matters are so diversified, that no single person would be able to understand the entirety in short time.

Any petroleum geological work involves at least two important aspects; 1. to increase general knowledge of the factors related to the work, 2. to improve analytical mind for interpreting the data and applying the result for practical exploration activities. The former may be called "descriptive petroleum geology", and the latter "analytical petroleum geology" or "petroleum prospecting".

There have been many petroleum geology books written by experts on the descriptive petroleum geology, but relatively few on the analytical petroleum geology.

At the Department of Petroleum Geology, the Faculty of Earth Sciences of King Abdulaziz University, students major petroleum geology at the undergraduate level. One of the courses in the Department is called "Petroleum Geology (411)" which teaches the analytical petroleum geology (petroleum prospecting). Prior to taking this course, the students had completed another course "Introduction to Petroleum Geology (311)" and other basic courses of geology and other sciences. In other words, the students are supposed to have the sound background on the general geology and the introductory petroleum geology before studying "Petroleum Geology".

The students are thus expected to have both the basic vocabulary of the petroleum geological terms and the understanding of some fundamental concepts. Using such basic knowledge, the students will study in this course (411) how to generate an exploration prospect by the analytical thinking.

Although the amount of available data at the time of exploration is usually limited, the data is the most important and essential part of the petroleum prospecting and evaluation. As described in Chapter 1 of this book, there are seven important factors for the formation of a petroleum accumulation, such as 1. reservoir, 2. trap, 3. cap rock, 4. secondary and 5. primary hydrocarbon migration, 6. hydrocarbon generation, and 7. source rock. The amount of available data usually decreases in this order. Because of this reason, the chapters of this book are arranged in the same order, although the chronological or logical order is opposite to this order.

In addition, some of the concepts and techniques involved in reservoir, trap and seal or cap rock are basic and fundamental in understanding the other factors, so that the students would be able to develop the basic knowledge before tackling the other difficult problems with poorer data control. Therefore, the chapters of this book have been arranged in the order opposite to chronological, but in the Introduction of Chapter 9, the chronological method of practical application is reviewed.

Three important points were stressed when writing this book; 1. relatively easy logics and expressions, 2. application for the Middle East region, particularly for Saudi Arabia, and 3. computer applications. At the end of each chapter, there are selected problems for which each student is expected to answer. The main purpose of these exercises is to review the main points discussed in each chapter.

I sincerely hope that use of this book in the classrooms will be helpful in teaching petroleum geology at King Abdulaziz University and elsewhere.

Acknowledgement

I wish to express my deepest appreciation to His Excellency, Dr. R.M.S. Obaid, President of King Abdulaziz University for writing the Foreword of this book. Dr. A.S. Tashkandy, Secretary General of the University's Scientific Council, kindly granted his full support for this publication.

I wish to thank Dr. A.R. Bakor, Dean, and Dr. A.N. Basahel, former Dean, of the Faculty of Earth Sciences for their efforts in help developing the Department of Petroleum Geology. Drs. F.M. Marzouki and M.A. Gazzaz, Vice Deans, not only encouraged but also supported various teaching and research activities of the Department.

During the process of evaluating my manuscript for publication, Professor A.M. Shanti, former Dean of the Faculty and member of the Scientific Council of the University, kindly granted his full support for my work.

Dr. F.A. Sharief, Head of the Petroleum Geology Department, has always been most cooperative for my work. Without his understanding and support, I think that this book could not be completed. Two other members of the Department, Messrs. M.S. Khan and H. Al-Khatib also contributed to this book, through their discussions with me in the last several years.

The recent research works conducted by the four graduate students, Messrs. I.H. Huwaidi, I.A.N. Sail, K.A. Bagabas, and H.E. Abdalla, significantly improved the contents of this book.

In the last twenty five years, I have been benefited with many valuable discussions with my colleagues in North America, Europe, and Asia. I wish to express my deepest appreciation to all of these petroleum geology experts.

For drafting and photographic reproduction, I was fortunate to have valuable supports from the Department of Photo and Structural Geology of the Faculty, headed by Dr. F.A. Zakir. I would like to extend my appreciation to Messrs. M.Y. Ali Khan and L. Sopart for their excellent works of drafting and photographic reproduction.

I wish to thank Dr. S.M. BaMashmous, Director of the Scientific Publishing Centre of the University, and Mr. F. Abdel-Aal, Head of the Publishing Department and other staff members of the Publishing Centre for their help in producing this book.

For the reproduction of the figures by various authors in this book, I was fortunate to have the official permissions from the following scientific organizations, publishers, or journals; American Association of Petroleum Geologists, Canadian Society of Petroleum Geologists, Elsevier Scientific Publishing Company, Institut Francais du Pétrole, Journal of Petroleum Geology, Society of Petroleum Engineers of AIME, Springer-Verlag Berlin, The University of Texas at Austin (Bureau of Economic Geology and Center for Energy Studies), and World Oil.

At last but not least, I thank my son, Albert J. Magara, for his assistance in computer programming.

Kinji Magara
Faculty of Earth Sciences,
King Abdulaziz University,
Jeddah, Saudi Arabia

Contents

Chapter 1

Petroleum Occurrences and Petroleum Geology

■ Introduction. ■ What is petroleum geology ?
■ Factors controlling oil accumulation. ■ Problems.

Introduction

More than 600 sedimentary basins and sub-basins are known in the world (Huff 1979). Out of these sedimentary basins, approximately a quarter by number and a half by both area and volume have petroleum production (see Fig. 1, Klemme 1980). Petroleum production has been established in many larger basins. Most producing regions are in the continents of the Northern Hemisphere.

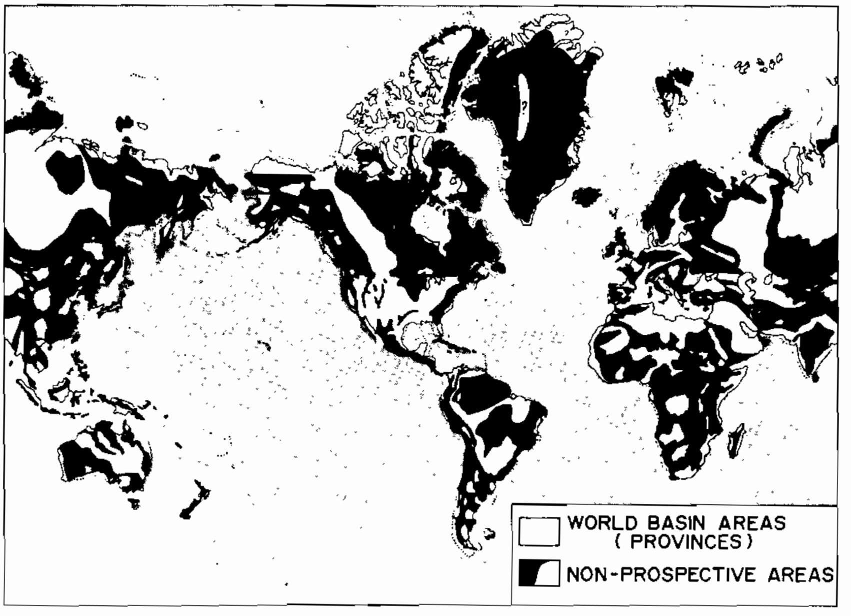

Fig. 1. Map showing prospective basins and nonprospective areas of the world (from Klemme 1980). Courtesy of Journal of Petroleum Geology.

According to Klemme, about three-quarter by number of the world sedimentary basins are non-productive, approximately one-third of which have never been drilled for exploration of petroleum deposits, due either to natural or political reasons.

A petroleum deposit is normally kept in one of the following traps or by a combination of these as follows: 1. structural, 2. stratigraphic, and 3. hydrodynamic. Wilson (1975) proposed another trap type called "diagenetic", which is primarily a result of the diagenetic processes in sedimentary rocks.

Although future exploration will probably have to rely more on discovering stratigraphic, hydrodynamic, and diagenetic traps, experience has shown that most of the known petroleum accumulations in the world are trapped structurally or by a combination of structural and other mechanisms. There are two types of structural trap: 1. anticline or dome, and 2. fault. Since White (1885) proposed his classical anticlinal theory, that type of trap has been accepted as the more important.

What is Petroleum Geology ?

Petroleum geology is a branch of the geological sciences using concepts and techniques which are applicable for exploration and exploitation of petroleum deposits in sedimentary rocks. Although the classical methods of discovering petroleum deposits, such as the surface geological survey and search for surface oil and gas shows, are still effective in many frontier basins, modern petroleum geologists working in oil producing basins tend to utilize a variety of indirect methods, such as gravity, magnetic, and seismic surveys, wire-line logging, geochemical survey and logging, remote sensing, etc., in addition to their classical and direct methods.

In short, a petroleum deposit may be discovered by the use of many geological, mineralogical, geophysical, and geochemical concepts and techniques; an application of petroleum geology.

Petroleum production (or development) geology is the second but important branch of petroleum geology, after petroleum exploration geology. It is known that only about one third of the oil inplace in the reservoir can be produced by the primary recovery method. Secondary and tertiary methods could increase the oil recovery by some 15%. This suggests that probably more than 50% of the oil inplace cannot be produced by using the presently available recovery techniques. I believe that the petroleum production geologist can contribute a great deal to increases of the oil recovery from the existing oil fields.

Factors Controlling Oil Accumulation

Figure 2 shows seven important factors we must consider in petroleum exploration:

1. Reservoir and effective pore spaces.
2. Trap.
3. Seal or cap rock.

4. Secondary hydrocarbon migration.
5. Primary hydrocarbon migration.
6. Hydrocarbon generation and maturation.
7. Source.

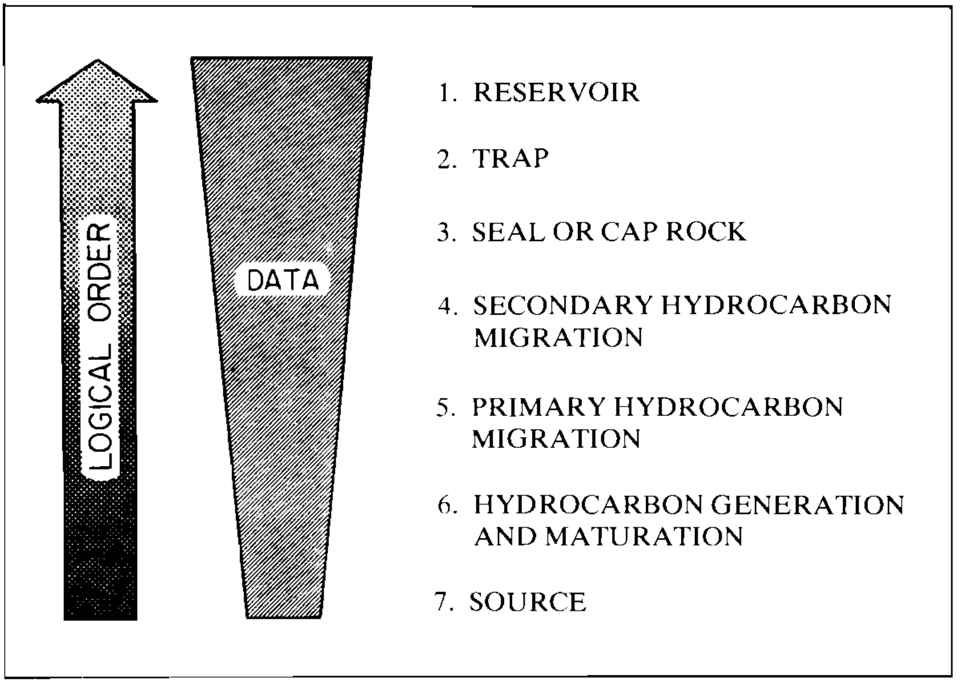

Fig. 2. Seven important factors for oil/gas accumulation (from Magara 1981b). Courtesy of American Association of Petroleum Geologists.

Out of this list, items 1, 2, 3, and 7 are rock (or material) itself or certain forms of sedimentary rocks, whereas items 4 to 6 are both physical and chemical processes related to a petroleum accumulation.

The chronological and logical order of occurrence of these factors is from item 7 to 1; hydrocarbons were generated from source rocks, moved from source to reservoir by the primary migration agent, and migrated within the reservoir by the secondary migration process. Before and after such hydrocarbons reach a trap, they must be sealed by cap rocks. At the final trapping position, the reservoir must have sufficient porosity and permeability for petroleum production.

Although from item 7 to 1 is the order in terms of timing, the abundances of available subsurface data do not usually follow it. We usually have good control of data on such items as reservoir, trap, and seal, once a first well has been drilled in a structure. There are usually many unsolved problems regarding primary and secondary migration. Source rock and hydrocarbon generation can be studied by organic geochemical methods if the source rock exists at the location where the well was drilled. However, if hydrocarbons were generated in the synclinal areas and migrated into the anticline, the data from the anticline have little value in evaluation source potential and level of hydrocarbon generation.

In summary, although it would be ideal to have sufficient information on all the factors listed in Figure 2, the amount of the available data usually decreases from item 1 to 7, especially when only a few wells have been drilled in an area.

Most petroleum accumulations were considered to be accompanied by all the factors listed in Figure 2. But, the presence of all of these factors in a certain area today does not necessarily indicate a petroleum accumulation. It could be that the timing of their occurrence in this area was not appropriate, so that petroleum either could not accumulate properly or was lost later. I believe that a proper interpretation of the relative timing of these geological factors will help us to discover more petroleum accumulations.

Out of the seven factors listed in Figure 2, items 2, 3, 4, 5, and 6 may be interpreted in terms of timing of their occurrence.

Problems

1. What is the proportion of the oil producing sedimentary basins in the total of about 600 in the world ?
2. List four types of traps for petroleum accumulations.
3. Define petroleum geology.
4. List seven important factors for the formation of an oil accumulation in the chronological order of occurrence.
5. Out of the seven factors above, which factors can be interpreted in terms of timing of their occurrence ?

Chapter 2

Reservoir Properties

- Introduction.
- Porosity.
- Porosity - permeability relationship.
- Secondary porosity and permeability.
- Problems.

Introduction

Petroleum deposits are normally found in pore spaces and fracture openings of a rock called "reservoir". The capacities of the reservoir rock both to hold and to yield petroleum are porosity and permeability. Porosity is expressed as a fraction or percentage of pore spaces in the total volume of the rock. On the other hand, permeability is the measure of the ease with which fluids (oil, gas, or water) may move through the interconnected pores of the rock.

Porosity

It is commonly accepted in the oil industry that the minimum porosity percentages for effective oil and gas reservoirs are about 10 and 5, respectively. If the porosity is less than the minimum value, economical production of petroleum may not be expected. This is particularly true if most pore spaces are of intergranular type. When some fracture porosity is developed, porosity less than those shown above may be productive.

Porosity of a given reservoir can be controlled by the original depositional factors of the reservoir and also by the postdepositional diagenetic factors. The original depositional factors for a reservoir of the intergranular type may be listed as follows:

1. Average grain size.
2. Sorting of grains.
3. Angularity (sphericity) of grains.
4. Surface roughness of grains.
5. Presence of ductile material, particularly clays.

The diagenetic factors are as follows:

1. Burial depth.
2. Geologic age.
3. Geothermal gradient.
4. Chemical composition of formation water, which may be important in pre-

cipitating some minerals and cement.

5. Tectonic forces which could cause fracture porosity.
6. Circulation of ground water, which could leach out some grains and cements by solution.
7. Formation of diagenetic clay minerals.
8. Early migration of petroleum into a reservior, which could preserve porosity.

Although estimating porosity before drilling can be critical in some exploration prospects, it is generally quite a difficult task because the evaluations of the depositional and diagenetic factors mentioned above are not easy.

Once an empirical relationship of reservoir porosity vs. depth is established in an area, it may be used for predicting porosity at any other location within the area. Figure 3 shows two of such relationships for sandstones at different geothermal gradients in the northeast Pacific arc-related basins. Figure 4 depicts the relationships for both shale and sandstone reported by Proshlyakov (1960).

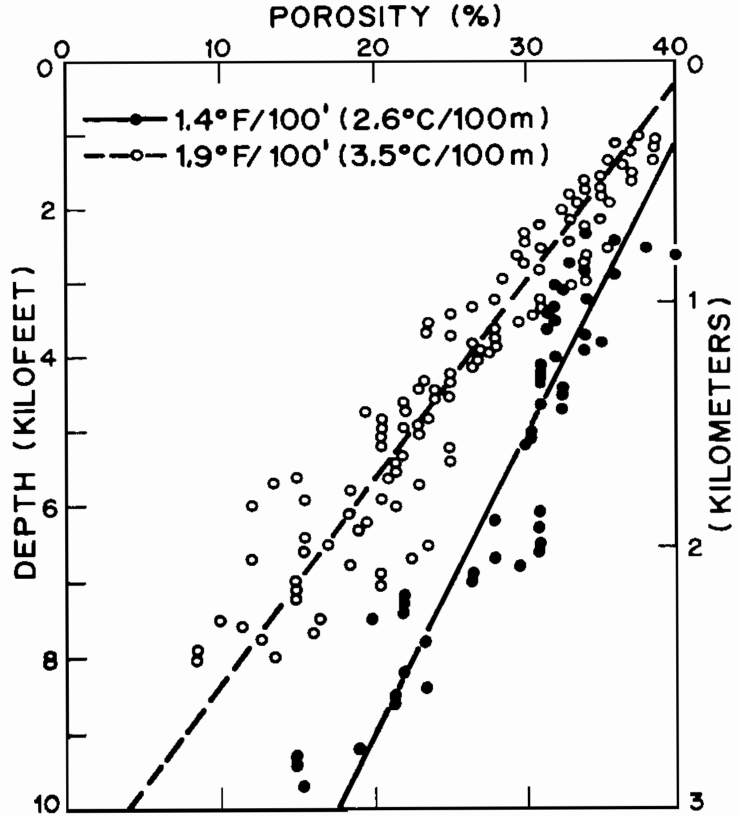

Fig. 3. Two porosity-depth relationships of sandstones associated with two different geothermal gradients in the Northeast Pacific arc (from Stephenson 1977 after Galloway 1974). Courtesy of American Association of Petroleum Geologists.

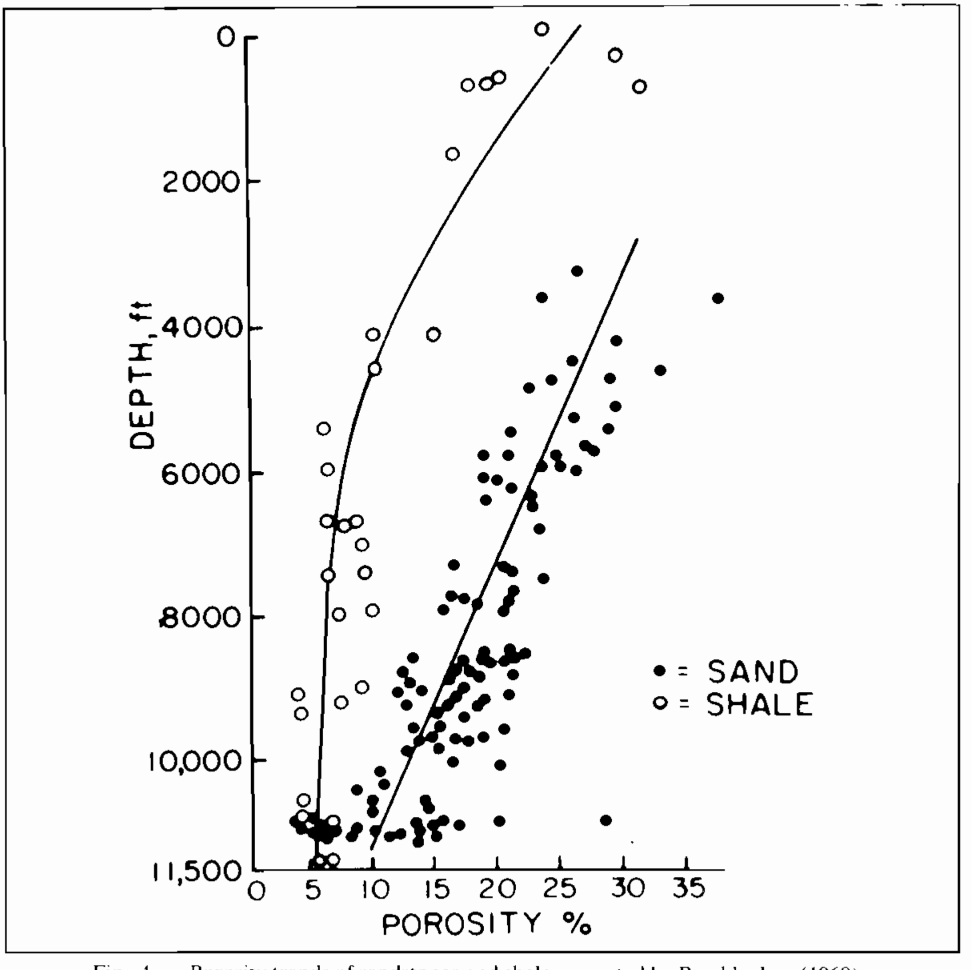

Fig. 4. Porosity trends of sandstones and shales reported by Proshlyakov (1960).

Porosity-Permeability Relationship

Because permeability is another important factor in determining reservoir quality, many attempts have been made to cross-correlate porosity with permeability.

Theoretically speaking, permeability, k, may be related to porosity, ϕ, by the following equation (adapted from Levorsen, 1967);

$$k = C \cdot \frac{\phi^3}{(1-\phi)^2} \cdot \frac{1}{S^2} \tag{1}$$

where C is constant and S is specific surface area. This relationship means that permeability increases as porosity increases and/or specific surface area of the grains decreases. Note that the specific surface area decreases as the average grain size increases.

With respect to the empirical relationship of porosity and permeability, Archie (1950) proposed such relationships for the Upper Wilcox sandstone in Texas and the Nacatoch sandstone in Louisiana (Fig. 5). This figure shows that about 3% increase in porosity produces ten-fold increase in permeability. A similar example from the same general area is shown in Fig. 6. Figure 7 depicts another relationship of the Bradford sandstone in Pennsylvania reported by Ryder (1948).

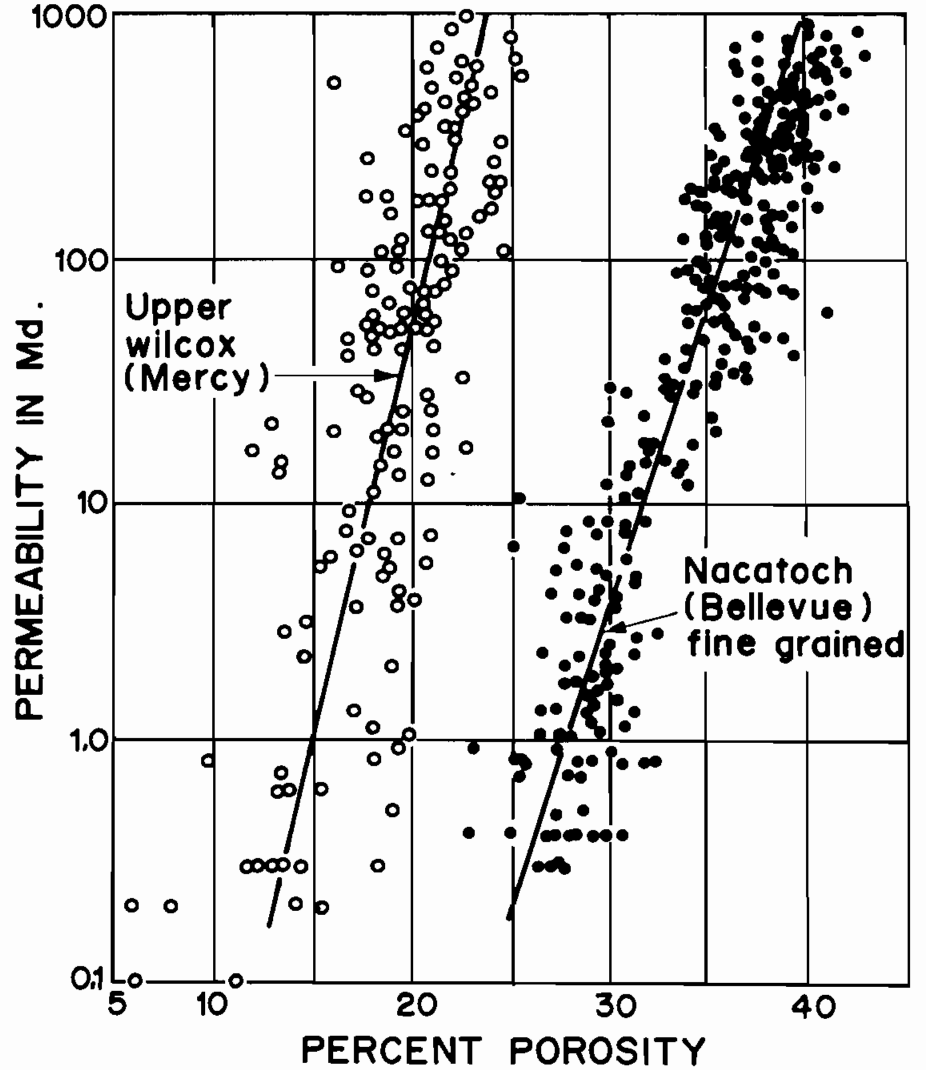

Fig. 5. Porosity-permeability relationships of Upper Wilcox sandstone (Eocene) at Mercy, Texas, and the Nacatoch sandstone (Upper Cretaceous) at Bellevue, Louisiana (from Archie 1950). Courtesy of American Association of Petroleum Geologists

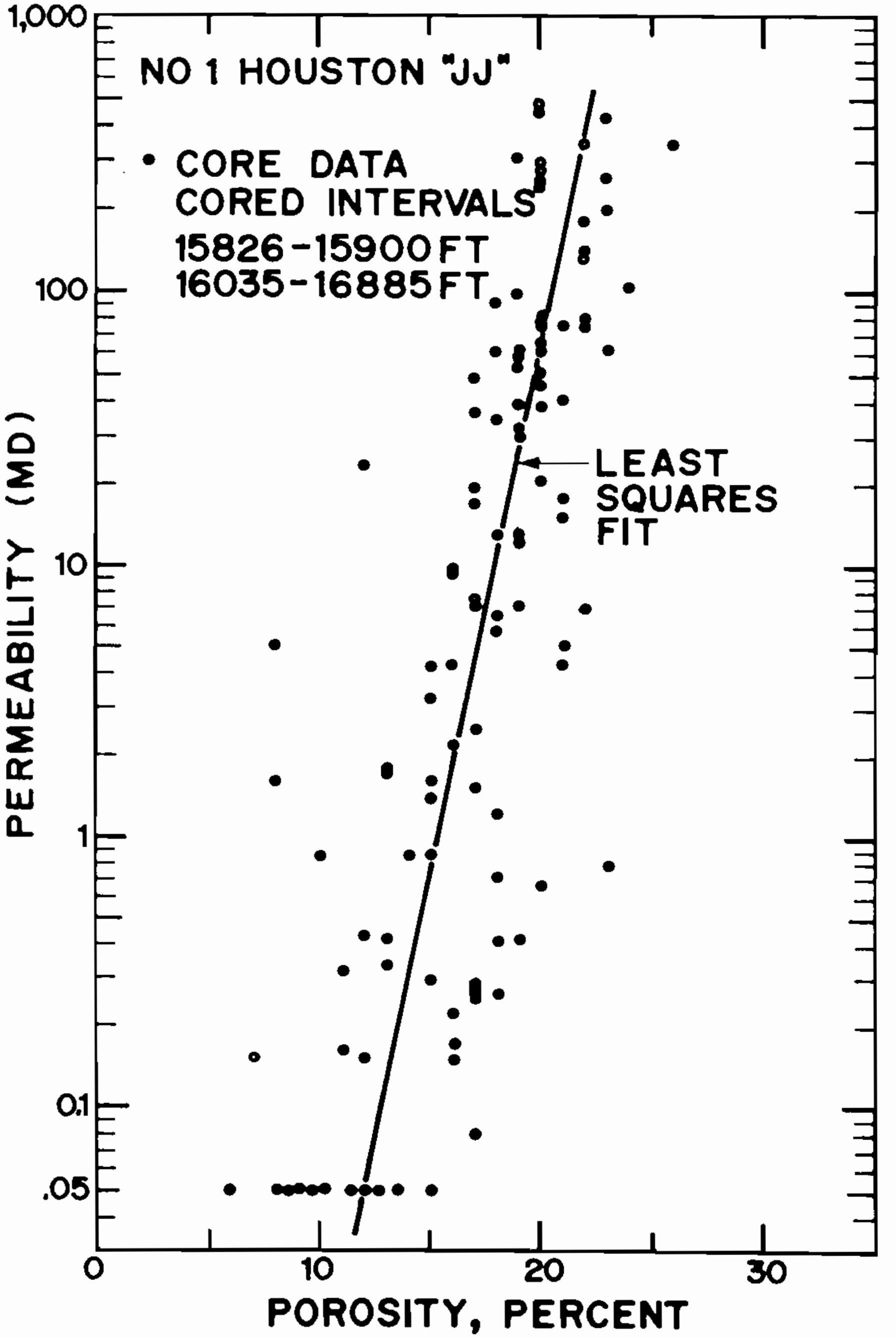

Fig. 6. Porosity-permeability relationship from Texas (from Bebout *et al.* 1978). Courtesy of Bureau of Economic Geology, University of Texas at Austin.

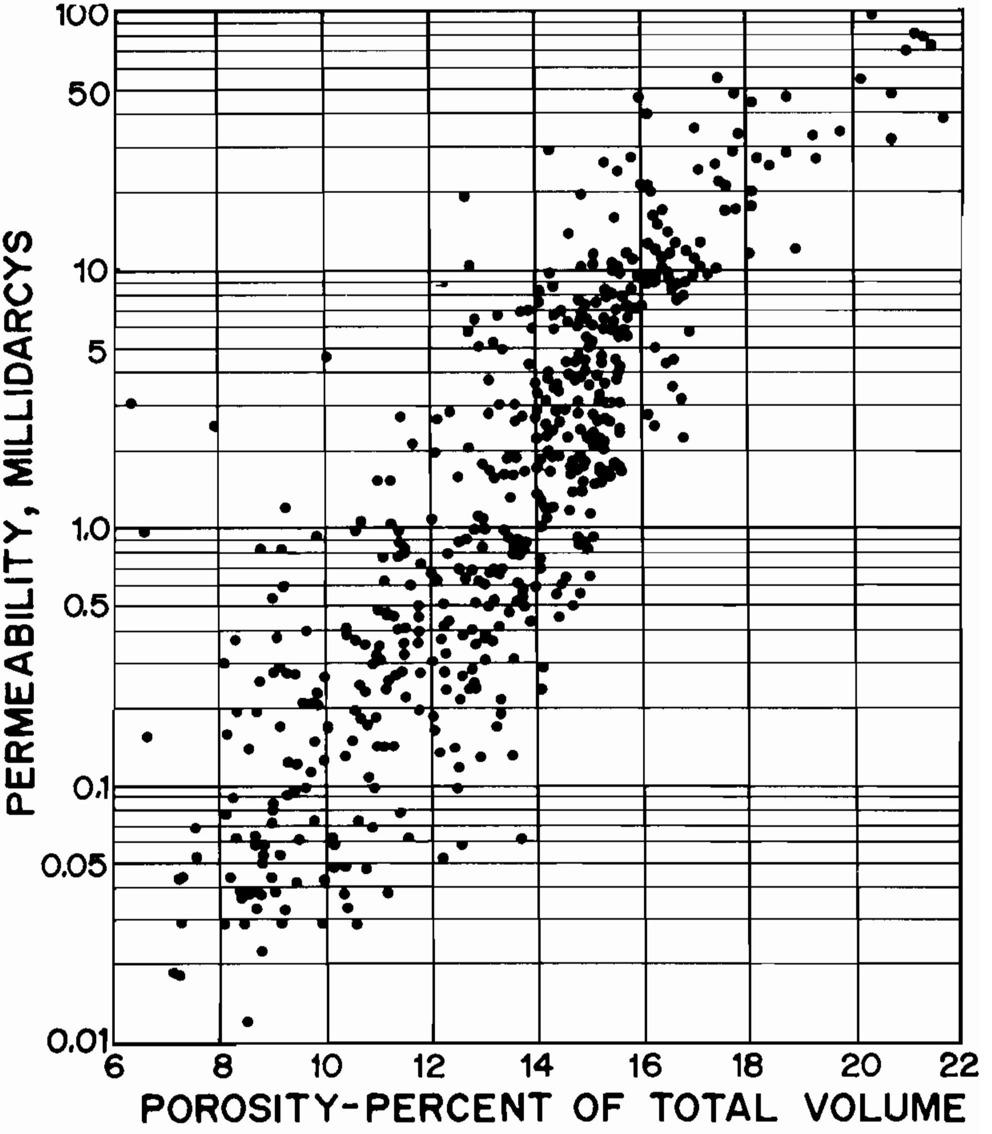

Fig. 7. Porosity-permeability cross plot of Bradford sandstone (Middle Devonian), Pennsylvania (from Ryder 1948). Courtesy of World Oil.

Secondary Porosity and Permeability

Because of the increased depth, temperature, and geologic age, primary porosity normally decreases with burial depth. Permeability will also decrease as porosity decreases. If, however, secondary porosity is developed by either fracturing or solution of mineral grains and cements, both porosity and permeability at depth can be abnormally high.

From the study of the Mackenzie Delta, Canada, Schmidt and McDonald (1979) suggested that if sandstone was cemented by calcite at shallow burial depths and later reached the thermal maturation stage of organic matter, calcite cement could be leached out by low pH fluid, causing significant secondary porosity. During the thermal maturation stage, organic matter, particularly of land-derived type, produced carbon dioxide, the dissolution of which in water could cause acidic environments (low pH). In such acidic environments, calcite would be dissolved but quartz could be more stable.

Kharaka *et al.* (1977) reported tbe reduction of pH in formation water from the deep geopressured interval in Texas Gulf Coast (Fig. 8). Significant secondary porosity at depth of the same general area was reported by Loucks *et al.* (Fig. 9, 1979).

In the Middle East region, the Asmari limestone (Oligocene-Miocene age) of the Zagros folded belt of Iran has been known for its high oil-productivity associated with secondary porosity and permeability. The region experienced a period of extremely fast sedimentation prior to the strong tectonic movements which formed the Zagros thrusts and folded belt.

Such fast sedimentation would have caused abnormal fluid pressure in relatively deep sections (Magara 1978c), and vertical charging of the high-pressured fluids may have caused natural hydro-fractures (Magara 1981a). During and after the uplifting and erosional periods, additional fractures may also have been formed, mainly due to relaxation of subsurface stress condition (Magara 1981a).

Generation of carbon dioxide and formation of carbonic acid from organic maturation proposed by Schmidt and McDonald (1979) may have also opened secondary porespace by dissolution of calcite in the reservoir.

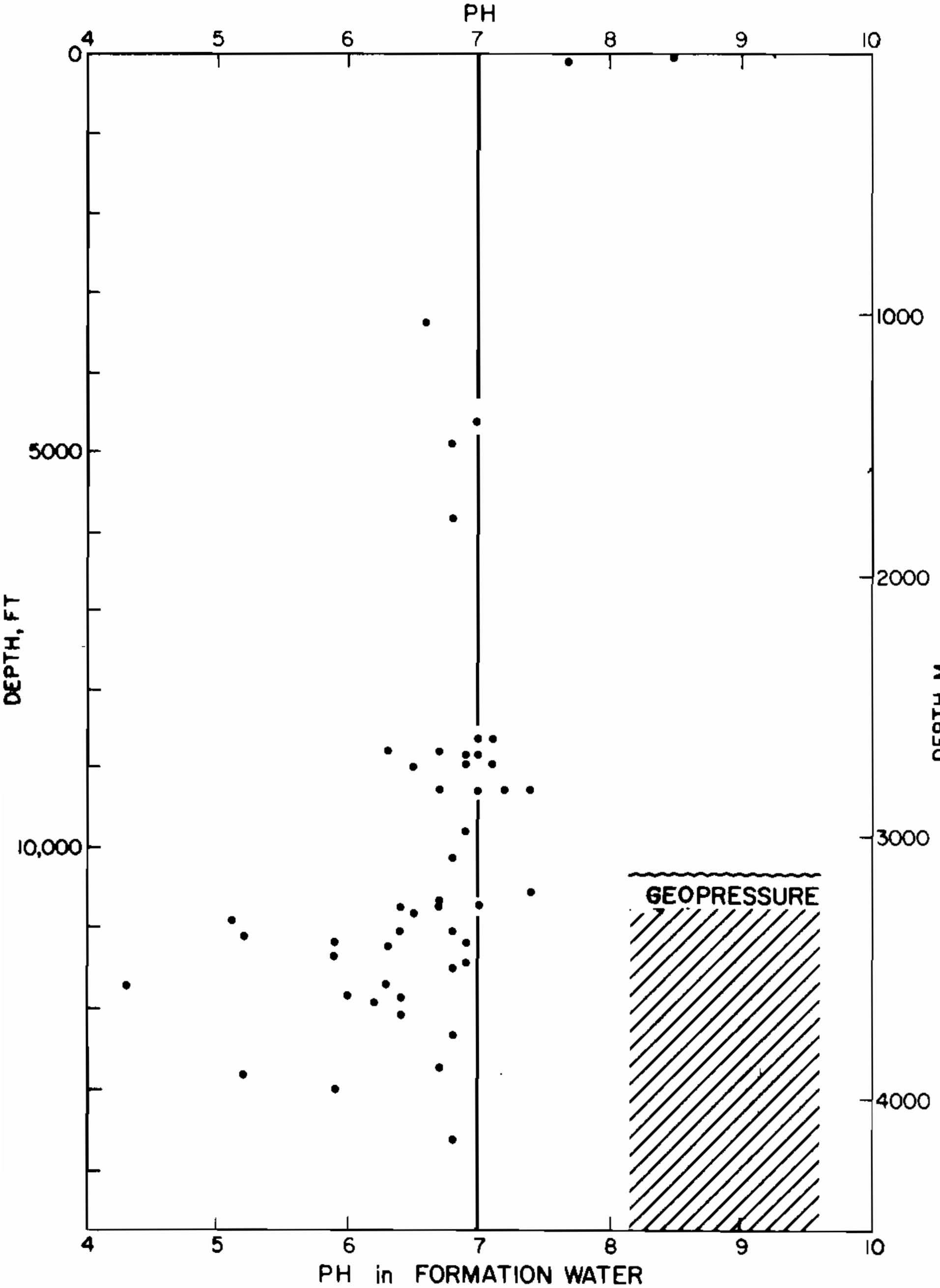

Fig. 8. Plot showing pH of formation waters versus depth in Texas Gulf Coast. Data derived from Kharaka *et al.* (1977).

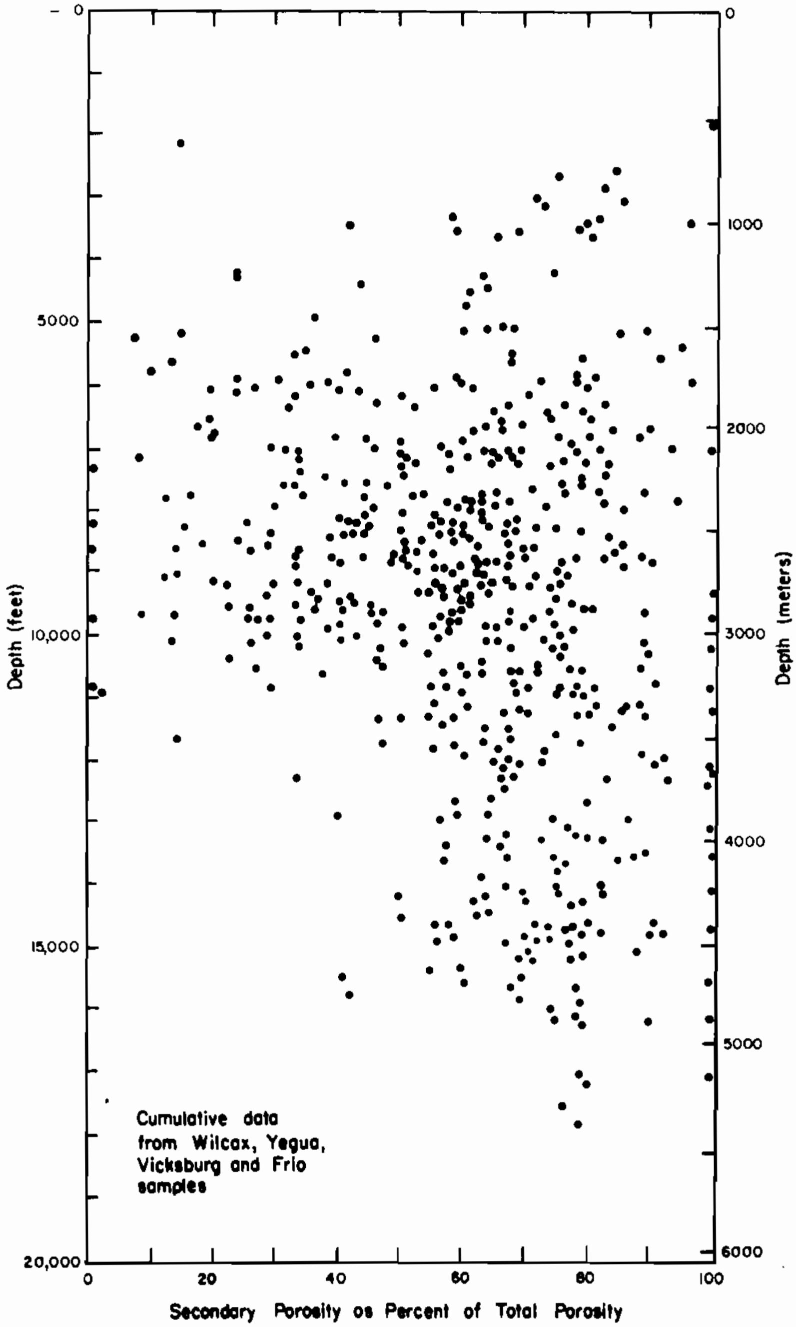

Fig. 9. Secondary porosity as per cent of total porosity versus depth for Lower Tertiary sandstones (from Loucks *et al.* 1979). Courtesy of Bureau of Economic Geology, University of Texas at Austin.

Problems

1. List depositional factors affecting porosity of a reservoir rock.
2. List diagenetic (post-depositional) factors causing changes of porosity of a reservoir.
3. Explain theoretical relationship among permeability, porosity, and specific surface area of grains.
4. Explain Archie's empirical relationship between porosity and permeability.

Chapter 3

Traps for Hydrocarbons

- Introduction. ■ Drainage efficiency.
- Sealing capacity. ■ Time of trap formation.
- Compaction correction of burial history plot.
- Problems.

Introduction

As described in Chapter 1, our future exploration for petroleum must be directed toward discoveries of stratigraphic, hydrodynamic, and diagenetic traps. However, the historical data shows that many oil accumulations have been found in structural traps, particularly in anticlinal and domal structures.

Scarcity of the stratigraphic, hydrodynamic, diagenetic, and fault traps may be mainly attributed to difficulty of finding these traps because of their subtle nature. There must also be some other geologic reasons that these traps are not as common as the anticlinal trap; in this respect, we may consider drainage efficiency and sealing capacity.

Drainage Efficiency

To form a commercial accumulation, concentration of a sufficient amount of petroleum must be attained in the subsurface reservoir. During the secondary migration stage, petroleum most likely migrated by the buoyancy force from structural lows to a high (crest). In case of an anticlinal or domal trap, the secondary migration could have taken place from all directions to the crest (or the drainage angle is 360°, see Fig. 10).

As shown in Figure 11, on the contrary, the drainage angle of most stratigraphic and fault traps is approximately a half the angle for the anticlinal trap. In other words, from the standpoint of the drainage angle, the former trap has only about 50% efficiency of the latter. In case of a combination trap of the stratigraphic and hydrodynamics, the drainage angle is about 180° as well.

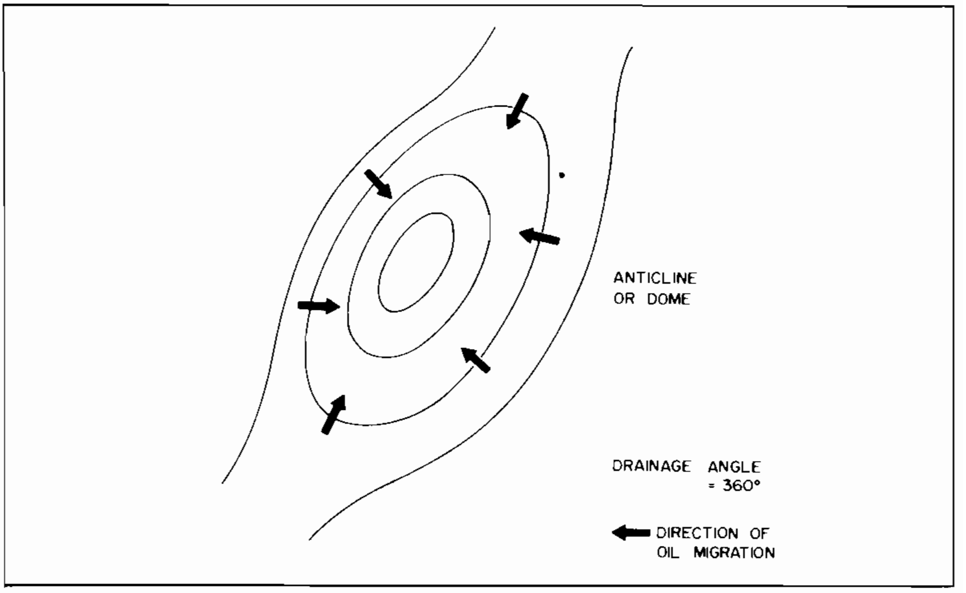

Fig. 10. Schematic diagram showing directions of secondary oil migration toward an anticline or dome.

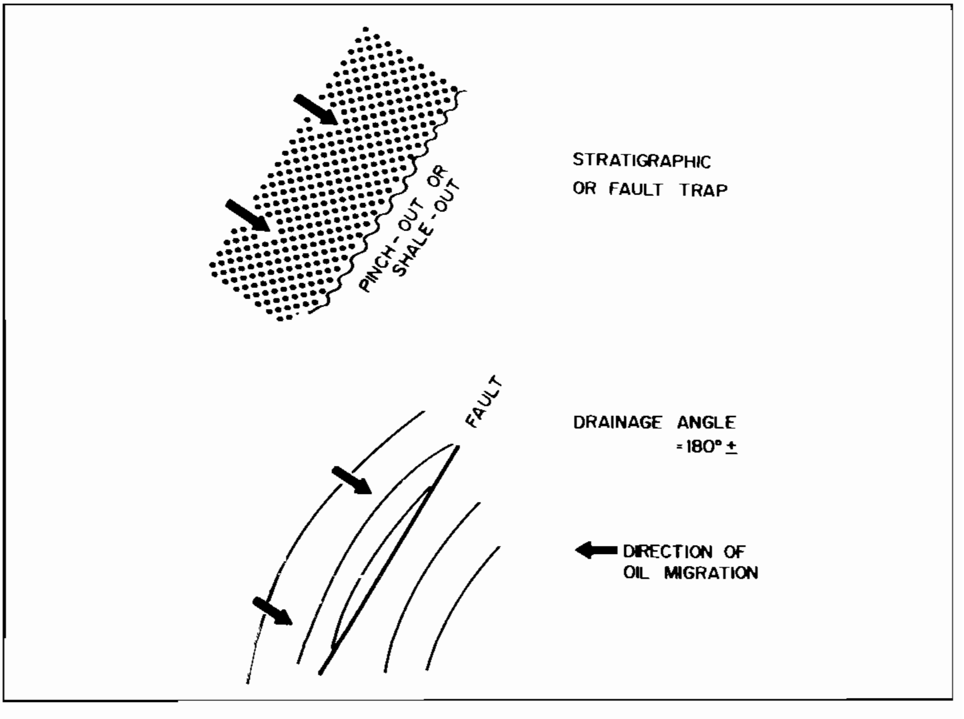

Fig. 11. Schematic diagram showing directions of secondary oil migration in cases of stratigraphic and fault traps.

Sealing Capacity

In case of either the anticlinal or the stratigraphic (pinch-out, shale-out, or unconformity) trap, the contact between the reservoir and cap rock was relatively stable for a long geological period. In such a case, the accumulated hydrocarbons can be kept safely in the reservoir.

In case of a fault trap, however, the downthrown block could have been moved either continuously or intermittently with respect to the upthrown block in the geologic past (see Fig. 12). During the successive period of fault movement, the sealing efficiency would have changed greatly as depicted in Fig. 12 (stage 1 = good sealing condition, stage 2 = poor sealing condition). In other words, fault traps are considered to be relatively unstable traps in most cases.

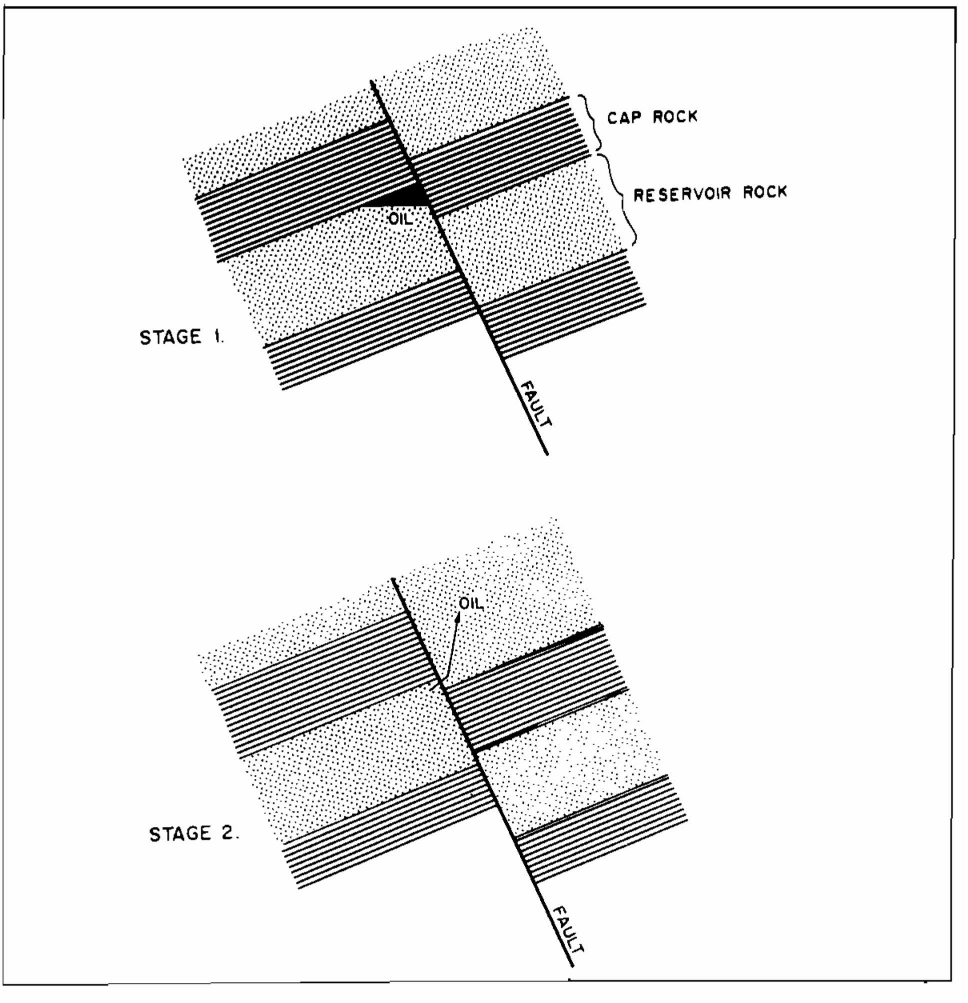

Fig. 12. Sealing efficiency of a fault trap; stage 1 - effective, and stage 2 - ineffective (or loss of oil).

Another example of the unstable trap is hydrodynamics. Since this trapping mechanism is controlled by fluid behavior, the trapping and sealing efficiency could have changed greatly in the geologic past, with possible change of fluid potential. Fluid potential is controlled mainly by the elevations of both intake and outlet areas and also by the supply of fluid (water), so that it is quite difficult to believe that the fluid potential stayed constant for a long geologic period that was necessary for retaining a significant amount of petroleum in the trap.

In summary, from the drainage efficiency and sealing stability viewpoints, the anticlinal and domal structures are more effective traps than any other traps. Although I have no intention to deny the significance of the other traps in the future exploration, the anticlinal trap is probably the most effective and stable trap.

Time of Trap Formation

For concentrating a large quantity of hydrocarbons in a trap, the timing of its formation is an important factor. This means that, by the time of major petroleum generation and migration, an effective trap must have existed to form a commercial accumulation.

Figure 13 shows schematic cross sections of two anticlines, A and B. Four depositional surfaces are shown by four lines, labelled 1 to 4; 1 shows the surface of a reservoir and 4 indicates the present depositional (or land) surface. At A, the central portion of the bed between surfaces 1 and 2 is thinner. This suggests that the anticline was probably developed between stages 1 and 2, with the formation thinning indicating its crest. Another possibility is that the differential loading or sedimentation, that took place between stages 1 and 2, created the anticline at the same time.

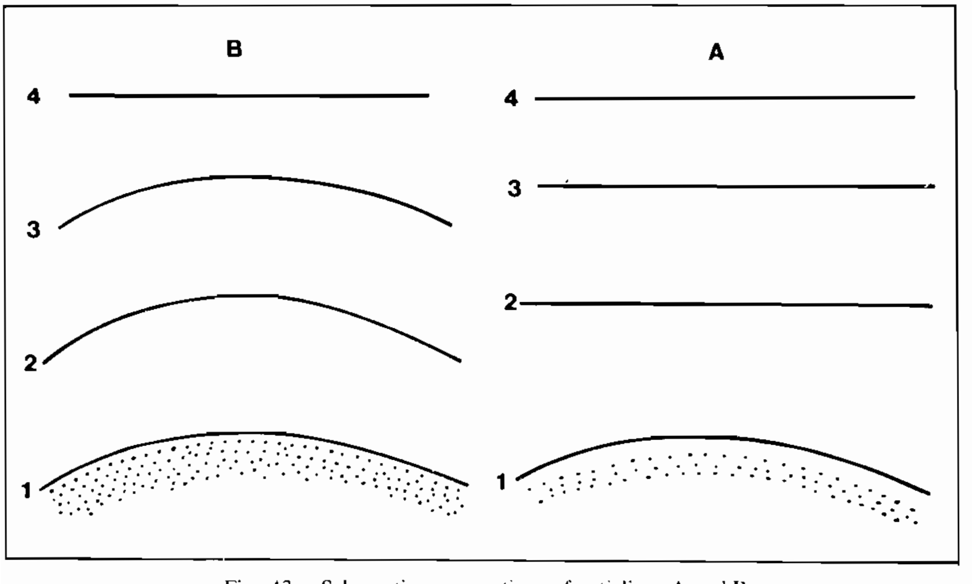

Fig. 13. Schematic cross sections of anticlines A and B.

In any situation, the bed-thinning makes it possible to estimate the time of the anticline formation as between stages 1 and 2. By applying the same concept, one could be able to interpret the time of trap development at B as between stages 3 and 4.

In summary, trap A was developed earlier than trap B. Therefore, if all the other factors for the formation of an oil accumulation are the same, the former trap has a better chance of containing petroleum than the latter.

For interpreting a more general case, which is usually more complicated geologically, a burial-history plot is recommended to construct. Using a geologic column of a synclinal area shown in Fig. 14, one would be able to construct a burial history plot for the Triassic reservoir, whose present depth is 14,500 ft and whose geologic age is 225 million years. Five depositional and burial stages may be identified; 1. end of deposition of the reservoir (225 million years ago - M.Y. ago), 2. end of Triassic (180 M.Y. ago), 3. end of Jurassic (135 M.Y. ago), 4. end of Cretaceous (70 M.Y. ago), and 5. present (0 M.Y. ago). These five stages are shown by numbers in the burial history plot of Figure 15.

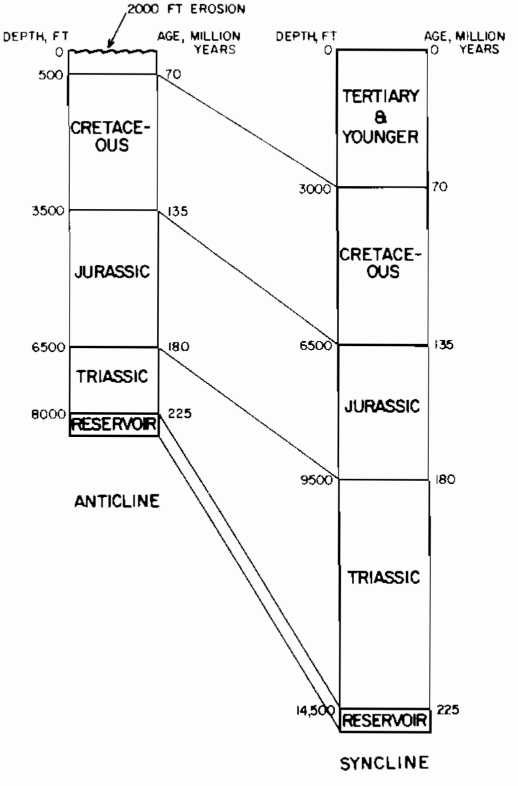

Fig. 14. Geologic columns representing anticlinal and synclinal areas.

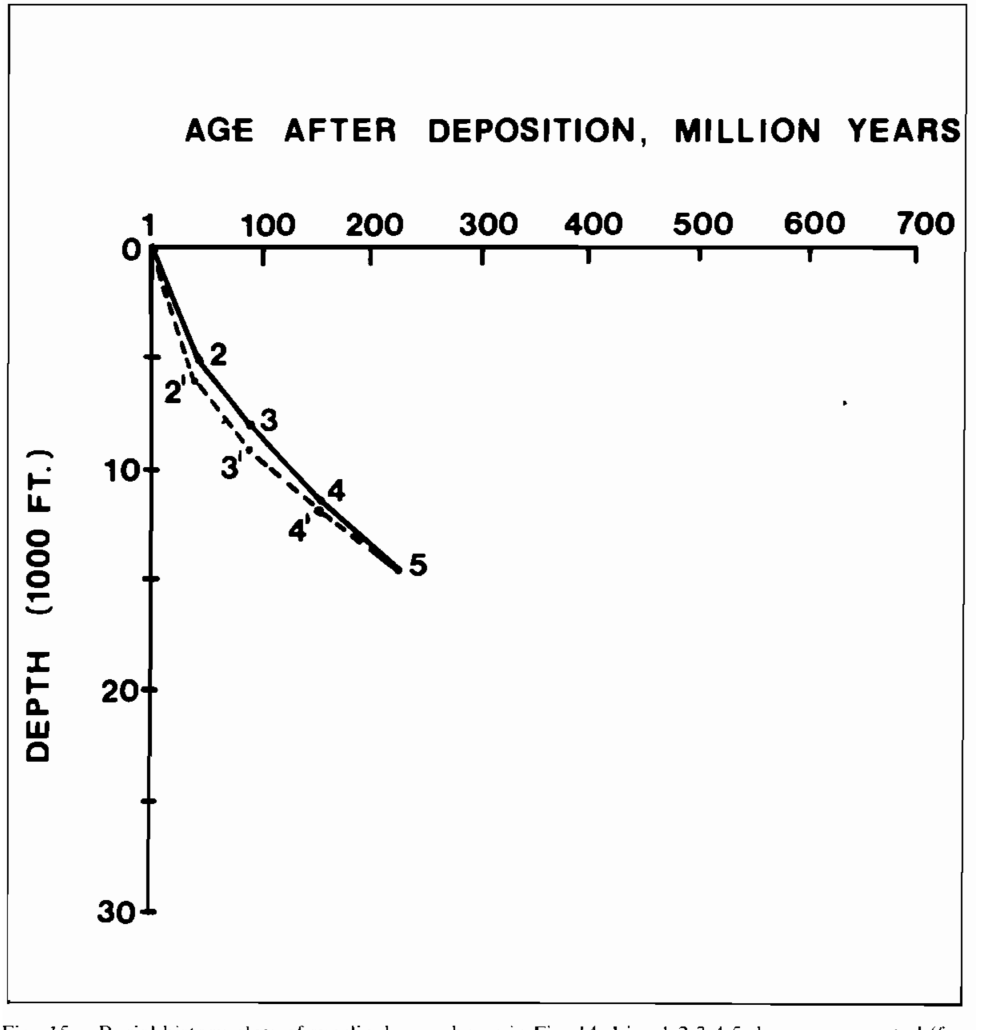

Fig. 15. Burial history plots of synclinal area shown in Fig. 14. Line 1-2-3-4-5 shows uncorrected (for compaction) burial history and line 1-2′-3′-4′-5 represents compaction-corrected burial history.

As described above, stage 1 is the time when deposition of the reservoir section had just been completed. At stage 2 or the end of Triassic age, the reservoir had been buried to 5,000 ft, because that is the thickness of the Triassic formations above it (14,500-9,500 ft, Fig. 14). If the effect of sediment compaction is considered, the burial depth at that time must have been more than 5,000 ft, because a 5,000 ft section today ought to have been thicker than 5,000 ft when it was less deeply buried (or at the end of Triassic). The age of the reservoir at stage 2 was 45 million years since deposition (225-180 M.Y.). Both points 2 and 2′ in Fig. 15 show uncorrected and corrected (for compaction) burial depths at stage 2.

The burial depths and geologic ages of the reservoir at successive stages of burial are shown as points 3, 4, and 5 (uncorrected) or 3', 4', and 5 (compaction corrected) in Fig. 15.

Time of trap formation can be estimated by constructing two burial history plots from both synclinal and anticlinal areas (for the geologic columns, see Fig. 14). The anticlinal area experienced significant erosion (2,000 ft) after the Tertiary deposition. Burial histories of both areas are shown in Fig. 16. The synclinal area experienced continuous burial from stage 1 to 5, whereas the anticlinal area had two periods of trap formation: 1. a slow burial (stages 1 and 2), and 2. a slow burial followed by significant uplift (stages 4 and 5); the erosional period is shown by a wavy line in Fig. 16. These two periods of trap development can be inferred by the tendency of the two burial-history lines from both areas to separate from each other. No compaction correction has been made in the plots of Fig. 16.

Between the two periods, the two burial lines are almost parallel, indicating that both synclinal and anticlinal areas subsided at almost the same rate.

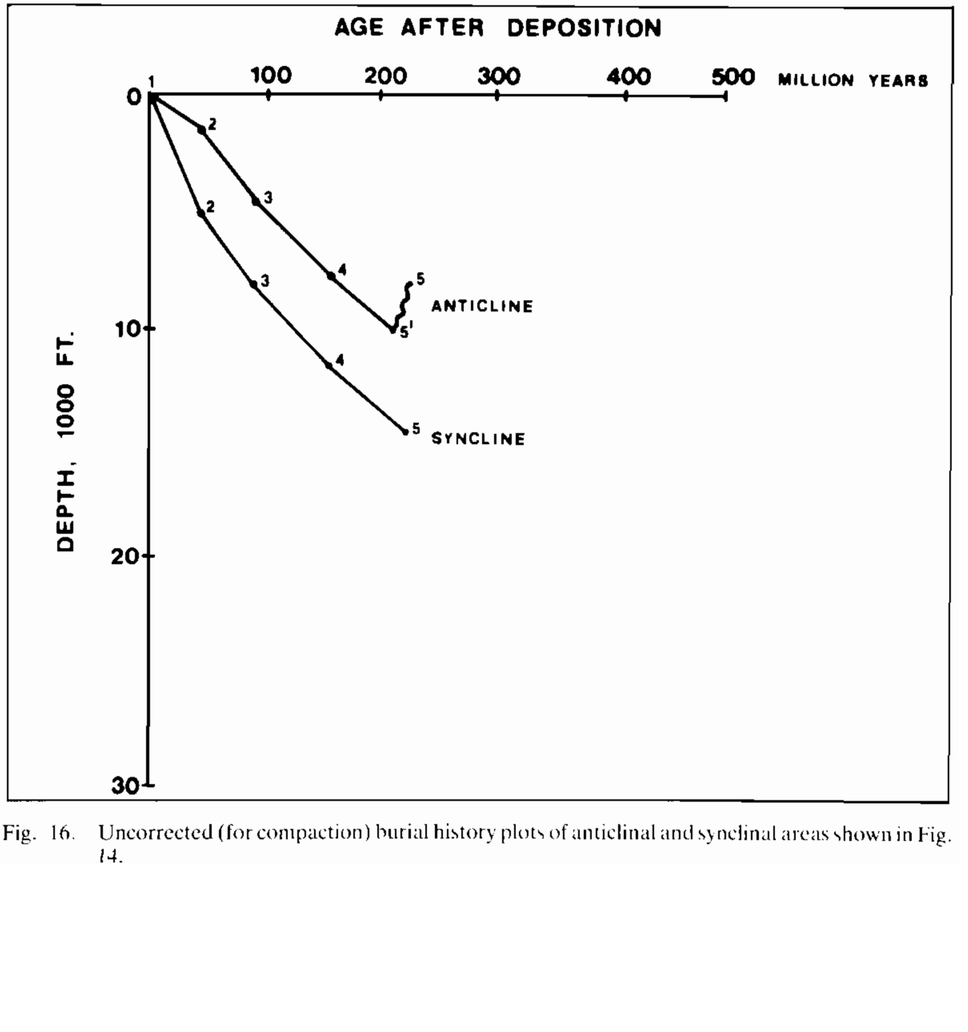

Fig. 16. Uncorrected (for compaction) burial history plots of anticlinal and synclinal areas shown in Fig. 14.

Rate of Loading (or Sedimentation) and Trap Formation

Although changing slopes of the burial-history lines from both synclinal and anticlinal areas indicate the status of trap formation, whether or not these two lines are separate from each other, is sometimes unclear on the plots. In such a case, rate of loading or sedimentation can be calculated and applied for estimating time of trap formation.

For a given geologic period, the rate of loading or sedimentation can be shown for both areas as follows;

$$R_A = \frac{\Delta D_A}{\Delta T} \tag{2}$$

$$R_S = \frac{\Delta D_S}{\Delta T} \tag{3}$$

where R_A and R_S are the rates of burial or sedimentation for both anticlinal and synclinal areas, respectively. ΔD_A and ΔD_S are the burial depth differences for both areas between the beginning and the end of a given geologic period, and ΔT is the geologic time interval of the period.

Rate of trap formation (R_T) can be defined as the difference between the rates of burial of both areas shown in equations (2) and (3), or

$$R_T = R_S - R_A = \frac{\Delta D_S - \Delta D_A}{\Delta T} \tag{4}$$

Using the burial history plots shown in Fig. 16, the rates of both burial and trap formation were calculated for the entire geologic period, and are shown in Table 1. Large positive values of R_T indicate periods of significant trap formation; in this example, the periods between stages 1 and 2 and between stages 5' and 5 during the erosion can be shown as the most important. Figure 17 depicts a graphical presentation of the trap formation for the case shown in Table 1.

Table 1. Rates of burial of anticlinal (R_A) and synclinal (R_S) areas, and of trap formation (R_T), for the case shwon in Fig. 16.

	Anticline R_A	Syncline R_S	Difference R_T
Stage 1			
	33.3	111.1	+77.8
Stage 2			
	66.6	66.6	0.0
Stage 3			
	46.2	53.8	+7.6
Stage 4			
	41.7	42.9	+1.2
Stage 5' (before erosion)*			
	-200.0	42.9	+242.9
Stage 5 (after erosion)			

unit : ft/million years

* Based on erosional period of 10 million years.

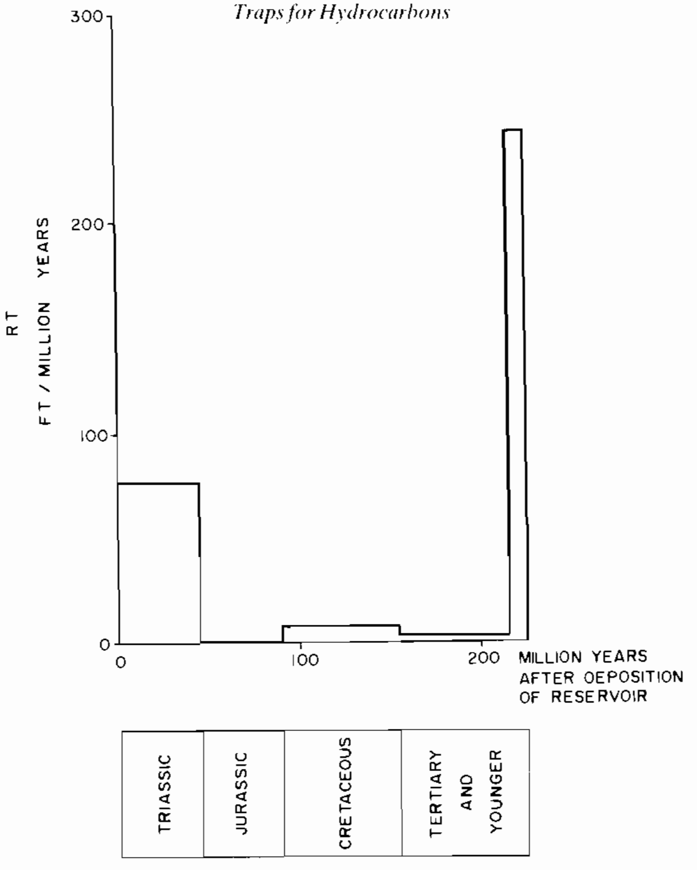

Fig. 17. Plot of rate of trap formation, R_T, based on data of Fig. 14.

A computer program was written for the IBM Personal Computer to plot both burial history and rates of trap formation (Fig. 17). The program is shown in Appendix A.

Compaction Correction of Burial History Plot

In Fig. 15, the burial history plot when the compaction correction is made is shown by line 1-2'-3'-4'-5, the middle part of which is shifted downward from the uncorrected line 1-2-3-4-5. Both cases show identical depths at the beginning (stage 1) and at the end (stage 5) of the burial history, but, at the intermediate stages of 2, 3 and 4, some compaction corrections are necessary.

If the sediment compaction is simply the result of fluid expulsion from it, the following mass balance relationship could be established;

$$V(1 - \phi) = V_0 (1 - \phi_0)$$

or

$$V_0 = V \frac{1 - \phi}{1 - \phi_0} \qquad (5)$$

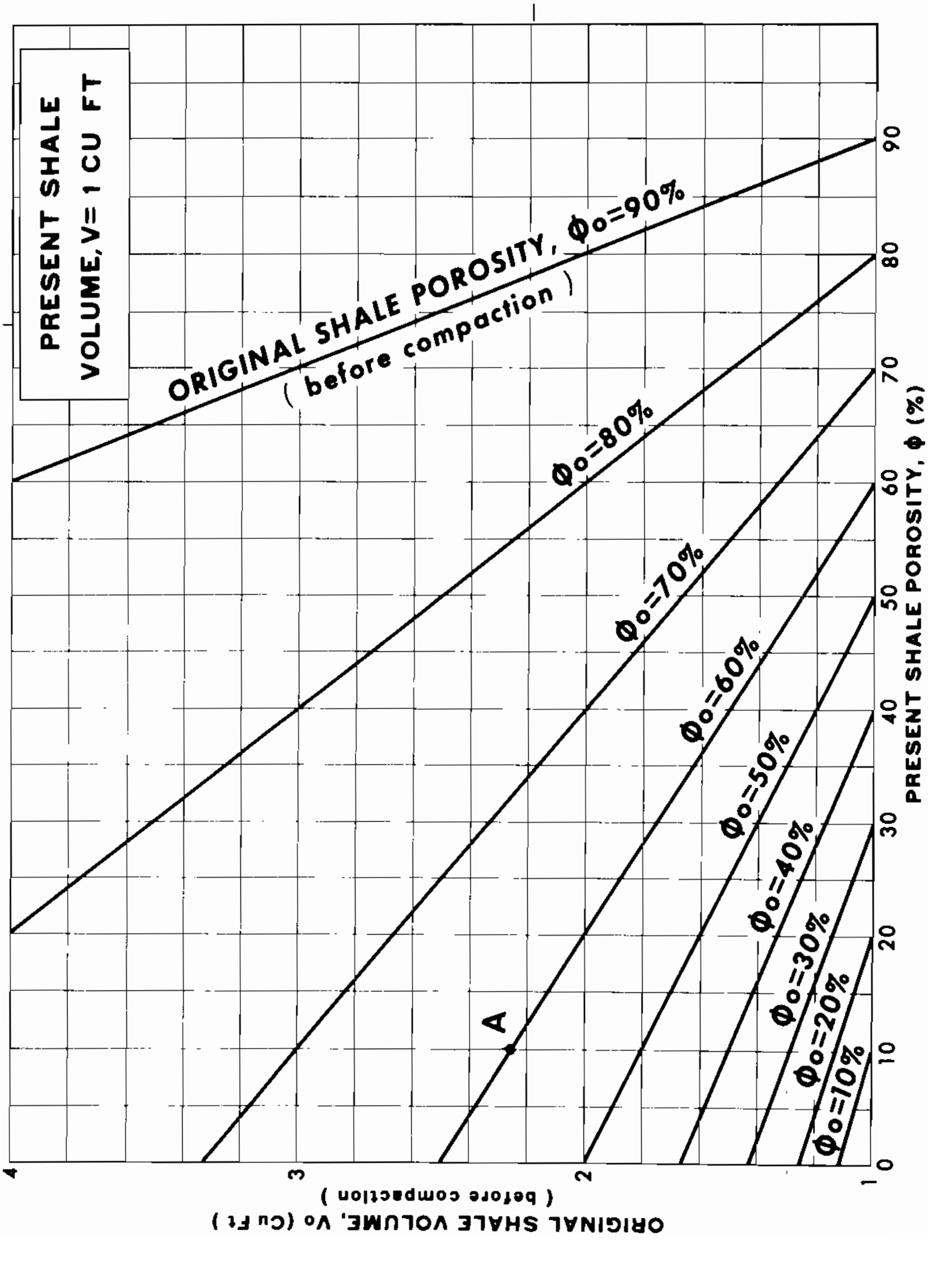

Fig. 18. Graph relating original and present shale porosities to original shale volume.

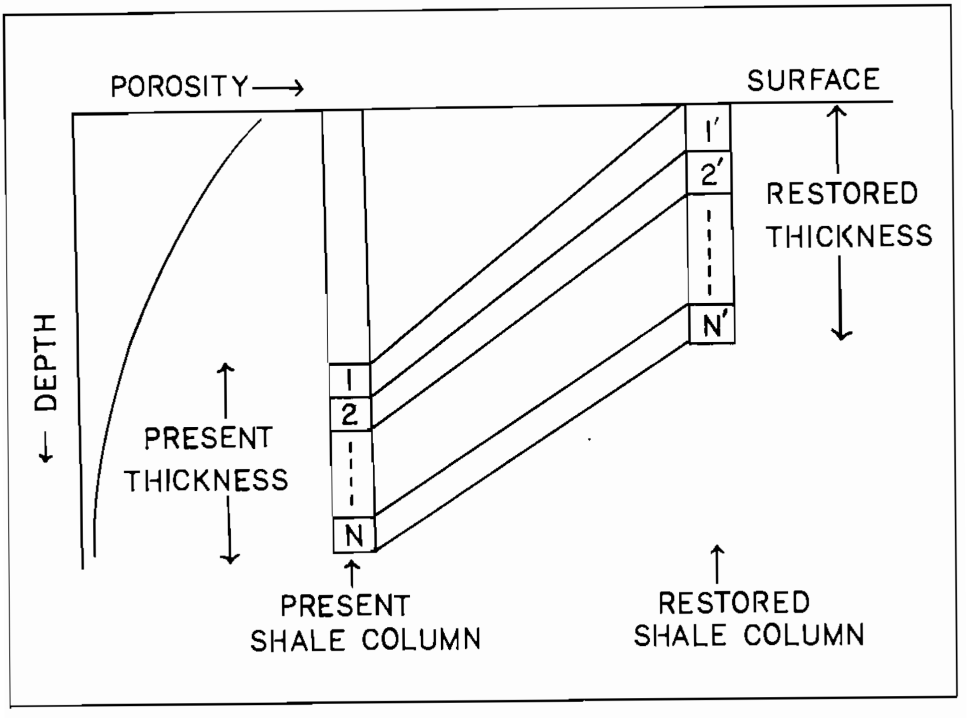

Fig. 19. Schematic diagram showing method of restoring present thickness to original thickness before compaction.

where V_0 and V are volumes of the sediment before and after compaction, and ϕ_0 and ϕ are its porosity values before and after compaction, respectively.

If a vertical sediment column with a unit base area is considered and if compaction occurred primarily in the vertical direction through an increase of overburden pressure, the volume terms in equation (5) can be replaced by new thickness terms, T_0 and T, before and after compaction, respectively, as;

$$T_0 = T \frac{1 - \phi}{1 - \phi_0} \tag{6}$$

In solving either equation (5) or (6), a convenient chart of Fig. 18 can be used. Point A in this figure is based on $\phi_0 = 60\%$ and $\phi = 10\%$ and the estimated V_0 (or T_0) on the vertical scale is 2.25 ft^3 (or 2.25 ft). In this chart, the present sediment volume after compaction, V (or thickness, T) is 1 ft^3 (or 1 ft). The result of calculation shows that the original volume of 2.25 ft^3 (or thickness of 2.25 ft) was reduced to 1 ft^3 (or 1 ft) by compaction and fluid expulsion.

The above estimation is identical to the result of the direct calculation using equation (5) or (6), as follows;

$$V_0 \text{ or } T_0 = 1 \times \frac{1 - 0.1}{1 - 0.6} = 1 \times \frac{0.9}{0.4} = 2.25 \text{ ft}^3 \text{ or ft.}$$

When a thick formation with changing porosity with depth is to be restored to that at shallower burial depths, more laborious steps must be taken. These steps are shown diagrammatically in Fig. 19. Let us suppose that column 1-N, which is deeply buried (see left-hand column), is to be restored to shallower burial depths (see right-hand column). A porosity-depth relationship is necessary to estimate the porosity values at both present (after compaction) and restored (before compaction) stages.

Let us take unit 1 from the present column and restore it at the surface shown as unit 1′ (restored column), using equation (6). The thickness of this unit was greater at that stage. The restoration of the other units must continue to the final one, N. The sum of the restored thicknesses from unit 1 to N is computed and is interpreted to be the true burial depth of the unit N when unit 1 was at surface or was being deposited.

Problems

1. Explain the main reasons why both anticlinal and domal traps are usually easier to find and more productive than the other types of traps.
2. Using the geologic data shown in Fig. 20, construct burial history plots of the reservoir at both synclinal and anticlinal locations.
3. Using the above data, calculate the rate of loading or sedimentation for the five successive periods for both synclinal and anticlinal locations.
4. From the result of 3, calculate the rate of trap formation for these periods. Then, describe the most significant period(s) of trap formation.

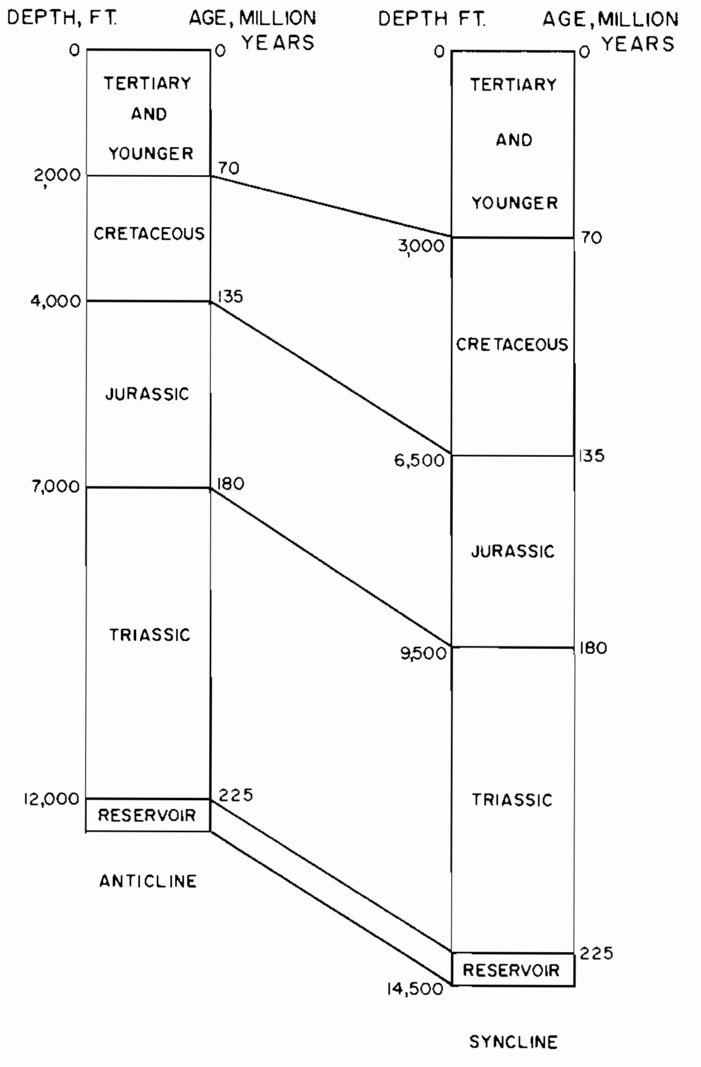

Fig. 20. Geologic columns of anticlinal and synclinal locations.

Chapter 4

Cap Rocks and Sealing Efficiency

- Introduction. ■ Capillary seal.
- Capillary pressure curve. ■ Pressure seal.
- Pressure-sealing time and depth.
- Summary. ■ Problems.

Introduction

It has been widely known that shale and anhydrite are the two main sealing rocks or cap rocks for hydrocarbon accumulations. Tight limestones can also be a seal. There are two important physical characters of rocks involved in the determination of sealing capacity; 1. ductility, and 2. high capillary pressure or low permeability.

Most anhydrite caps are effective, because of their extremely low (or practically nil) permeability and of their ductile nature. Some undercompacted shales, which are called pressure seals (Evans *et al.* 1975), also have both low permeability and high ductility. Even in these rocks, fractures may be developed by the imbalance between the subsurface stress and fluid pressure (Magara 1981a), but such fractures could be closed quickly if the rock is ductile.

In cases of normally compacted shale and tight (and probably dense) limestone, their high capillary pressure and low permeability are the main reasons of their being good cap rocks.

Cap rock may be defined as a rock which tends to retard the vertical escape of hydrocarbons from a trap. I believe that in most traps a small amount of vertical loss of hydrocarbons is inevitable, but, as long as the loss is significantly less than the amount migrating into the trap, a commercial accumulation can be formed. In other words, there would be no need of having an absolute seal or cap rock to form a hydrocarbon accumulation in the subsurface.

Another important point with respect to the cap rock is that a rock, which effectively seals hydrocarbons but not water, is necessary in forming an entrapment. This means that hydrocarbons are being sieved effectively by the cap rock, while formation water escapes upward from the trap.

If, for the sake of argument, the cap rock is an absolute seal for both water and hydrocarbons, then virtually no water would migrate from synclinal areas to the crest. Because water's compressibility is extremely low, water cannot move into the crestal area unless water already existing in the crest is being removed to the surface. Movement of water is an essential factor of hydrocarbon migration in most cases.

Capillary Seal

Berg (1975) offered an equation to estimate the maximum height of oil column, Z_0, held by the capillary pressure;

$$Z_0 = \frac{2\gamma\left(\frac{1}{r_t} - \frac{1}{r_p}\right)}{g\,(\rho_w - \rho_0)} \tag{7}$$

where γ is the interfacial tension between oil and water, r_t and r_p the pore-throat radius of cap rock and pore radius of reservoir rock, respectively, g the gravity acceleration, and ρ_w and ρ_0 the densities of water and oil, respectively.

A well-sorted, fine-grained sandstone with a porosity of 26% was considered by Berg. Such a natural aggregate may approximate a rhombohedral packing of uniform spheres in which pore sizes are 0.154D, 0.225D, and 0.414D, D being the sphere diameter.

The graph in Fig. 21 shows the critical height of oil column as estimated by these assumptions: if the column of oil exceeds this critical height, the oil will move upward; otherwise, it will stay under the seal. In this model, the reservoir rock, whose grain size, D, is 0.2 mm, is overlain by the same or a finer-grained rock. The critical height of the oil column (vertical scale) is shown for a given grain size (horizontal scale) and given density difference ($\Delta\rho$) between water and oil. For example, an oil column of 150 ft can be retained by silt of 0.01 mm grain size, if the density difference ($\Delta\rho$) is 0.2g/cm^3.

If water is moving due to hydrodynamic force in the reservoir, the critical height of oil column, Z_{ot}, can be expressed differently (Berg 1975);

$$Z_{ot} = \frac{2\gamma\left(\frac{1}{r_t} - \frac{1}{r_p}\right)}{g\,(\rho_w - \rho_o)} \pm \left(\frac{\rho_w}{\rho_w - \rho_o}\right)\frac{dh}{dx}\cdot X_o \tag{8}$$

where $\frac{dh}{dx}$ is the inclination of fluid-potential surface measured from potentiometric map and X_o the horizontal width of oil accumulation (Fig. 22).

The optional sign ($\pm$) in equation (8) refers to flow direction: the positive sign corresponds to down-dip flow and the negative to up-dip flow. In other words, a greater hydrocarbon column can be retained if there is a down-dip flow or down-dip potential gradient. The sealing capacity of a given cap rock is usually less for gas than for oil, because the buoyancy term, $\rho_w - \rho_o$ (or may be, $\rho_w - \rho_g$ for gas) in both equations (7) and (8) is greater for gas.

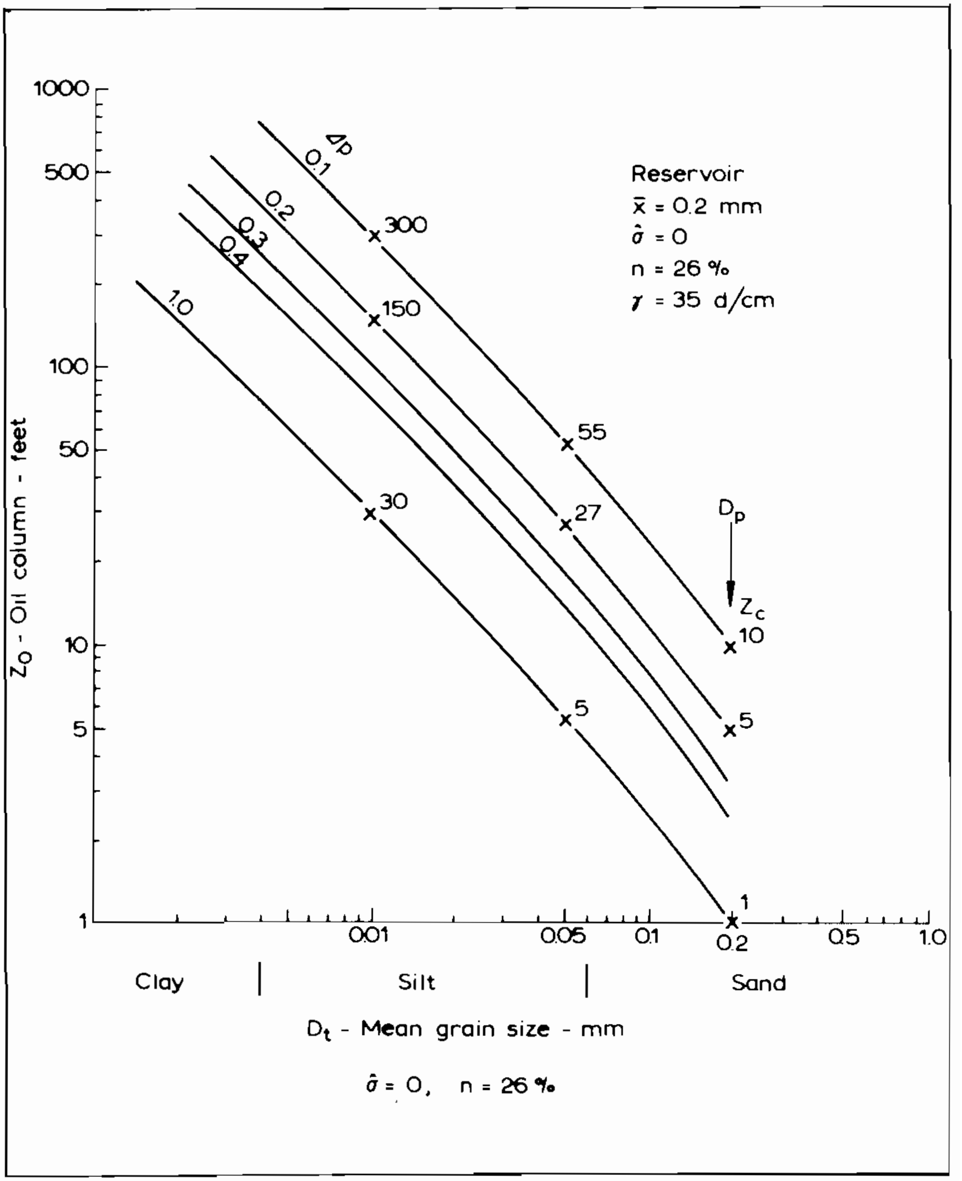

Fig. 21. Graph relating mean grain size of cap rock and density difference ($\Delta\rho$) between water and hydrocarbons in reservoir to height of oil column (Z_o). Refer to text for explanation (Berg 1975). Courtesy of American Association of Petroleum Geologists.

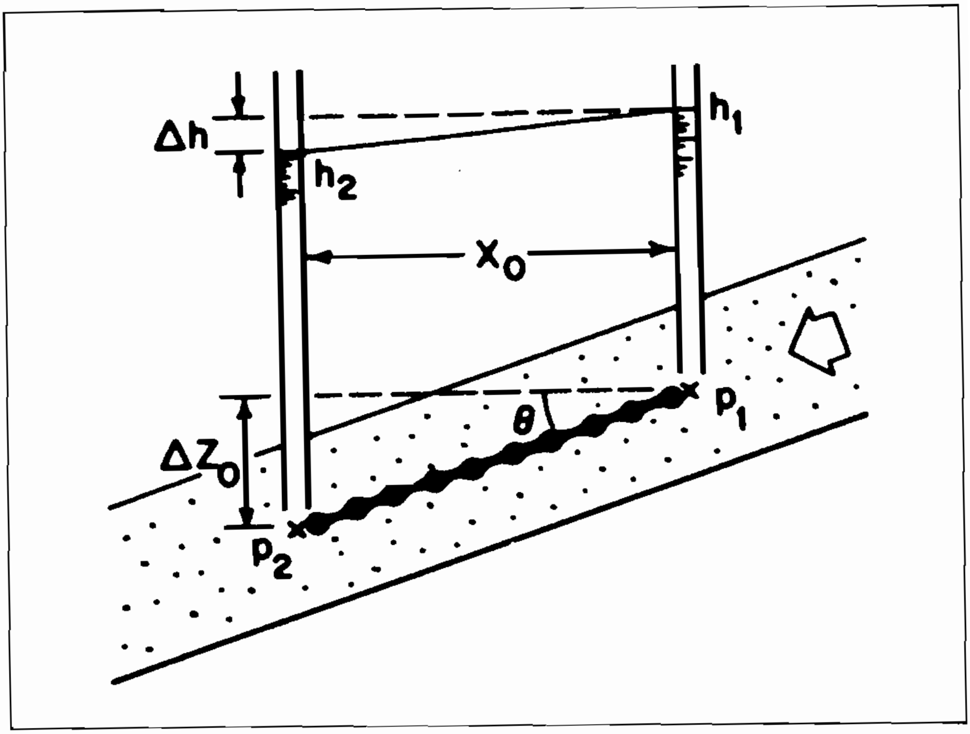

Fig. 22. Schematic diagram of oil stringer held in aquifer by downdip flow of water (Berg 1975). Courtesy of American Association of Petroleum Geologists.

In general, the capillary sealing capacity tends to increase with increasing sediment compaction, because of the reduction in pore size and of the increase in the proportion of structured water in shale which further retard the movement of water.

Capillary Pressure Curve

To evaluate pore geometry of a core, capillary pressures are sometimes measured by injecting oil (or mercury) into the water-saturated core. Examples of capillary pressure curves of a reservoir and a cap rock are shown in Fig. 23.

In the reservoir curve, the pressure necessary to force the oil (or mercury) to enter the rock is named as displacement pressure, $P_{d(reservoir)}$. After the displacement pressure is exceeded, the curve becomes nearly flat, showing that it takes very little additional pressure to increase the oil (or mercury) saturation (or to decrease water saturation). After this stage, the curve becomes more vertical, suggesting that additional pressure does not significantly increase the oil (or mercury) saturation (or decrease water saturation). During this final stage, only very small pore spaces are available for injection of oil (or mercury). The water saturation at the final stage is called "irreducible water saturation, $S_{w.irr(reservoir)}$".

A homogeneous, porous, and permeable reservoir is usually characterized by relatively small P_d and $S_{w,irr}$ values. A poor reservoir or a good cap rock, on the contrary, tends to have relatively large P_d and $S_{w,irr}$ values which are shown by curve "cap rock" in Fig. 23. In this case, to inject oil into the cap rock, thc minimum pressure shown by "A" is necessary.

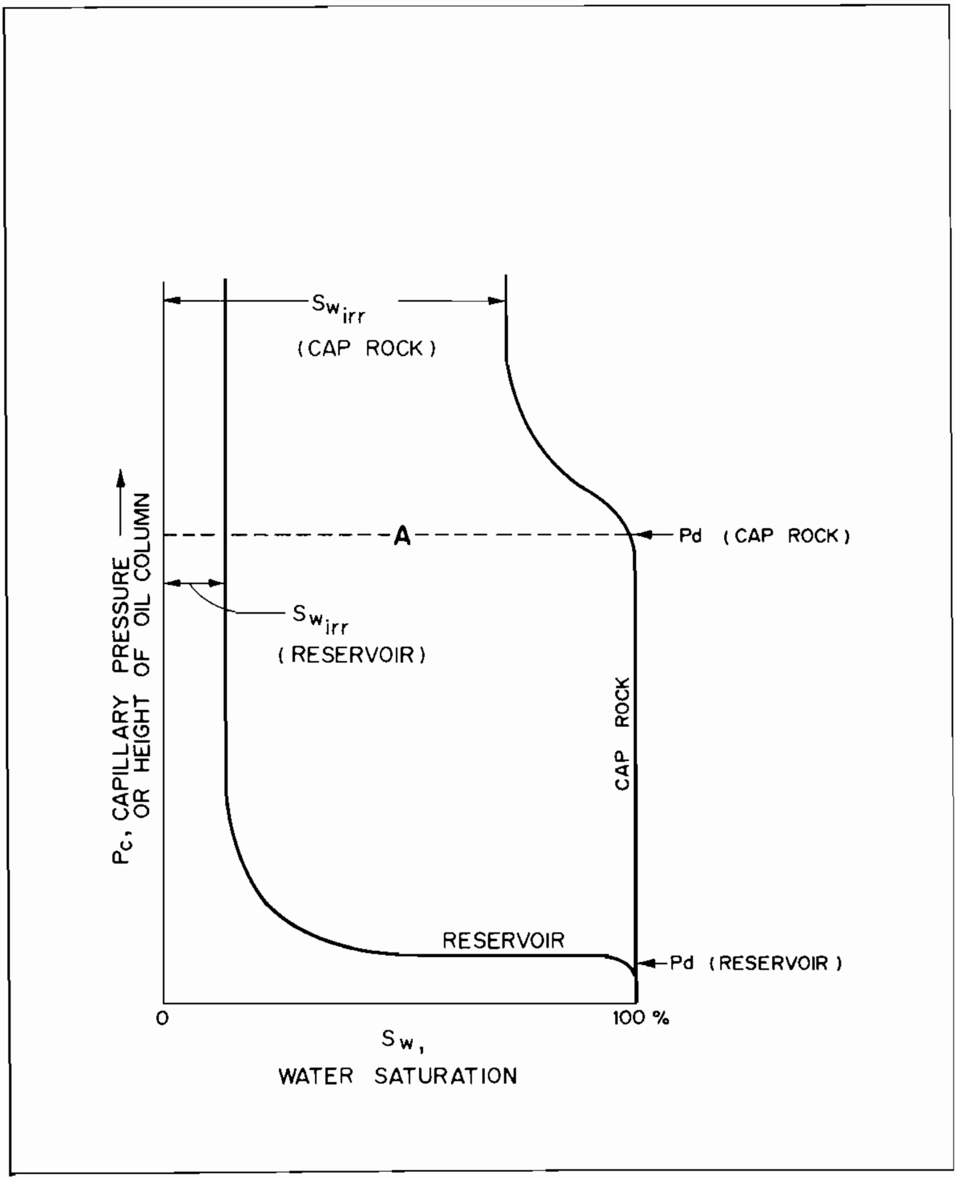

Fig. 23. Schematic capillary pressure curves of reservoir and cap rocks. Refer to text for explanation.

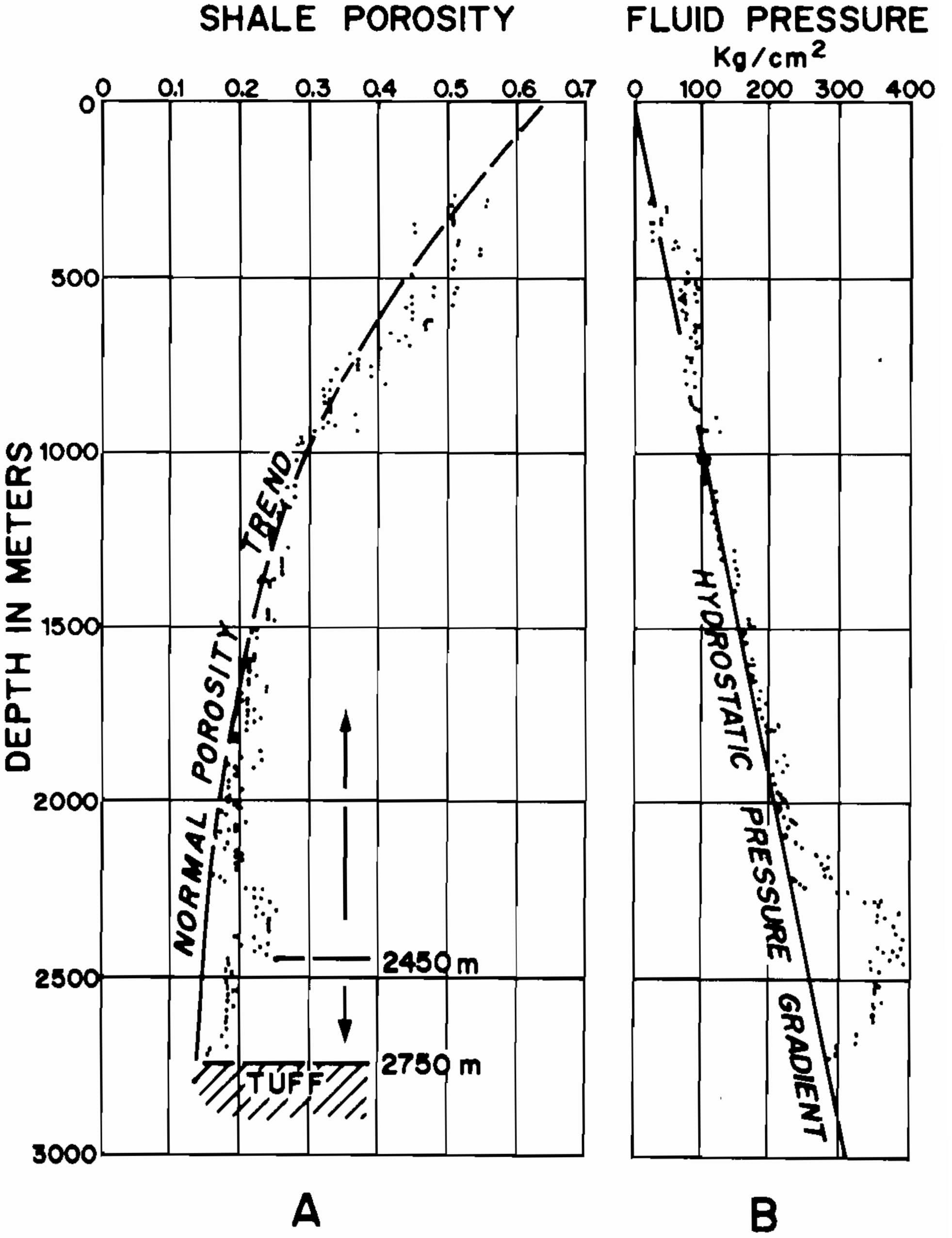

Fig. 24. Example of pressure seal at Shiunji SK-21, Japan. Refer to text for explanation (from Magara 1968). Courtesy of American Association of Petroleum Geologists.

In a hydrocarbon reservoir, pressure of the hydrocarbon phase in excess of water pressure increases upward due to buoyancy. This excess hydrocarbon pressure can be shown as $(\rho_w - \rho_h)$ H.g, where ρ_w and ρ_h are densities of both water and hydrocarbons, H the height of hydrocarbon column, and g the gravity acceleration. Therefore, the capillary pressure (P_c) on the vertical axis of Fig. 23 may be replaced by the term related to the height of the hydrocarbon column.

If the excess pressure of such a hydrocarbon column exceeds level A in Fig. 23, the hydrocarbons will be injected into the cap rock (or lost upward). Otherwise, the hydrocarbons will be retained in the reservoir. In summary, a higher P_d value of the cap rock tends to keep a thicker hydrocarbon column.

Pressure Seal

Slightly undercompacted shales can act as pressure seals. An excellent example from Japan is shown in Fig. 24, in which the undercompacted shales between about 2,250 and 2,450m (see A) have fluid pressures in excess of the hydrostatic pressure (see B). These excess fluid pressures in the shales are believed to have helped in holding hydrocarbons (gas in this case) in the volcanic tuff reservoir below about 2,750m.

Another example is shown in Fig. 25 which depicts both sandstone % and calculated fluid pressure of shales of a well in the Gulf Coast, Louisiana. The shales between about 7,000 and 9,000 ft are believed to be acting as pressure seals for hydrocarbons trapped below 9,000 ft. Figure 26 is an example of pressure seal from the northern Canada.

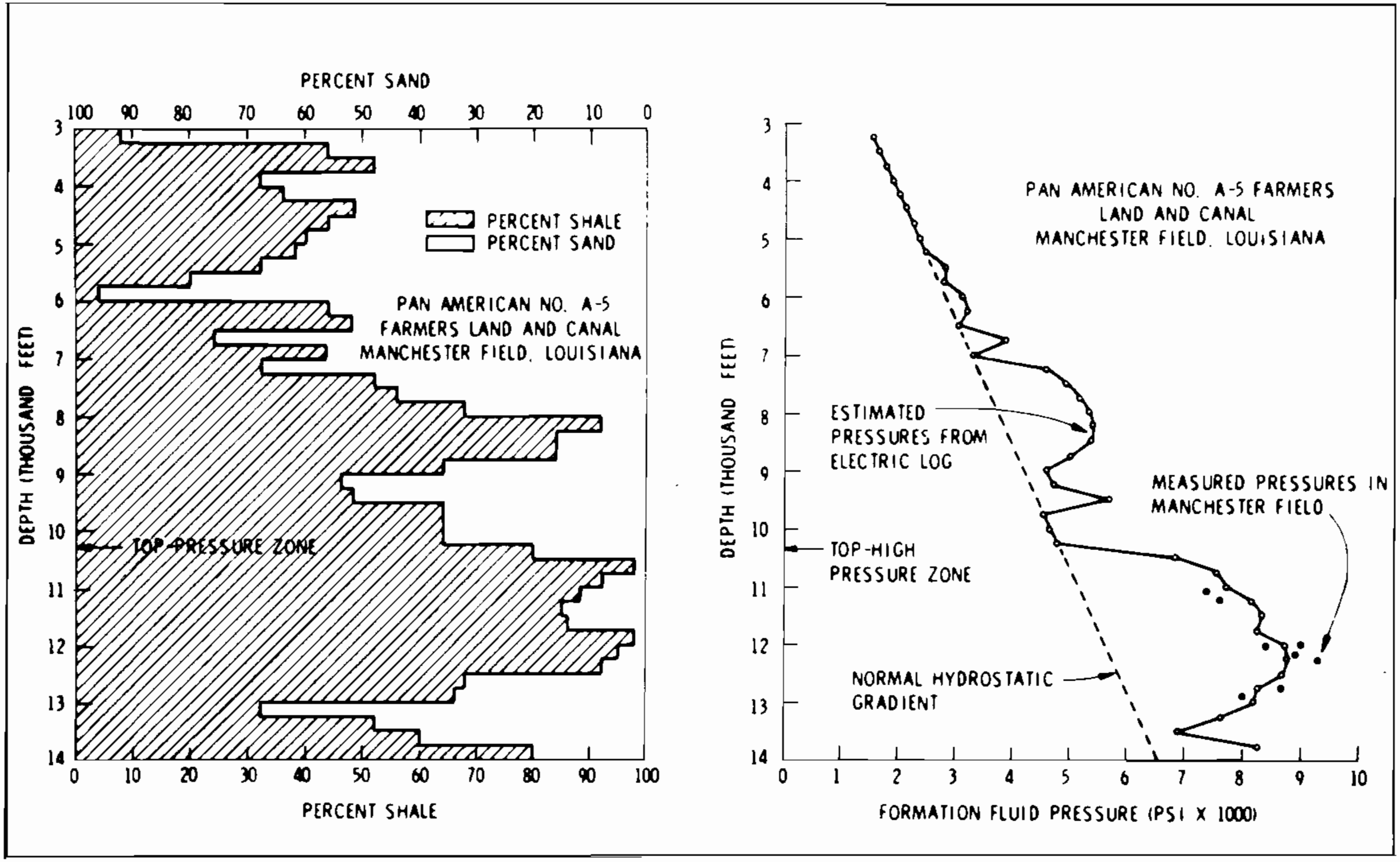

Fig. 25. Example of pressure seal in Gulf Coast. See text for explanation (from Schmidt 1973). Courtesy of American Association of Petroleum Geologists.

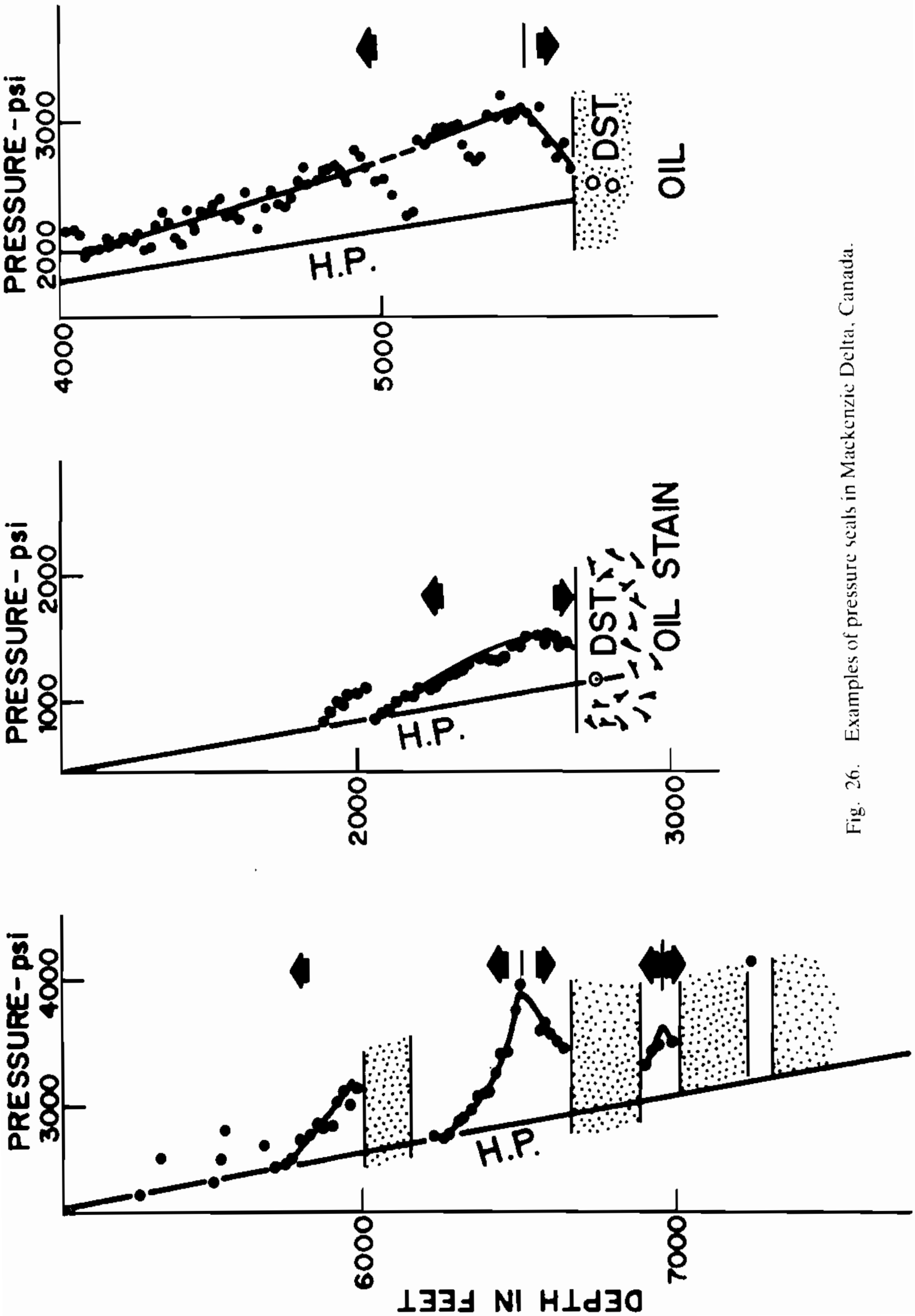

Fig. 26. Examples of pressure seals in Mackenzie Delta, Canada.

Pressure-Sealing Time and Depth

Unlike capillary seals, most pressure seals are believed to have been developed long after deposition. These undercompacted shales generally underwent relatively normal compaction in the earlier stages of their history, until their permeability had been reduced to a level beyond which normal fluid expulsion and normal compaction became impossible mainly due to the reduced permeability and fluid mobility (Magara 1978a). The shale compaction rate would then have slowed down, and undercompaction have resulted. Possible compaction histories of the undercompacted shales (pressure seals) are shown in Fig. 27.

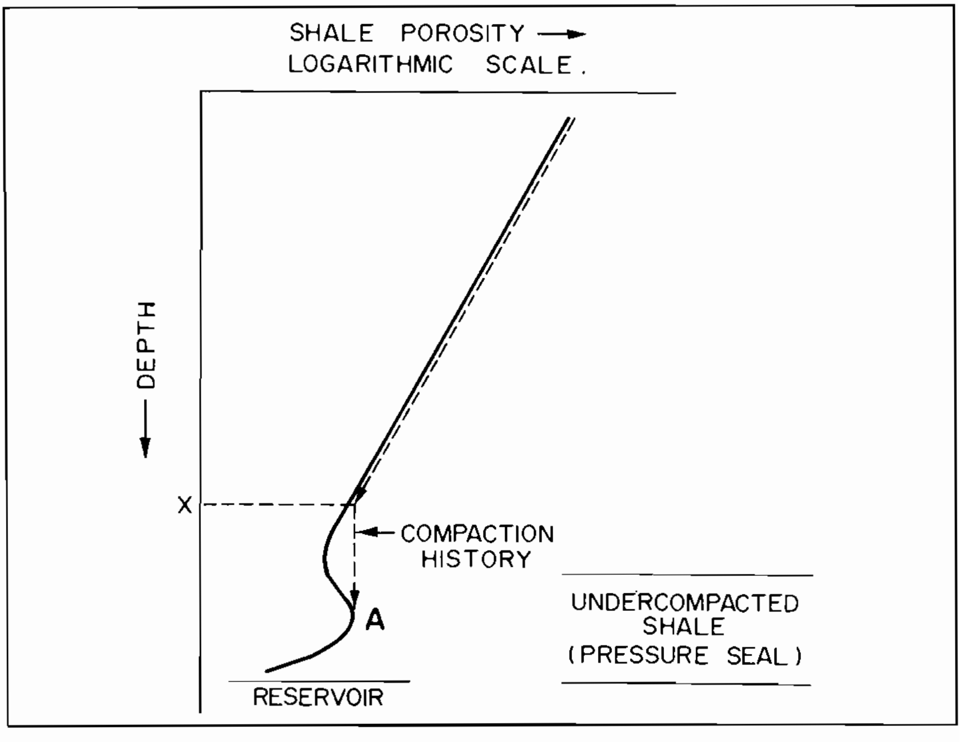

Fig. 27. Schematic diagram showing sealing depth (X) of pressure seal at A.

The depth at which normal compaction and normal fluid expulsion for shale A (most undercompacted) ceased is shown as X in Fig. 27. This is the estimated depth at which shale A reached the stage of restricted fluid expulsion, or the sealing depth. Possible deepest sealing depth, which corresponds to possible latest sealing time (geologically speaking), can be estimated by drawing a near vertical line from shale A and finding the intercept depth with the normal compaction trend line shown as X in Fig. 27. The actual sealing depth could have been slightly shallower than this depth, but the difference between the actual and possible deepest sealing depths may not be too large in most cases.

If this sealing depth (X) is plotted on a burial history plot such as shown in Fig. 28, corresponding sealing time can be estimated at X'. This is possible latest sealing time and the actual sealing time may have been slightly earlier than this estimate. Estimation of the sealing depth and time at an anticlinal location is most important, because most hydrocarbons tend to escape upward there if there is no effective seal.

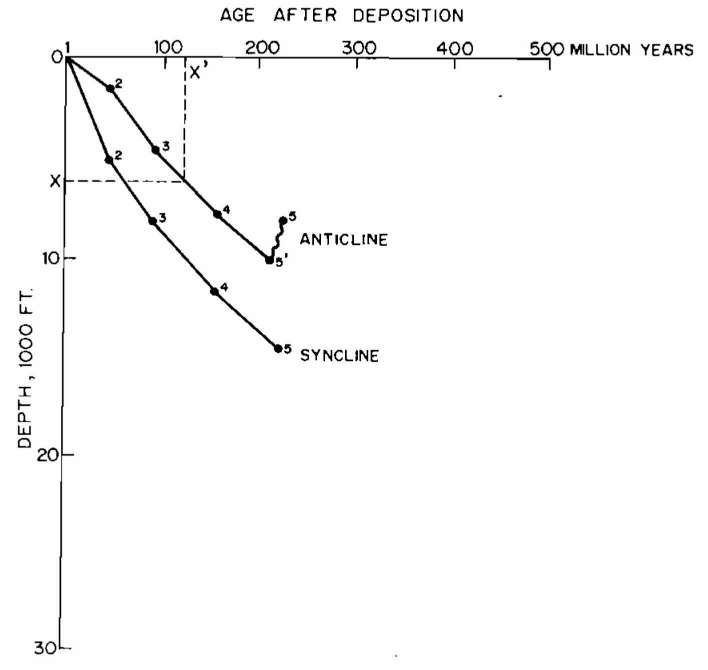

Fig. 28. Schematic diagram showing method of estimating sealing time (X') determined from sealing depth (X) in Figure 27.

Although absolute timing (or absolute geologic age) of seal development is not important, its timing relative to trap formation, and hydrocarbon generation and migration is a critical factor in assessing a prospect: by the time a trap was formed and hydrocarbons migrated into it, an effective seal must have been developed over the reservoir to form a significant accumulation.

Summary

The capillary seal is effective only when hydrocarbons have their own phase separate from water, whereas the pressure seal could be effective for any form of hydrocarbons, either separate from or soluble in water. Because the solubility of oil in water is much smaller than that of gas, the capillary seal tends to hold most oil accumulations effectively, but may not be good enough for many gas accumulations. In such cases, an additional sealing capacity by pressure seals would be helpful in keeping a high gas column. Note also that, because of greater buoyancy force of gas, gas tends to leak out more easily and quickly. In such a case, the presence of the pressure seal would become important.

It is known that most pressure seals are developed in relatively young sedimentary rocks (usually Cretaceous or younger). Timing analysis of a pressure seal using a burial history plot described above is quite useful in these younger rocks.

Problems

1. Describe effective sealing conditions for a trap.
2. Using Fig. 21, estimate the critical height of oil column, if the cap rock is clay of 0.005mm grain size and the density difference between the oil and water is 0.3 g/cm^3.
3. In the above example, if fluid is moving downdip, can we expect greater or smaller height of oil column over the height estimated above ?
4. Explain the method of estimating both depth and time of pressure seal development.

Chapter 5

Secondary Hydrocarbon Migration

■ Introduction. ■ Buoyancy. ■ Hydrodynamics.
■ Differential entrapment. ■ Problems.

Introduction

Once hydrocarbons from source rocks enter reservoir rocks, they will encounter various physical conditions that did not exist in the source rocks:

1. larger pore spaces
2. fewer capillary restrictions
3. less semisolid or structured water
4. less fluid pressure.

These new conditions generally help to enlarge and connect the hydrocarbon globules, which can cause significant buoyant force. The reduced capillary restrictions will allow this buoyancy to move the interconnected globules to a higher structural position in the reservoir. In other words, formation of a trap is an important factor in migrating hydrocarbons at the secondary stage. The structured water will be explained in the next chapter.

Buoyancy

If some structural relief, due to loading imbalance and/or late-stage uplift and erosion, is formed, the interconnected globules of hydrocarbons will be able to move to a higher structural position, provided the buoyant force exceeds the capillary restrictions.

The critical height of oil column, Z_o, for oil accumulation insuch a case is given as follows by Berg (1975);

$$Z_0 = \frac{2\gamma\left(\frac{1}{r_t} - \frac{1}{r_p}\right)}{g\,(\rho_w - \rho_0)} \tag{7}$$

as explained in Chapter 4.

Fig. 21, in Chapter 4, shows the critical height of oil column as estimated from this equation. If the oil column exceeds this critical height, the oil will move; otherwise, it will stay. In this model, D, the average grain size of the reservoir rock, is 0.2mm

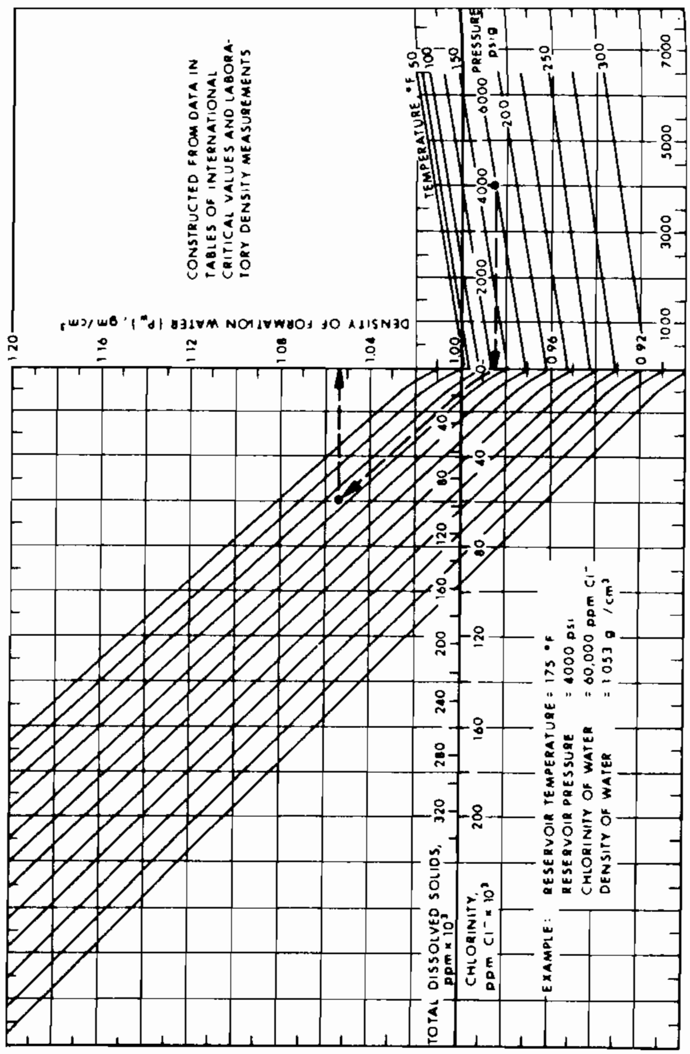

Fig. 29. Nomograph to determine density of formation water at subsurface conditions (from Schowalter 1979). Courtesy of American Association of Petroleum Geologists.

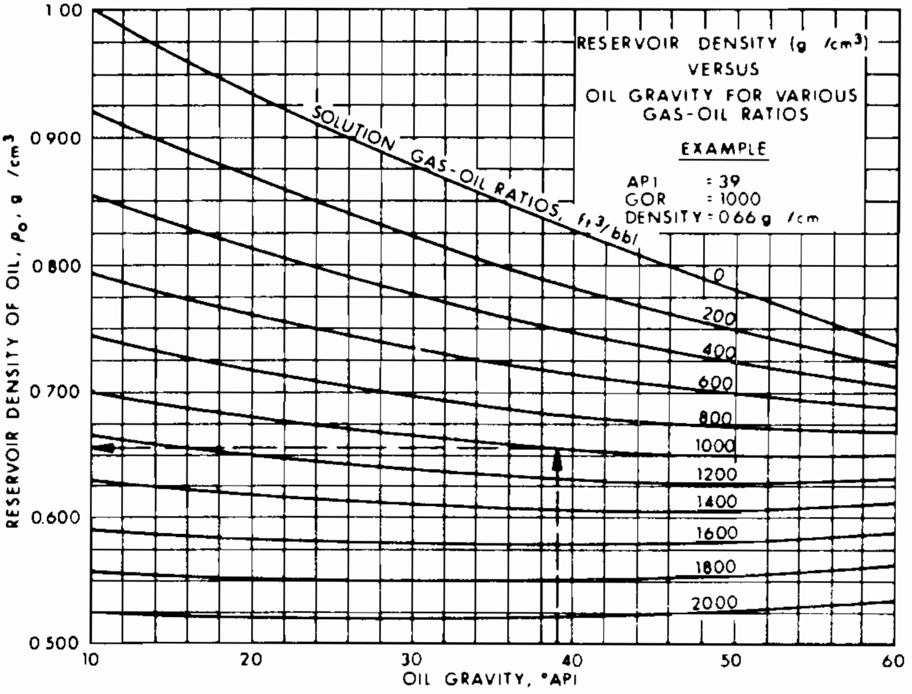

Fig. 30. Nomograph to determine subsurface oil density from API gravity and solution gas-oil ratio (from Schowalter 1979). Courtesy of American Association of Petroleum Geologists.

and the reservoir is overlain by the same or finer-grained rock. The critical height of the oil column (vertical scale) is shown for a given grain size (horizontal scale) and given density difference ($\Delta\rho$) between water and oil.

If, for example, the height of the oil column exceeds 5 ft when the fluid-density difference is 0.2 g/m^3 and the reservoir grain size is 0.2mm, the oil moves upward within the reservoir. If the reservoir rock becomes finer upward, or is overlain by other finer rock, a taller oil column is required for upward migration.

The density of water is controlled by pressure, temperature, and the amount and kinds of dissolved solids. Fig. 29 provides a means of evaluating the densities of formation water (Schowalter 1979). Schowalter stated: "In situations where the dominant negative ion is chloride, the chloride-ion concentration scale can be used. For waters that contain appreciable amount of negative ions other than chloride, the upper scale for total dissolved solids should be used."

Estimating the density of oil in the subsurface is more complicated, because it depends on the composition of oil and dissolved gases, temperature, and pressure. Fig. 30 can be used to arrive at a workable estimate of the density of oil under subsurface conditions from the stock-tank API gravity and the solution gas-oil ratio (Schowalter 1979).

Schowalter proposed three nomographs (Figs. 31, 32, and 33) to estimate manually the density of gas in the subsurface. The equation used to develop these nomographs is

$$\rho_g = 1.485 \times 10^{-3} \frac{mp}{ZT} \tag{9}$$

where ρ_g is the subsurface density of gas (g/cm^3), m the apparent average molecular weight, p the absolute pressure (lb/sq in), Z the compressibility factor, and T the absolute subsurface temperature (Rankine).

The interfacial tension between oil and water is significantly different from that between gas and water, under laboratory conditions. Hocott (1938), however, showed that, at higher pressures and temperatures, the interfacial tensions of both oil and gas with water approach 30-35 dynes/cm (Fig. 34). This is the basis on which Berg assumed the interfacial tension of 35 dynes/cm when constructing Fig. 21 (in Chapter 4).

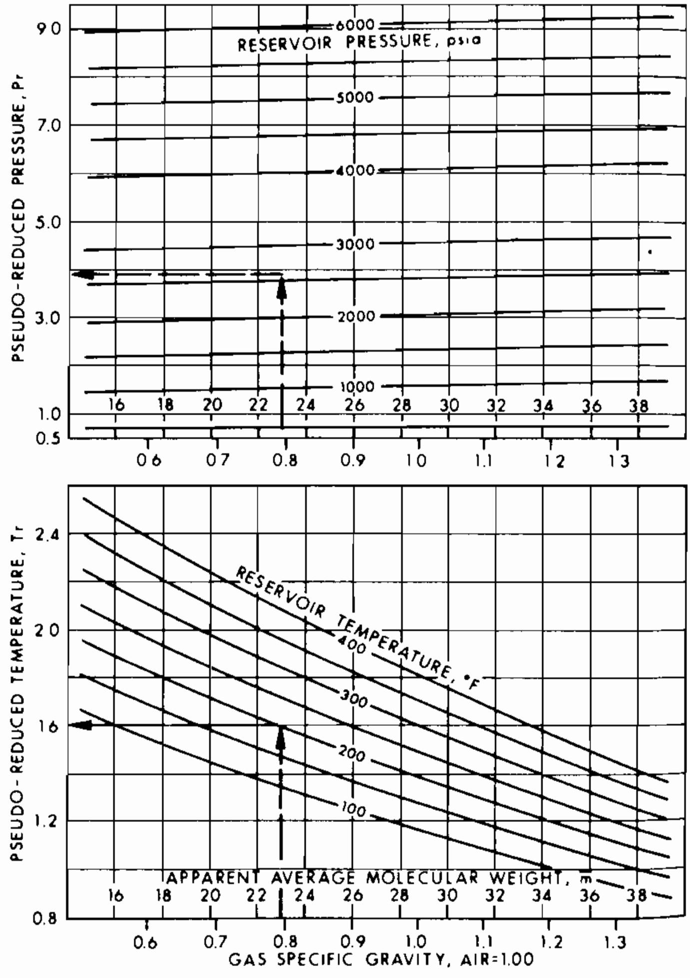

Fig. 31. Nomograph to determine density of gas jointly with Fig. 32 and 33 (from Schowalter 1979). Courtesy of American Association of Petroleum Geologists.

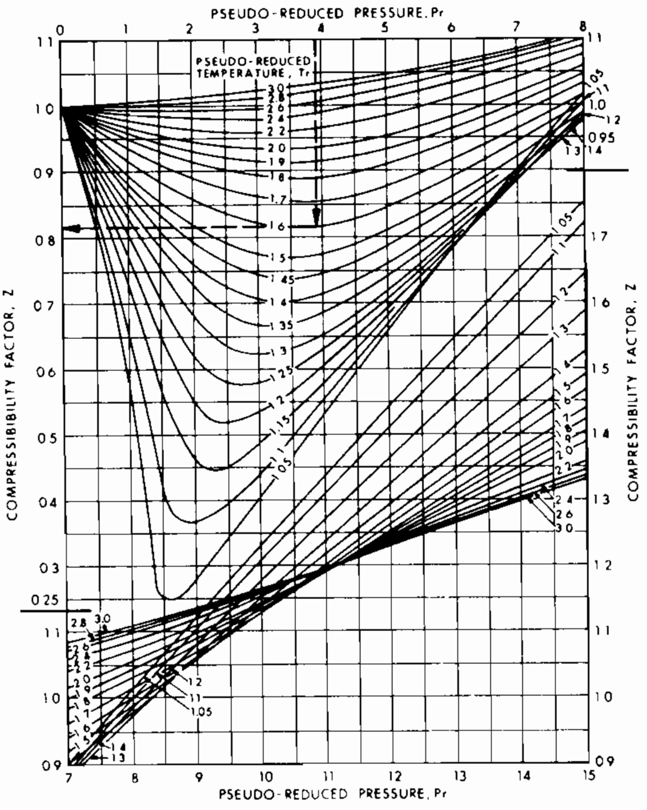

Fig. 32. Nomograph to determine density of gas jointly with Fig. 31 and 33 (from Schowalter 1979). Courtesy of American Association of Petroleum Geologists.

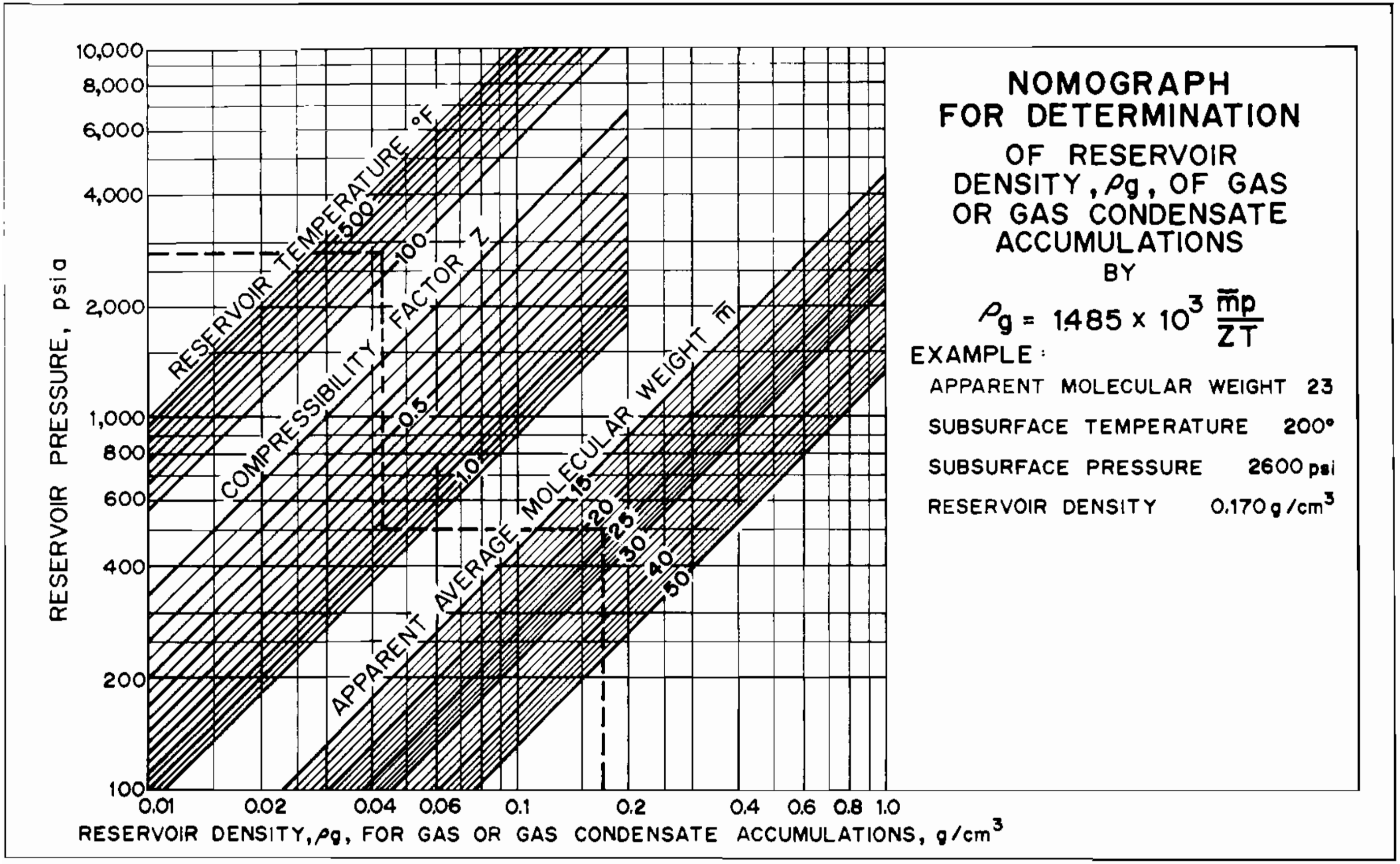

Fig. 33. Nomograph to determine density of gas jointly with Fig. 31 and 32 (from Schowalter 1979). Courtesy of American Association of Petroleum Geologists.

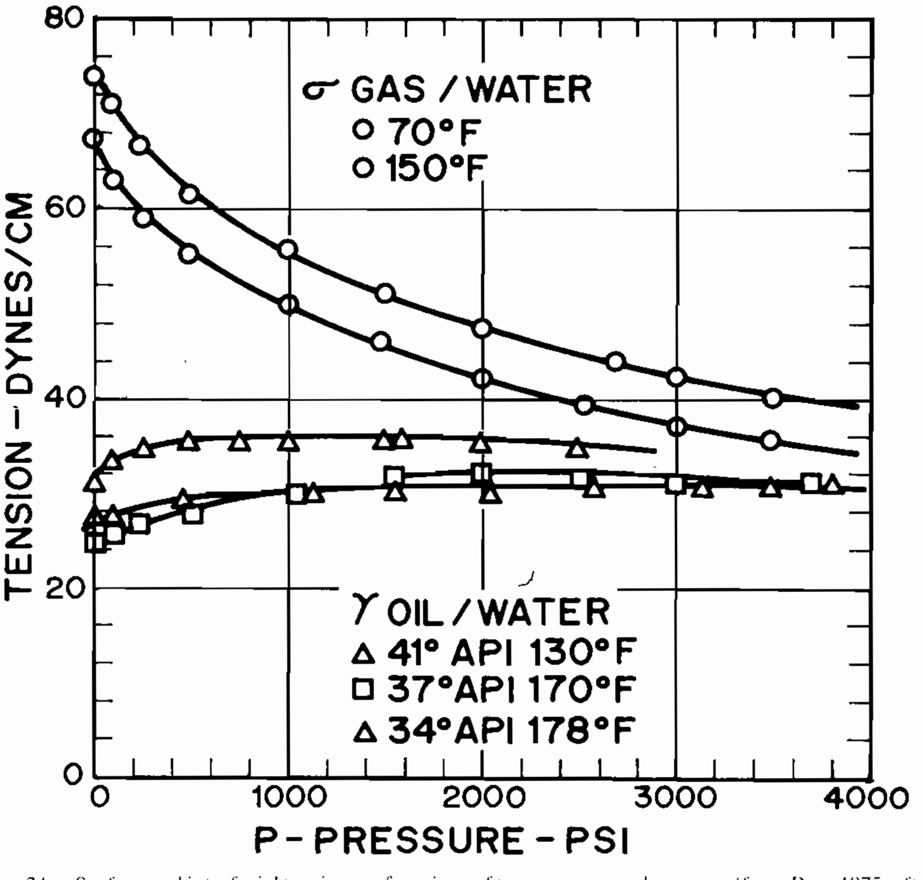

Fig. 34. Surface and interfacial tensions as functions of temperature and pressure (from Berg 1975, after Hocott 1938). Courtesy of Society of Petroleum Engineers at AIME.

If buoyancy were the principal cause of secondary petroleum migration, such migration would have taken place when or after active structuring or trap development occurred. For secondary migration, of course, the reservoir must have received a sufficient amount of oil or gas through primary migration.

Although buoyancy itself may suffice to move hydrocarbons in many reservoir rocks, other forces such as sediment compaction, aquathermal effect, and possibly clay-mineral dehydration may also influence secondary migration. In many cases, however, the directions of migration due to these different causes are the same as that due to buoyancy - from a structurally deeper place to one that is shallower.

If the directions of fluid flow resulting from these other causes are different from that of the flow caused by buoyancy, hydrocarbon accumulations may be forced to move to locations other than the tops of structures, or they may be completely lost from the sedimentary basin.

Hydrodynamics

Schematic examples of this type of accumulation are shown in Fig. 35. This figure depicts combinations of structural and hydrodynamic conditions in the subsurface; the accumulation is moved downdip by the hydrodynamic force.

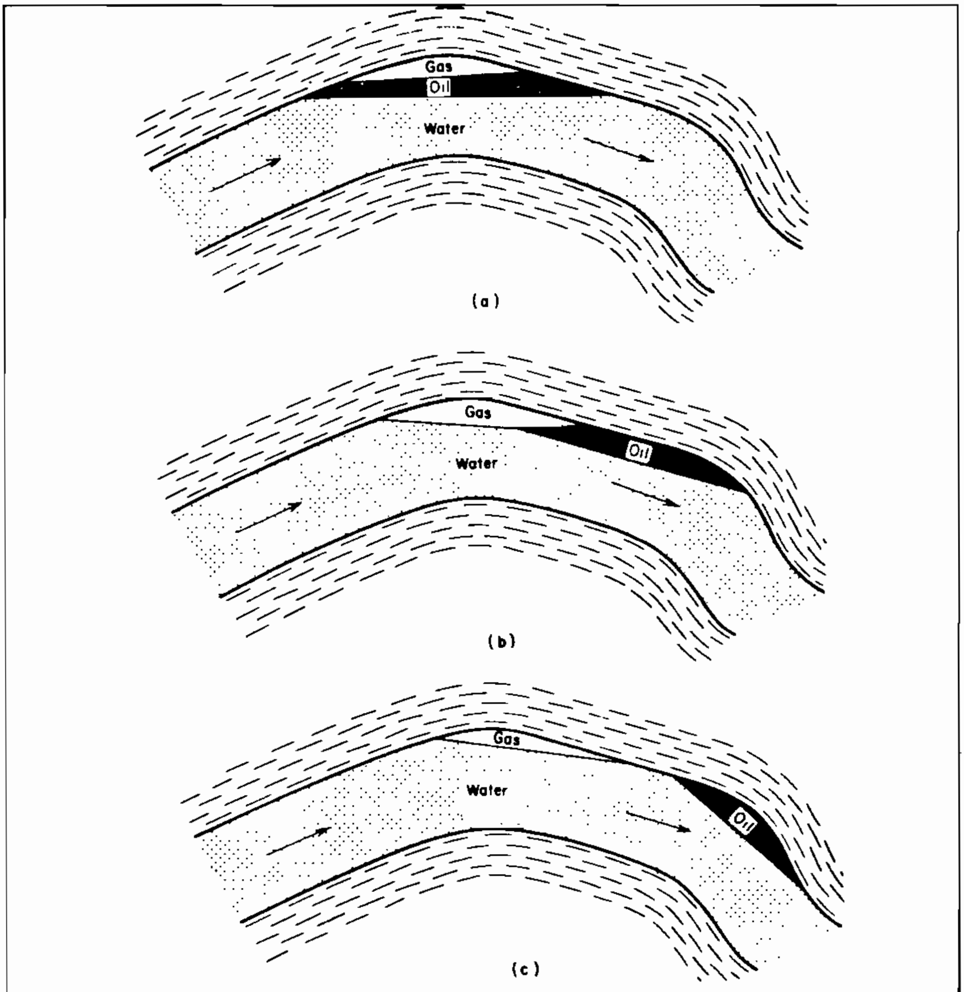

Fig. 35. Types of hydrodynamic oil and gas accumulations in sandstone reservoir; (a) gas entirely underlain by oil, (b) gas partly underlain by oil, (c) gas and oil accumulations separated (from Hubbert 1953). Courtesy of American Association of Petroleum Geologists.

The inclination of the oil (or gas)/water contact is given by Hubbert (1953) as follows:

$$\frac{dZ}{dX} = \frac{\rho_w}{\rho_w - \rho_h} \cdot \frac{\Delta h}{\Delta X} \qquad (10)$$

where $\frac{dZ}{dX}$ is inclination of oil (or gas)/water contact, ρ_w the density of water, ρ_h the density of hydrocarbons, and $\frac{\Delta h}{\Delta X}$ the inclination of potentiometric surface.

The elevation of the potentiometric surface of a reservoir can be estimated by making an imaginary water column whose weight corresponds to the measured or estimated formation-water pressure in the subsurface. The inclination of the potentiometric surface may be obtained if at least three measured or estimated water-pressure values are available within an area.

A hydrodynamic condition may be caused either by motion of meteoric water that penetrates from the surface into subsurface rocks or by movement of the sediment source or of the compaction water.

If an oil or gas accumulation is trapped in such a hydrodynamic environment, the oil (or gas)/water contact must be inclined in the direction of declining potentiometric elevation. However, an apparent inclination of oil (or gas)/water contact does not necessarily mean a hydrodynamic condition. It could also result from changing capillary pressure due to the changes in pore size and pore geometry caused by changing lithology, subsurface stress and diagenesis. Wilson (1975) proposed the importance of diagenetic effect in forming petroleum accumulations, some of which have tilted oil (or gas)/water contacts.

If faults effectively seal hydrocarbons, the difference of oil/water contact levels in different fault blocks also could cause an apparent tilt, as shown in Fig. 36. This apparent tilt has nothing to do with hydrodynamic conditions.

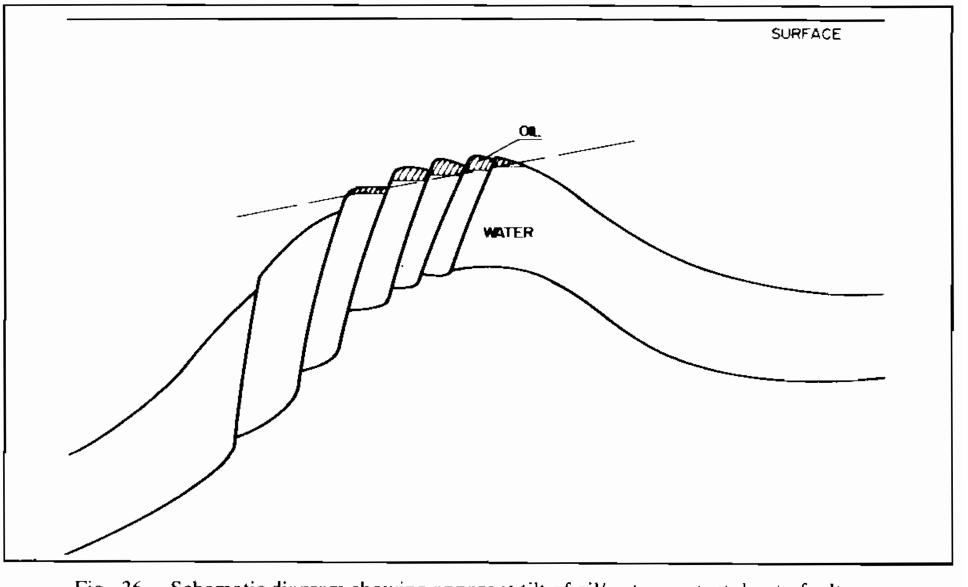

Fig. 36. Schematic diagram showing apparent tilt of oil/water contact due to faults.

Water-salinity change from fresher water in the intake area to more-saline water in the deeper parts of a basin is sometimes regarded as an indicator of hydrodynamic conditions. But salinity change does not necessarily mean hydrodynamic conditions in the sense used by many hydrodynamics geologists.

If fresh meteoric water was in contact with saline formation water during the geological past, we would find a gradual salinity change in the subsurface from diffusion, even if the water was static. Another possibility is that meteoric water has disturbed the relatively shallow formation water by circulating locally through it and thereby freshening it, but has not completely penetrated the deeper parts of the basin. In such a case, too, we would see gradual salinity change, but they would not imply the hydrodynamic condition in the sense used by the hydrodynamic geologists.

Under true hydrodynamic conditions, water drives into the deep subsurface and replaces some or all of the formation water. If such hydrodynamic conditions continued for some period of geologic time, then should not we have almost completely fresh water throughout the basin, rather than gradual changes in salinity? Figure 37 shows an example of salinity maps in Japan, where gradual salinity changes are observed but hydrodynamic conditions do not appear to exist.

For a hydrodynamic state to continue to exist in the subsurface, the following conditions at least must be met:

1. There must be proper outlets and passageways for water moving in a basin.
2. There must be a difference in fluid potential to cause the water to move.

Although the second condition is usually considered, the first one tends to be overlooked by some hydrodynamics geologists. The validity of the conclusions made from these hydrodynamics studies in different parts of the world must, therefore, be re-examined.

Differential Entrapment

If both oil and gas are generated in the deepest parts of a sedimentary basin, and if the basin contains a series of connected structures or traps, gas will occupy the deepest (or fist) trap, and oil will spill out to the shallower traps. As shown in Fig. 38 (Gussow, 1954), if this process continues, we will find oil accumulated in the higher traps and gas in the lower.

Gussow listed many examples of differential entrapment of this type, but the same situations (deeper gas and shallower oil) may also be explained by the concept of stages of petroleum maturation (deep gas and shallow oil - see Chapter 7) and also possibly by differences in source-rock type (see Chapter 8).

Gill (1979) showed examples of differential entrapment in the Michigan Basin (Figs. 39 and 40). He denied the possibility in this basin that the observed partitioning between oil and gas is caused by differences in source type, depth of burial, or pressure and temperature (or maturation). He then concluded that, "... except for Gussow's theory, all the alternative explanations examined by the writer (Gill) were

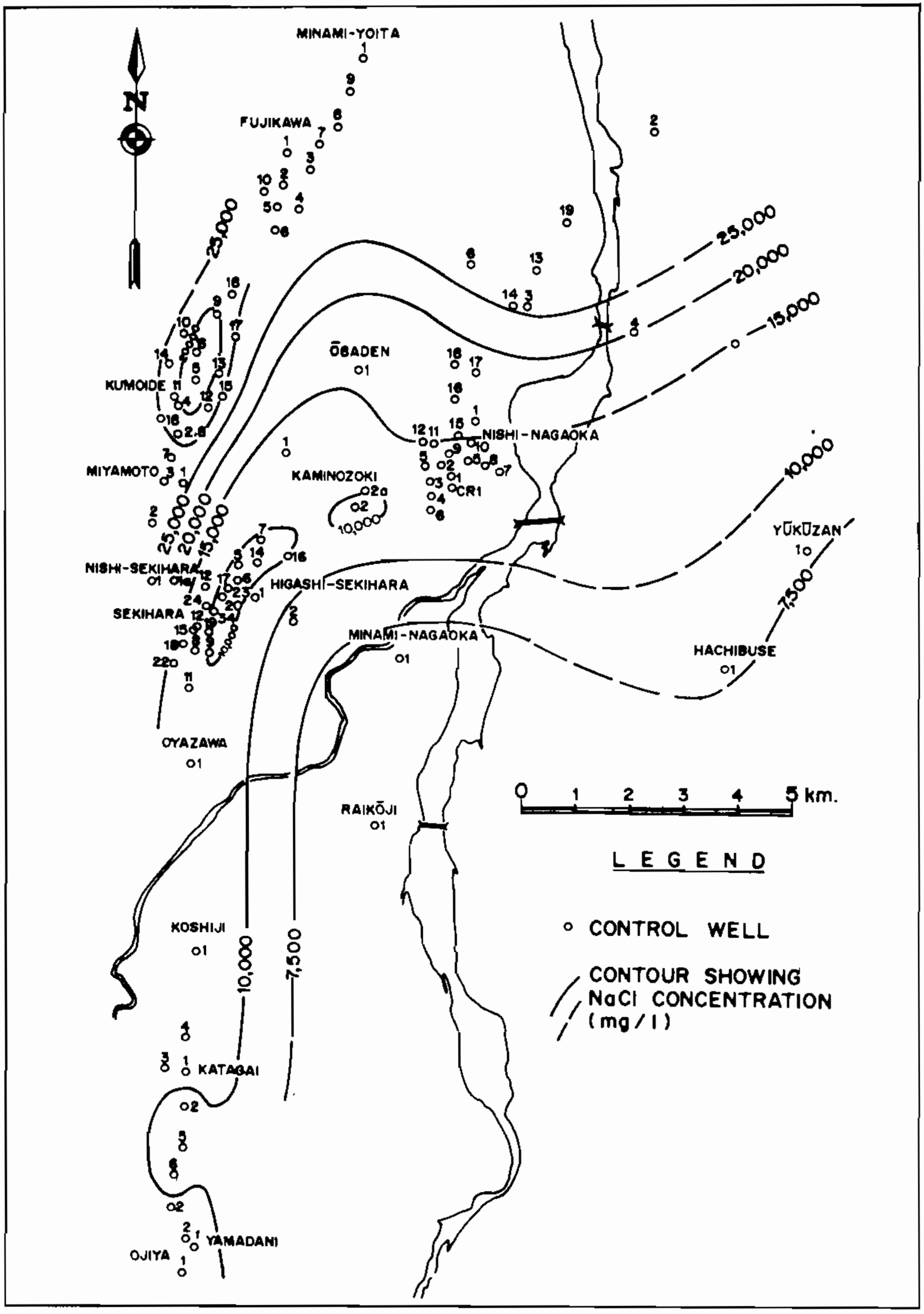

Fig. 37. Isoconcentration map (of NaCl) of Nagaoka agglomerate reservoir, Japan (Magara 1968). Courtesy of American Association of Petroleum Geologists.

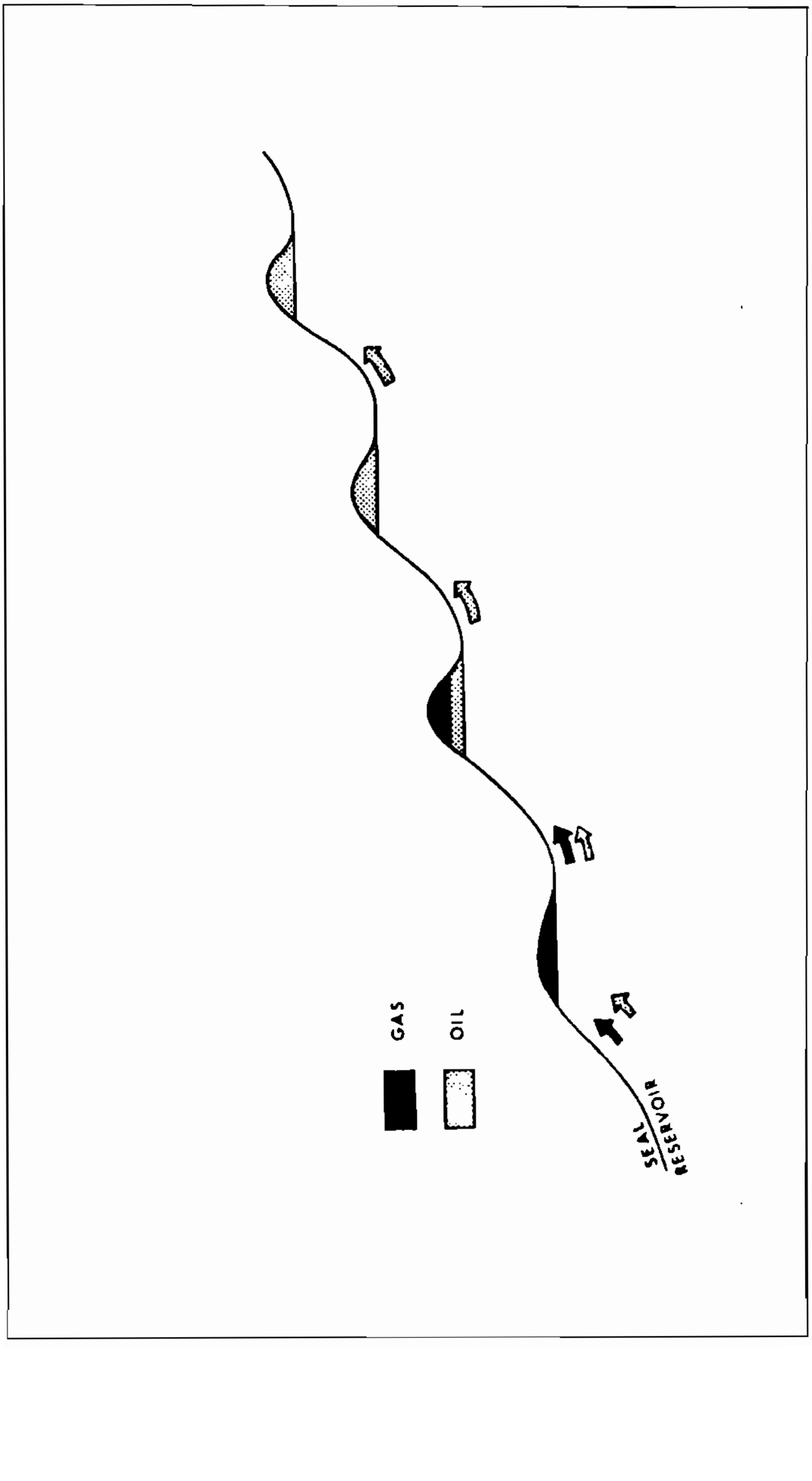

Fig. 38. Diagram showing structural differential entrapment of oil and gas. For series of traps that spill updip, gas will be differentially entrapped downdip from oil (from Gussow 1954). Courtesy of American Association of Petroleum Geologists.

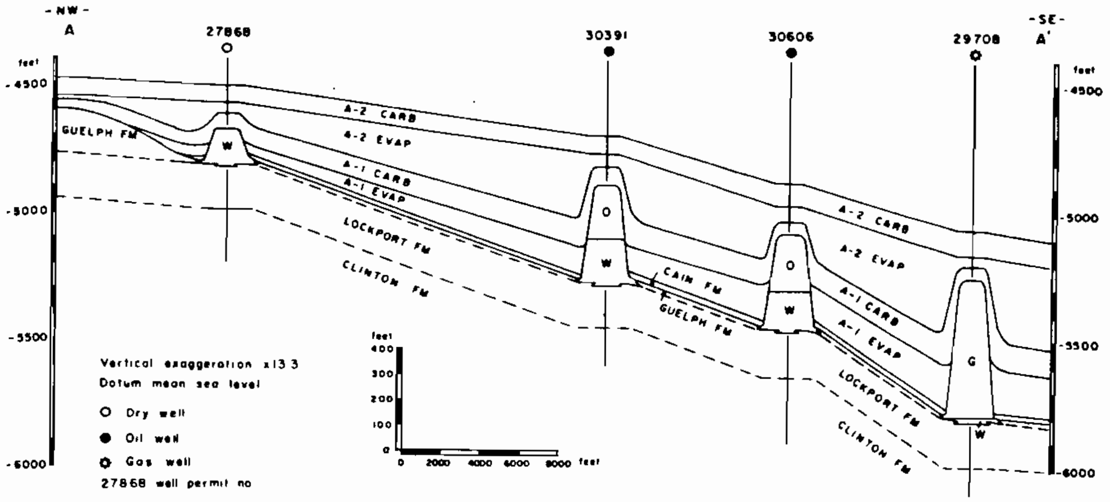

Fig. 39. Geologic cross section across pinnacle reef belt in Grand Traverse County, northern Michigan (W = water, O = oil, and G = gas). Gussow's differential entrapment concept seems applicable in this area (Gill 1979). Courtesy of American Association of Petroleum Geologists.

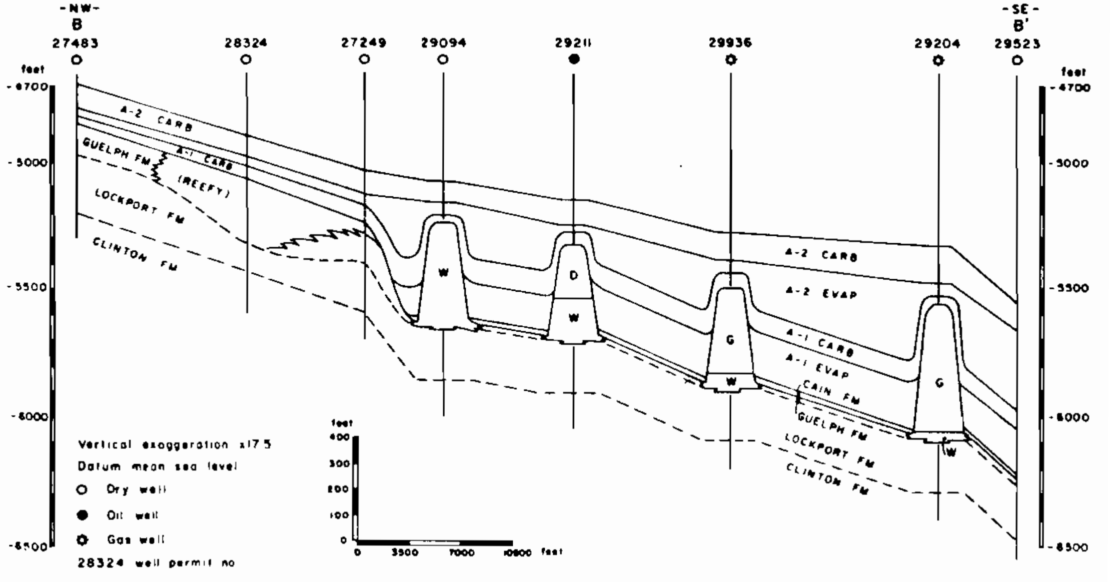

Fig. 40. Geologic cross section across pinnacle reef belt in Kalkaska County, northern Michigan. Symbols are same as in Fig. 39 (Gill 1979). Courtesy of American Association of Petroleum Geologists.

found to suffer from certain weaknesses, as they failed to account adequately for all the observations" (p. 617).

Schowalter (1979) recently postulated a different reservoir model in which a series of capillary pressure barriers tend to hold certain height of hydrocarbon columns (Fig. 41). When oil and gas are present as separate phases in a stratigraphic trap, gas will be at the upper part of the trap and will be trying to break through the barrier. The amount of oil leaking updip may be smaller than the amount of gas. As this type of migration process continues, the shallower traps may become saturated by gas, and the deeper traps by oil, as shown in Fig. 41. This is a situation exactly the opposite of the continuous reservoir depicted in Fig. 38.

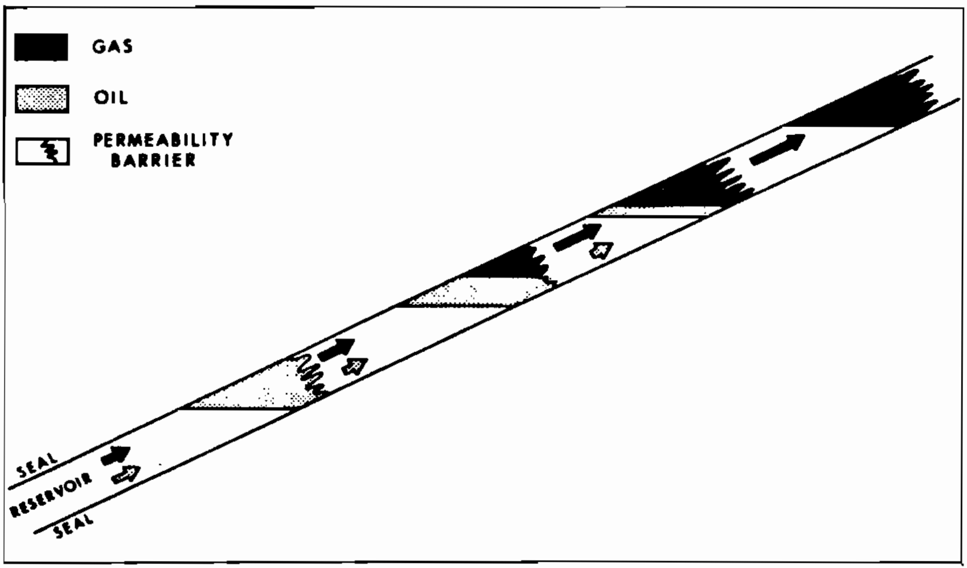

Fig. 41. Stratigraphic differential entrapment of oil and gas. For series of traps that leak updip, oil will be differentially entrapped downdip from gas (Schowalter 1979). Courtesy of American Association of Petroleum Geologists.

Problems

1. List four major differences of physical conditions between source rocks and reservoir rocks.
2. Describe the critical physical condition that hydrocarbon globules are able to move to a higher structural position.
3. Explain the hydrodynamics concept proposed by Hubbert (1953).
4. Explain the differential entrapment concept by Gussow (1954).

Chapter 6

Primary Hydrocarbon Migration

- Introduction. ■ Molecular solution.
- Micellar solution. ■ Oil-droplet expulsion.
- Importance of structured water in primary oil migration.
- Oil-film migration. ■ Compaction-fluid movement.
- Aquathermal fluid migration. ■ Osmotic fluid movement.
- Fluid movement due to clay dehydration.
- Generation of gas. ■ Capillary pressure.
- Buoyancy. ■ Diffusion. ■ Problems.

Introduction

Primary migration is defined as the movement of petroleum from nonreservoir and source rocks to reservoir rocks, and is distinguished from its concentration and accumulation into pools of oil and gas within the reservoir rocks, which is known as secondary migration.

At the stage of secondary migration, hydrocarbons are believed to migrate updip in the reservoir, primarily through buoyancy effect. Therefore, if the reservoir section is porous and permeable enough to allow the hydrocarbons to move, and if it has some structural relief, the hydrocarbons would be able to migrate updip and to concentrate into a pool within a trap. There must also be some density difference between hydrocarbons and formation water.

However, the discussion of primary migration must be conducted in a different manner. This is because hydrocarbons, at the time of primary migration, were probably disseminated in the form of small globules in fine-grained rocks, which would imply very little buoyancy. The capillary restrictions of fine-grained rocks, however, are relatively very large, so that movement of such small globules is considered by several investigators to be very difficult. If, on the other hand, most hydrocarbons are in solution in water, they could be quite free to move.

Regarding the form of hydrocarbons at the time of primary migration, there are basically three different possibilities : molecular solution, micellar solution, and a separate hydrocarbon phase.

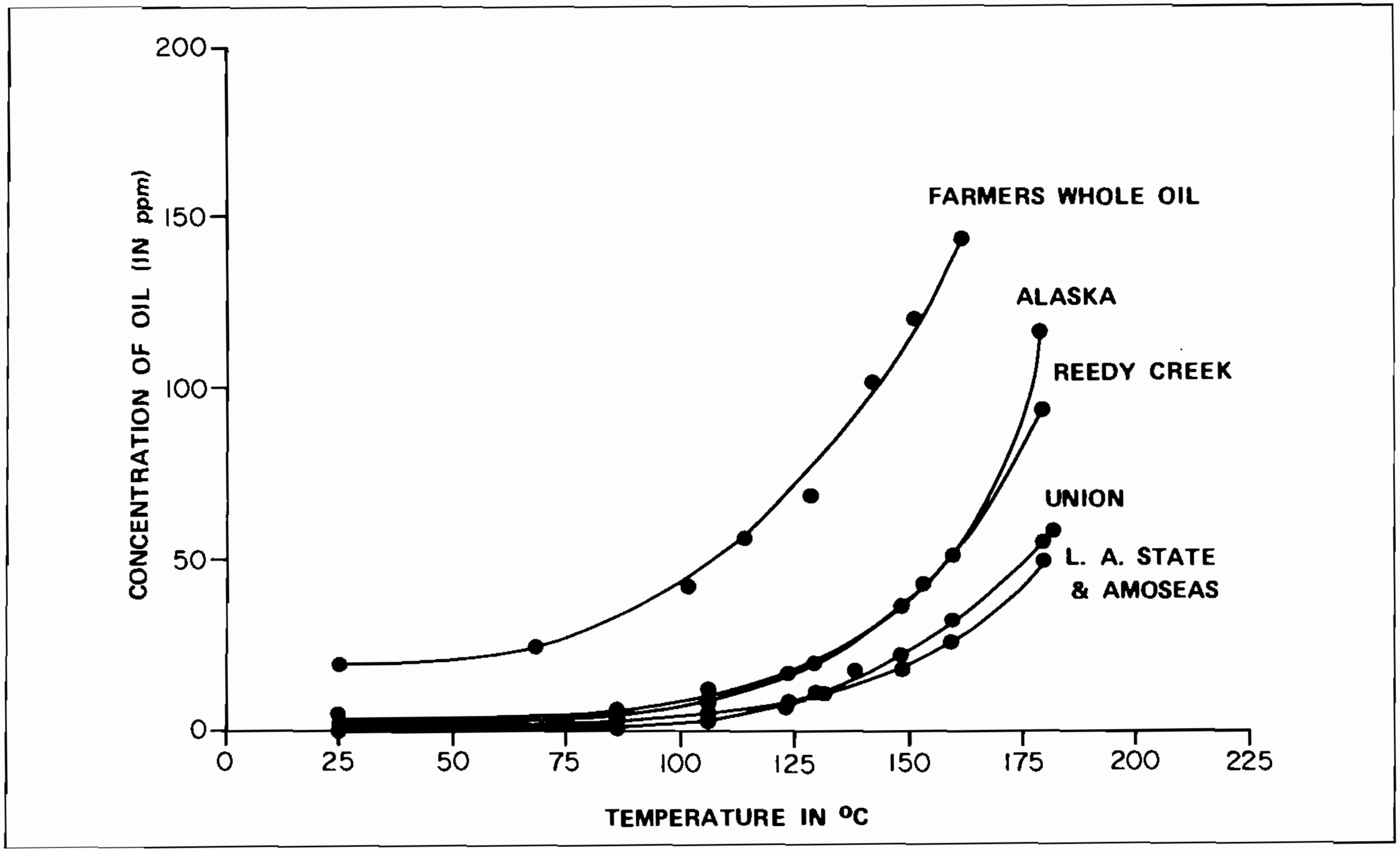

Fig. 42. Solubilities of two whole oils (Wyoming Farmers and Louisiana State) and four topped oils (Amoseas Lake, Reedy Creek, Alaska and Union Moonie) as functions of temperature in water. Topping temperature is 200°C (392°F) (from Price 1976). Courtesy of American Association of Petroleum Geologists.

Molecular Solution

If most hydrocarbons at the primary migration stage were in the form of molecular solution, there would be no capillary restrictions to movement. Hydrocarbons would thus be able to move either with movement of water, or by molecular diffusion without movement of water.

The molecular solubility of liquid hydrocarbons in water at relatively high temperatures was extensively studied by Price (1976). Figure 42 illustrates the results of Price's experiments. The highest solubility was observed with the Farmers whole oil sample in Fig. 42. The solubility of this oil at 160°C is approximately 150 ppm, and the curve shows an increasing tendency toward solubility with increasing temperature. These temperature values are much higher than the known range of 60 to 150°C for most oil accumulations (Magara 1977a).

On the other hand, Dickey (1975) stated that the flowing stream would have to contain at least 10,000 ppm of hydrocarbons at the time of primary migration, on the basis of his own estimate of the amount of migrating hydrocarbons in compaction fluid.

Magara (1977a) offered another approach to estimating the required concentration of oil in the flowing stream, using Tissot and Pelet's (1971) analytical data of amounts of hydrocarbons, resins and asphaltenes in Devonian shales in Algeria. Figure 43 shows the results in mg/g organic carbon. This figure shows that the amount of hydrocarbons decreases toward the reservoir, indicating primary hydrocarbon migration. On the other hand, the amounts of resins (NSOs) and asphaltenes in the shales remain relatively constant.

The difference in hydrocarbon concentration at the 14 m point and at the near-reservoir point is about 40 mg/g organic carbon. Within this short interval of 14 m, it would be reasonable to assume that the level of total hydrocarbon generation per gram of organic carbon is nearly constant. Therefore, we may be able to state that the 40 mg represents the lowest possible amount of hydrocarbons expelled per gram of organic carbon from the shale closest to the reservoir.

On the basis of the above estimate and the estimated amount of compaction water expelled, Magara (1977a) concluded that the amount of hydrocarbons in the flowing stream can be estimated to be at least 8,000 ppm. Vyshemirsky *et al.* (1973) made experiments with squeezing a mixture of clay, liquid hydrocarbons and water up to 300 atm. They found that the amount of hydrocarbons squeezed with water was much more than could be accounted for by solution mechanism alone.

From the above statement, it is obvious that the greater proportion of liquid hydrocarbons must have moved in their own phases.

Another difficulty in accepting solution as the principal mechanism for primary migration is that the composition of hydrocarbons accumulated in most pools usually cannot be related to the relative solubilities of the different classes of hydrocarbons.

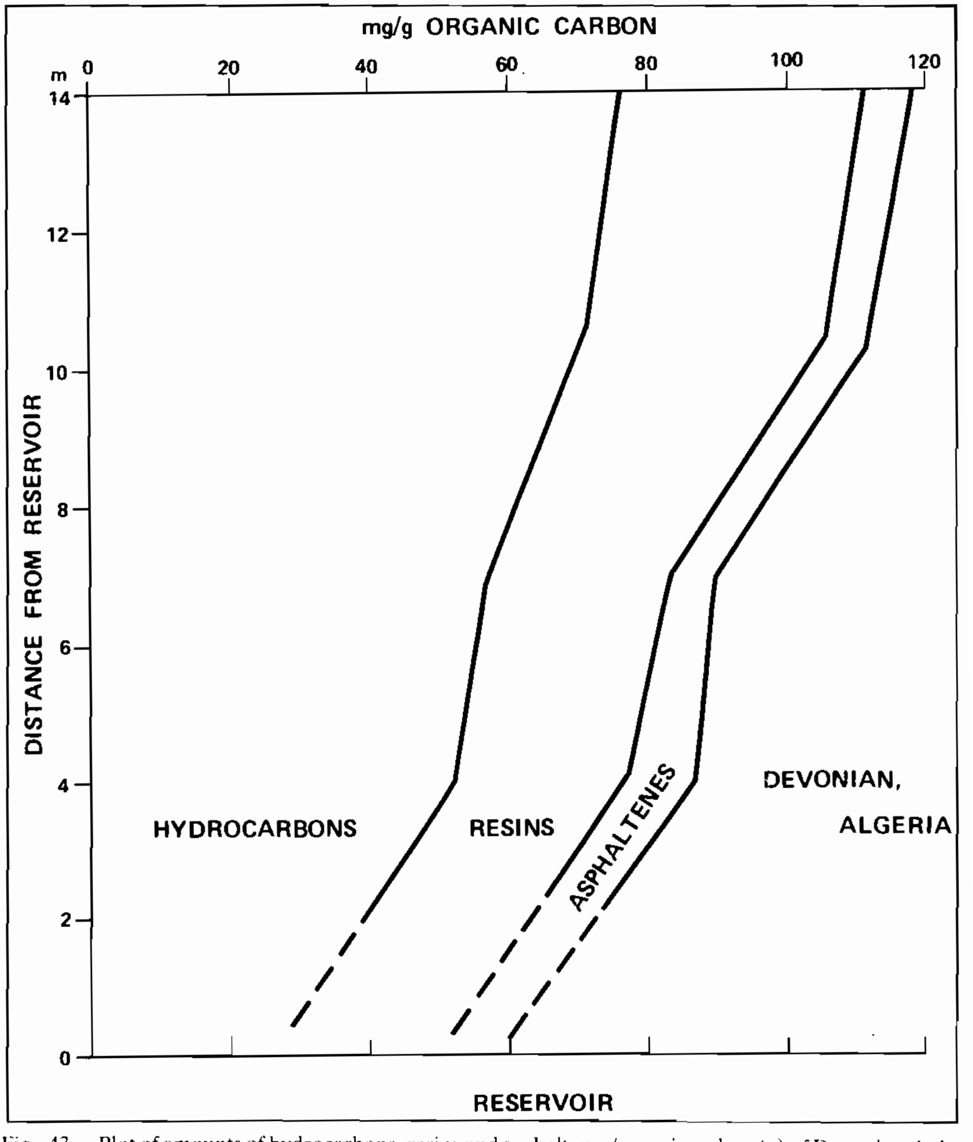

Fig. 43. Plot of amounts of hydrocarbons, resins and asphaltenes/organic carbon (g) of Devonian shales adjacent to reservoir in Algeria. Original data are derived from Tissot and Pelet (1971).

In other words, if solution were the principal mechanism for migration, the composition of accumulated hydrocarbons would have to be governed by the relative solubilities of the different kinds of hydrocarbons. However, the real subsurface data do not support this possibility.

McAuliffe (1978) stated that, " ... the water solubilities of hydrocarbons vary significantly with hydrocarbon class (alkanes, cyclo-alkanes, aromatics, etc.) and decrease markedly with increasing molecular weight within a class (Fig. 44). The relative composition of crude petroleum with respect to the relative water solubilities of petroleum hydrocarbons suggests that solution is not a reasonable migration mechanism."

As a matter of fact, Tissot and Pelet's (1971) geochemical data shown in Fig. 43 suggest that hydrocarbons were expelled preferentially over resins (NSOs) which are more soluble. Therefore, we may be able to conclude that molecular solution cannot be the principal mechanism for primary migration.

From the above observations and interpretation, we may be able to conclude that primary migration of liquid hydrocarbons is a matter of the exclusion of relatively insoluble but mobile material from source rocks.

In the case of primary migration of gas, however, the situation can be completely different. Fig. 45 (from Bonham 1978) shows that the solubility of natural gas in water at high temperatures is relatively high. If compaction water that is saturated with natural gas moves from a synclinal area where pressure is extremely high to the crest of an anticline where pressure is relatively low, a significant amount of gas must be separated in the latter area because of the lower solubility of gas there. I believe that most gas accumulations can be explained by this simple mechanism.

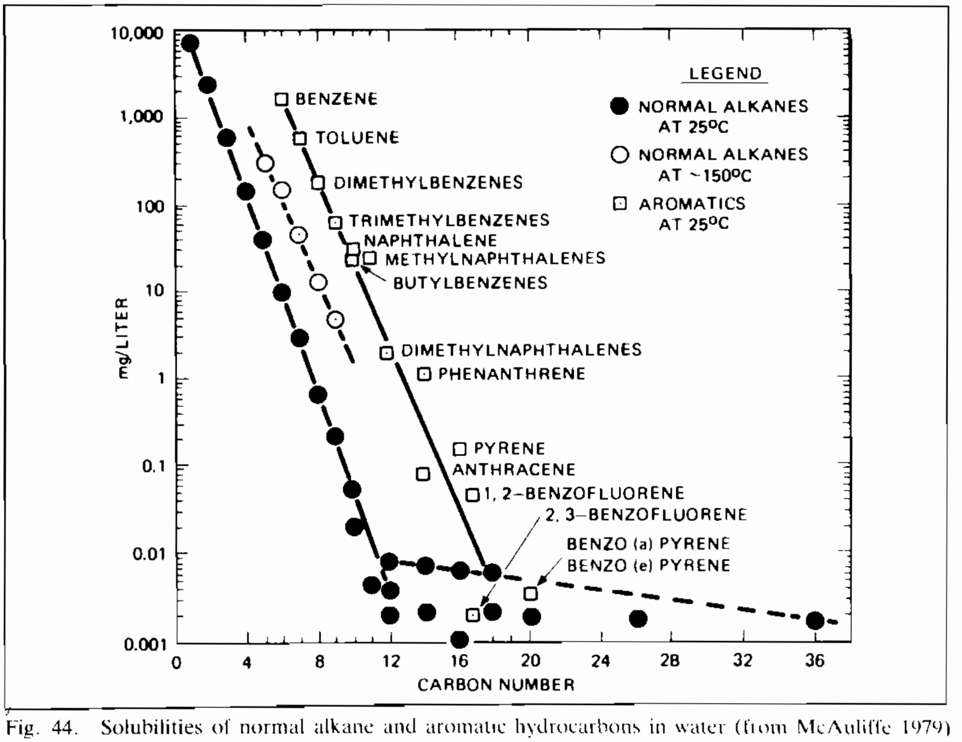

Fig. 44. Solubilities of normal alkane and aromatic hydrocarbons in water (from McAuliffe 1979) Courtesy of American Association of Petroleum Geologists.

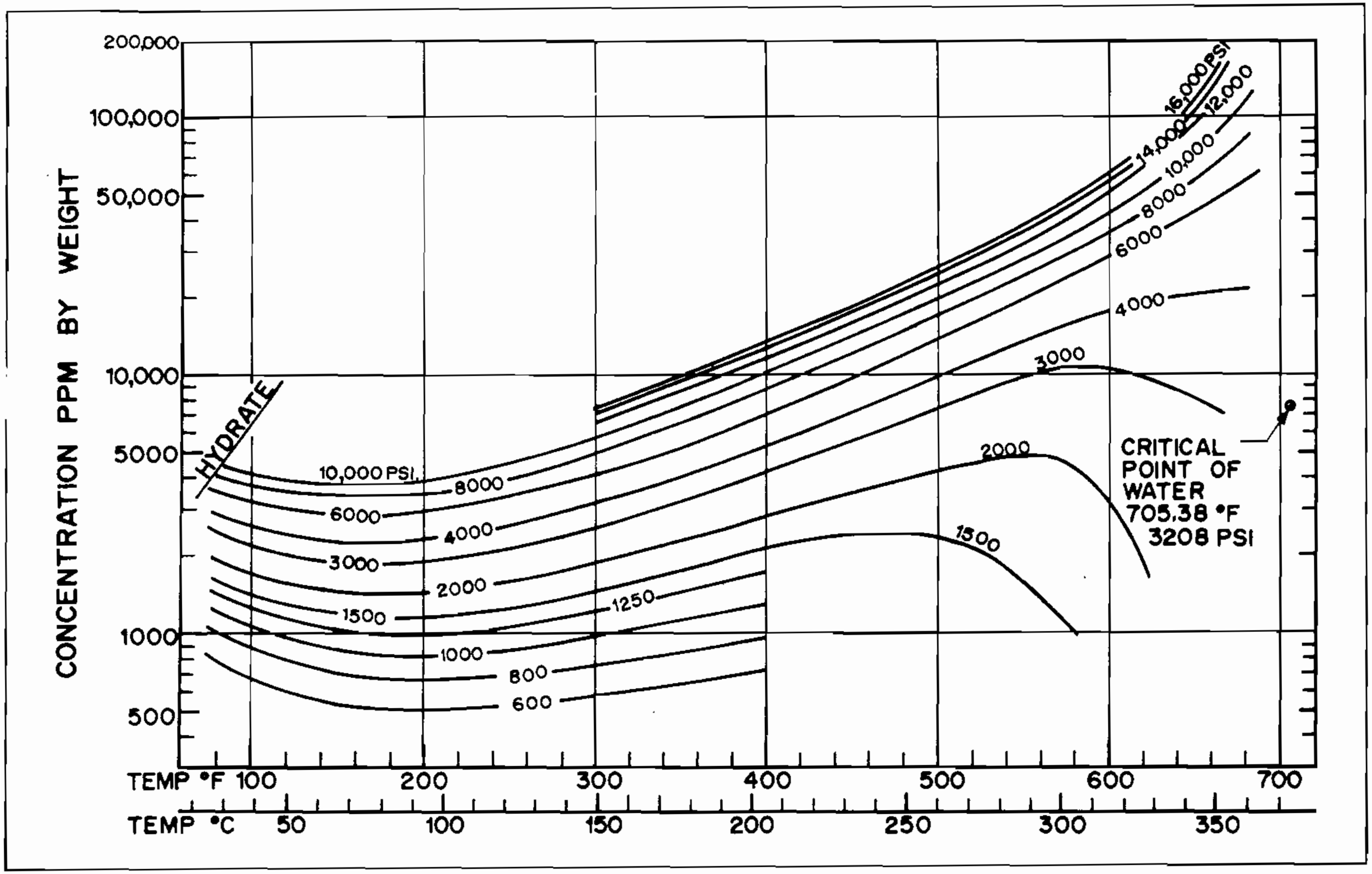

Fig. 45. Solubility of methane in water (from Bonham 1978). Courtesy of American Association of Petroleum Geologists.

Micellar Solution

Baker (1962) proposed another solution mechanism called micellar solution. He suggested that hydrocarbon solubility is substantially high if the water contains micelles formed by the soaps of organic acids. There are, however, several reasons for questioning the plausibility of Baker's proposal as the principal mechanism of hydrocarbon migration in the subsurface.

First of all, there is no evidence that such solubilizing micelles exist in significant quantities in shales. Even if they do exist in shales, they would not be able to move easily because these micelles are relatively large molecules. Second, the micelles may increase the solubility of the heavier hydrocarbons in water only to a few parts per million – nowhere near the 10,000 ppm or more that appears to be necessary (Dickey 1975). The third objection to accepting micellar solution as important in primary migration is that the process whereby the hydrocarbons carried by the fluid (water, micelles and hydrocarbons) are unloaded at the final trapping position in the reservoir cannot satisfactorily be explained.

Oil-droplet Expulsion

As mentioned earlier, the expulsion of oil droplets from shales has been believed by many geologists and geochemists to be an extremely difficult process; primarily because the basic concepts of capillary pressure were developed in coarse-grained reservoirs. Oils already trapped in these coarse-grained rocks cannot easily move upward into the overlying shales because of capillary restrictions by the shales, although there is usually significant buoyant force due to the density difference between the oil and the water. In other words, the movement of oil from coarse- to fine-grained rocks is very difficult.

However, primary migration occurs from fine- to coarse-grained rocks, so that the capillary pressure difference may have helped the movement of the oil droplets. Nevertheless, for an oil droplet to have moved within the fine-grained source rock may still be considered very difficult.

According to Berg (1975), capillary pressure, P_c is given as :

$$P_c = 2\gamma\left(\frac{1}{r_t} - \frac{1}{r_p}\right) \tag{11}$$

where γ is the interfacial tension between oil and water, r_t the radius of pore throat (see Fig. 46), and r_p the radius of pore space (see Fig. 46).

Berg (1975) stated that, " ... natural aggregate may approximate a rhombohedral packing of uniform spheres in which pore sizes are 0.154D, 0.225D, and 0.414D, where D is sphere diameter" (Graton and Fraser 1935). Then he went on : " ... the migration path through the aggregate is by means of alternate pores of diameter 0.225D and 0.414D that are connected by pore throats of diameter 0.154D" (Fig. 47).

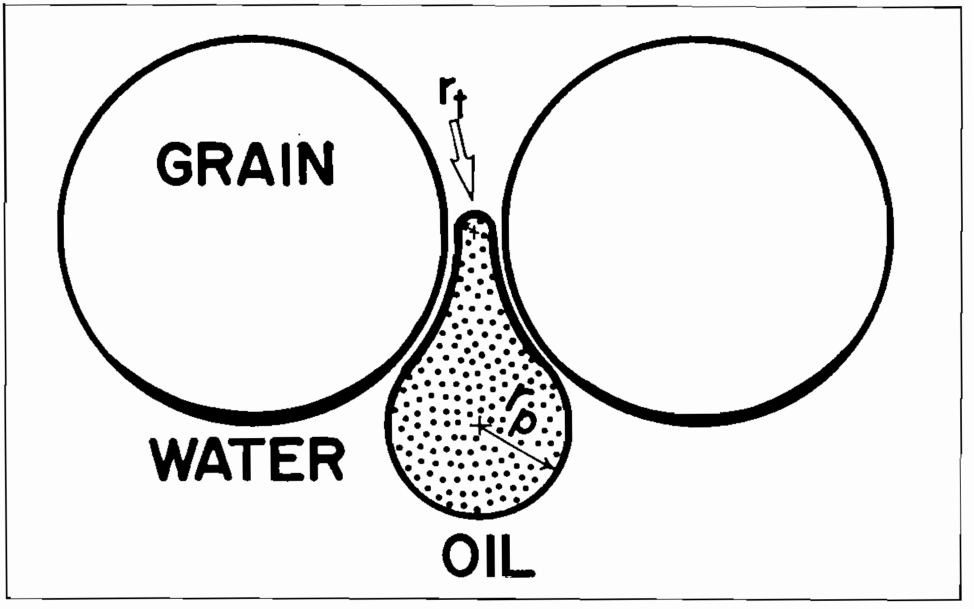

Fig. 46. Schematic diagram showing an oil droplet in sandstone reservoir. Symbols, r_t and r_p, represent radii of porethroat and porespace, respectively.

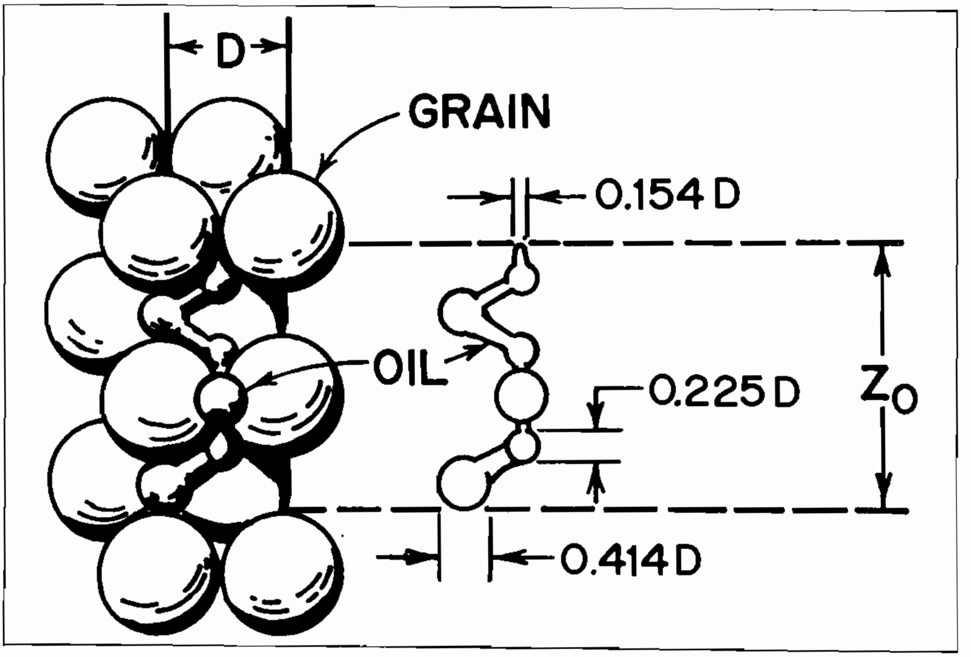

Fig. 47. Schematic diagram of globules connected through pores in rhombohedral packing of uniform spherical grains where D is grain diameter and porosity is 26 per cent (Berg 1975). Courtesy of American Association of Petroleum Geologists.

Therefore, we may be able to define r_t and r_p in equation (11) as follows (Berg 1975) :

$$r_p = \left(\frac{1}{2}\right)(0.414D) \tag{12}$$

$$r_t = \left(\frac{1}{2}\right)(0.154D) \tag{13}$$

where D is the grain diameter.

By introducing equations (12) and (13) into equation (11), Berg obtained :

$$P_c = \frac{16.3}{D} \cdot \gamma \tag{14}$$

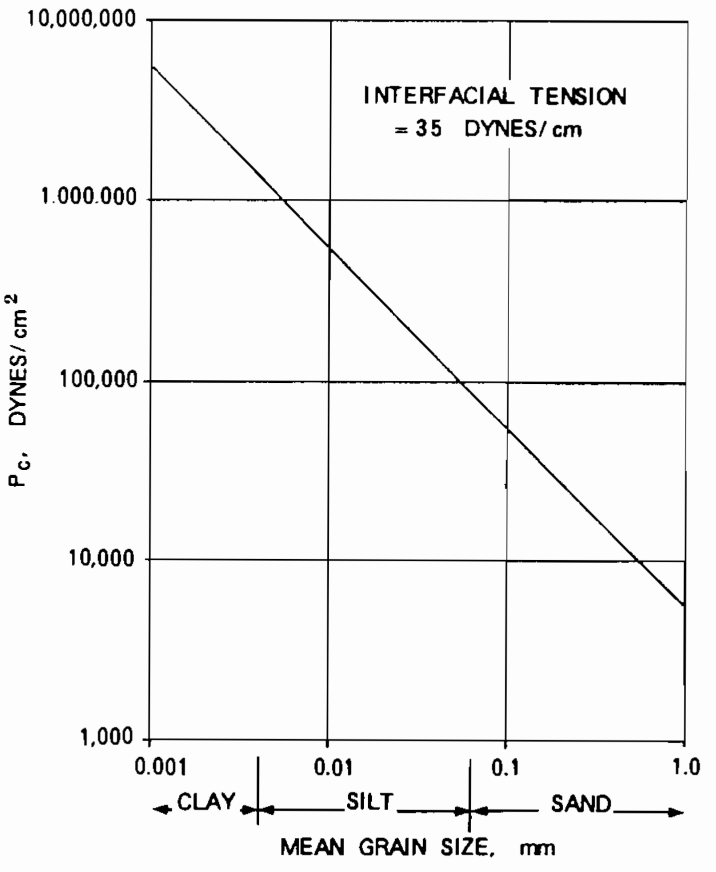

Fig. 48. Graph showing relationship between capillary pressure, Pc, and mean grain size of rhombohedrally packed spheregrains. Interfacial tensions is assumed to be 35 dynes/cm.

Equation (14) means that capillary pressure increases as the mean grain diameter decreases. Fig. 48 shows the relationship between calculated capillary pressure, P_c, in dynes/cm^2, and mean grain size, based on the above assumptions and equation (14). The relationship shown in Fig. 48 may be used to conclude that, on the basis of the model described above (Figs. 46 and 47), movement of an oil bubble in fine-grained rocks is an extremely difficult process.

Although the previous model seems to represent adequately a condition in a coarse-grained reservoir rock, it may not be a reasonable model in fine-grained rocks.

Figure 46 shows an oil bubble whose top end has a radius smaller than that of the bottom end. The difference in these two radii can cause a significant capillary pressure in fine-grained rocks (equation 11 and Fig. 48). However, if the radius of the bottom end is reduced by some physical force and if r_p becomes nearly equal to r_t in equation (11), the capillary pressure, P_c, will approach zero, or

$$P_c \rightarrow 0$$

when

$$r_p = r_t$$

As suggested by Hobson in 1954, the distortion of a small oil droplet in shales may be accomplished by the rearrangement of grains associated with compaction. If the water in shales is mostly structured or semisolid, such distortion of the oil droplet can occur even more easily, because the droplet interfaces with solid and semi-solid materials only in shales.

An analogy to this situation is toothpaste (oil) in an aluminum tube (grains and structured water). By squeezing the aluminum tube, we can change the shape of the toothpaste in any way we wish. We can also squeeze the toothpaste out of the tube quite easily.

On the other hand, if the tube contains a large quantity of water (liquid) with a small amount of toothpaste (oil), changing the shape of the toothpaste is not as easy as before. Although squeezing the water out is easy, the toothpaste cannot be readily pushed out until the water is almost completely drained from the tube, or until the toothpaste interfaces directly with the tube.

More recently, McAuliffe (1979) stated that "... oil and gas are generated in, and flow from (kerogen) network" (p. 761). He believed that oil or gas flowing in this network would not be subject to interfacial tension.

It is, however, doubtful that such a continuous network of organic matter is developed, because of the relatively low concentration of the organic matter (on the order of a few per cent of less) in most source rocks.

Importance of Structured Water in Primary Oil Migration

Figure 49 shows plots of the density and viscosity of bound or structured water in montmorillonite derived from Martin (1962) and Low (1976). Both density and viscosity increase as the amount of water in the clay decreases. In other words, density and viscosity would increase as clays or shales compacted.

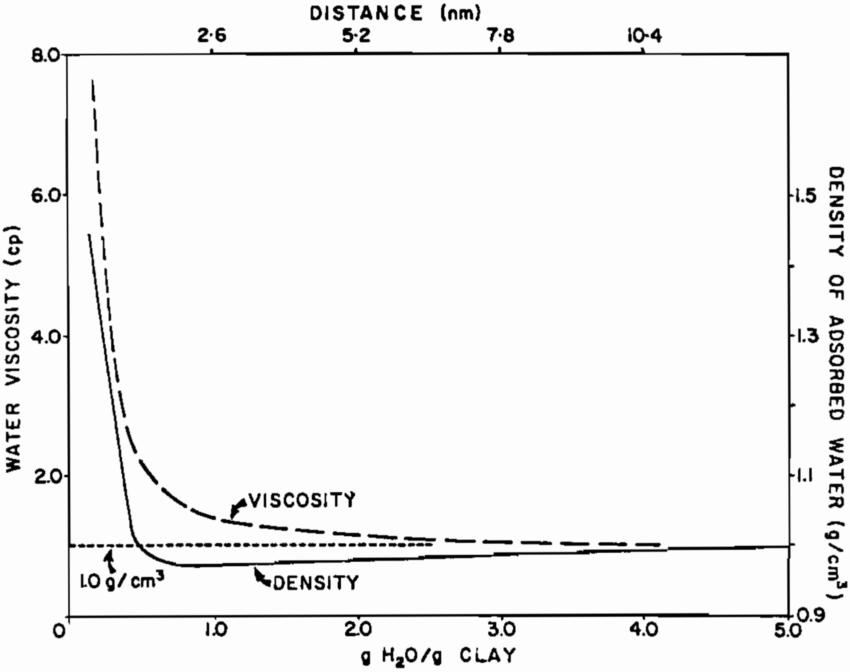

Fig. 49. Density and viscosity of adsorbed or structured water in montmorillonite. Data are derived from Martin (1962) and Low (1976).

Dickey (1975) recently proposed the importance of the presence of structured water in primary oil migration, with the backing of a wide variety of current knowledge on shale pore-water chemistry and physics, shale pore-space geometry, fluid flow , etc. Using the concept of relative permeability in sandstones, he stated that, "... oil will move along with the water only if it occupies about 20 percent or more of the pore volume" (p. 341). Dickey also guessed that the residual-oil saturation in shales may be less than 10 per cent and possibly as low as 1 per cent, because a considerable fraction of the internal surfaces of shales can be oil-wet (p. 342).

Figure 50 illustrates a schematic relationship of the relative permeability and oil (or water) saturation. The critical residual-oil saturation is indicated by an X. The figure for X in shales may be between 10 and 1 per cent. If this critical oil saturation is exceeded, oil can flow along with water. If, for example, the oil saturation is at X′, a small amount of oil will move with a large quantity of water.

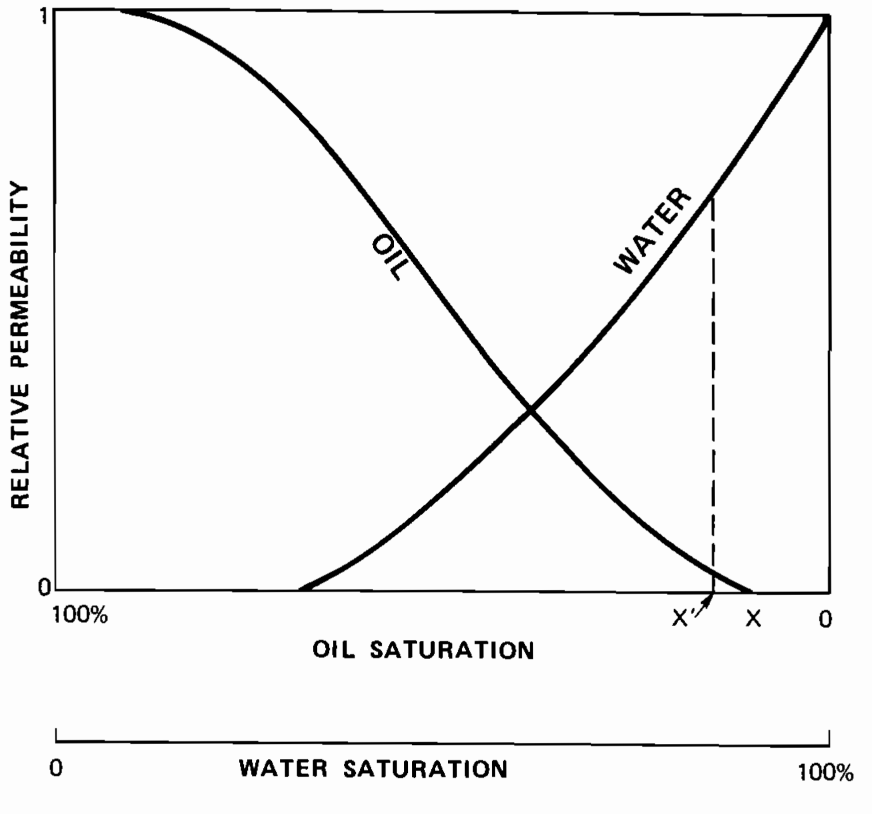

Fig. 50. Schematic diagram showing relative permeability - water (or oil) saturation relationship for sandstone (Magara 1978a). Courtesy of Canadian Society of Petroleum Geologists.

On the basis of the above concepts, Magara (1978a) stated that, "if, for example, the oil saturation in the total water (solid and liquid) is 100 ppm (0.01 wt%), and if only 1 per cent of the water is in liquid phase (and 99% is solid), the oil saturation in the liquid water will be 10,000 ppm (1 wt%)". Assuming that the density of oil is 0.8 g/cm^3 and that of water 1 g/cm^3, this figure will correspond to about 1.2 vol. per cent. After some liquid water is expelled with or without a small amount of oil, then the saturation of oil in the liquid phase in the shale pores will increase, causing more oil migration. As the liquid water is further expelled as the shales compact, the absolute permeability will be reduced to an extremely low level and movement of the total fluids (water and oil) may eventually become very difficult.

Figure 51 depicts the possible variation in oil saturation as liquid water is gradually removed. The two diagonal lines refer to the original oil concentration of 10 ppm and 100 ppm, respectively, when the liquid water occupies 10 per cent of the bulk shale volume.

If the liquid water is continuously expelled to the level of 0.01 per cent remaining (there would be a lot of structured or semisolid water left in the shales), the respective oil saturations in the liquid phase will become 10,000 ppm (1 wt %) and 100,000 ppm (10 wt %). The corresponding volume percentages are about 1.2 and 12 per cent, respectively. The oil may move along with the water at this stage.

To simplify a complicated problem, the above discussions have assumed that the boundary between the semisolid and liquid waters is clearcut. However, in the actual shales, the change from liquid water phase to semisolid phase is considered to be quite gradual as depicted in Fig. 49.

Based on the theoretical consideration of specific surface area of montmorillonite, Magara (1978a) estimated that about 40-50 per cent of the montmorillonite clay or shale would be relatively structured. Fig. 52 shows the lines marking 40 and 50 per cent water added to Dickinson's (1953) shale porosity-depth relationship for the Gulf Coast. This figure shows that the 40-50 per cent porosity level of shales can be attained at relatively shallow depths, such as those of 500 to 1,000 ft. In other words, the critical compaction level at which the amount of liquid water becomes extremely small, facilitating possible oil-phase migration, would be reached at a very shallow depth – at which stage there may not have been enough oil generated to enable any effective oil migration.

As suggested by Van Olphen's (1963) experiments, if the structured water is not effectively removed by overburden pressure alone, the compaction of montmorillonitic shale may have to terminate entirely. In the actual subsurface, however, it does not, because heat may help release some of the relatively structured water. Also, some of the relatively less structured water may be expelled hydraulically if the threshold pressure is exceeded.

We commonly observe the gradual decrease of porosity with depth within normally compacted sections, which implies that water has been expelled from the shales one way or another. In order to keep this relatively small amount of liquid water in shale, the liquid water generated must be expelled effectively over a period of geologic time. In other words, generation of liquid water and its expulsion must take place hand in hand. Good drainage is a necessary condition. If the heat generates liquid water, but that water cannot move out and thus stay in shale pore spaces, the concentration of oil in the liquid phase will become very small.

The latter situation may be observed in the deep, undercompacted shales of many relatively young sedimentary basins, in which most of the structured water in montmorillonite has become relatively free pore-water because of the possible clay-

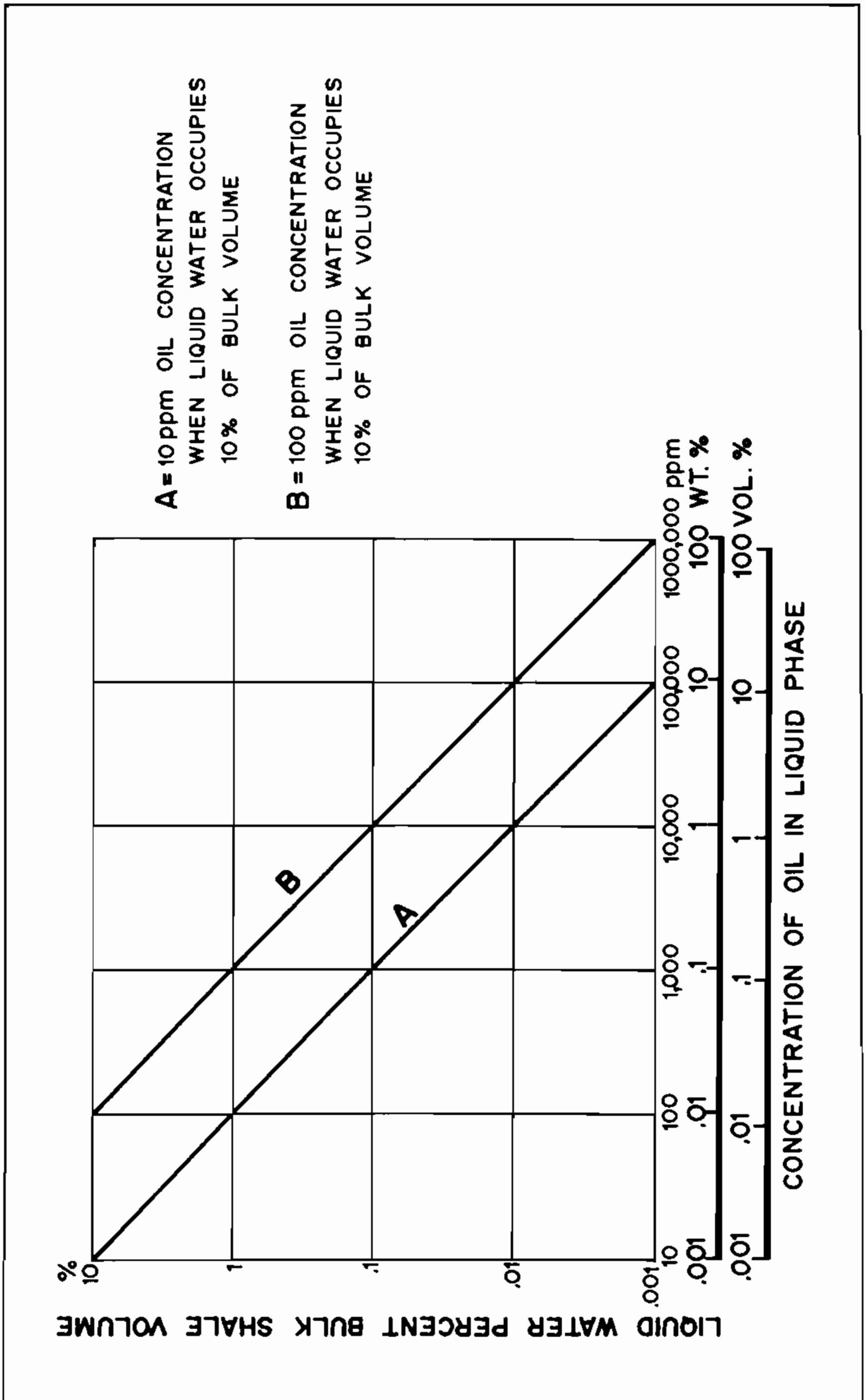

Fig. 51. Graph showing increasing tendency of concentration of oil in liquid phase as liquid-water per cent in shale decreases, assuming no oil migration (Magara 1978a). Courtesy of Canadian Society of Petroleum Geologists.

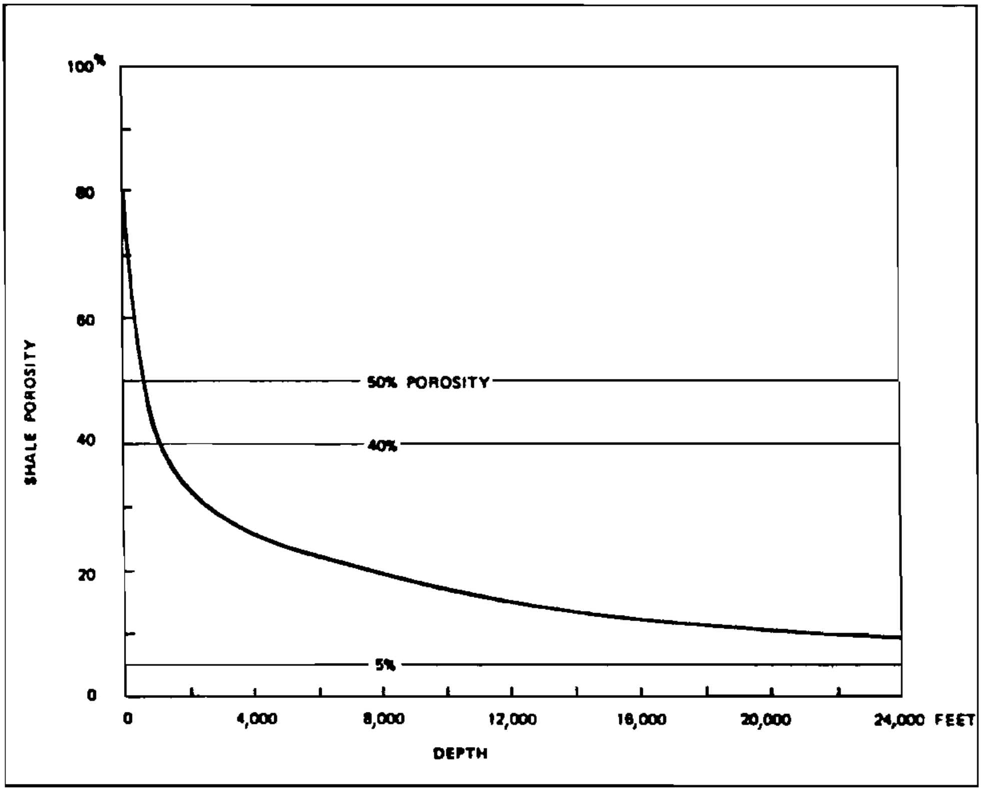

Fig. 52. Shale porosity - depth relationship in Gulf Coast by Dickinson (1953). 5% porosity line represents possible semisolid or structured water per cent in illitic shales and 40-50 per cent porosity zone indicates such in montmorillonitic shales (Magara 1978a). Courtesy of Canadian Society of Petroleum Geologists.

mineral conversion from montmorillonite to illite by relatively high temperature (Burst 1969). However, in these deep undercompacted shales, the liquid water generated seems not to have been expelled for lack of good permeable zones. Fluids may still be moving through these massive shales at an extremely slow rate, but effective migration in the oil phase is not likely because the oil saturation in the liquid phase is so low. A small amount of oil may, however, move in solution in water even in such massive shales.

We may thus be able to conclude that, to have effective primary migration of oil in the oil phase, most of the liquid water available in the shales must be expelled effectively to maintain a relatively high oil saturation in the liquid phase. The longer the sediments maintain effective drainage, the greater the chances of primary oil migration, other geological and geochemical conditions being equal. This may explain why most oil pools have been discovered in relatively low-pressure zones (Timko and Fertl 1971), where drainage conditions are considered to have been excellent.

On the basis of the above concepts, Magara (1978a) proposed a model for primary migration in the oil phase, as shown in Fig. 53. The top diagram shows a schematic of relative permeability vs. degree of shale compaction. As the shale compacts the relative permeability to water decreases and that to oil increases. Nevertheless, even with this increased relative permeability to oil, the absolute permeablity of the shale will continually decrease as the shale becomes more compacted (middle diagram in Fig. 53). Assuming that the pressure gradient in the shale remains relatively unchanged during compaction, oil migration in the oil phase will reach its maximum at an intermediate, not a late, compaction stage. After the intermediate compaction stage, oil-phase migration will decline as the absolute permeability of the shale decreases (bottom diagram, Fig. 53).

With our current knowledge of primary oil migration, it is not possible to pinpoint the time of most effective migration, which depends on the physical, chemical and geological conditions described above. Using the previously described model, we may be able to state that primary oil migration can occur at a relatively early or intermediate stage of burial after the generation of a significant amount of oil.

Another approach to estimating time of primary oil migration is based on the subsurface observation of different kinds of water, such as lattice, structured, and free pore-water, derived from a cross plot of the shale porosities from sidewall neutron and formation-density logs (Youn 1974). Youn studied shale samples from several wells in the Beaufort Basin, Canada. The mathematical relationship determined by the least-squares method is as follows :

$$\phi_{SNP} = 7.65 + 1.14 \cdot \phi_{FDC} \tag{15}$$

where ϕ_{SNP} is shale porosity from sidewall neutron log in %, and ϕ_{FDC} shale porosity from formation-density log in %.

This relationship is shown by a thick diagonal line in Fig. 54. The bulk-density scale is also shown along with the porosity scale at the bottom of the diagram. The porosity/bulk-density relationship is determined on the basis of matrix density of shales being 2.72 g/cm^3 and water density 1.00 g/cm^3 (Youn, 1974).

The equal-porosity relation (porosities from both neutron and density logs are identical) is shown by a thin diagonal line ("EQUAL POROSITY LINE") in Fig. 54. In comparing Youn's empirical relation with the equal-porosity line, we realize that the porosity determined from the neutron log is 8-20 per cent higher than that from the density log.

This difference may be explained by the fact that the neutron log reads all the hydrogen atoms as porosity while in the density log the porosity is calculated on the basis of the matrix or grain density being 2.72 g/cm^3. Shale matrix or grains usually contain some lattice water (mainly OH water) which is part of the clay minerals.

In short, porosity from the neutron log indicates the total of the lattice, structured

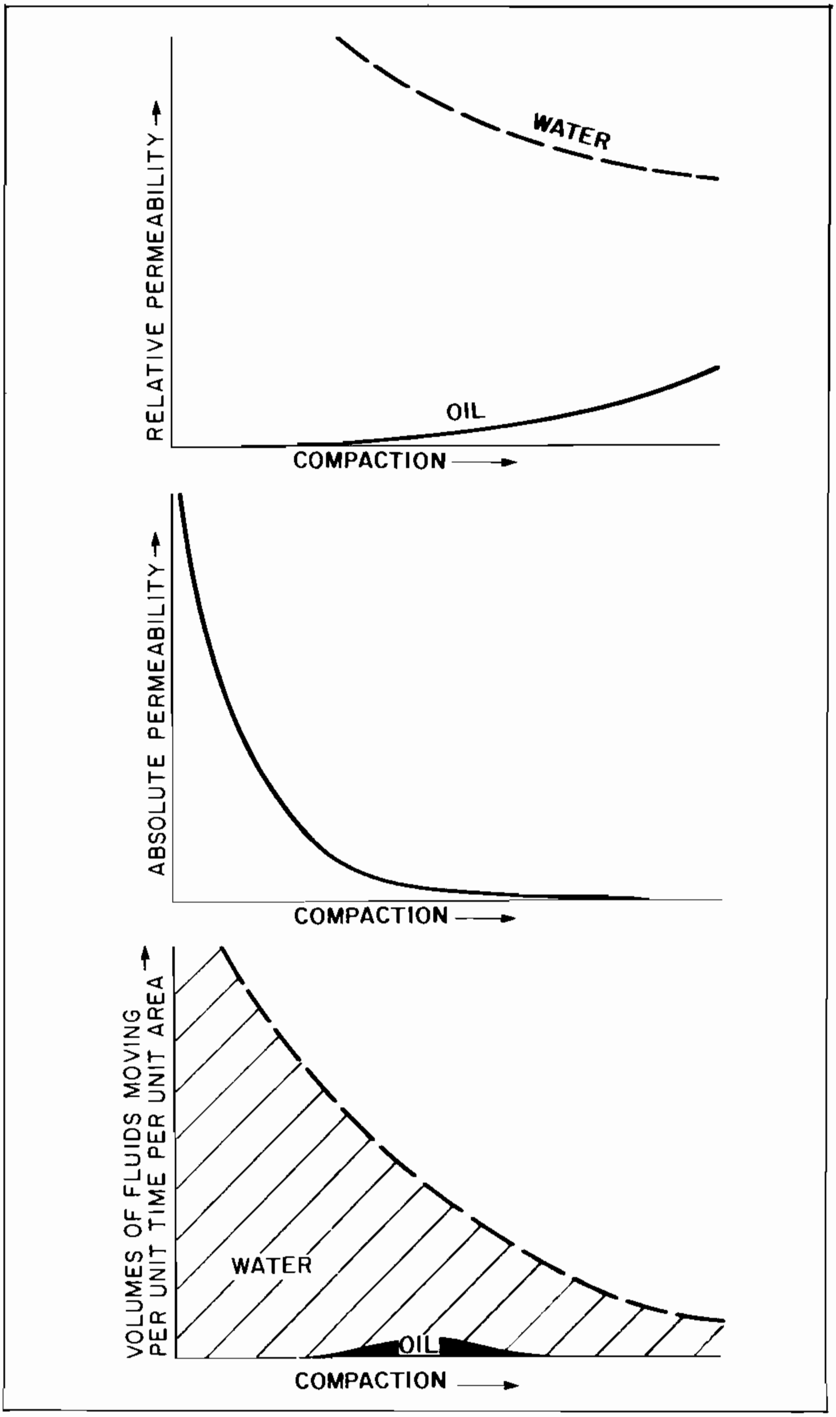

Fig. 53. Hypothetical relationships of relative permeability, absolute permeability, and fluid movement to degree of compaction (from Magara 1978a). Courtesy of Canadian Society of Petroleum Geologists.

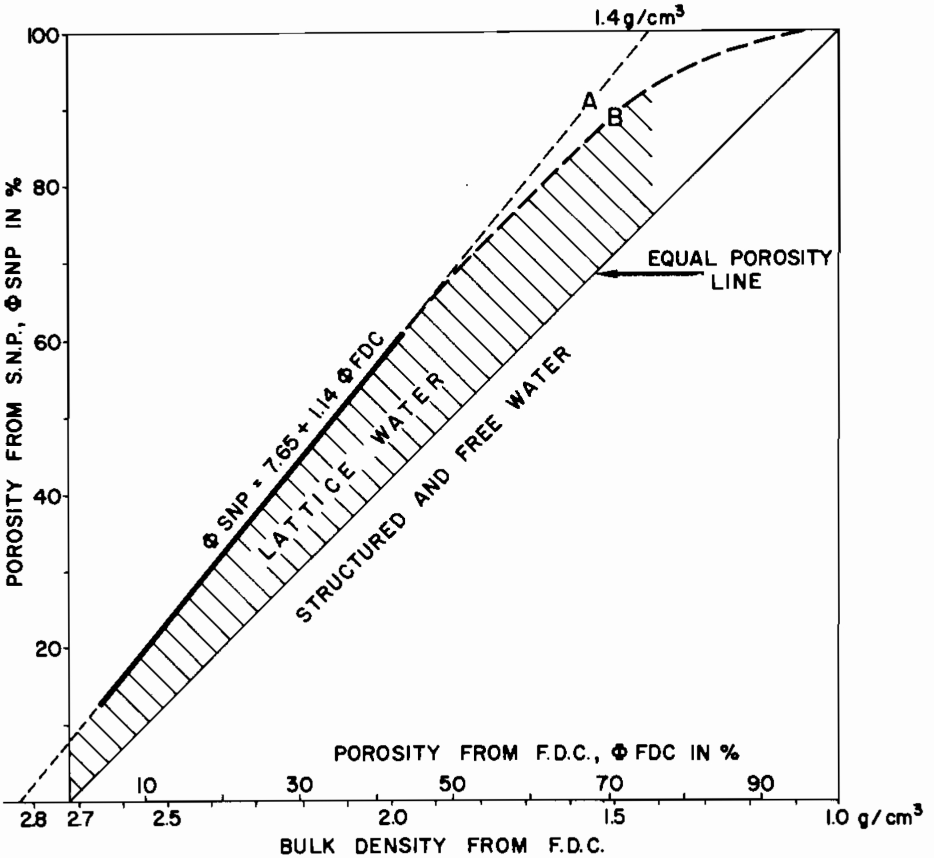

Fig. 54. Porosity cross plot of Beaufort shales, Canada, from sidewall neutron and formation density logs. Data from Youn (1974).

(or bound) and relatively free pore waters, but porosity derived from the density log includes bound and free pore waters only.

The empirical relationship is extrapolated to the upper end of Fig. 54 as shown by a dashed line A. The density corresponding to 100 per cent neutron porosity is approximately 1.4 g/cm^3. It is quite interesting to note that this (lattice) water density figure (1.4 g/cm^3) is almost the same as the highest bound-water density shown in Fig. 49. In other words, the density of water closest to the clay surface (bound water) seems to be quite similar to the density of water within the clay minerals (lattice water).

Although an extrapolation of Youn's empirical relationship by a straight line (A) may indicate the density of lattice water, the actual relationship at a higher porosity range ($>$ 50%) of clays or shales may be shown by a curved dashed line (B). This is because, when porosity is truly 100 per cent or there is 100 per cent water, both logs must read the same porosity (100%). Therefore, the relationship must be connected to the 100 per cent porosity point.

In Fig. 54, the empirical porosity relation is extrapolated to 0 per cent neutron porosity as well. The density corresponding to this point is about 2.84 g/cm^3, which is considered to be the density of clays or shales without lattice water (dry clay or shale density).

Although the hypothetical line (B) is drawn in the porosity range of 50 and 100 per cent, in the actual subsurface and surface clay porosity greater than 80 per cent may not exist. Therefore, the possible range of clay or shale porosity may be between 80 and 0 per cent.

Figure 54 shows that, in the very early stages of compaction (F.D.C. porosity 80-50%), the amount of lattice water shown by the shaded area is unchanged; compaction is caused primarily by the expulsion of free water at these stages.

In the intermediate and later stages of compaction (F.D.C. porosity 50-0%), the amount of lattice water shown by the shaded area in Fig. 54 decreases with compaction. This decrease may suggest that at these stages chemical and mineralogical changes of shales take place in addition to mechanical compaction and fluid expulsion, and even that some lattice water may be converted into other forms of water (bound and free).

Martin's (1962) density relation and Low's (1976) viscosity relation are transferred to the porosity cross plot in Fig. 55. The density and viscosity lines in Fig. 55 intercept the bottom axis (porosity from F.D.C.) at different porosity values, suggesting that as the shales compact, they must expel more dense and viscous water.

Because of the worldwide evidences of the tendency of shale porosity to decrease with depth (Fig. 56), it may be stated that even the viscous water was expelled from shales one way or another. Relatively high temperatures in the subsurface may have helped the shales to move the water by reducing viscosity slightly.

The rate of expulsion of water, however, slows down with depth, as is observed from the porosity-depth curves for different parts of the world (Fig. 56). This slowdown may suggest that as shales become more compacted, the viscosity of the water they contain continues to increase, despite the higher subsurface temperatures.

It is known that both the density and the viscosity of oil decrease with increasing burial depth or subsurface temperature (Levorsen 1967). We may thus be able to conclude that, at the earliest stages of oil generation, the viscosity of the oil may be greater than that of the water being expelled. At these earliest stages, the water may be preferentially expelled, leaving the viscous oil behind. At some point in the compaction history of shales, the viscosity of the oil may become less than that of the water then being expelled. This is because the viscosity of the oil decreases continuously with burial depth while that of the water being expelled increases continuously (Fig. 55).

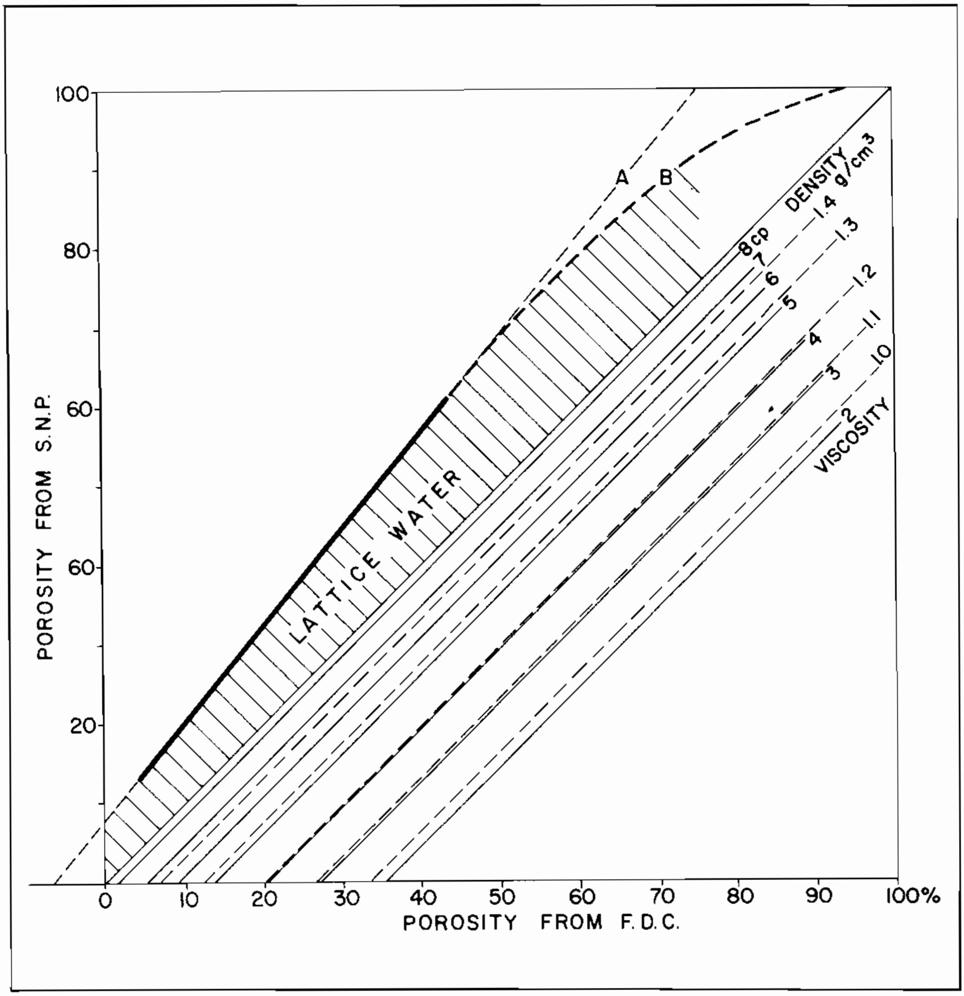

Fig. 55. Porosity cross plot of Beaufort shales, Canada, combines with possible variations of density and viscosity of structured or absorbed water.

When this critical level of burial depth or compaction is reached, the oil may flow preferentially, resulting in significant primary oil migration.

Oil-film Migration

The permeability of shales in the direction parallel to the bedding planes is much greater than in the perpendicular direction. A number of investigators also believe that, if oil migrates in its own phase, the oil phase must be continuous. Reasoning from these two basic ideas, several geologists and geochemists proposed that oil will migrate as a thin film in the souree rocks. The principal direction of primary oil migration in this case would, therefore, be parallel to the bedding planes.

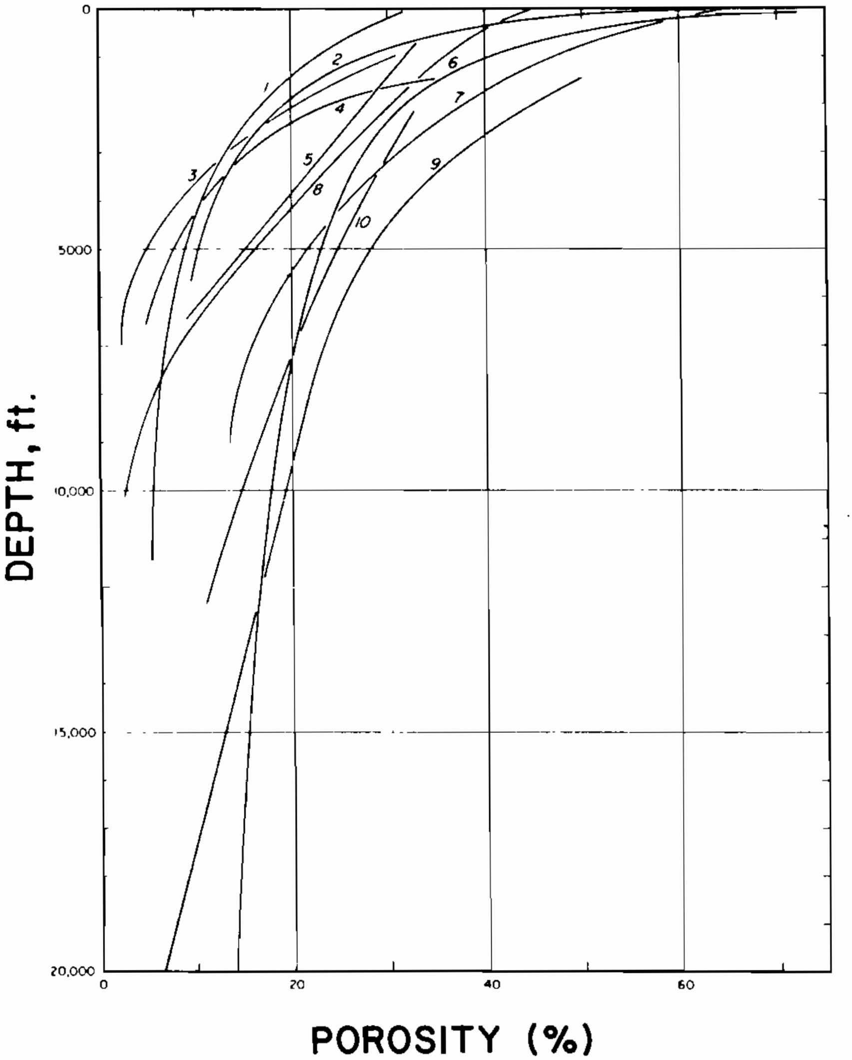

Fig. 56. Relationship between porosity and depth of burial for shales and argillaceous sediments (from Rieke and Chilingarian, 1974). Courtesy of Elsevier Scientific Publishing Company.
1 = Proshlyakov (1960); 2 = Meade (1966); 3 = Athy (1930); 4 = Hosoi (1963); 5 = Hedberg (1936); 6 = Dickinson (1953); 7 = Magara (1968); 8 = Weller (1959); 9 = Ham (1966); 10 = Foster and Whalen (1966).

Regarding the first points, Magara (1978a) recently stated : "The direction of oil and water movement does not have to be predominantly along layer parallel to the bedding planes. The permeability in the direction parallel to the bedding plane is usually higher than in that perpendicular to the bedding. However, in most shales the pore-pressure gradient is usually much higher vertically than horizontally". Fluid flow is controlled by both permeability and pressure gradient under a given viscosity level, so that there may be more fluid moving vertically than horizontally. If, for example, the permeability in a horizontal direction is 100 times more than it is in a vertical direction, but the vertical pressure gradient is 1,000 times more than the horizontal pressure gradient, then the amount of vertical fluid movement per unit area per unit time is 10 times the amount of horizontal movement.

Regarding the second point, it is obvious that, in order to overcome the capillary restrictions of shales, there is no need to have a continuous oil phase such as a film. As mentioned earlier, if the radii of both ends of an oil droplet become nearly equal, the capillary pressure will be reduced significantly. The size of the oil droplet or the continuation of the oil phase is not a main controlling factor in reducing the capillary pressure under these conditions. If some hydraulic pressure gradient exists in shales, the oil droplet will be able to move along with the water.

In summary, although there is no reason to deny oil movement in the form of a thin film, this type of movement is not the sole requirement for active primary oil migration. Oil would be able to move vertically in shales in the form of small oil droplets, as well as in the horizontal direction.

For the sake of argument, however, let us now assume for a moment that primary oil migration occurs along the layers parallel to the bedding planes, and that there is no chance of oil moving vertically in the source rocks. If this assumption is valid, then virtually no oil will migrate from the overlying and underlying shales into a reservoir of large areal extent, such as that shown in Fig. 57A. If a sandstone pinches out or becomes shalier in one direction, as shown in Fig. 57B, there would be some oil migration from the shaly facies to the sandy zone. However, I believe that explaining the world's major oil accumulations in terms of only the second, shale-out model would be extremely difficult, not to say unrealistic.

Tissot and Pelet's (1971) geochemical analysis in Algeria also suggests that oil can migrate in the vertical direction in shales (Fig. 43).

Compaction-fluid Movement

If the conditions necessary for primary oil migration are developed by the generation of oil, the presence of a large quantity of structured or semisolid water, and the resulting distortion of shape of an oil droplet, then the oil may be able to move by the hydraulic force developed in shales.

There are several possible causes for the development of such hydraulic force. The most important one is, of course, sediment loading, which has been known for many years and recently discussed by Magara (1977b) on a theoretical basis. The cumulative volumes of the expelled compaction fluid were estimated, by using Dickinson's (1953) porosity-depth curve, and a simplified Gulf Coast model. In this model, the

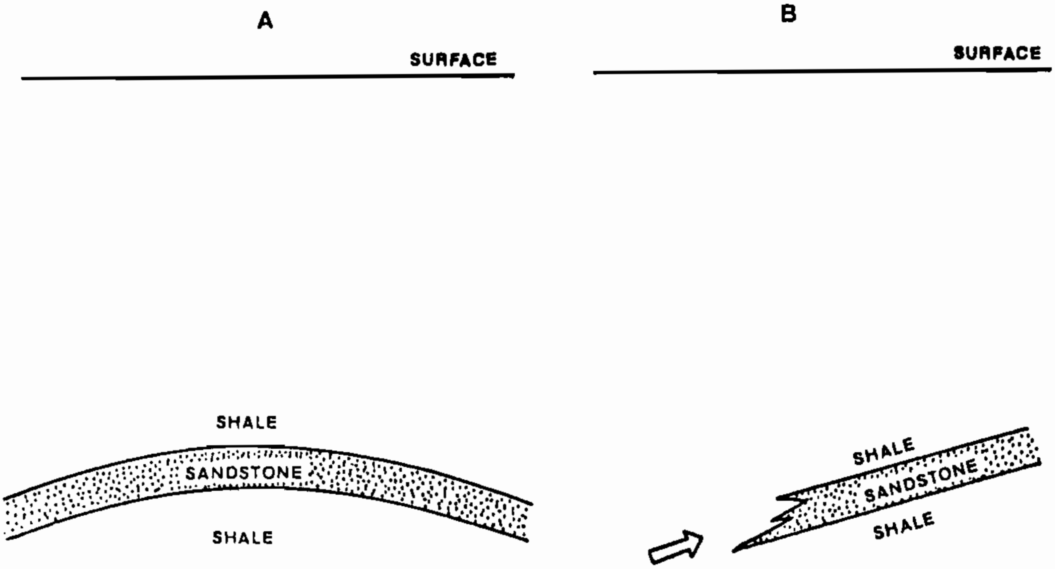

Fig. 57. Schematic diagrams showing sandstone reservoirs of large areal extent and of lateral pinch-out.

upper sequence is composed of sandstone-shale interbeds in which most fluids have moved horizontally, and the lower sequence of massive and homogeneous shales where the compaction fluid has moved vertically upward. The horizontal migration distance in the upper sequence is assumed to be 10 miles and the total thickness of the sedimentary column 33,000 ft (10 km). Figure 58 shows the cumulative volumes of fluid loss since burial to 2000 ft from a shale column whose base area is 1 sq ft. The respective depths to the boundaries of the upper and lower sequences are assumed to be 9,500 ft and 12,500 ft.

It is interesting to note that the cumulative fluid-volume plot based on the model that simulates the Gulf Coast sedimentary basin resembles the oil-production frequency plot for the same area (Burst 1969). On the basis of the concept of oil-droplet migration caused by the presence of structured or semisolid water, a greater amount of expelled fluids means a greater chance of a higher percentage of structured water being present in the source rocks, because more of the movable (or liquid) water has been expelled. Oil or gas may thus be able to move from the source rock relatively easily.

A fact that could affect the significance of shale compaction and fluid expulsion in petroleum migration is that the rate of compaction decreases continuously as the shales become more deeply buried. In other words, by the time the source rocks had reached deep burial where the temperature was high enough to generate hydrocar-

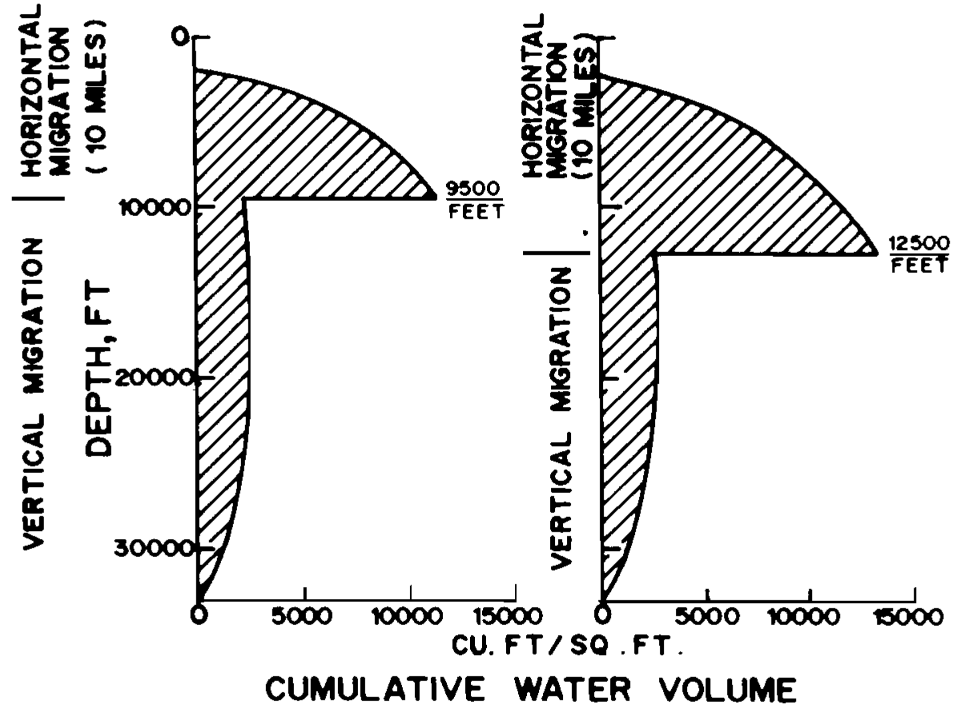

Fig. 58. Cumulative water-loss volumes from shales in Gulf Coast (combined vertical and horizontal migration model). From Magara (1976). Courtesy of American Association of Petroleum Geologists.

bons, the expulsion of compaction fluid might have become too slow and insignificant to be an effective agent in primary migration.

If fluids expand at such depths, the expansion might facilitate late-stage fluid expulsion.

Aquathermal Fluid Migration

Barker (1972) proposed the concept of aquathermal pressuring for the generation of abnormal pressures, using the pressure-temperature-density diagram for water (Fig. 59). The vertical scale is pressure in psi, and the horizontal scales are temperature in both centigrade and Fahrenheit. Density values in g/cm^3 (and specific volume values in cm^3/g) of water are shown along the isodensity line. The original data for constructing this diagram were obtained from Kennedy and Holser (1966). The three heavy lines show the three temperature-pressure relationships when the geothermal gradient is 25°C/km (1.37°F/100 ft), 18°C/km (1°C/km (1°F/100 ft) and 36°C/km (2°F/100 ft). In these cases, it is assumed that the water pressure increases hydrostatically with depth.

These three heavy lines intercept water isodensity lines whose values decrease as the pressure (or burial depth) increases. This progression to lower densities and

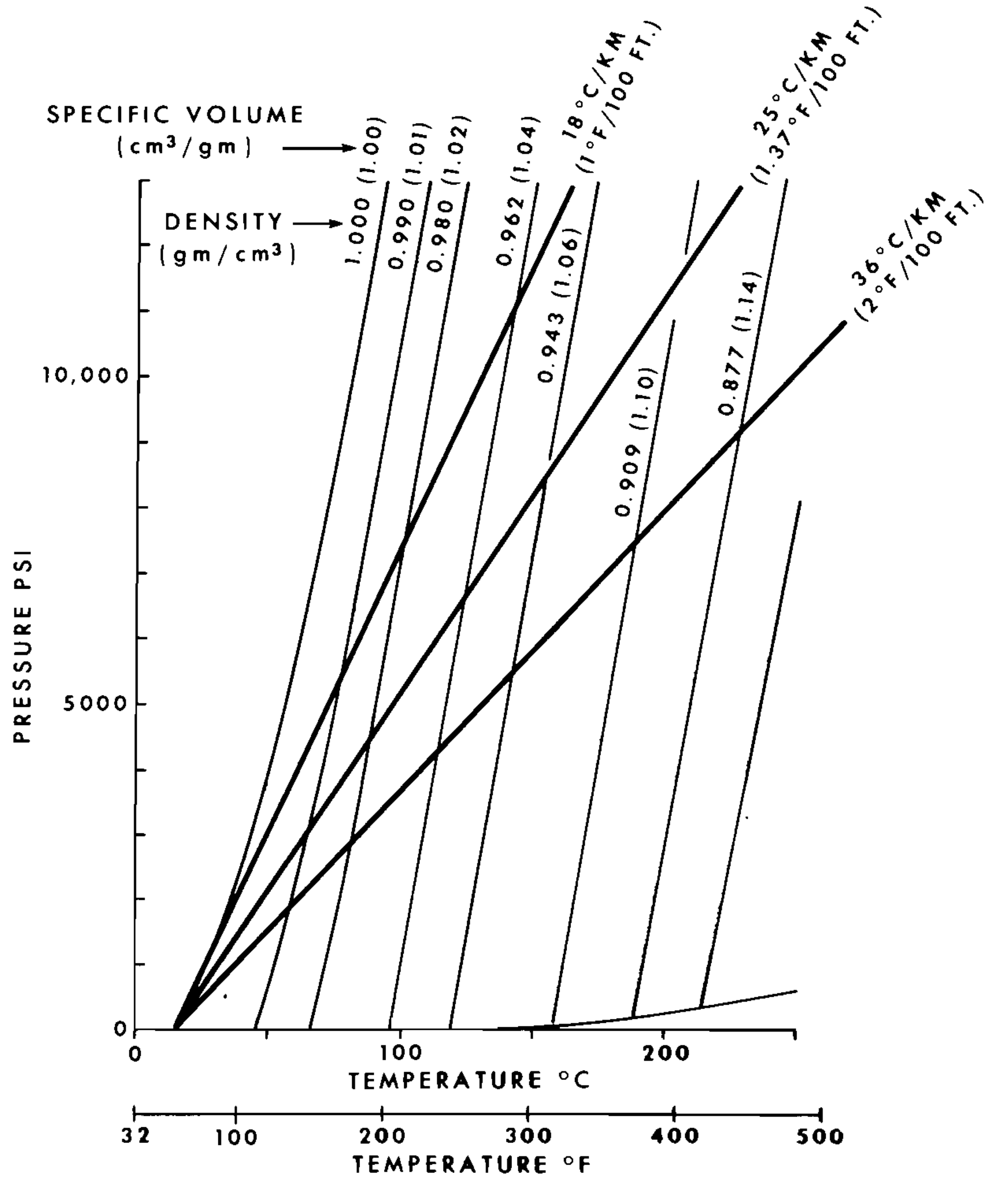

Fig. 59. Pressure-temperature-density (or specific volume) diagram for water. Three geothermal gradient-lines of 25°, 18°, and 36°C/km for hydrostatically pressured fluid are superimposed on a basic diagram derived from Barker (1972). Courtesy of American Association of Petroleum Geologists.

higher specific volumes means that a given weight of water expands with burial. The reason is that the increase of pressure caused by the hydrostatic gradient is inadequate to hold the water volume constant. The amount of expansion can be estimated from the specific volume values (cm^3/g), shown in brackets in Fig. 59.

For the geothermal gradient of 25°C/km (1.37°F/100 ft), for example, the specific volume increases from 1 cm^3/g at 0 psi pressure to 1.10 cm^3/g at 11,600 psi, corresponding to a burial depth of about 25,000 ft. Thus, a 10 per cent expansion results from about 25,000 ft of burial. That is a significant amount.

Figure 60 shows continuous expansion of water for the three geothermal gradients, where the specific volume of water (cm^3/g) is shown on the vertical scale and the depth (ft) on the horizontal scale. At 20,000 ft, for example, about 3 per cent expansion has occurred for the geothermal gradient of 1°F/100 ft, about 7 per cent expansion for 1.37°F/100 ft, and 15 per cent for 2°F/100 ft.

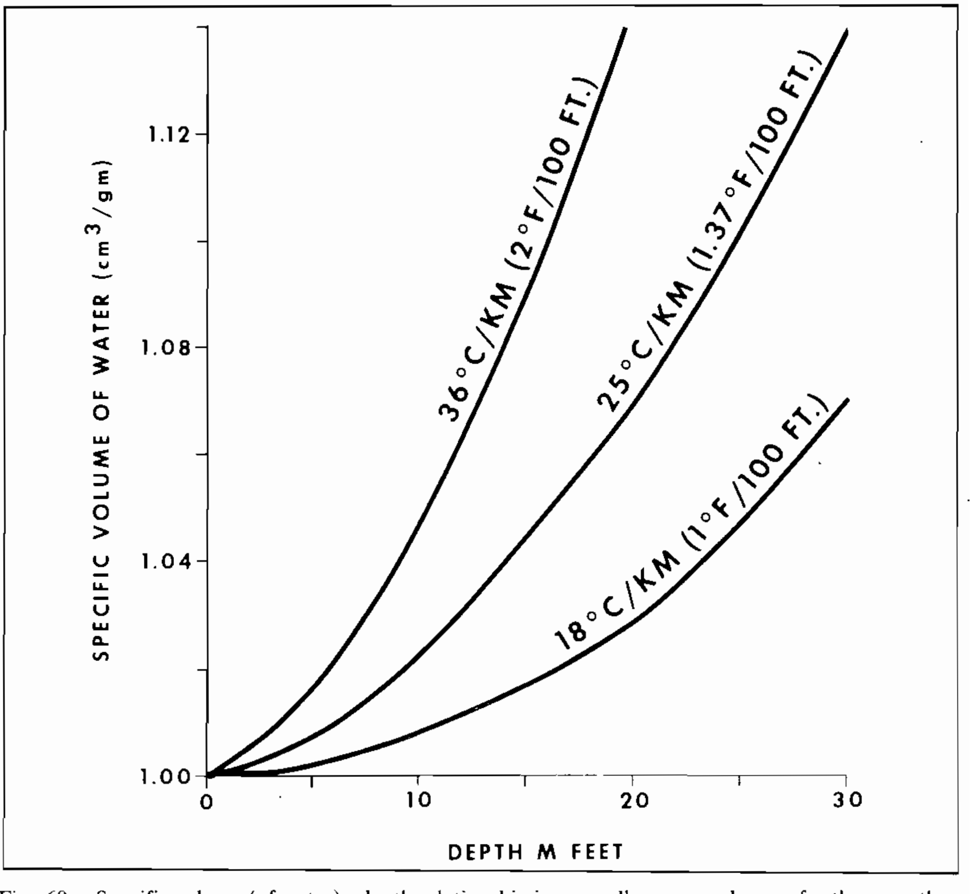

Fig. 60. Specific volume (of water) - depth relationship in normally pressured zones for three geothermal gradients of 25°, 18°, and 36°C/km (from Magara 1974b). Courtesy of American Association of Petroleum Geologists.

This figure shows that the rates of increase in specific volume, or rates of expansion, increase with depth. Because the amount of water expelled by compaction decreases with burial depth, such a late-stage water expansion will facilitate fluid migration at depth.

If rock grains expand, this phenomenon would create more intergrain space; thus more space for water. Its effect, however, is considered to be relatively very small – about 1/15 that of water.

The direction of fluid migration due to aquathermal effect is from a deep section to a shallow one, or from a basin center to its edges. These directions are essentially the same as those of fluid movement caused by sediment compaction. In summary, the significance of aquathermal effect is simply to increase the effectiveness of compaction-fluid flow at deep burial.

The hydraulic forces caused by sediment compaction and aquathermal effect are considered to be important in moving the oil droplets remaining in a source rock that contains a relatively large percentage of structured water.

Osmotic Fluid Movement

In most sedimentary basins, formation-water salinity increases with depth or with increasing compaction. These salinity values are usually higher than that of sea water (about 35,000 ppm). The principal cause of these increase in water salinity with compaction would be ion filtration by shales.

There are also several laboratory tests which have demonstrated ion filtration by clays (Engelhardt and Gaida 1963; McKelvey and Milne 1962). Figure 61 shows the result of the experimental work by Neglia (1979), indicating the decreasing concentration of the solutions expelled from Na-montmorillonite with increasing pressure. The concentrations of the solutions remaining in the clay will thus increase with increasing pressure or compaction.

Magara (1974a) showed the pore-water chlorinity-porosity relationships (Fig. 62) of shales in the Burgan field (Kuwait) and in three fields in Texas, analized by Hedberg (1967). The relation between porosity and chlorinity, which can be converted to salinity (NaCl) by multiplying by 1.65, in the Burgan data can be approximated by a hyperbola; the chlorinity increases as the porosity decreases. In addition, most of the Texas data fall within the extension of the general Burgan trend. The data shown in Fig. 62 are evidences of the effect of ion filtration by subsurface shales.

Therefore, if we combine the concept of ion filtration and a shale-porosity profile such as that shown in Fig. 63A, a shale-salinity profile like the one in Fig. 63C may be drawn. The salinity varies inversely with the shale porosity; it increases as the the porosity decreases. Figure 63B, on the other hand, shows a possible pore-pressure profile in the shale which is caused primarily by the shale compaction effect. The fluid would move from the center to the edges of each shale bed, toward sandstones, because of pressure differentials resulting from unbalanced compaction.

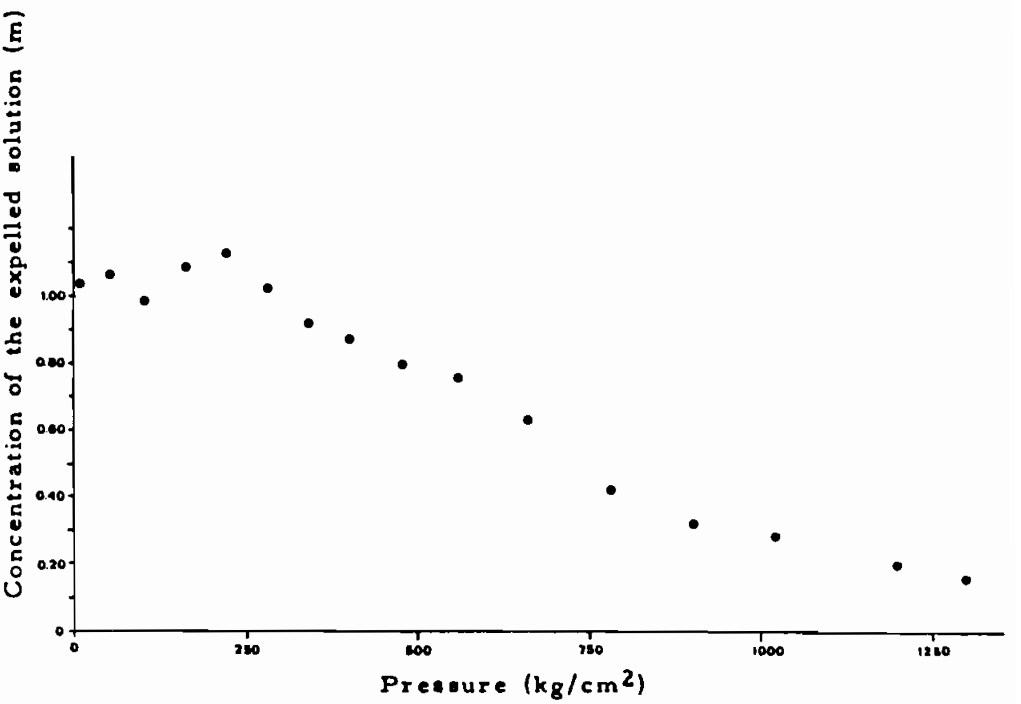

Fig. 61. Salinity of water expelled during compaction from Na-montmorillonite suspension dispersed in 1.0 NaCl moral solution (from Neglia 1979). Courtesy of American Association of Petroleum Geologists.

Such unbalanced compaction of shale is commonly observed at intermediate depths in relatively young sedimentary basins, where permeable sandstones are interbedded with shales. It seems that the maximum fluid expulsion and maximum porosity reduction occurred in the shales directly above and below the sandstones. The porosity in the middle of a shale bed may remain relatively high, because the fluids were not easily expelled.

On the basis of the salinity profile shown in Fig. 63C, we may be able to conclude that osmotic force tends to move water from the center to the edges, or from a fresher to a more concentrated site, within each shale bed. The directions of fluid flow due to osmotic effect are essentially the same as those due to sediment compaction as discussed above.

In the model shown in Fig. 63, if water expands from aquathermal effect, this water also will move from the center to the edges within a shale bed, because more expansion can be expected at a point of higher porosity (or more water).

In conclusion, the directions of fluid flow due to compaction, aquathermal and osmotic effects are essentially the same, from the center to the edges of each shale bed intercalated by two permeable sandstones (Fig. 63).

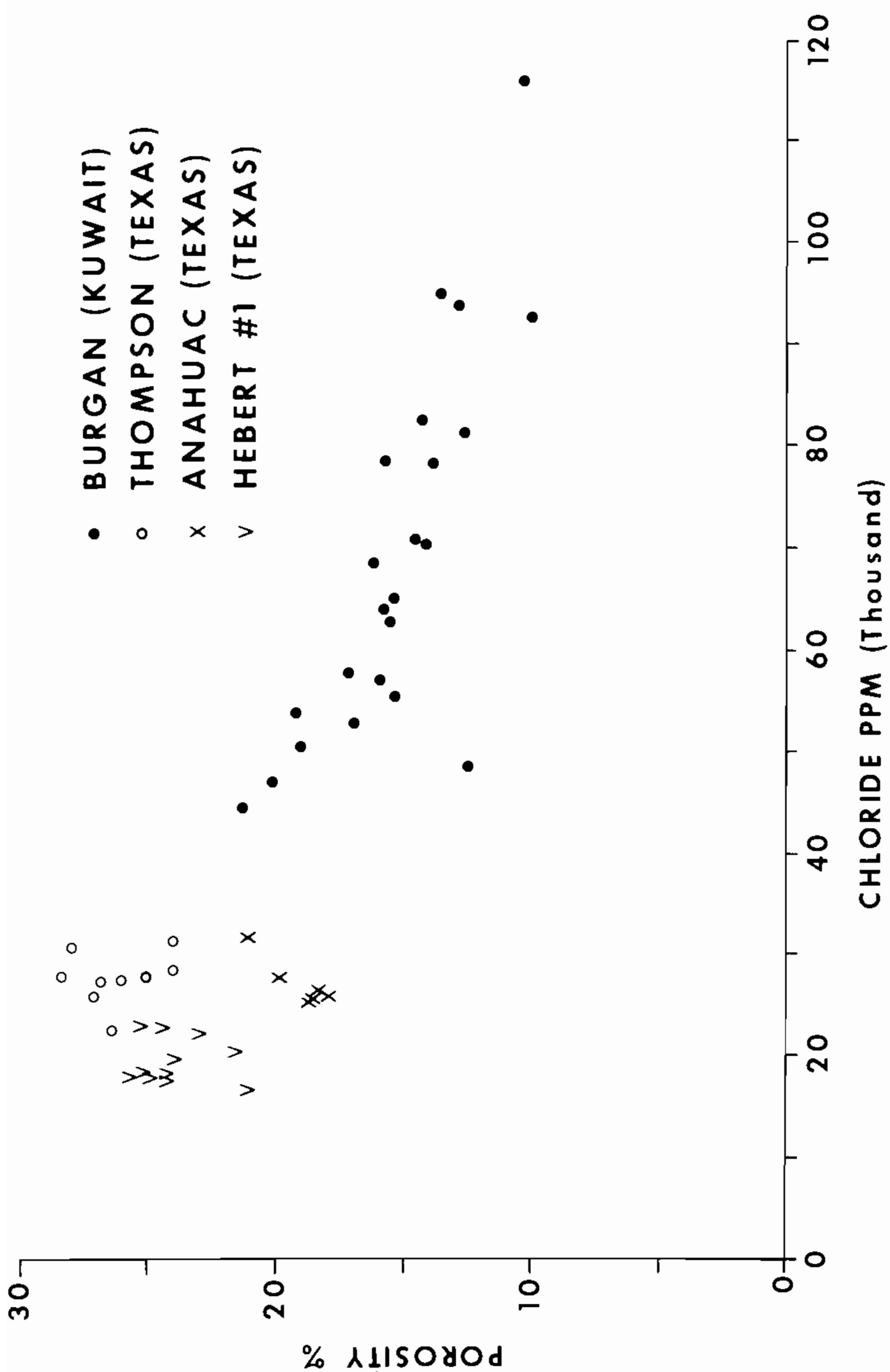

Fig. 62. Shale porosity-chlorinity relationship, Kuwait and Texas. Data are derived from Hedberg (1967).

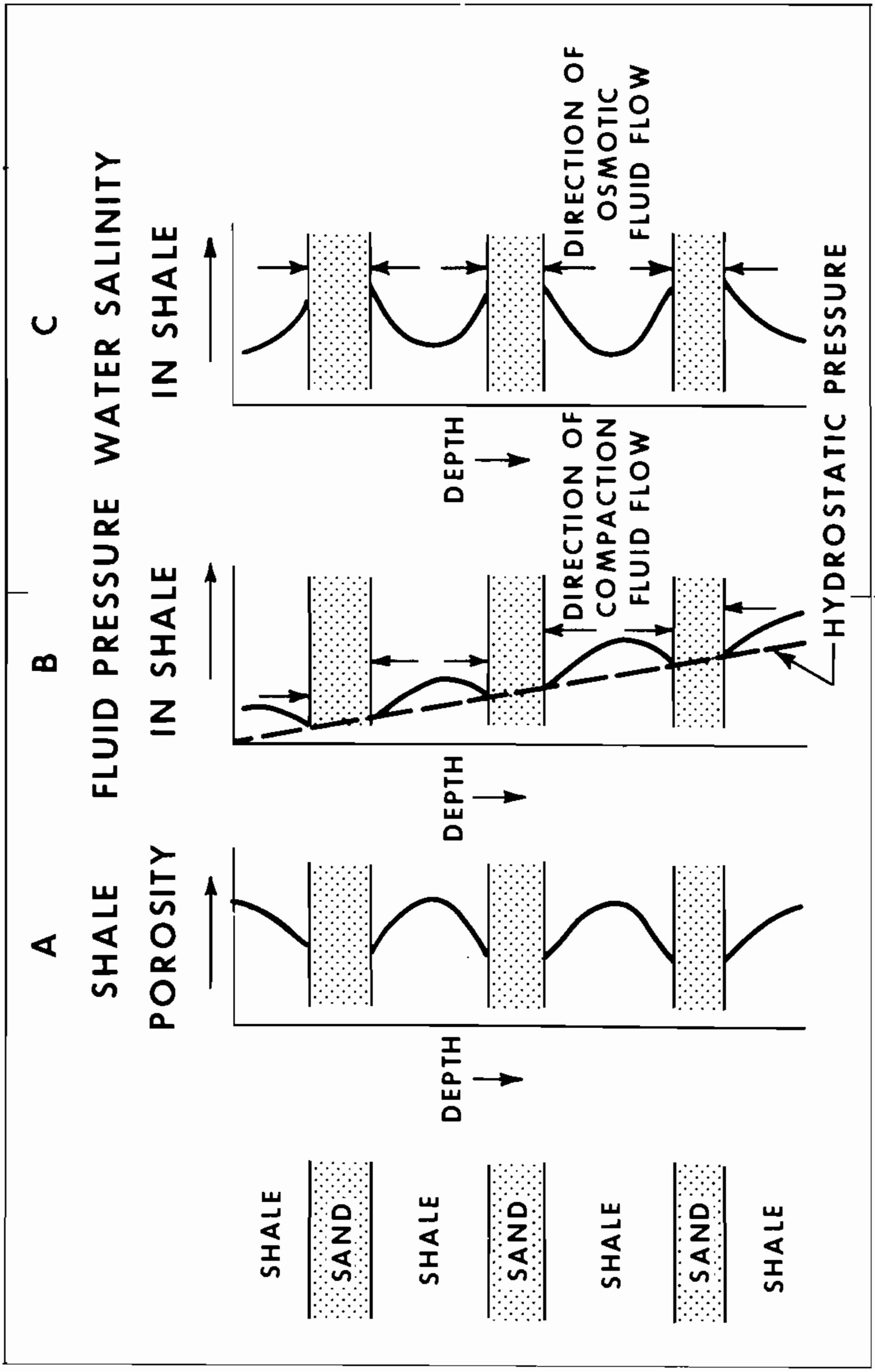

Fig. 63. Schematic diagram showing shale porosity, fluid pressure, and pore-water salinity distribution in interbedded sand-shale sequence (from Magara 1974a). Courtesy of American Association of Petroleum Geologists.

Fluid Movement Due to Clay Dehydration

From his study of clay-mineral composition in the Gulf Coast shales, Powers (1967) concluded that alteration of montmorillonite (or smectite) to illite begins at a depth of about 6,000 ft and continues at an increasing rate to a depth, usually about 9,000-12,000 ft, where there is no montmorillonite left. According to Powers, this alteration provides a mechanism for desorbing the last few layers of adsorbed or bound water in clay, and transferring it into interparticle locations as free water. If the last few water layers are denser than free water (Fig. 49), this released water will tend to increase its volume. If water expansion is restricted, the pore-water pressure will increase to abnormally high levels.

Martin's (1962) adsorbed-water density plot (Fig. 49) shows that approximately the first five water layers could be denser than 1 g/cm^3. If, therefore, these bound-water layers were converted to free water (1 g/cm^3), there must be a significant volume expansion. However, as Martin's plot shows, the density of water layers away from the above interval (first to fifth water layers) is less than 1 g/cm^3. When the adsorbed water becomes free, these water layers, whose density is less than 1 g/cm^3, must also become free-water layers (or water of 1 g/cm^3 density). In other words, some contraction of water volume must take place.

In summary, on the basis of Martin's (1962) data, there is a possibility of volume expansion of the first five water layers at the time of montmorillonite-illite conversion. At the same time, however, the volumes of the other water layers will contract somewhat. All of these water layers exist in clays. Therefore, there may be almost no net volume expansion of water at the time of clay-mineral conversion.

Powers (1967) apparently ignored the effect of the possible contraction in the volume of water whose original density is less than 1 g/cm^3, and concluded that clay-mineral conversion would result in a volume expansion between 2.5 and 20 per cent. He considered this phenomenon the most important agent in causing abnormal pressures in the deeper parts of sedimentary sequences in the Gulf Coast.

According to Burst (1969), clay dehydration depends mainly on subsurface temperature; the average dehydration temperature in the Gulf Coast being 221°F. For this conversion, certain chemical conditions for potassium fixation would also be required. He proposed phase change and possible expansion of bound water at the time of clay-mineral conversion as important agents for flushing hydrocarbons.

From a comparison of oil-production frequency with the level of significant clay-mineral conversion, Burst concluded that peak oil production can be expected about 1,500 ft above the dehydration level. Magara (1976), however, argued that, at the same level in the Gulf Coast area, the shales usually reached maximum compaction and the peak oil-generation stage (at least in most synclinal areas), so that the oil could have been flushed by compaction fluids that had been moved by mechanical sediment compaction and aquathermal effect.

The principal reason that Powers and Burst proposed montmorillonite-illite conversion as being important in flushing water and petroleum is that to remove adsorbed water by pressure alone under laboratory conditions (25°C) is known to be extremely difficult. Van Olphen (1963) showed at 25°C the pressure needed to remove the last interlayer of water is 65,000-70,000 psi, and that needed for the second-to-last water interlayer is 30,000 psi. These pressure values are considerably higher than the pressure at depths less than 20,000 ft. In other words, overburden pressure alone may not suffice to release at least the last two layers of bound water.

If, however, interlayer water is released by clay dehydration in response to temperature rise, and subsequently remains in the pore spaces as free water, the same overburden pressure will be sufficient to flush it out of the shales, provided good drainage conditions are available.

Because essentially, in all the world's sedimentary basins temperature increases with depth, the bound water will be released in one way or another, provided that suitable chemical conditions prevail. Therefore, the laboratory model of the constant temperature (25°C) would not represent a realistic condition in the subsurface. Whether the water released by clay-mineral conversion can be flushed out of the shales or not depends on the general drainage conditions. Drainage conditions usually improve as the percent or number of interbedded sandstones and/or the areal extent of these sandstones increase.

In other words, I believe that clay-mineral conversion would not suffice for flushing hydrocarbons out of shales unless good drainage conditions are established. This situation may be observed in the deep, undercompacted shales of the Gulf Coast, from which most of the bound water has been released by relatively high temperatures (Burst 1969). However, the liquid water generated seems not to have been expelled for lack of good permeable zones. For further discussions refer to Magara (1975a).

It may be concluded that, although montmorillonite-illite conversion will provide a significant amount of free water at depth, effective migration of hydrocarbons would not occur if there is no good drainage. This may explain why most oil pools have been found in zones of relatively low pressure (Timko and Fertl 1971), where drainage conditions are generally excellent.

Generation of Gas

Hedberg (1974) proposed the importance of the generation of gas, especially of methane, for causing shale diapirs and primary hydrocarbon migration. The volume expansion associated with the generation of gas is known to be quite significant, so that this phenomenon could indeed result in diapirs and primary migration. Quantifying such an effect, however, is not an easy task at present.

Bray and Foster (1980) proposed that carbon dioxide and hydrocarbon gases dissolved in pore water could facilitate migration of liquid hydrocarbons.

Capillary Pressure

A separate oil droplet can move from fine- to coarse-grained rocks by capillary pressure. Therefore, if the grain size increases continuously from source to reservoir rock, capillary pressure may help to move the oil droplets. However, conditions in the subsurface are generally less ideal; the grain size in the source rock remains low and relatively constant, then suddenly increases at the interface with the reservoir rock. For an oil droplet to move in fine-grained rock is generally very difficult unless its shape is significantly distorted.

The presence of structured water in shales, as discussed in the preceding sections, would help change the shape of an oil droplet, and provide conditions for it to move by hydraulic forces.

Buoyancy

Buoyancy force or pressure, P_B, caused by an oil bubble whose height is Z_o, is given as

$$P_B = (\rho_w - \rho_o) \cdot g \cdot Z_o \qquad (16)$$

where ρ_w is density of water, ρ_o density of oil, and g gravity acceleration.

If this buoyant force exceeds the capillary pressure, P_c, then the oil bubble will move in the upward direction. By combining equation (16) with (11), we obtain.

$$(\rho_w - \rho_o) \cdot g \cdot Z_o \geqq 2\gamma \left(\frac{1}{r_t} - \frac{1}{r_p} \right) : \text{ movement.}$$

$$\text{and } (\rho_w - \rho_o) \cdot g \cdot Z_o < 2\gamma \left(\frac{1}{r_t} - \frac{1}{r_p} \right) : \text{ no movement.}$$

In most source rocks, very tiny oil droplets are probably disseminated, so that the buoyant force caused by each droplet would be relatively very small. Therefore, buoyant force alone is usually not sufficient to cause significant primary migration.

Diffusion

For oil in solution in water, diffusion can be an important agent in primary migration. From the preceding discussions, however, it is obvious that most oil must exist in a separate phase, so that diffusion cannot be a principal mechanism for oil migration.

The solubility of gas in water, however, is relatively high (Fig. 45), so that gas can migrate by molecular diffusion. Gas also can migrate in water with physical movement of the water, caused by sediment compaction. Which mechanism is more significant for gas migration is not well understood.

There is an opinion that most oil and gas migrated by diffusion, having moved from a point of higher to a point of lower concentration. Several investigators call this phenomenon "primary migration by chemical gradient". For oil/gas migration to result from this diffusive mechanism, a certain amount of oil or gas must have been generated at, at least, one point in the source rock, resulting in some gradients of oil/gas concentrations toward a reservoir. Such gradients would generally become more significant as more hydrocarbons were generated. Therefore, to argue that this mechanism is the principal one for primary migration is to imply that the generation of hydrocarbons is almost the sole cause of primary migration, in that a certain critical amount of hydrocarbons generated in source rock migrates automatically.

However, for the several reasons mentioned above, this type of simple logic cannot apply in actual subsurface situations. In other words, the generation of hydrocarbons does not in itself seem to guarantee their migration. Whether the generated hydrocarbons can migrate or not depends on other physical and geological conditions, such as the presence of structured water, good drainage conditions (presence of permeable beds), higher temperature, ... etc.

The generation of hydrocarbons is important because without it there would be no hydrocarbons to move anywhere. However, a significant amount of hydrocarbon generation does not have to be followed by significant migration. Most of the generated hydrocarbons may have to stay in source rocks forever if the conditions are not suitable for migration. A good example of this kind is "oil shales".

For the sake of argument, let us now assume, for a moment, that the chemical gradient is the most important agent for hydrocarbon migration. Let us assume too that a significant oil accumulation has been created by this mechanism. As soon as the oil accumulated, a significant negative gradient would have developed around the accumulation, because the concentration of oil in the accumulation is quite high, whereas the concentration in the rocks above and below the accumulations are (usually) quite low. This negative chemical gradient could cause a significant movement of oil into the surrounding rocks as soon as a small amount of oil has accumulated.

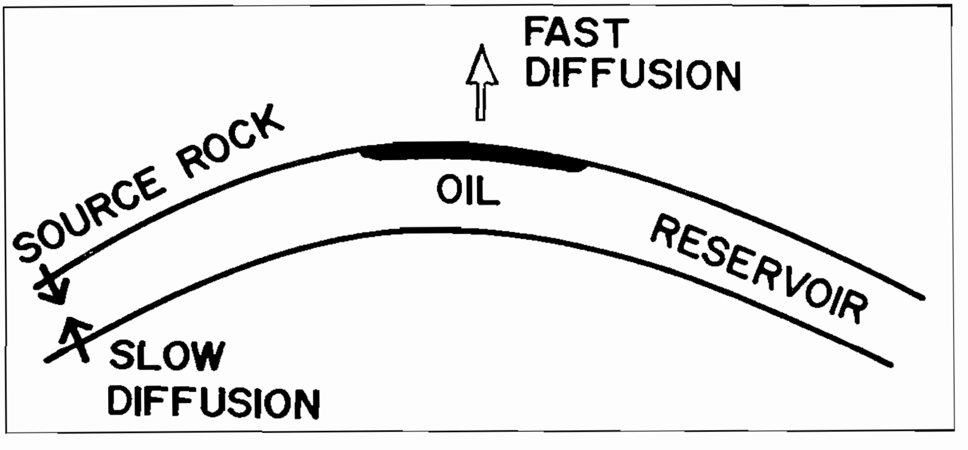

Fig. 64. Schematic diagram showing concept of migration and loss of oil by diffusion. See text for explanation.

The accumulated oil would be lost at a rate much faster than the rate of accumulation, because the difference in concentration of oil between the accumulation and the cap rocks must be much higher than that of oil between the source rock and the reservoir, in the synclinal areas (Fig. 64). From applying this concept, we may be able to conclude that diffusion cannot be the principal cause of primary hydrocarbon migration.

Problems

1. Which condition is the most important at the time of primary hydrocarbon migration; molecular solution, micellar solution, and separate hydrocarbon phase?
2. Explain the importance of aquathermal effect on primary hydrocarbon migration.
3. Explain osmotic fluid migration.
4. Is diffusion a plausible mechanism of primary hydrocarbon migration?

Chapter 7

Hydrocarbon Generation and Maturation

■ Introduction. ■ Generation and maturation of hydrocarbons. ■ Lopatin's method. ■ Problems.

Introduction

In evaluating a source rock potential, four important factors may be considered ; 1. organic richness, 2. type of organic matter, 3. level of hydrocarbon generation and maturation, and 4. expulsion efficiency of the generated hydrocarbons. Items 1 and 2 will be discussed in Chapter 8 and item 4 is included in Chapter 6, while item 3 is the main problem being discussed in this chapter.

Most of the problems being discussed in Chapters 7 and 8 are related to modern organic geochemistry – a highly specialized branch of science of petroleum geology. There are so many recent developments in this field made by organic geochemists working in the petroleum industry and academia. It is strongly recommended for the readers to study the basics of organic geochemistry using the textbooks written by Tissot and Welte (1978) and Hunt (1979).

Generation and Maturation of Hydrocarbons

Most petroleum hydrocarbons have been generated by a thermal process in the subsurface from various organic matters deposited in the geological past. Connan (1974) documented a time-temperature function by examining accumulated oils of known geologic ages and the maximum (or present) temperatures. Solid circles in Fig. 65 indicate the data he obtained. This figure shows that the younger the rocks, the higher the temperture needed to generate hydrocarbons in them.

During the continuous burial of organic matter, it experienced gradual changes of color from yellow through brown and dark brown to black, as hydrocarbons were being produced from it. Reflectance of the light on the polished surface of the organic matter also changes depended upon the elapsed geologic time and temperature.

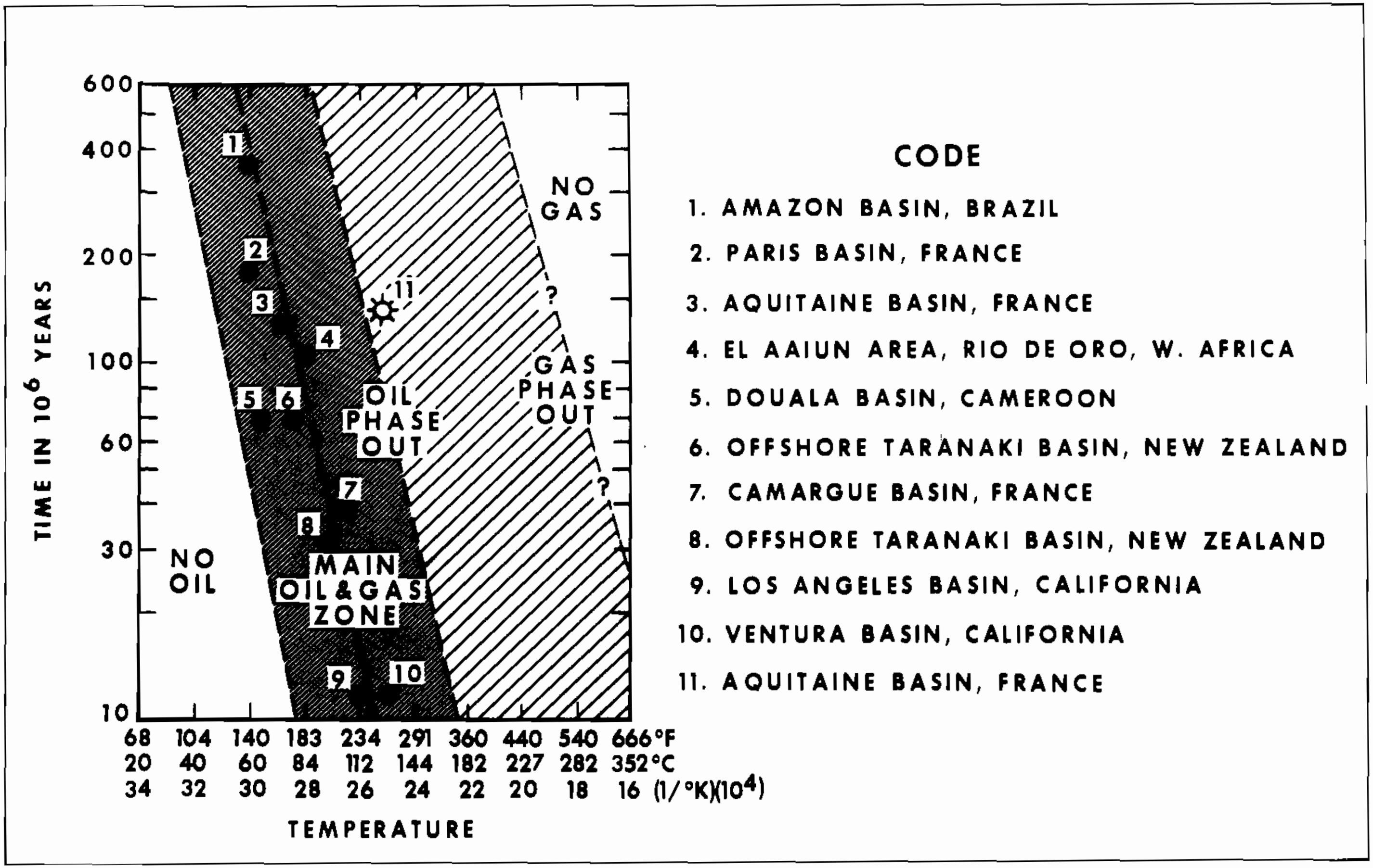

Fig. 65. Time-temperature relationship of petroleum genesis (from Hunt 1974, based on Connan 1974). Courtesy of Society of Petroleum Engineers of AIME.

There are two basic methods of evaluating the status of petroleum generation and organic maturation : 1. visual, and 2. geochemical. The first method is based on the color (or light reflectance) change of the organic matter (kerogen) and the second method estimates the compositional change of kerogen due to maturation. Figure 66 correlates these various methods with the stages of oil, wet gas, and dry gas generations.

Stages of organic maturation can also be estimated on the basis of extracted hydrocarbons and organic matter (in this case, bitumen, or soluble organic matter in solubent). Figure 67 shows examples of extractable hydrocarbon plots in Japan. This method is sometimes unreliable because a significant portion of the generated hydrocarbon could have been expelled from the source rock. In such a case, the result of interpretation can be misleading. By the way, the efficiency of hydrocarbon expulsion is an important factor in assessing the source rock potential.

Another method of evaluating the maturity of source rocks is pyrolysis, by which a sample is heated by an equipment (*e.g.*, Rock Eval) and the amount of hydrocarbons already existing and to be generated with deeper burial (with higher temperature) are estimated, along with the estimation of amounts of CO_2 and H_2O. Figure 68 shows examples of plots of both hydrogen and oxygen indices derived from the pyrolysis. For details of these methods, refer to the works of Tissot and Welte (1978) and Hunt (1979) mentioned before.

Among all the methods of source rock evaluation, the vitrinite reflectance is probably the one most commonly used in the petroleum industry. Unless an organization has its own organic geochemical laboratory, these samples for the vitrinite reflectance measurements are sent to one of the agents specializing in this type of work. For most petroleum geologists, therefore, it is not essential to learn the technique of the vitrinite reflectance measurement, but is advisable to understand and to apply the result of the measurements for practical applications.

To measure vitrinite reflectance, we would need subsurface samples which can be obtained from drilled wells. In most petroleum prospect evaluation, however, it is preferable or sometimes necessary to estimate the reflectance even before drilling. We may also wish to estimate the vitrinite reflectance of a synclinal area where drilling may never take place. However, such estimate in the syncline is important because most oil in the trap may have moved from the synclinal area.

Waples (1980) developed a new method for estimating vitrinite reflectance using a burial history plot. This method is based on Lopatin's (1971) fundamental concept of petroleum generation and maturation.

Lopatin's Method

Chemical reaction rate theory predicts that temperature dependence on maturity is exponential. It is generally accepted that the reaction rate will be doubled if the temperature is raised by 10°C. After constructing a burial history plot and defining

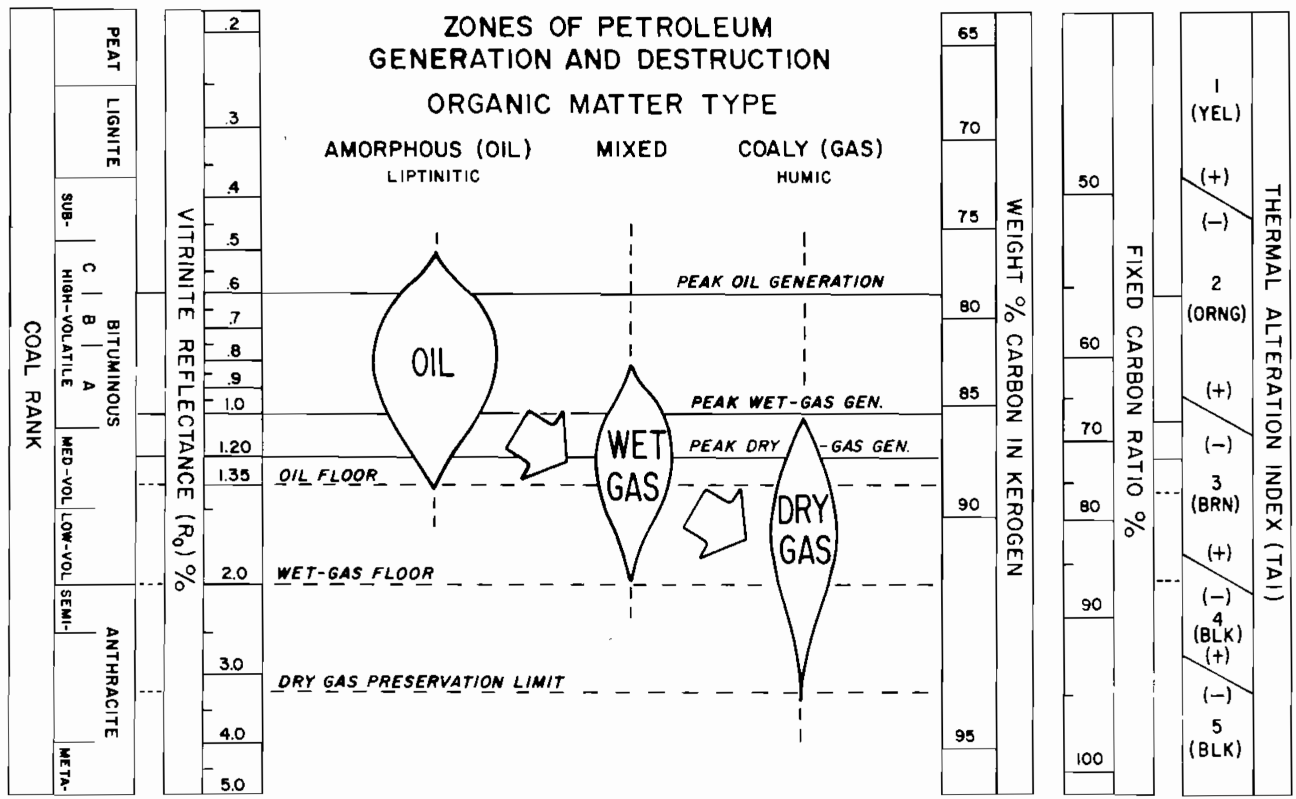

Fig. 66. Correlation of coal-rank scale with various maturation indices and zones of petroleum generation and destruction (from Dow 1978). Courtesy of American Association of Petroleum Geologists.

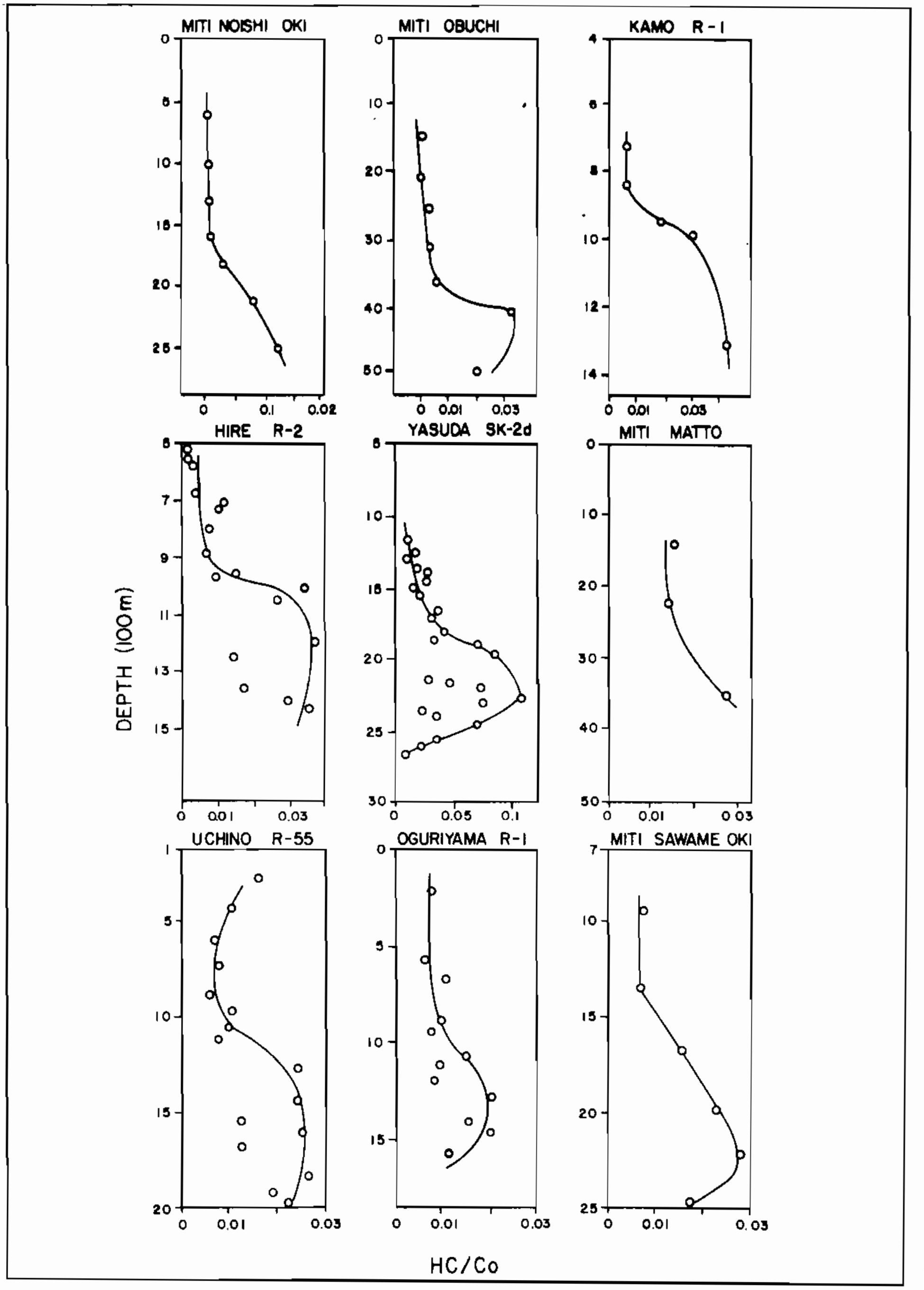

Fig. 67. Examples of extracted hydrocarbon (HC) analysis in Japanese sedimentary basins; Co = organic carbon (from Asakawa and Fujita 1979).

the temperature intervals of 10°C each, one would be able to calculate the time-temperature index (or integral, TTI) as follows,

$$\mathrm{TTI} = \sum_{n\ min}^{n\ max} (\Delta T_n)\,(r^n), \qquad (17)$$

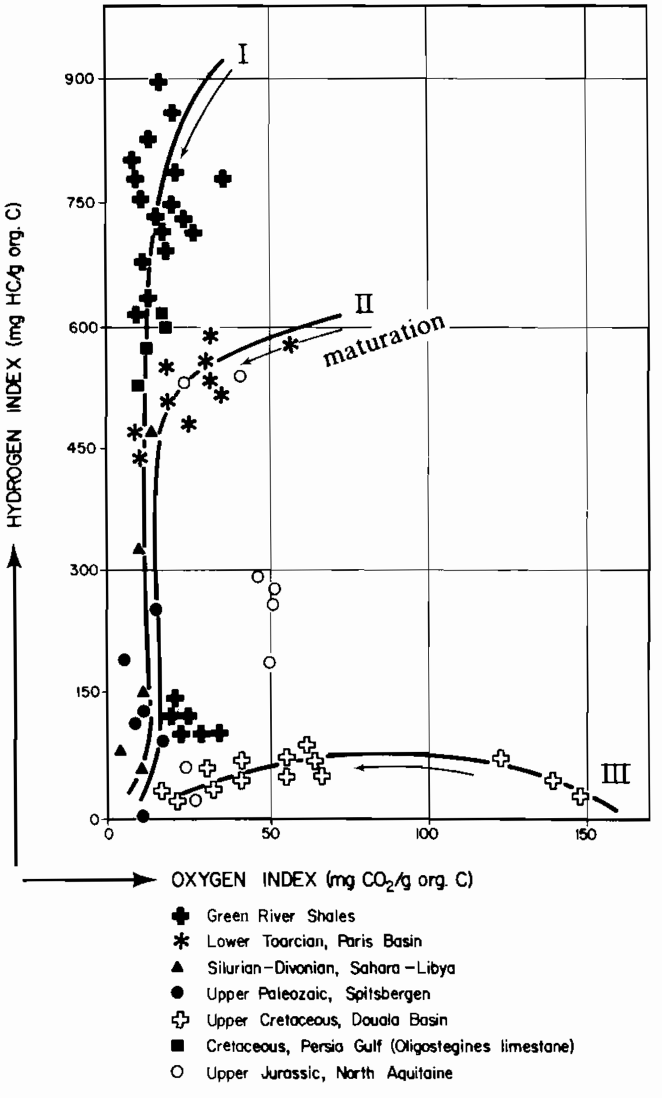

Fig. 68. Classification of source rocks by pyrolysis indices (from Espitalie *et al.* 1977). Courtesy of Institut Francais de Pétrole.

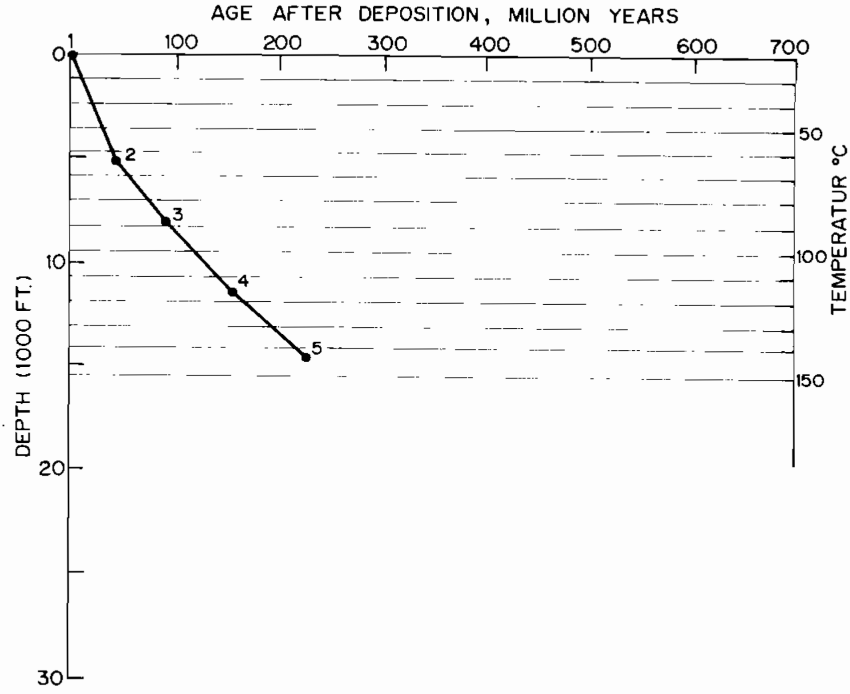

Fig. 69. Burial history plot of synclinal area shown in Fig. 14. Horizontal lines show temperature increments of 10°C each for time-temperature-index calculation. See text for explanation.

where n max and n min are the n-values of the highest and lowest temperature intervals encountered, ΔT_n the length of time spent by the sediment in the temperature interval, n, and r the base of the reaction factor (normally 2). Table 2 shows the values of r^n for different temperature intervals.

The values of TTI were calculated using the burial history plot shown in Fig. 69 (for the geologic data for constructing this plot, refer to Fig. 14 in Chapter 3). The surface temperature and geothermal gradient are assumed to be 68°F (20°C) and 1.5°F/100 ft respectively. Based on this geothermal gradient, a vertical interval (or thickness) of 1,200 ft corresponds to a 10°C increase in temperature. The geologic time period in millions of years within each temperature interval was estimated and multiplied by the reaction factors mentioned above (Table 2), to obtain the TTI (Table 3). Cumulative TTI was also calculated and converted to vitrinite reflectance, R_o (Table 3), using the empirical relationship by Waples (Fig. 70).

Table 2. List of temperature interval, index value, n, and temperature factor, r^n, for ealculation of time-temperature index (TTI) (From Waples, 1980).

Temperature Interval, °C	Index Value, n	Temperature Factor, r^n
20- 30	–8	2^{-8}
30- 40	–7	2^{-7}
40- 50	–6	2^{-6}
50- 60	–5	2^{-5}
60- 70	–4	2^{-4}
70- 80	–3	2^{-3}
80- 90	–2	2^{-2}
90-100	–1	2^{-1}
100-110	0	1
110-120	1	2
120-130	2	2^2
130-140	3	2^3
	m	2^m

Table 3. Sample results of time-temperature index (TTI) and vitrinite reflectance (R_o) estimation based on burial history plot of Fig. 69.

Temperature Interval, °C	r^n	Time, Million years	TTI	Cumulative TTI	R_o
20- 30	1/256	11	0.04	0.04	–
30- 40	1/128	11	0.09	0.13	–
40- 50	1/64	11	0.17	0.30	–
50- 60	1/32	11	0.34	0.64	–
60- 70	1/16	17	1.06	1.70	0.45
70- 80	1/8	18	2.25	3.95	0.50
80- 90	1/4	19	4.75	8.7	0.60
90-100	1/2	22	11.0	19.7	0.70
100-110	1	22	22.0	41.7	0.85
110-120	2	25	50.0	91.7	1.10
120-130	4	28	112.0	203.7	1.45
130-140	8	28	224.0	427.7	1.70
140-150	16	2	32.0	459.7	1.75

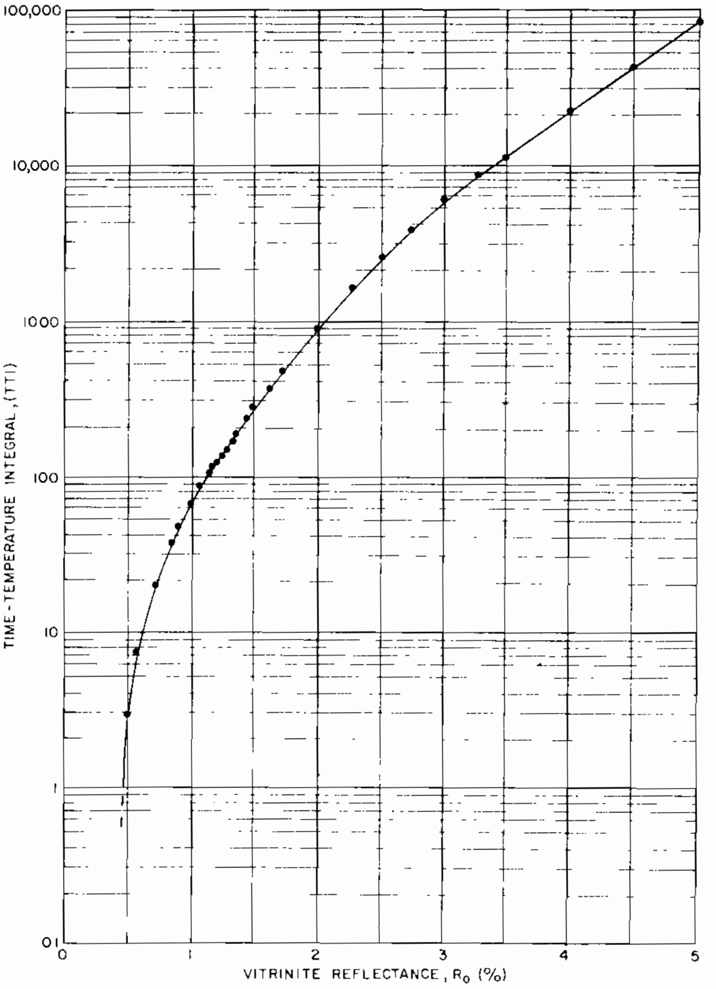

Fig. 70. Empirical relationship between time-temperature index (TTI) and vitrinite reflectance (R) derived from 402 samples studied by Waples (1980).

From Fig. 66, the values of vitrinite reflectance, R_o, can be correlated with the stages of oil and gas generation as follows:

R_o,%	Hydrocarbons
Less than 0.6	No major generation
0.6 -1.0	Major oil generation
1.0 -1.35	Oil and wet gas generation
1.35-2.0	Wet and dry gas generation*
2.0 -3.0	Dry gas generation

Using these stages, the geologic time periods for generation of different types of hydrocarbons can be estimated (see Fig. 69 and Table 3);

No major generation	0-98 million years after deposition of reservoir (225-127 million years ago)
Major oil generation	98-157 million years after deposition of reservoir (127-68 million years ago)
Oil and wet gas generation	157-185 million years after deposition of reservoir (68-40 million years ago)
Wet gas generation	185-225 million years after deposition of reservoir (40-0 million years ago).

The result of estimation suggests that the rock has reached the stage of the major wet gas generation.

For an instantaneous estimation of vitrinite reflectance when a burial history was relatively simple and uniform, use one of a series of charts included in Appendix B. If a burial history was more complicated, the formal calculation methods of TTI and R_o as described in this chapter must be used.

It may be pointed out that the result of the vitrinite reflectance measurements can be used only as a possible indicator of organic maturation, rather than a sole guarantee for a large amount of oil generation, because the vitrinite itself is not a prime oil-producer in source rocks. This method has been widely used because the relationship between the reflectance and organic maturation has already been well-established and also vitrinite is present in most sedimentary rocks. The level of organic maturation indicated by the vitrinite reflectance can thus be used as a clue to understanding the true oil generation and maturation which are controlled by the availability of suitable types of organic matter (mainly marine), as well.

* Dry gas means CH_4, or methane gas, and wet gas is other heavier petroleum gas.

Problems

1. State two basic methods of evaluating maturity of source rock.
2. Explain Lopatin's concept of the time-temperature index for estimating the stages of petroleum generation and maturation.
3. Using the geologic data of the synclinal location shown in Fig. 20, estimate TTI and R_o. Note that the surface temperture is 86°F (30°C) and the geothermal gradient is 1.2°F/100 ft.

Chapter 8

Richness and Types of Organic Matter

■ Introduction. ■ Relationship between sedimentation rate and organic carbon per cent. ■ Types of organic matter. ■ Problems.

Introduction

It is widely accepted that the organic richness (or organic carbon %) is one of the most important factors controlling the quality of source rocks. The minimum organic carbon % for an effective source rock is usually considered to be 0.5 for clastic rocks and 0.4 for carbonate. Another factor influencing the source rock quality is the type of organic matter.

Momper (1978) considered that the source rock is the most important among the seven controlling factors for petroleum accumulations (Fig. 2 in Chapter 1), because nothing else matters if there is no source rock.

Figure 71 shows the distributions of the average organic carbon %, of number of giant oil and gas fields, and of the amount of expandable clay throughout the geologic time, constructed by Barker (1977). A giant oil field contains more than 0.5 billion bbl of recoverable oil and a giant gas field has more than 3 trillion ft^3 of recoverable natural gas. They contain nearly 75% of the world's known petroleum reserves. The curve for the total petroleum reserve is essentially the same as the number of the giant fields, except for lower values for the Tertiary section (Barker 1977).

Barker then concluded that the organic-carbon-concentration curve follows the trend of the giant-field petroleum abundance curve much better than does the expandable clay-mineral curve. It may, therefore, be concluded that, although the other factors such as organic matter type and maturity are also important, the concentration of organic carbon in sedimentary rocks is one of the controlling factors in accumulating a significant amount of petroleum.

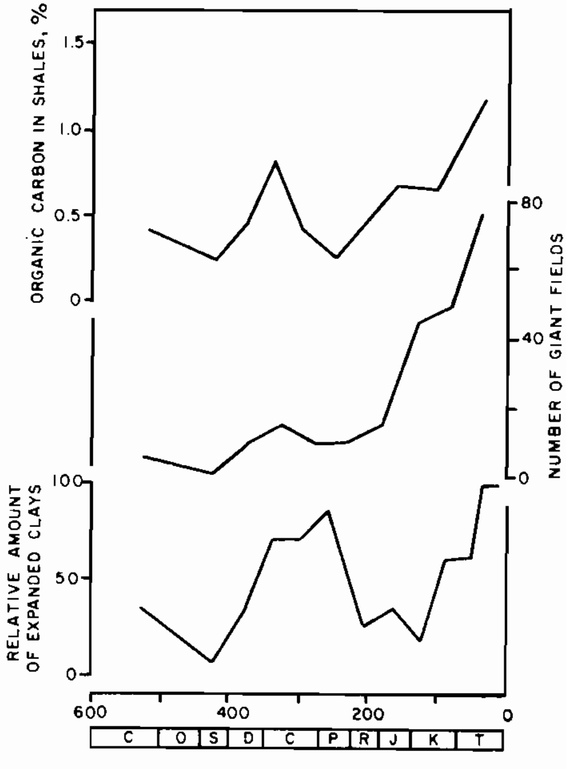

Fig. 71. Variation throughout time of average organic carbon content of shales, number of giant fields, and relative amount of expandable clay (from Barker 1977). Courtesy of American Association of Petroleum Geologists.

Relationship between Sedimentation Rate and Organic Carbon Percent

It is expected that a relationship between depositional environment and concentration of organic matter exists because production, transportation, and destruction or preservation of organic matter can be controlled by the environmental factors. Dow (1978, p. 1588) states that, "If the supply of organic matter is constant, its concentration in sediments should be inversely related to the depositional rate of mineral particles. Therefore, areas of high sedimentation rates, such as deltas, should contain sediments with relatively low organic-carbon concentrations. If the sedimentation rate is too slow, however, much of the organic matter reaching the bottom may be consumed by heterotrophic organisms before it can be protected by burial. Intermediate sedimentation rates which minimize the effects of both dilution and consumption commonly result in the most organic-rich sediments". He then concluded that "the most organic-rich sediments are deposited in areas of high organic productivity, where the supply of bottom oxygen is minimal, the water is reasonably quiet, and sedimentation rate of mineral particles is intermediate".

Figure 72 depicts the maximum organic carbon % and the rate of sedimentation for the Canadian Arctic region. Powell's (1978) large number of data (about 300 samples) was used to establish the maximum organic carbon %. Correction for the effect of compaction was not made in Fig. 72. The result suggests that the organic carbon % is highest at the sedimentation rate around 80 ft/million years.

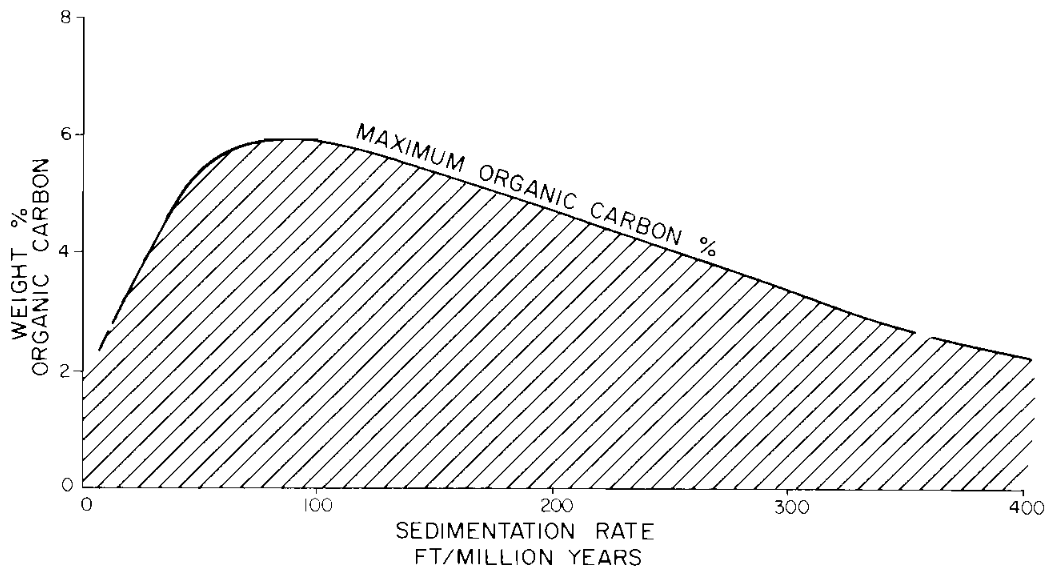

Fig. 72. Graph showing relationship between maximum organic carbon % and sedimentation rate for Canadian Arctic region. Data derived from Powell (1978).

Figure 73 is a plot of the organic carbon % against the sedimentation rate for the Pennsylvanian and Permian rocks of the Palo Duro and Midland Basins of Texas (data after Dutton 1980). The highest organic carbon % corresponds to 80-90 ft/million years (rate of sedimentation).

A similar plot on logarithmic paper, constructed by Ibach (1982) using the Deep Sea Drilling Project (DSDP) data is shown in Fig. 74. Depositional environment and geologic age are shown in this Figure. Lithologic zonation of the same data is made in Fig. 75, in which black shale has the highest % of organic carbon. The summary plots of the linear regression analyses for the data of different lithologies are shown in Fig. 76, suggesting that the range of the peak organic carbon % is from about 14 to 41 m/million years (or from about 46 to 134 ft/million years).

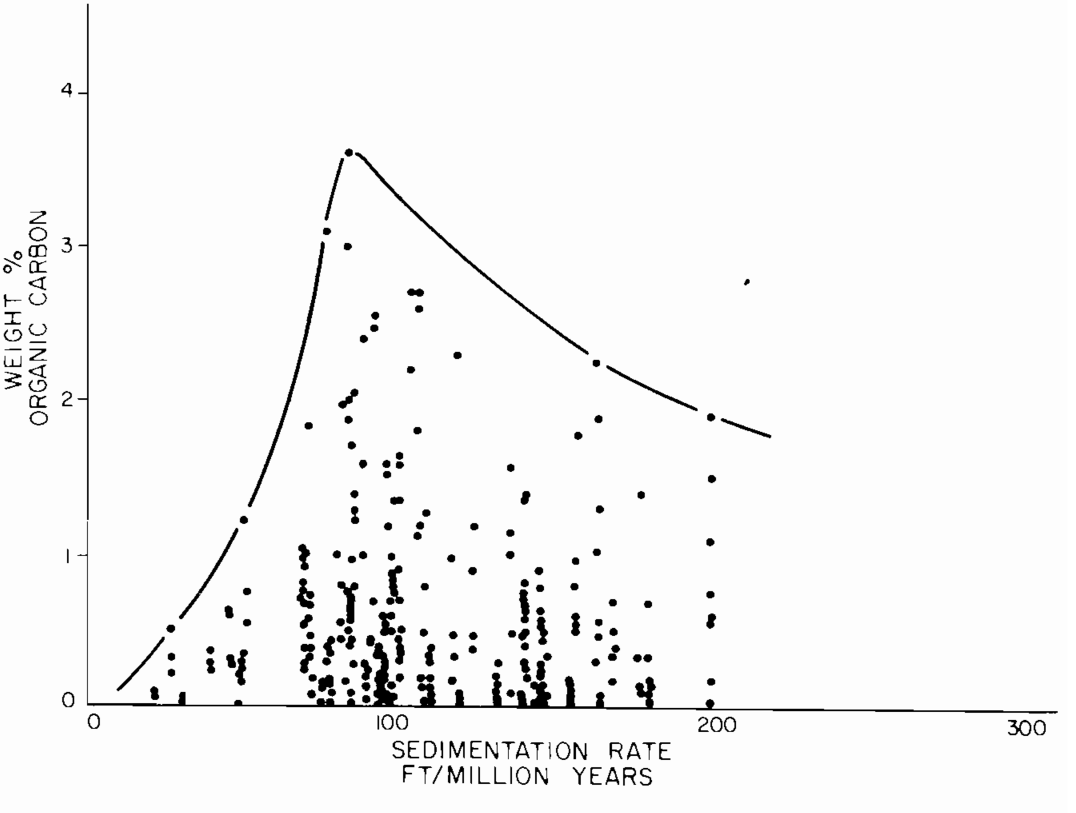

Fig. 73. Graph showing relationship between organic carbon % and sedimentation rate for Paleozoic rocks in Palo Duro and Midland Basins of Texas. Data from Dutton (1980).

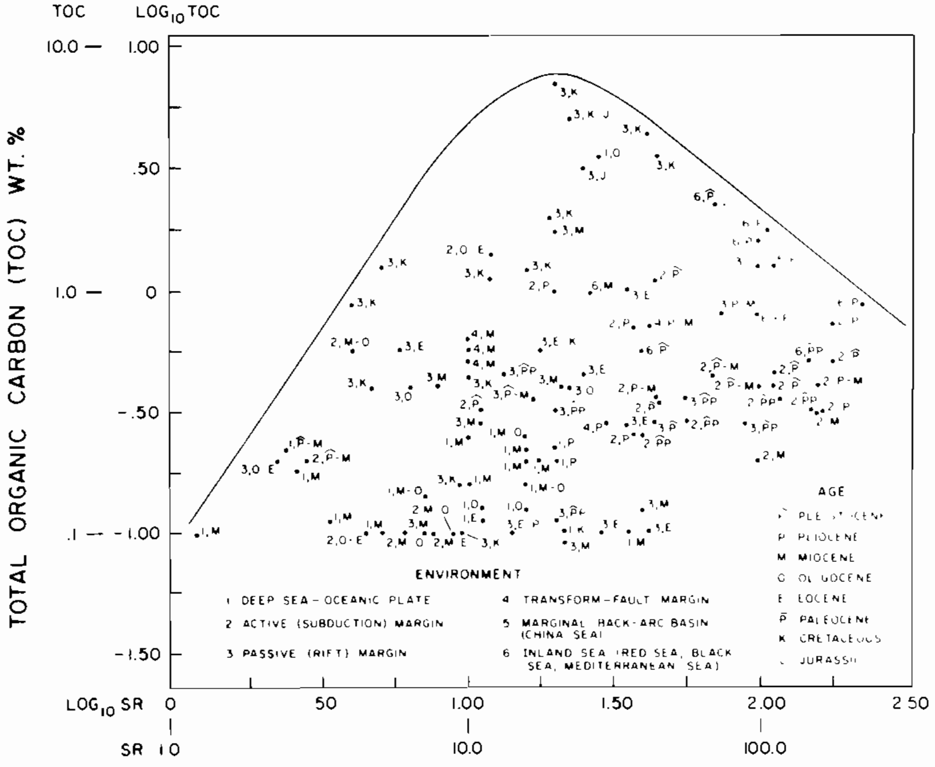

Fig. 74. Relationship between total organic carbon % and sedimentation rate from Deep Sea Drilling Project data: depositional environment and geologic age (from Ibach 1982). Courtesy of American Association of Petroleum Geologists.

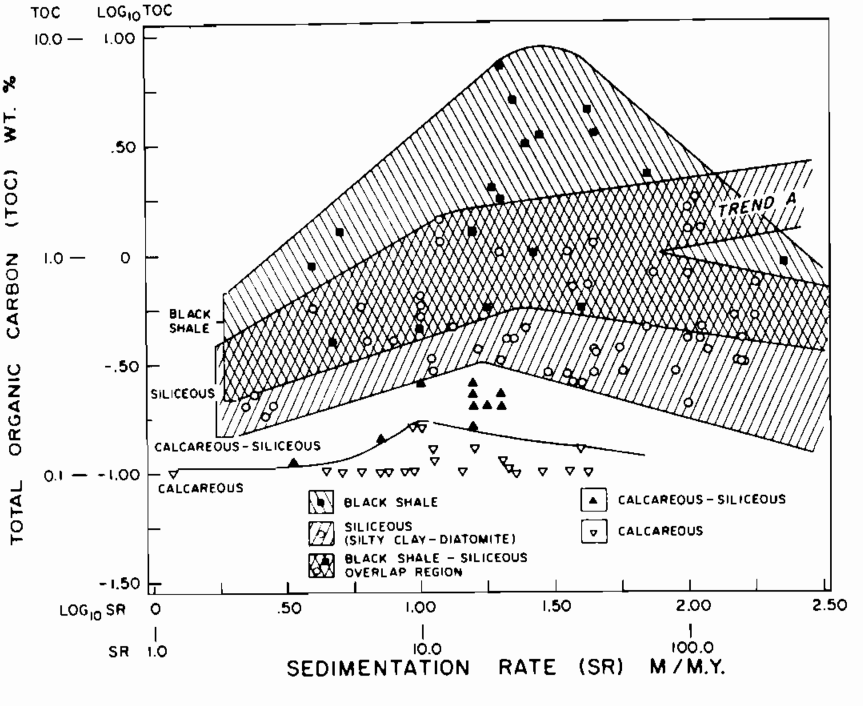

Fig. 75. Relationship between total organic carbon % and sedimentation rate from Deep Sea Drilling Project data: lithologic field zonation (from Ibach 1982). Courtesy of American Association of Petroleum Geologists.

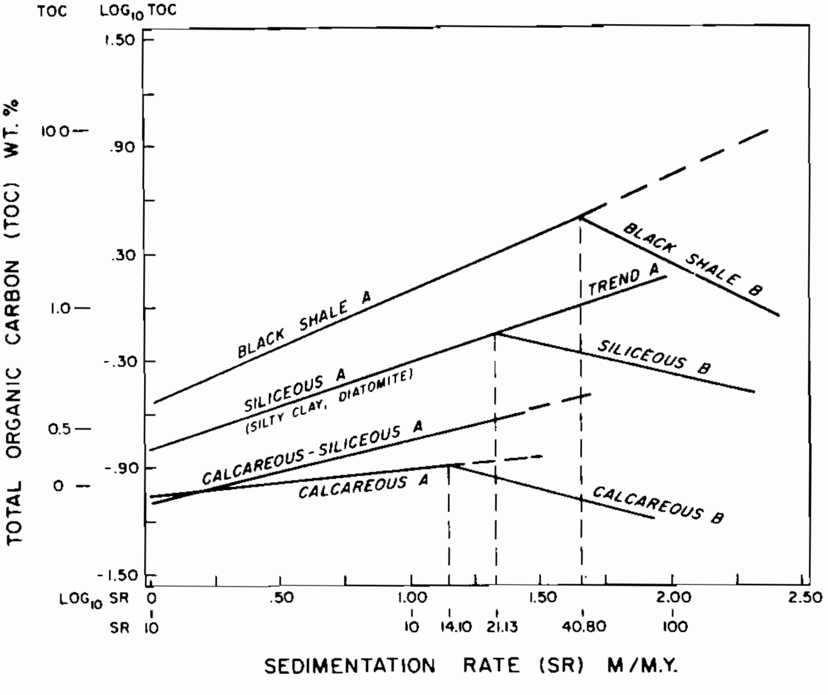

Fig. 76. Relationship between total organic carbon % and sedimentation rate from Deep Sea Drilling Project data: summary of lithologic field zonation (from Ibach 1982). Courtesy of American Association of Petroleum Geologists.

In all the examples shown above (Fig. 72-76), there seem to be optimum rates of sedimentation for accumulating the maximum organic carbon%. The optimum sedimentation rate may vary on changing environment of deposition.

For the oil producing regions in the Middle East, only a few data of organic carbon % have been reported. Figure 77 shows the isopach map of the Callovian and Oxfordian (Jurassic) source rocks in the Arabian Gulf with the total organic carbon greater than 1%. The thickest area is located in the middle of this Figure (see the 300 ft contour line) and corresponds approximately to the sedimentation rate of 70-85 ft/million years (Fig. 78, showing the average rate of sedimentation of the Jurassic formations).

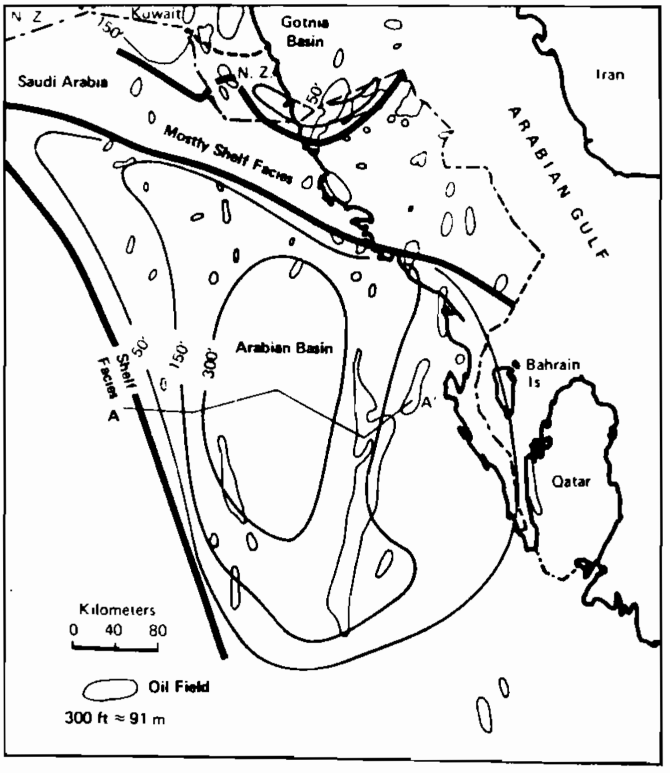

Fig. 77. Isopach map of Callovian and Oxfordian source-rock facies with total organic carbon ≧ 1 wt % (from Ayres *et al.* 1982). Courtesy of American Association of Petroleum Geologists.

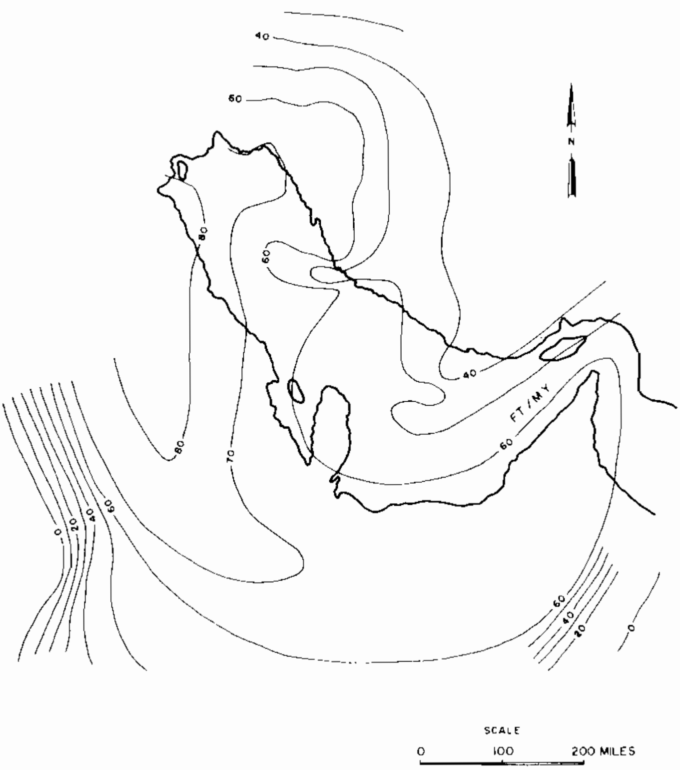

Fig. 78. Map showing average rate of sedimentation (ft/million years-M.Y.) of Jurassic formations in Arabian Gulf region.

It may be summarized that the optimum sedimentation rate for accumulating organic matter in the Jurassic source rocks in the Arabian Gulf region ranges between about 70 and 85 ft/million years which is not far from those obtained in the other regions.

The average sedimentation-rate maps of both the Cretaceous and Tertiary formations shown in Figs. 79 and 80 suggest a few potential source areas in this region, based on the 70-85 ft/million years sedimentation rate; for Cretaceous, near the head of the Gulf (near Kuwait) and the middle of the Rub al Khali Basin, and for Tertiary, the central part of the Gulf.

If a burial history plot is constructed in an area, it is possible to calculate the rate of burial (or sedimentation) and to relate it to the possible percentage of organic carbon which is an essential factor for the petroleum assessment.

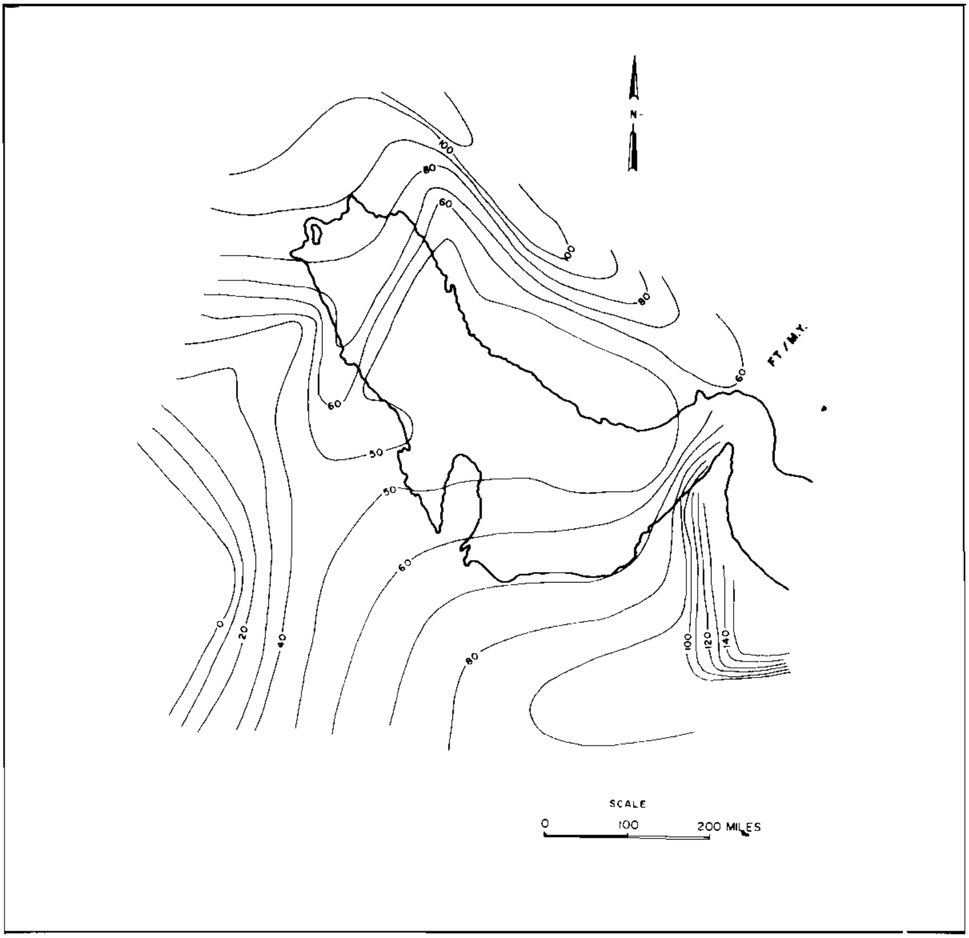

Fig. 79. Map showing average rate of sedimentation (ft/million years-M.Y.) of Cretaceous forrr ations in Arabian Gulf region.

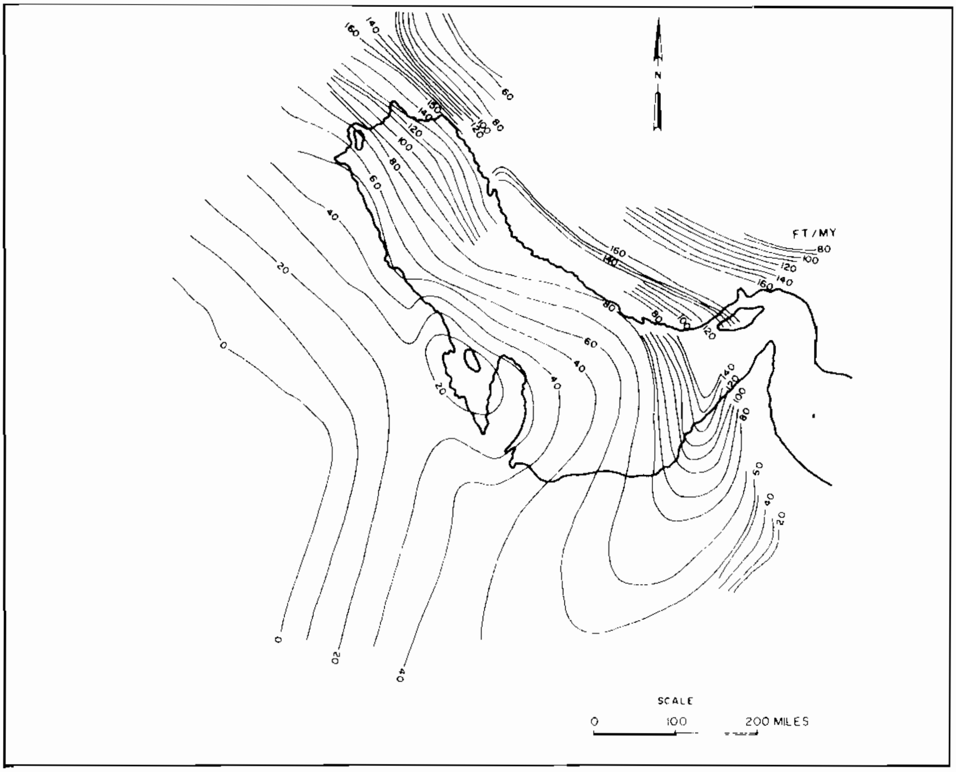

Fig. 80. Map showing average rate of sedimentation (ft/million years-M.Y.) of Tertiary formations in Arabian Gulf region.

Types of Organic Matter

To identify organic matter types, a van Krevalen-type diagram, in which H/C and O/C ratios from the elemental analysis are plotted, can be used. An example is shown in Fig. 81. The same plot can also be used for estimating level of organic maturation (see Chapter 7).

Three types which can be identified from the plot are types I, II, and III. Type I refers to kerogen having originally a high hydrogen content and a low oxygen content. This type of kerogen may be derived from an accumulation of algae. The well known Green River shales of Colorado and Utah belong to this type (Tissot 1977).

Type II refers to kerogen having a slightly lower hydrogen content than that of type I. This type may be derived from marine phytoplankton and zooplankton deposited in a confined environment. The Cretaceous source rocks of the Middle East belong to this type (Tissot 1977). Type III has a low original hydrogen content and a high oxygen content, and thus is usually considered as a prime gas source rather than an oil source. This type is primarily of terrestial origin.

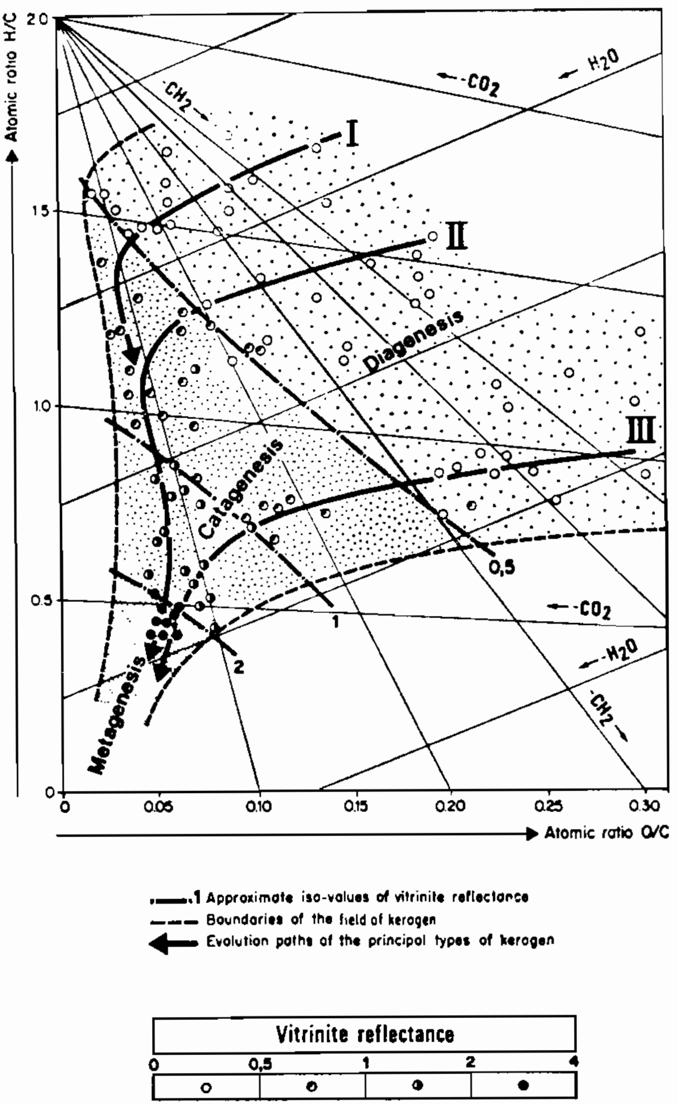

Fig. 81. Scheme of kerogen evolution based on elemental analysis results. Principal stages of petroleum generation and corresponding vitrinite reflectance values are shown for three main types of organic matter I, II, and III (from Tissot and Welte 1978). Courtesy of Springer-Verlag Berlin.

A similar interpretation of organic matter types can be made from the result of pyrolysis (see Fig. 68 in Chapter 7).

Visual identification under microscope is also commonly made in the petroleum industry. They sometimes identify three types, such as amorphous, cuticular, and woody or coaly organic matters, which may be correlated with types I, II, and III, respectively.

Problems

1. Explain the reason why the source rock and its organic concentration are the most important factors in accumulating petroleum.
2. What are the giant oil and gas fields?
3. Explain the relationship between the sedimentation rate and organic matter concentration.
4. Explain three types of organic matter which can be identified by the elemental analysis result.

Chapter 9

Petroleum Generation, Maturation, and Migration in Arabian Gulf Region

Introduction

Previous chapters describe the fundamental concepts of reservoir, trap, cap rock, primary and secondary hydrocarbon migration, hydrocarbon generation and maturation, and organic richness of source rock. In evaluating these geologic factors, we would need a substantial amount of subsurface data which are usually available after extensive drilling. However, for discovering a new oil field, such evaluation must sometimes be made with a limited amount of data which is available at that time. Before extensive drilling, data is usually scarce.

Even at a very early stage of oil exploration, a geologist would usually be able to work with at least two basic data ; 1. regional stratigraphy from the surface exposures which would provide him with a broad understanding of geologic ages and rock types involved, and 2. regional seismic sections which can be used in interpreting the subsurface structure.

Using these data, he would be able to construct a series of burial history plots of selected anticlinal and synclinal locations. The slope of a burial line would give him an idea of the burial or sedimentation rate, which could further suggests possible organic richness of the sediment (Chapter 8). The burial history data from the synclinal area is most valuable in this respect, because the syncline covers a greater area and is usually more mature than the anticline. If information of depositional environment and lithology is available, his prediction on organic richness would be improved.

Maturity of organic matter can also be estimated from the burial history plot, using Lopatin's method described in Chapter 7. Similar to the organic richness, the data from the synclinal area would be most useful for the maturity estimate. Regional geothermal gradient must be estimated or at least guessed for this work.

The difference of the burial rates between the anticlinal and synclinal locations would give ideas on the trap timing (Chapter 3) and secondary migration (Chapter 5). Primary migration may also have been influenced by burial which could cause sediment compaction and aquathermal fluid migration (Chapter 6).

If the pressure seal* is involved in this area, then both time and depth of the pressure seal development can be estimated by the method described in Chapter 4, using the burial history plot.

In short, except for the reservoir property, all the other geologic factors for forming a petroleum deposit (Fig. 2 in Chapter 1) can be evaluated through the use of the burial history plot. An important advantage of this method is that the evaluation can be made at a very early stage of exploration.

Following section will described examples of practical application of the method for estimating petroleum generation, maturation, and migration in the Arabian Gulf region.

Application for Arabian Gulf Region

Application of Lopatin's method for this region was made by Sail and Magara (1985), using the regional isopach maps constructed by Kamen-Kaye (1970). The isopach maps and the cumulative isopach maps which were made from the original isopachs can be used for understanding primary and secondary migration, as well as for petroleum generation and maturation.

At the time of primary migration, the generated hydrocarbons would have moved from a point of more excess fluid pressure due to sediment loading to a point of lesser one (see Chapter 8 of the book by Magara 1978c). Such a variation of sediment loading can be inferred from the study of the regional isopach maps. At the secondary migration stage, most hydrocarbons are believed to have moved from a paleo-structural low to a high due to the buoyancy effect. The cumulative isopach maps mentioned above will show the paleo-structural features. The stages of petroleum generation and maturation can also be estimated from the cumulative isopach maps.

Sail and Magara (1985) estimated both TTI and R_0 of the Jurassic base at various geologic stages in this region. Until the burial stage of the end of Cretaceous, most of the region showed immature or early mature stage at which only heavy oil generation could be expected. The major oil generation for the Jurassic formations was attained during the Tertiary period. Figure 82 shows the estimated stages of petroleum generation and maturation along with the burial contour map and R_0 values, at the end of Tertiary. Figure 83 shows a map of excess fluid pressure due to the Tertiary-sediment loading, which can be used to interpret the directions of primary hydrocarbon migration (The general direction is from northeast to southwest).

---

* Pressure seal may be identified from seismic interval velocity data which is usually shown at top of each seismic section.

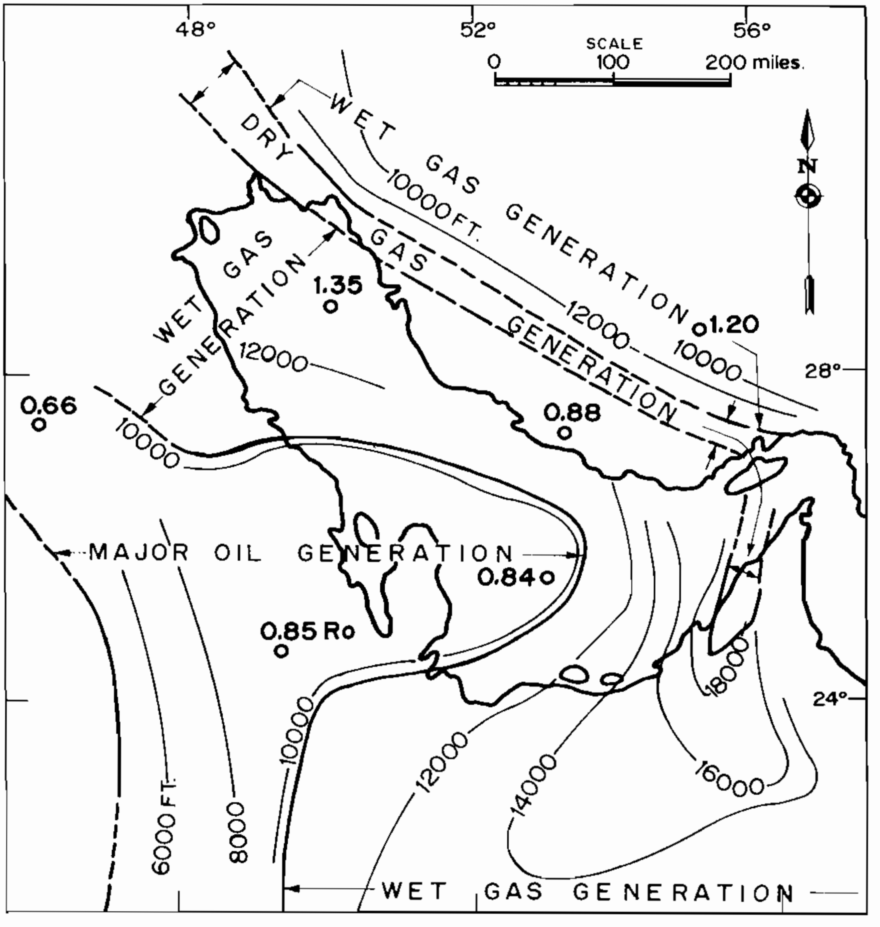

Fig. 82. Map showing hydrocarbon-generation zones of basal Jurassic formation at end of Tertiary period (from Sail and Magara 1985).

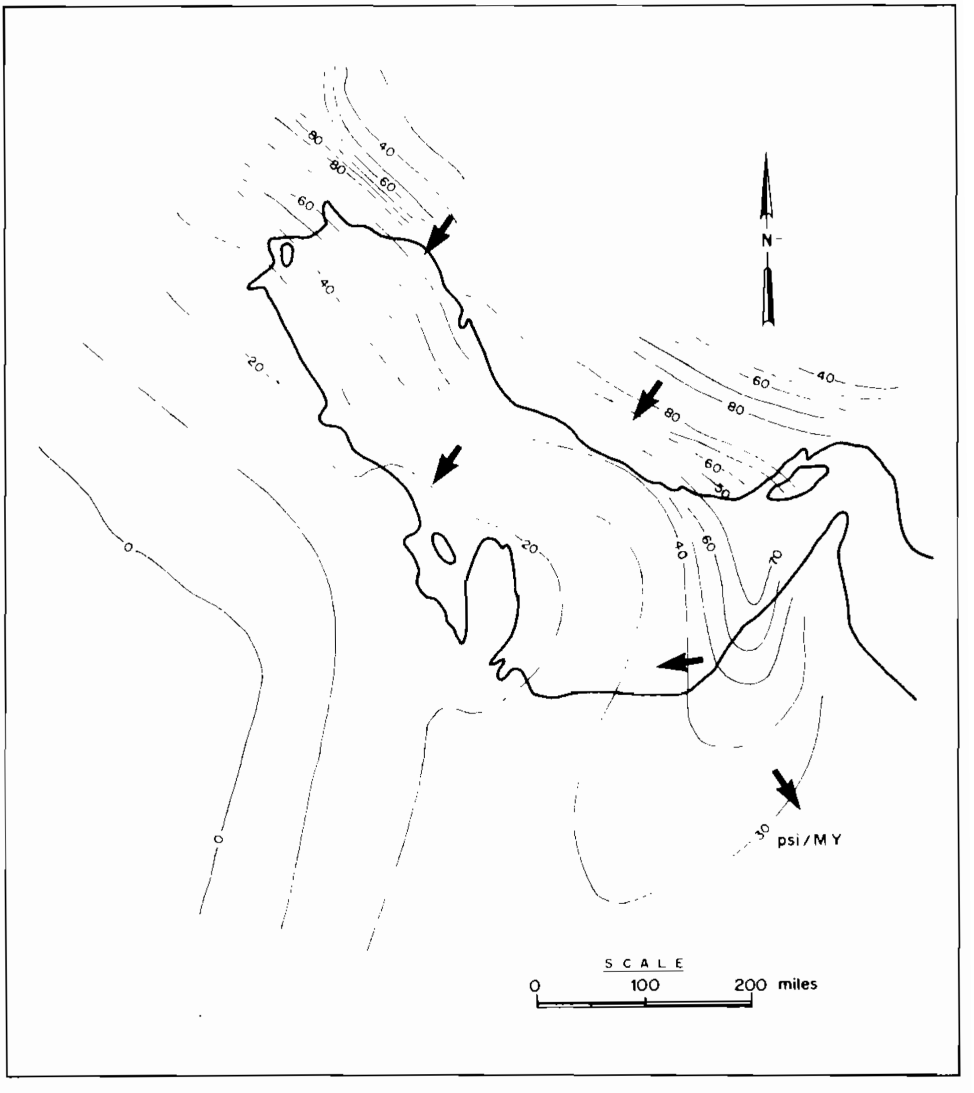

Fig. 83. Map showing rate of excess fluid potential increase (psi/million years-M.Y.) during Tertiary period in Arabian Gulf region. Arrows show inferred directions of primary hydrocarbon migration.

A comparison of the presence of the oil accumulations in the Jurassic formations with the estimated maturation stages is demonstrated in Fig. 84. Most of the oil fields fall in the area of the major oil generation.

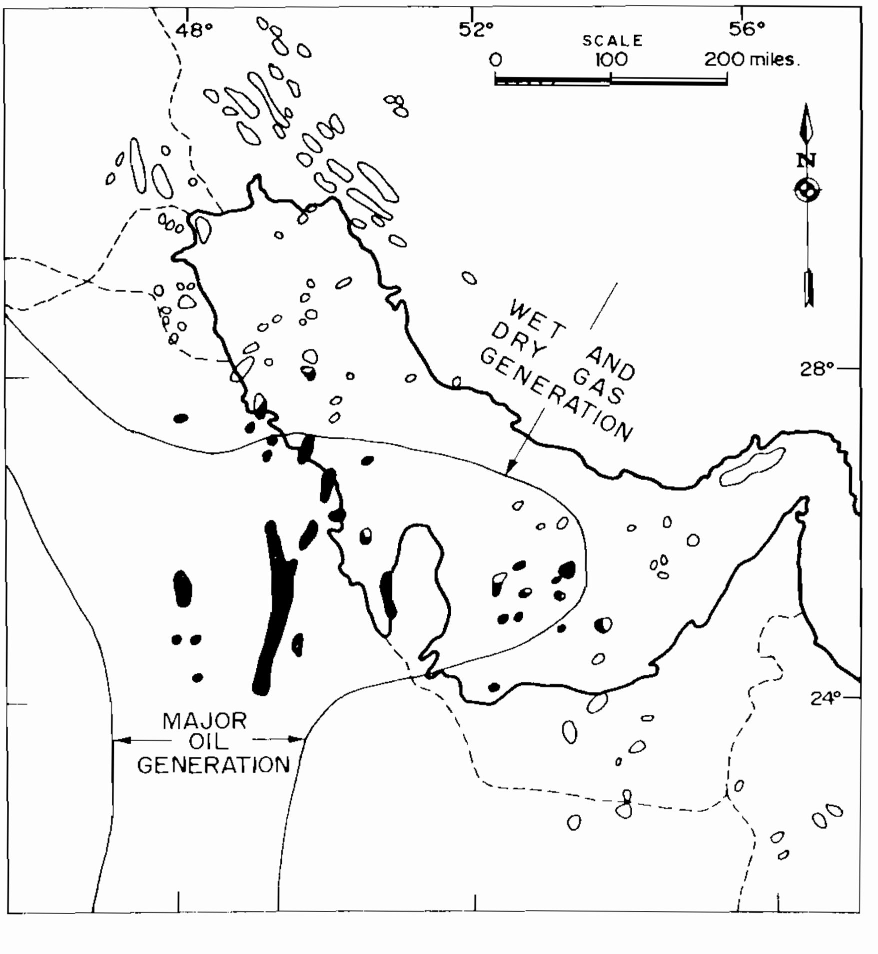

Fig. 84 Superposition of hydrocarbon-generation zones of basal Jurassic formation (Fig. 82) over oil field distribution map (Sail and Magara 1985).

Figure 85 shows a similar maturation map for the base of the Cretaceous formations at the end of the Tertiary period. The oil generating area covered the central part of the Arabian Gulf where most oil reservoirs of this age exist (Fig. 86). The general direction of primary migration in this period is the same as that shown in Fig. 83.

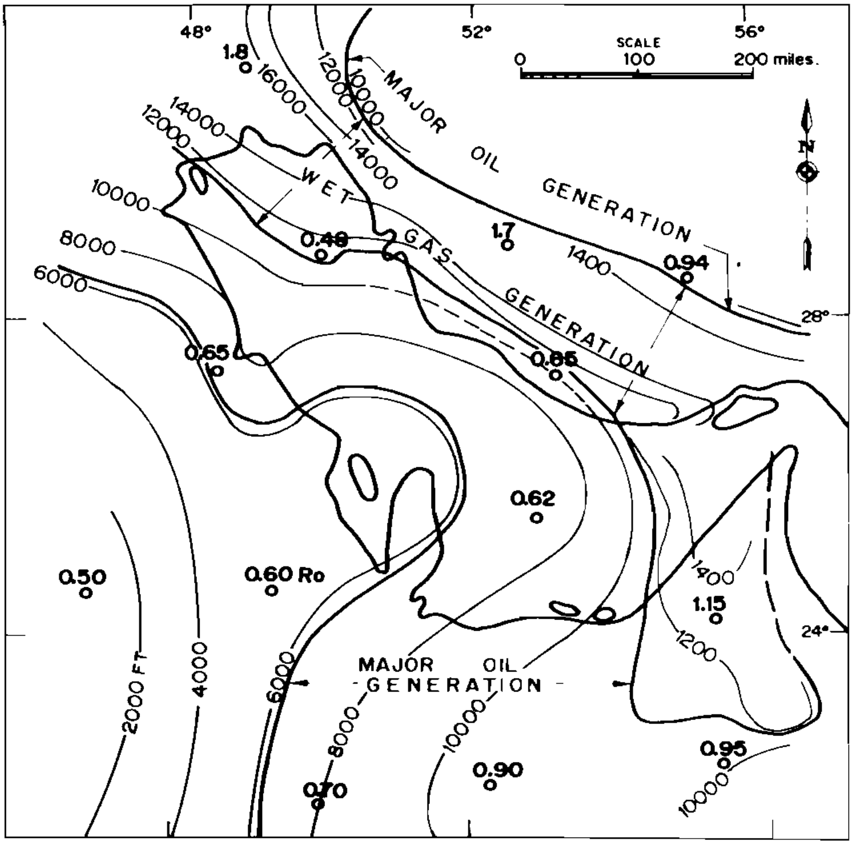

Fig. 85. Map showing hydrocarbon-generation zones of basal Cretaceous formation at end of Tertiary period in Arabian Gulf region (Sail and Magara 1985).

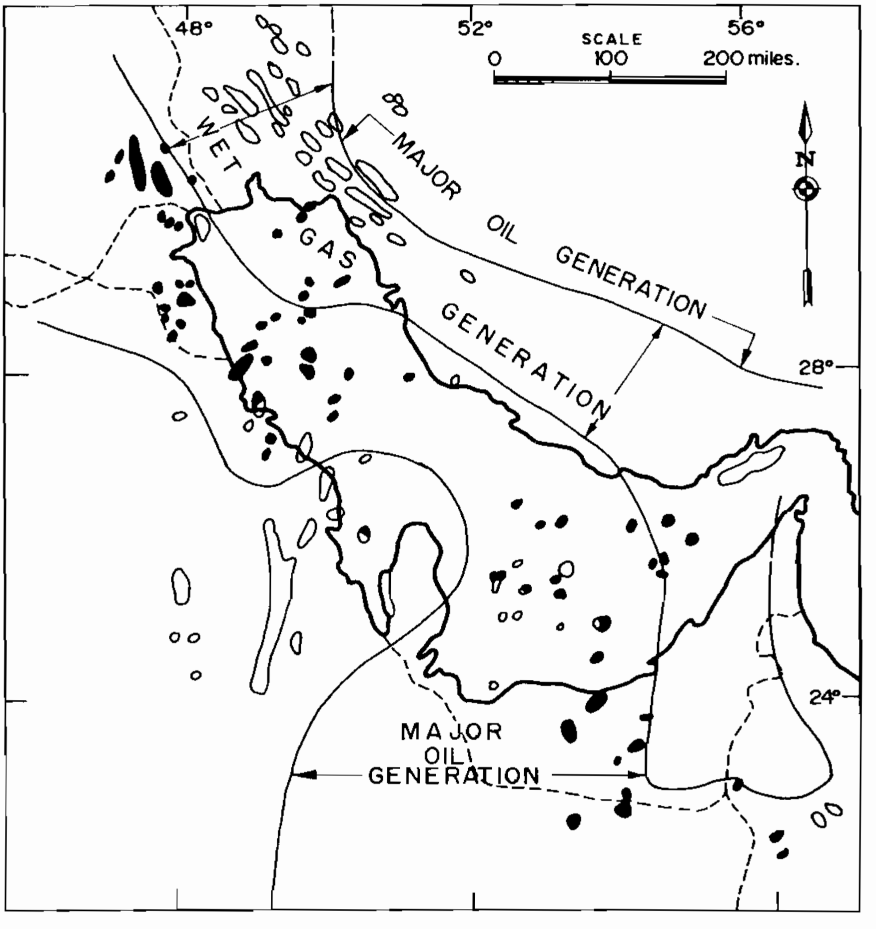

Fig. 86. Superposition of hydrocarbon-generation zones of basal Cretaceous formation (Fig. 85) over oil field distribution map (Sail and Magara 1985).

Figure 87 is a maturation map of the base of the Tertiary formations at the end of Tertiary, showing the major oil generation in the Zagros Mountain foothills. Most of the oil fields in the Tertiary formations fall within the Tertiary oil generation area (Fig. 88), with some exceptions caused by vertical oil migration from deeper source rocks.

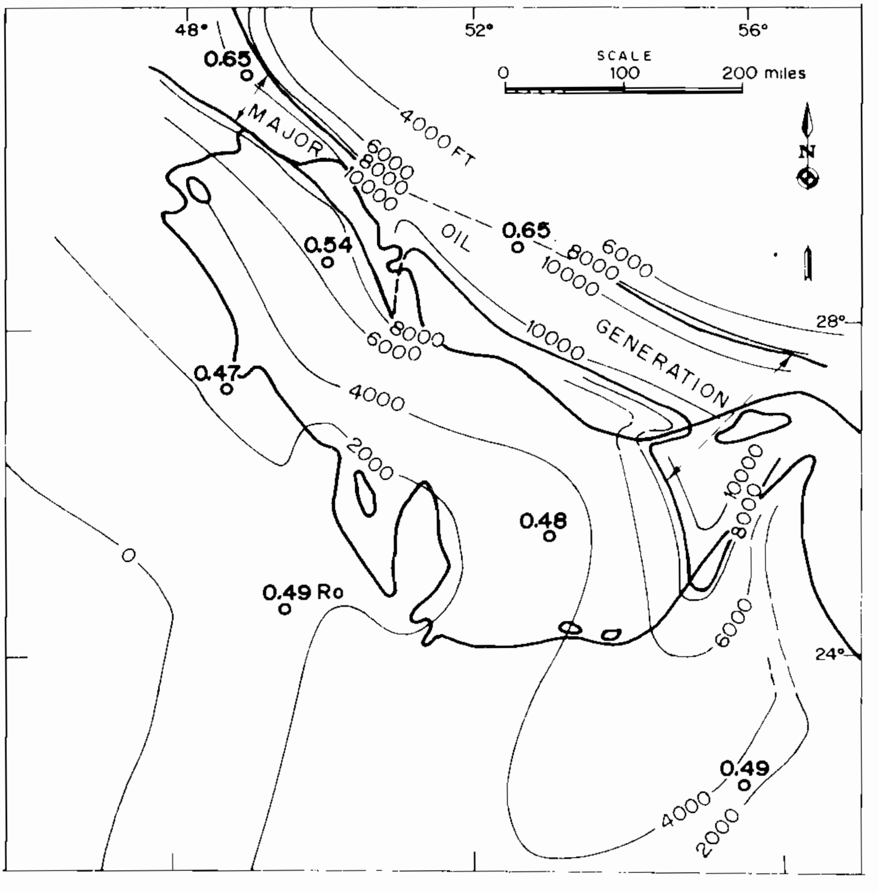

Fig. 87. Map showing hydrocarbon-generation zones of basal Tertiary formation at end of Tertiary period in Arabian Gulf region (Sail and Magara 1985).

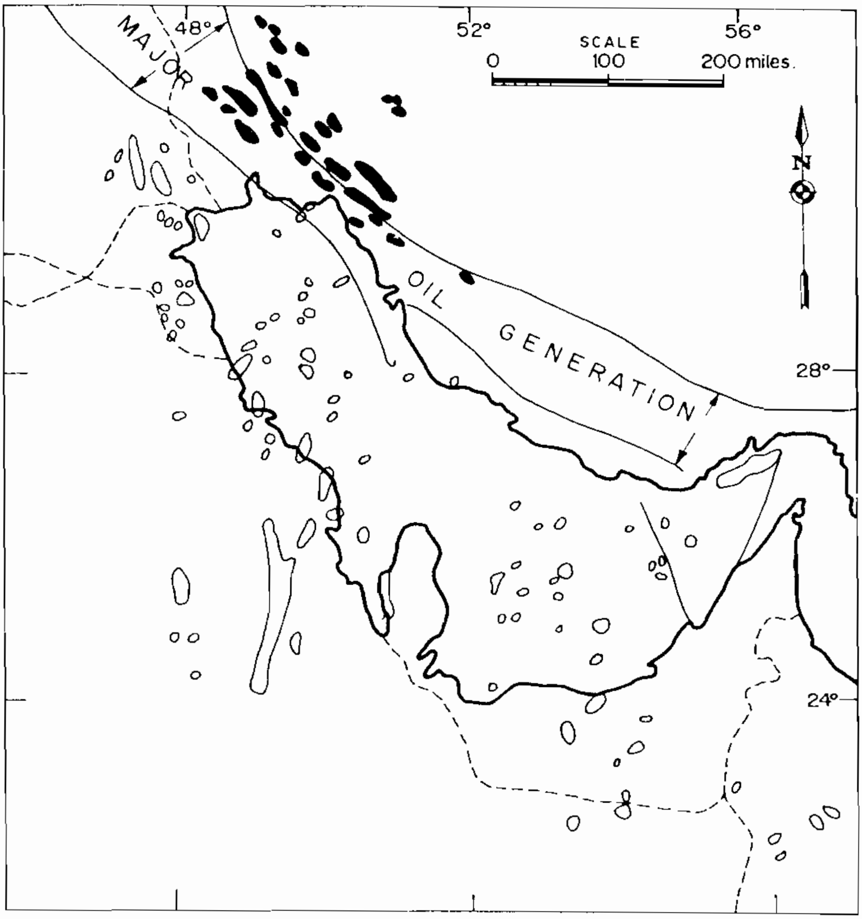

Fig. 88 Superposition of hydrocarbon-generation zones of basal Tertiary formation (Fig. 87) over oil field distribution map (Sail and Magara 1985).

Problems

1. Explain the methods of using a burial history plot for the estimations of organic richness, primary and secondary migration, hydrocarbon generation and maturation, timings of trap and cap rock formations.
2. Describe the major source areas for the Jurassic, Cretaceous, and Tertiary oil fields in the Arabian Gulf Region.
3. Show the principal and regional direction of primary hydrocarbon migration in the Arabian Gulf during the Tertiary period.

Chapter 10

Importance of Lithological Factors in Accumulations of Oil in Saudi Arabia

Introduction

In 1978, a theoretical model for predicting the optimum reservoir percentage for oil accumulations was proposed by Magara (1978b). This model is based on the average reservoir thickness, the frequency of interbedding of the reservoirs, and the average thickness of cap or source rock facies.

A computer program was written to calculate and plot the result, which was then compared with the occurrences of oil in the Jurassic formations of Saudi Arabia.

Because of the confidential nature of the subsurface reservoir data of this region, only the lithological data from the type localities (Powers *et al.* 1966), whose depositional environments are greatly different from those of the oil producing areas, were used for this study. Because of this reason, the validity of the result obtained may be in question in some cases. Nevertheless, both the model and the computer program seem to have a great potential for future applications.

Reservoir Thickness and Oil Accumulation

Curtis *et al.* (1960) proposed a statistical relationship between the ultimate recoverable oil in a sandstone and its average gross thickness, based on 7,241 reservoirs in the United States. Gas in the reservoirs was converted to an oil equivalent. In 1971, Smith *et al.* showed this relationship in a graphical form (Fig. 89), in which the original data are depicted by four horizontal lines and the average relationship is shown by a diagonal solid line (Recoverable Oil).

The mathematical form of the relationship given by Smith *et al.* is as follows :

$$I_o = C \cdot Y^2 \tag{18}$$

where c I_o, is oil in place, Y the average thickness of sandstones, and C the constant. The broken straight line in this figure indicates this relationship (Estimated In-Place Oil), suggesting that the volume of either the in-place oil or the recoverable oil is proportional to the square of the average thickness of sandstone.

Let us assume that there is a reservoir model whose width and length will be doubled when the thickness is doubled. The volume of the reservoir body, and possibly the total pore space of the reservoir, will increase in this case by a factor of eight. If the total pore space is the most important factor in determining the volume of oil, the oil reserve must increase by a factor of eight when the thickness becomes doubled.

The statistical evidence that the reserve increases by a factor of only four when the thickness is doubled suggests that the most important factor in determining the oil reserve is the contact area between the reservoir body and the surrounding rocks. This model seems to be quite reasonable if the main hydrocarbon source was in the surrounding rocks and the hydrocarbons were expelled from them during compaction and primary migration. The fluid expulsion efficiency would generally increase as the contact area increases.

If, on the contrary, the surrounding rocks are cap or sealing rocks, the contact is also very important in keeping the oil in the reservoir. Incorporation of possible minimum thickness of the effective cap rocks with the model may permit us to predict the optimum percentage of reservoir facies for oil accumulations.

If a different model is assumed, whose width and length do not become doubled when the thickness is doubled, the situation would be different. Such a case may be inferred from the range of accumulated oil for a certain reservoir thickness, as shown in Fig. 89.

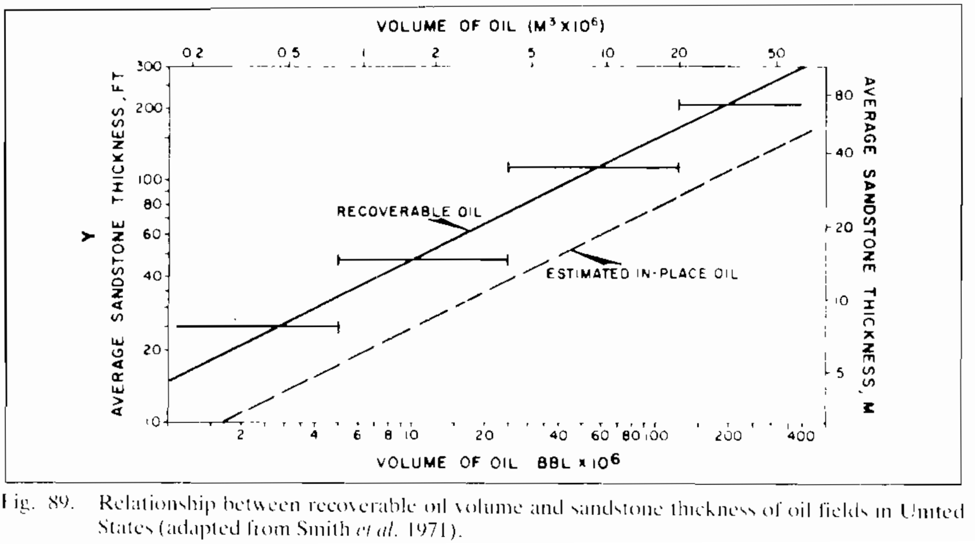

Fig. 89. Relationship between recoverable oil volume and sandstone thickness of oil fields in United States (adapted from Smith *et al.* 1971).

Cap Rock-Reservoir Model

In the former Magara's model, a combination of sandstone reservoirs and shales (source rocks) was considered. In this chapter, a combination of one of reservoirs (calcarenite, dolomite, sandstone, and porous limestone) and one of cap rocks (anhydrite, shale, or may be tight limestone) is used. The total thickness of the unit is 1,000 ft (Fig. 90), where a changing number of reservoirs are inserted. The reservoir thickness in this case is 40 ft.

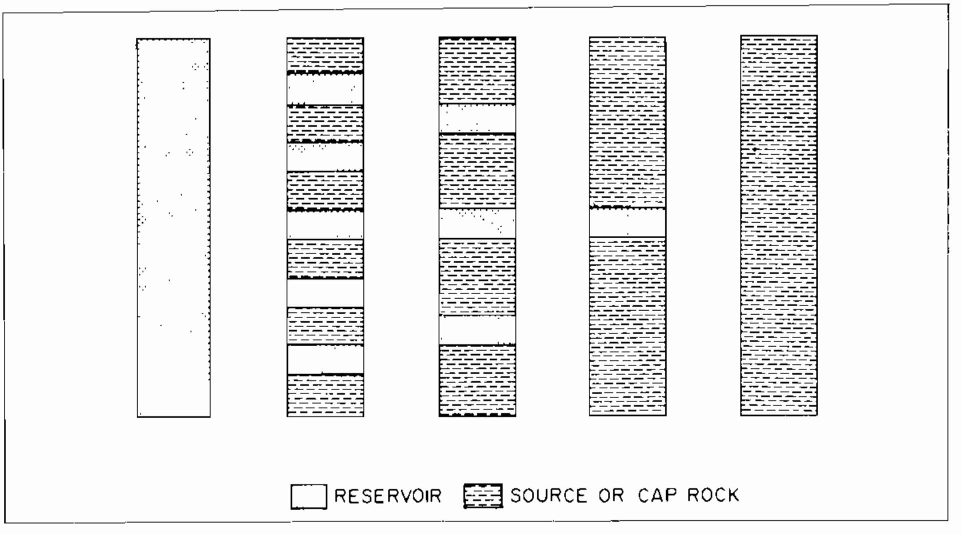

Fig. 90. Reservoir - cap rock model. Refer to text for explanation (from Magara 1978b). Courtesy of Canadian Society of Petroleum Geologists.

Changing reservoir percentage due to the change of the number of reservoir beds is shown in the top diagram of Fig. 91. The average thickness of the intercalating rocks will decrease as the number of the reservoirs or reservoir percentage increases. This situation is depicted in the middle diagram of Fig. 91. Although the average thickness of the intercalating rocks for a lower reservoir percentage is relatively large, only a certain minimum thickness is necessary for preventing the possible vertical leak of oil. For the following discussion, let us assume an arbitrary cut off of 100 ft, as shown by a solid line in the middle of the diagram (Fig. 91). With the cap-rock thickness less than 100 ft, oil can still be trapped but with less efficiency.

In the bottom diagram of Fig. 91, a product of the number of reservoirs and thickness of the intercalating beds (cap rocks) with a 100 ft cut off is depicted, to indicate the probability of having a proper combination of reservoirs and cap rocks. In this example, the product is maximum when the reservoir percentage is about 30.

A computer program predicting the optimum reservoir percentage was written and shown in Appendix C. Input parameters of the program are the average reservoir thickness and the minimum effective thickness of cap rocks.

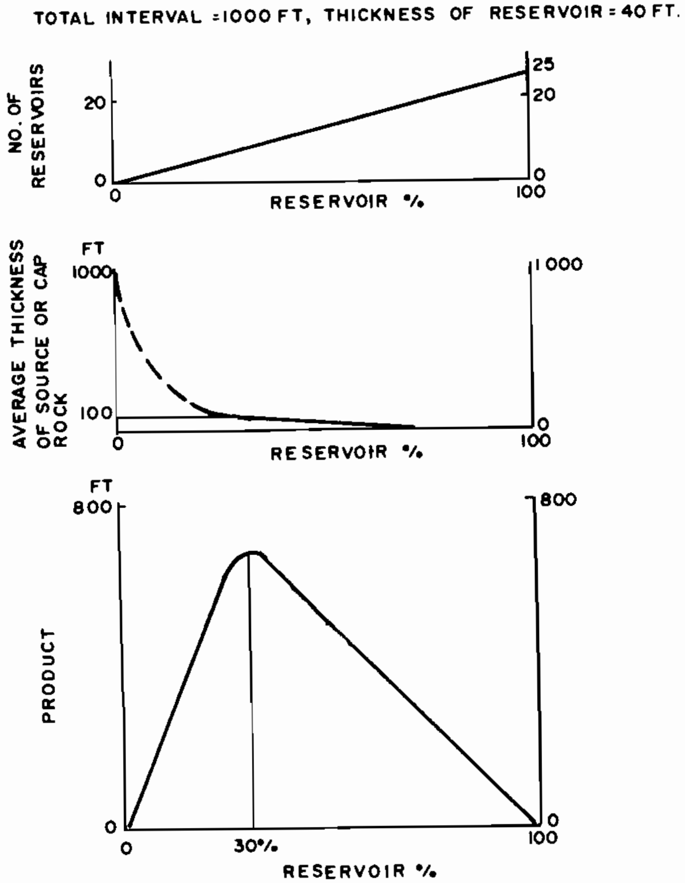

Fig. 91. Graph showing result of sample calculations using reservoir - cap rock model shown in Fig. 90 (adapted from Magara 1978b). Courtesy of Canadian Society of Petroleum Geologists.

Application for Jurassic Formations in Saudi Arabia

The average reservoir and cap rock thicknesses were obtained from the data of the type sections defined by Powers *et al.* (1966). The reservoirs include calcarenite dolomite, and sandstone, and cap rocks include anhydrite, shale, and aphanitic limestone. For the reservoir thickness, the average value for each formation was used. The minimum thickness of cap rocks for effective sealing was estimated to be 8 ft for anhydrite and 30 ft for other lithologies. The summary of the inputs and outputs for computer runs is included in Table 4.

Figure 92 shows the calculated product value corresponding to the actual reservoir percentage for each of the Jurassic formations. The number of the major oil reservoirs in each formation is also shown. Figure 92 shows a general agreement between these two plots, except the Marrat Formation, in which there is a chance of over-maturation. Oil in Marrat may have been converted to gas by the thermal effect.

Table 4. Inputs and outputs of computer runs for Jurassic formations in Saudi Arabia. *See* text for explanation.

Formation	Reservoir Thickness, ft	Cap Rock Thickness, ft	Maximum Product	Corresponding Reservoir %	Actual Reservoir %	Corresponding Product
Arab	4	8	640	35	51	520
Jubaila	40	30	400	57	62	400
Hanifa	30	30	480	55	63	400
Twaiq Mountain	30	30	480	55	20	160
Dhruma	10	30	720	28	18	470
Marrat	15	30	640	35	31	580

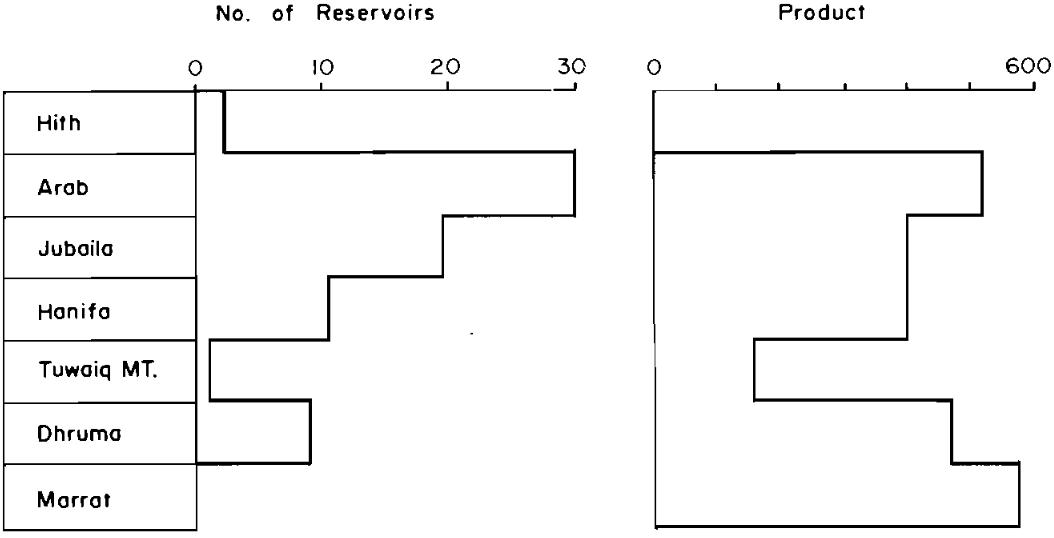

Fig. 92. Comparison of number of major oil reservoirs and computer-generated "product" of Jurassic formations in Saudi Arabia (from Huwaidi 1984).

Using Powers *et al.* (1966) data, the average thicknesses of each lithology of the Jurassic formations were estimated.

Lithology	Thickness, ft
Calcarenite	4
Dolomite	7
Sandstone	17
Limestone	13
Shale	20
Anhydrite	8

Using these thicknesses and the minimum effective cap rock thickness of 8 ft for anhydrite and 30 ft for other cap rocks, a series of the computer runs based on several hypothetical combinations of reservoirs and cap rocks were made as follows :

Reservoir	Cap Rock	Maximum Product
1. Calcarenite	Anhydrite	640
2. Sandstone	Shale	640
3. Dolomite	Anhydrite	480
4. Dolomite	Limestone	720
5. Calcarenite	Shale	880
6. Limestone	Anhydrite	360
7. Calcarenite	Limestone	840

The result indicates that, except items 3 and 6, the product value is more than 640. In such cases, a good combination of both reservoir and cap rock can be expected. To form an oil accumulation, of course, other factors such as a proper trap, high reservoir quality, high organic concentration, and proper maturation are also necessary.

As mentioned earlier in the chapter, the lithological data were derived from the type localities whose depositional environments are greatly different from those of the oil producing areas of the Kingdom. It would be desirable in the future that the same program will be applied for the data from the oil producing areas.

Lithological Composition of Jurassic Formations in Saudi Arabia

Using the lithological data of the Jurassic type sections in Saudi Arabia defined by Powers *et al.* (1966), a triangle plot was made by computer for each formation and for the entire Jurassic formations. This computer program not only plots the composition on the ratio-triangle graph, but also calculates the D-function and the relative entropy function described by Forgotson (1960). A value of the D-function closer to 100 (or the entropy function closer to 1) suggests relatively an even mixture of three lithological components (non-clastic rocks, sandstone, and shale in these cases), while a smaller value means that the composition belongs more or less to a single end-member (or component). Appendix C2 shows the computer program written for the I.B.M. Personal Computer.

Figures C3 to C9 in Appendix show the triangle plots for the Marrat, Dhruma, Tuwaiq Mountain, Hanifa, Jubaila, Arab, and the entire Jurassic formations, respectively. Note that a plot for Hith was not made because it is composed of 100% *anhydrite (non-clastic).*

Problem

Explain the relationship between the recoverable oil volume and gross sandstone thickness, based on the 7,241 reservoirs in the United States.

Chapter 11

Computer Applications for Oil Reserve and Resource Evaluations

- Introduction.
- Volumetric Monte Carlo simulation.
- Organic geochemical Monte Carlo simulation.
- Areal simulation of Random drilling.
- Problems

Introduction

Search for a petroleum deposit is fundamentally a scientific and technical matter, which can be handled by petroleum geologists working in the petroleum industry. Most of the basic problems involved in the search of petroleum were discussed in the preceding chapters of this book.

In the actual exploration, however, another important factor, economics, must also be considered. In this chapter, only a few economic problems will be discussed ; estimation of the recoverable oil/gas volume and of the discovery rate (success ratio) of exploration drilling.

Three computer programs using the random sampling method were developed ; 1. volumetric Monte Carlo simulation, 2. organic geochemical Monte Carlo simulation and 3. areal simulation of random drilling.

Volumetric Monte Carlo Simulation

In the petroleum industry, a method called "Monte Carlo simulation" has been widely used for assessing petroleum reserves and resources. In this method, a large number of trial calculations for oil reserves and resources is made using the computer-generated random numbers.

For each of the engineering and geological factors controlling a recoverable oil volume, we would be able to define a possible range and most probable value, such as "minimum", "maximum", and "most likely". Within each range, the computer generates values randomly. A set of randomly generated values of these engineering and geological factors will be used to compute a vlume of oil.

If a large number of random sampling is tried, then we would be able to expect to generate a large number of the assessed oil volumes, a distribution of which would give us the probability of finding oil pools.

Most natural events are known to be either normally or log-normally distributed. This type of distribution is usually shown by a bell-shaped curve (top of Fig. 93). The bottom diagram of Fig. 93 depicts a corresponding cumulative frequency curve. Using this type of distribution, we would be able to define the statistical minimum, most likely (or median), and maximum.

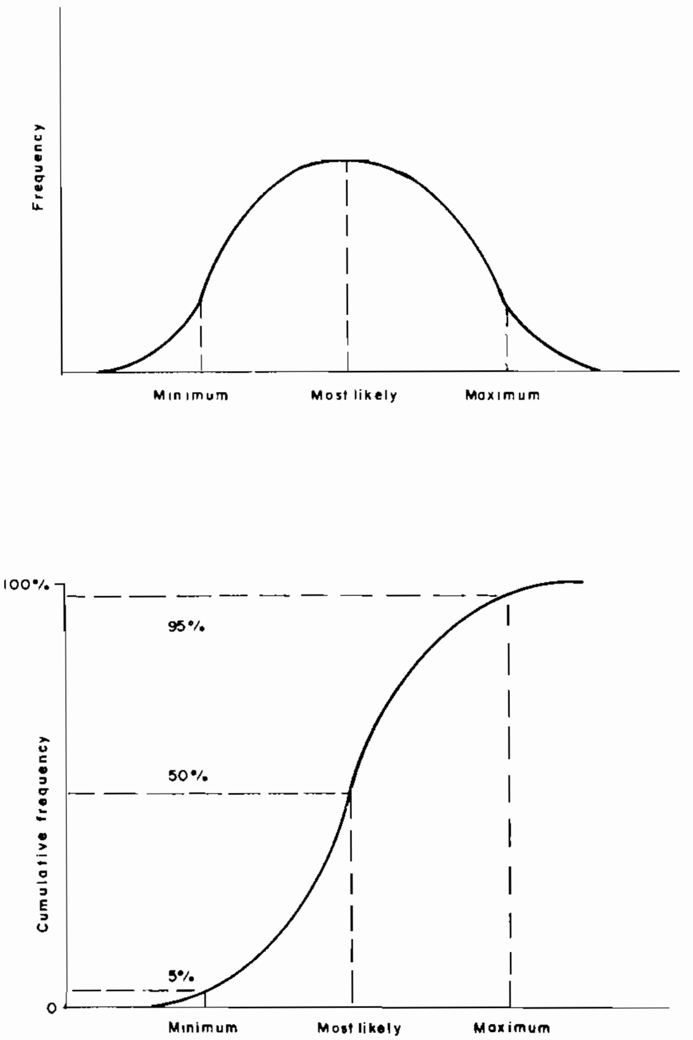

Fig. 93. Schematic diagram showing frequency and cumulative frequency distributions of a normally-distributed population.

In the available computer program, however, a simple triangle model shown in Fig. 94 is used. In this model, the computer generates random values of both engineering and geological factors, such as area of accumulation (A), thickness of reservoir (H), water saturation (S_w), porosity (ϕ), recovery efficiency (E_R), and formation volume factor (B_o), and then calculates recoverable oil volume (P) as follows,

$$P = A.H.(1 - S_w) \cdot \phi \cdot E_R / B_o \qquad (19)$$

The risked recoverable oil volume (P_R) can be given as,

$$P_R = A.H.(1 - S_w) \cdot \phi \cdot E_R (1 - F_R) / B_o \qquad (20)$$

where F_R is risk factor.

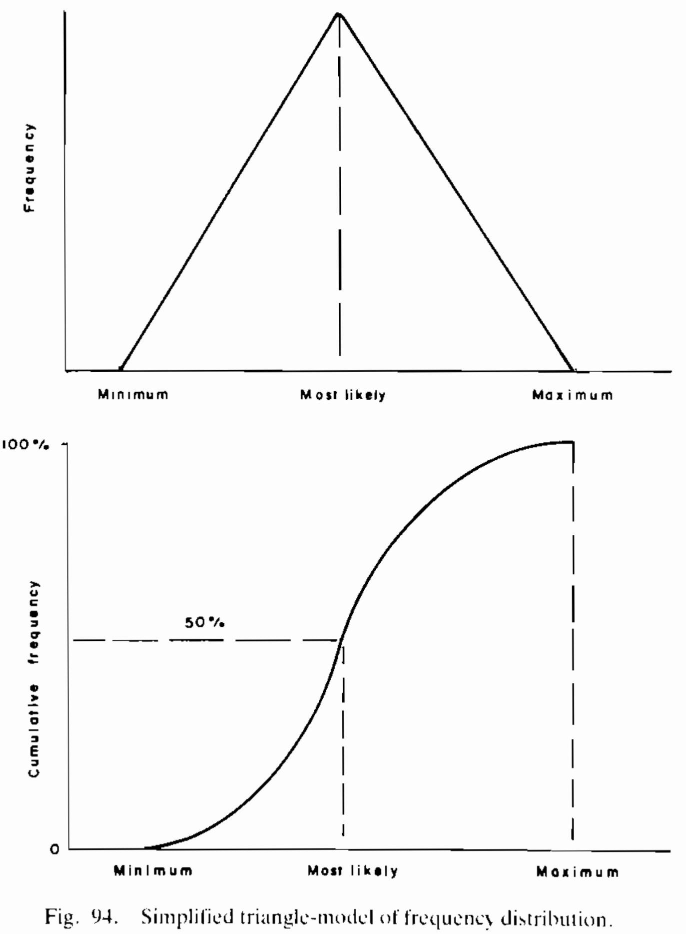

Fig. 94. Simplified triangle-model of frequency distribution.

The calculation is repeated by the computer a large number of times (usually 1,000 times or more, but because of the available small computer capacity, this program *repeats only 100 times*), *to* obtain a distribution of the assessed recoverable oil volumes. The oil volumes will then be arranged from small to large and the cumulative frequency distribution will be made. There are two cases of the probability distributions ; 1. based on cumulative number of cases, and 2. based on cumulative oil volume. They can be either risked or unrisked. The printout of the computer program, which was included in the M.Sc. Thesis by Huwaidi (1984), is shown in Appendix D1.

To conduct a sensitivity study of the model, a set of the standard input values was first determined.

	Minimum	Most likely	Maximum
Area, sq. km	29	30	31
Reservoir thickness, ft	150	180	200
Water saturation, %	9	10	11
Porosity, %	17	19	21
Recovery efficiency, %	30	33	35
Formation volume factor	1.05	1.08	1.11
Risk factor, %	40	50	60

Above hypothetical example simulates a relatively small oil field in the Kingdom of Saudi Arabia, containing about 500 million bbl of recoverable oil.

Secondly, a series of the computer runs were made for the sensitivity checks. In each run, most input factors stay the same as those used for the previous standard run, except only one factor which either increases or decreases.

Summaries of these computer runs are shown in Figs. 95-99. In each graph, the horizontal axis shows the field size in million bbl and the vertical axis indicates the probability of finding that field size or less.

1. Changing area (Fig. 95)

The reserve ranges from about 350 to 750 million bbl, with the median or most likely figure being between about 400 and 620 million bbl.

2. Changing reservoir thickness (Fig. 96)

The assessed values are ranging widely between about 390 and 620 million bbl for the most likely cases. The above results suggest that both the area and reservoir thickness have significant effects on assessment.

3. Changing water saturation (Fig. 97)

With the assumed range of water saturation, variation of the assessed oil reserve is not large.

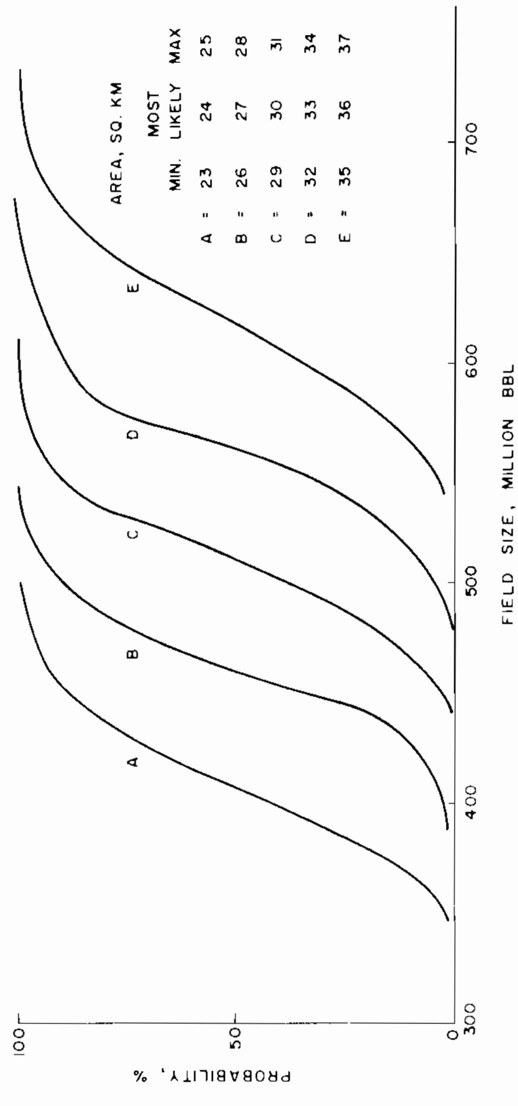

Fig. 95. Summary plots of changing producing area (adapted from Huwaidi 1984).

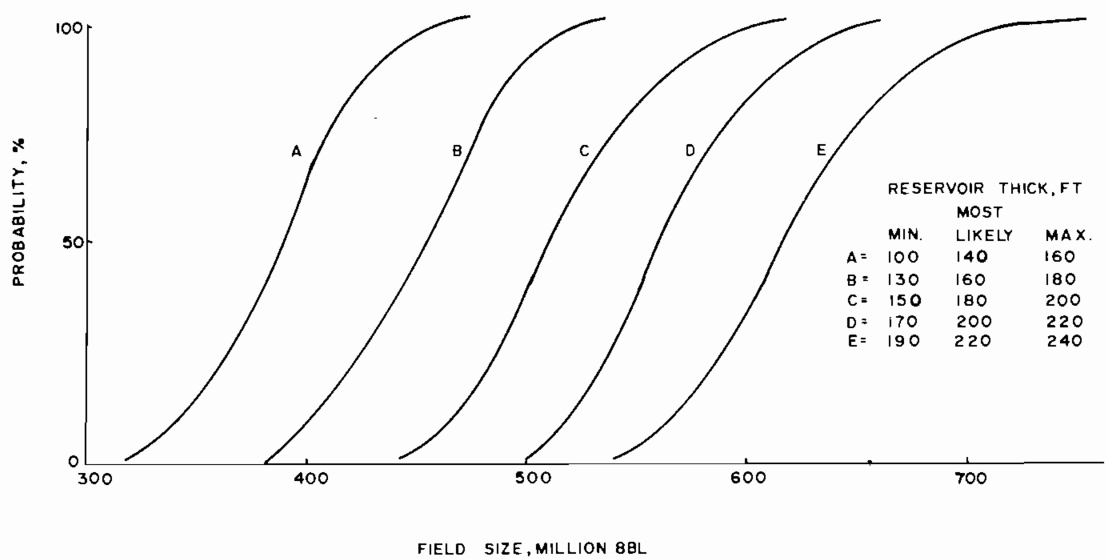

Fig. 96. Summary plots of changing reservoir thickness (adapted from Huwaidi 1984).

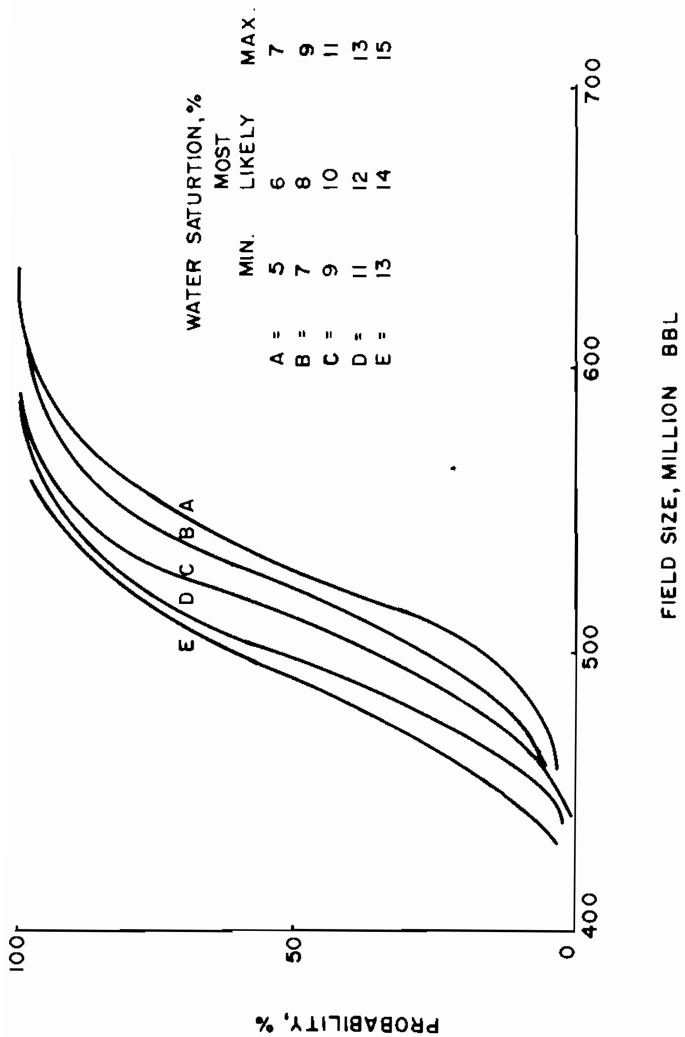

Fig. 97. Summary plots of changing water saturation (adapted from Huwaidi 1984).

4. *Changing porosity (Fig. 98)*

Porosity usually has a great influence on the assessment. For those values used for the sensitivity study, however, the reserve does not change greatly, ranging from about 450 to 560 million bbl for the most likely cases.

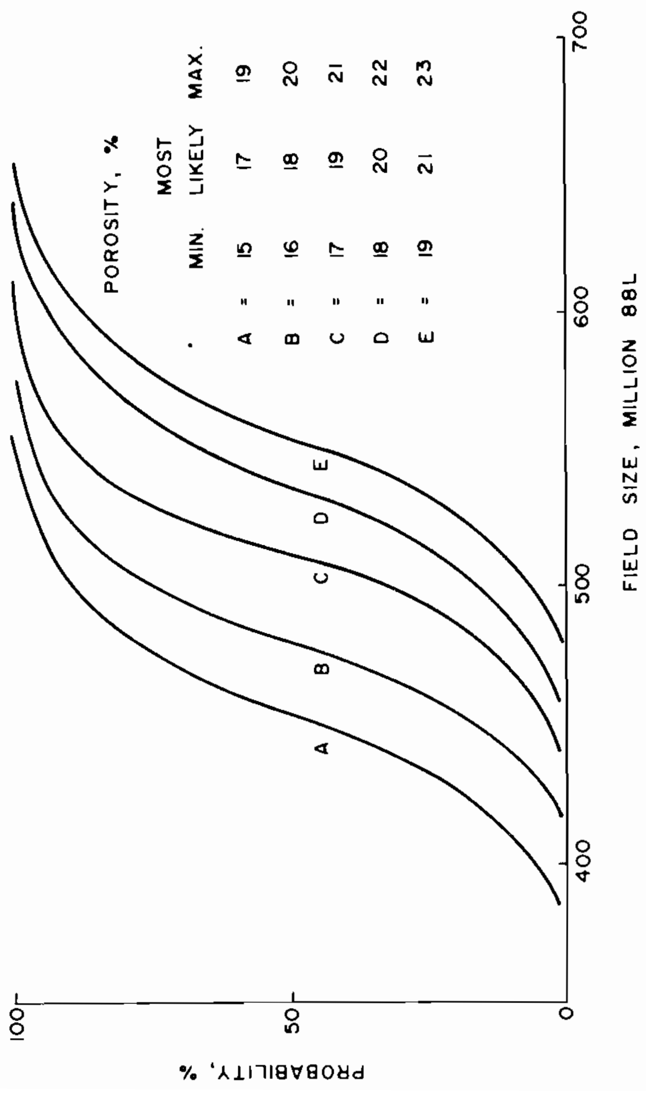

Fig. 98. Summary plots of changing porosity (adapted from Huwaidi 1984).

5. Changing risk factor (Fig. 99)

The risk may be considered as either remoteness or uncertainty from the known cases (oil fields). Such remoteness may be related with a geological location, a geological setting, or a technical difficulty, and a combination of these. To evaluate this effect, the risk factor changed in almost full range between 1 and 99%. The result shows a very wide range, between about 50 and 470 million bbl for the most likely cases.

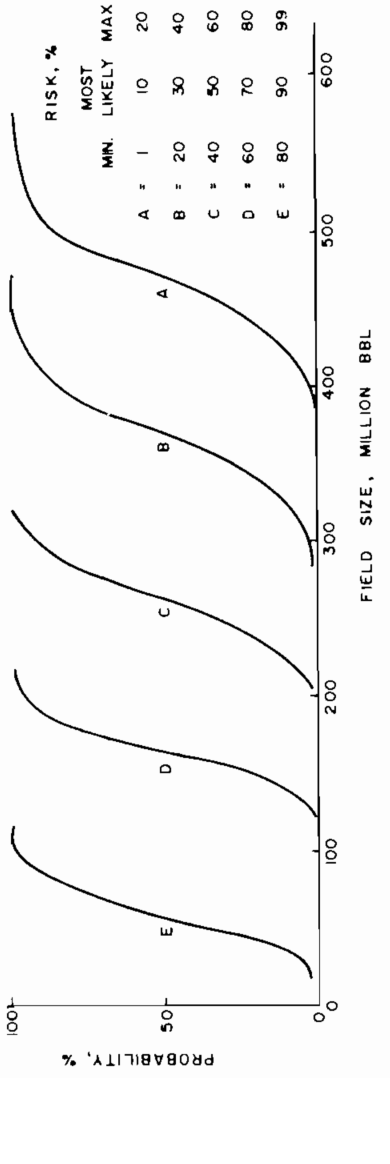

Fig. 99. Summary plots of changing risk factor (adapted from Huwaidi 1984).

Organic Geochemical Monte Carlo Simulation

Ayres *et al.* (1982) recently identified as the best source rocks in Saudi Arabia the thermally mature, thinly laminated, organic-rich carbonate rocks of the Jurassic age (Callovian-Oxfordian or equivalent to the Hanifa and Twaiq Mountain Formations, see Fig. 100). These rocks seem to have been deposited in an intrashelf basin.

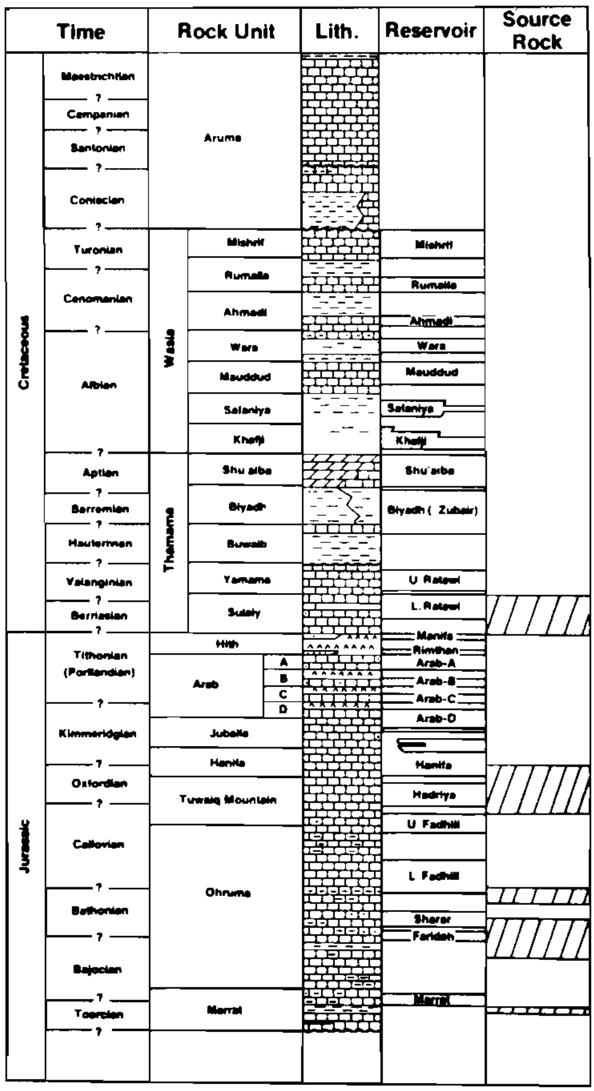

Fig. 100. Generalized Cretaceous and Jurassic stratigraphic section showing lithology, reservoir units, and source rocks (from Ayres *et al.* 1982). Courtesy of American Association of Petroleum Geologists.

Ayres *et al.* (1982) suggested extensive vertical migration of oil from these source rocks to reservoirs. The possibility of the vertical oil migration was also suggested by Young *et al.* (1977), based on their age-dating method of accumulated oil in this region.

Total organic carbon concentration of the Jurassic source rocks ranges from about 3 to 5 per cent (Ayres *et al.* 1982). Bitumen content is so high, that it often exceeds kerogen content and the hydrocarbon content is in order of several thousands ppm. The kerogen is mainly amorphous which is considered to be of the best type. Figure 77 in Chapter 8 shows Ayres *et al.'s* isopach map of the Callovian and Oxfordian source rocks.

Using a concept similar to the volumetric Monte Carlo simulation, another computer program was written (see Appendix D2 for program) and tested. According to Ayres *et al.'s* Jurassic-source-rock map, the area of distribution of the source rocks covers approximately 100,000 km^2. In the following trial runs, let us simulate the oil volumes over an area 1/100 of the total (or about 1,000 km^2). Based on Barker and Dickey's (1984) discussion on Ayres *et al.'s* work, the total recoverable oil volume (including the future discovery of about 50 billion bbl) of this area may be assumed to be about 270 billion bbl. One hundredth of this volume is thus 2.7 billion bbl. The hydrocarbon yield may be assumed to be about 200 mg/g organic carbon (which is equivalent to a few to several thousands ppm concentration) from the source rocks containing 3 to 5 per cent organic carbon.

Barker and Dickey (1984) recently estimated the volume of oil accumulated in this area and concluded that the source rocks identified by Ayers *et al.* (1982) (see Fig. 77) may represent only a part of all. Because the average source rock thickness from Figure 77 is about 150 ft, it may be more than doubled in the computer simulation to obtain the assessed figure of about 2.7 billion bbl.

The standard input factors are as follows,

	Minimum	Most likely	Maximum
Area, sq. km^2	900	1000	1100
Source rock thickness, ft	350	400	450
Organic carbon, wt. %	3	4	5
Hydrocarbon yield, mg/g O.C.	180	200	220
Trapping efficiency, %	40	50	60
Recovery efficiency, %	30	33	35
Risk factor, %	40	50	60

Twenty additional runs were made for the sensitivity study, and the summary plots are shown in Fig. 101 (changing source rock thickness ft), 102 (changing organic carbon, %), 103 (changing hydrocarbon yield, mg/g organic carbon), 104 (changing trapping efficiency, %), and 105 (changing risk factor, %). All the cases shown in these plots suggest wide ranges of the minimum, most likely, and maximum values of the assessed oil reserves.

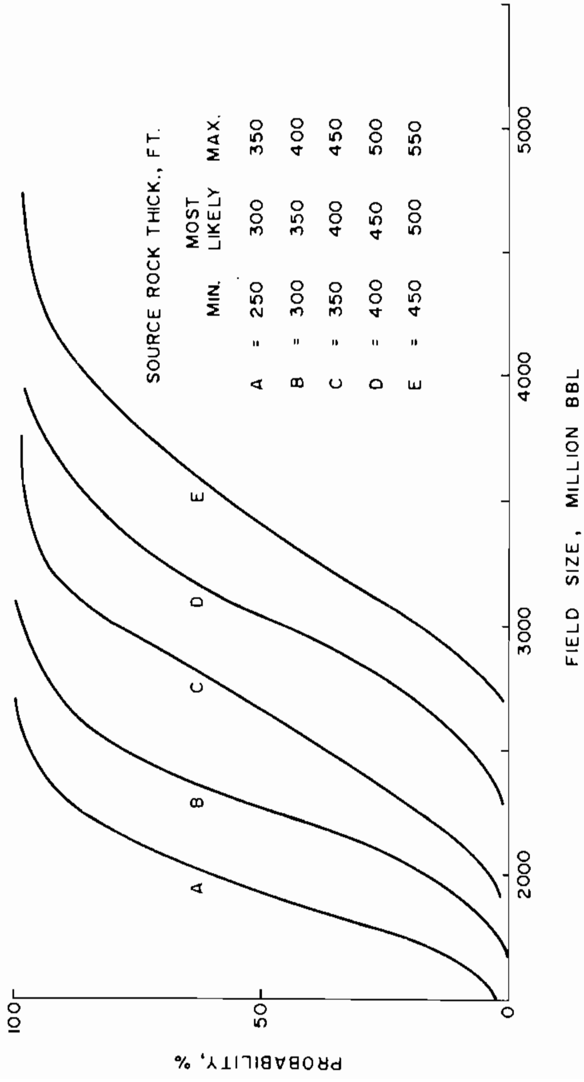

Fig. 101. Summary plots of changing source-rock-thickness (adapted from Huwaidi 1984).

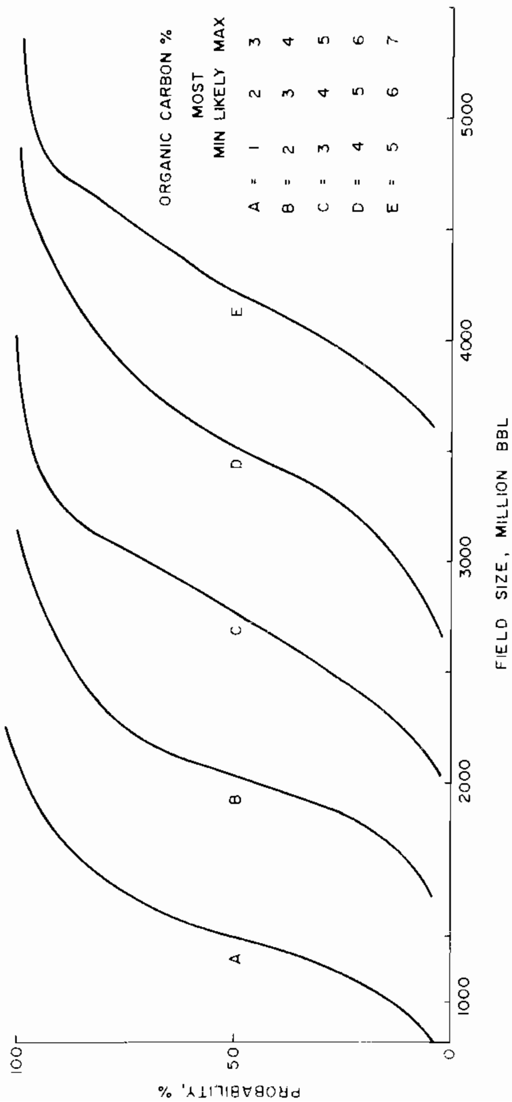

Fig. 102. Summary plots of changing organic carbon % (adapted from Huwaidi 1984)

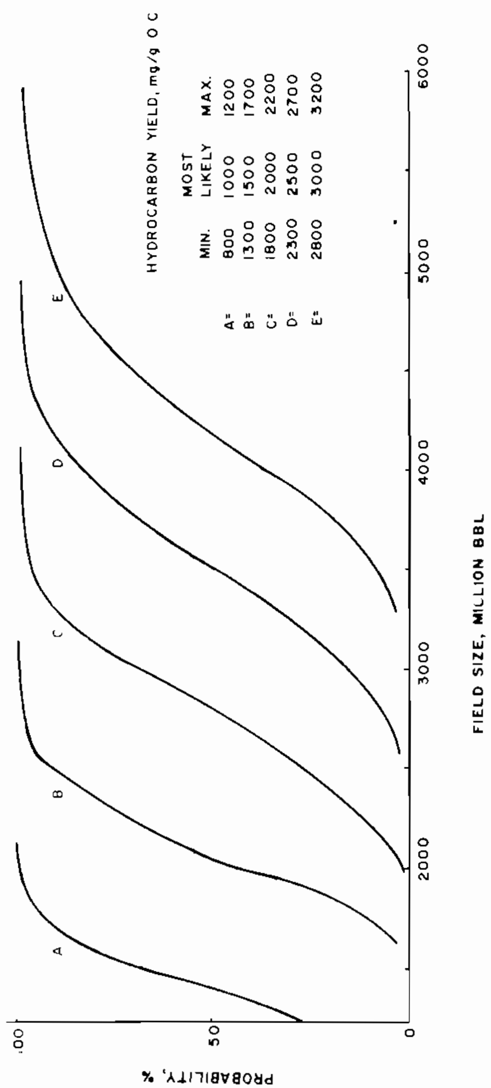

Fig. 103. Summary plots of changing hydrocarbon yield (adapted from Huwaidi 1984).

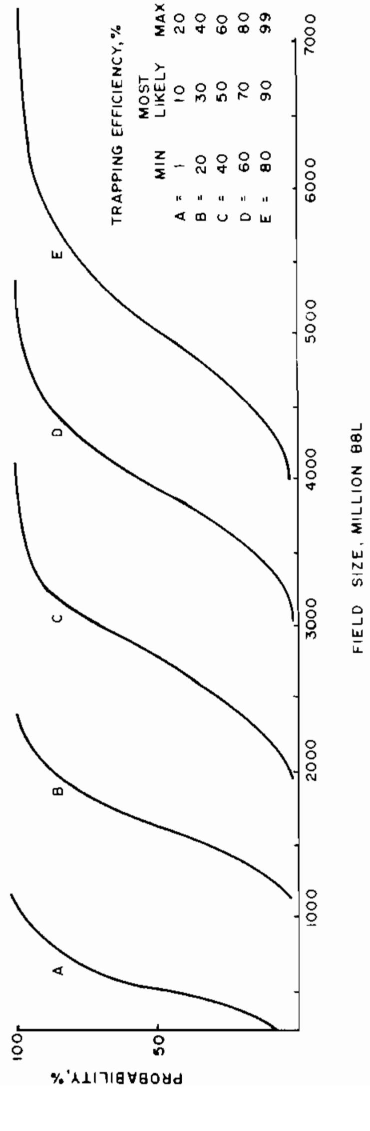

Fig. 104. Summary plots of changing trapping efficiency (adapted from Huwaidi 1984)

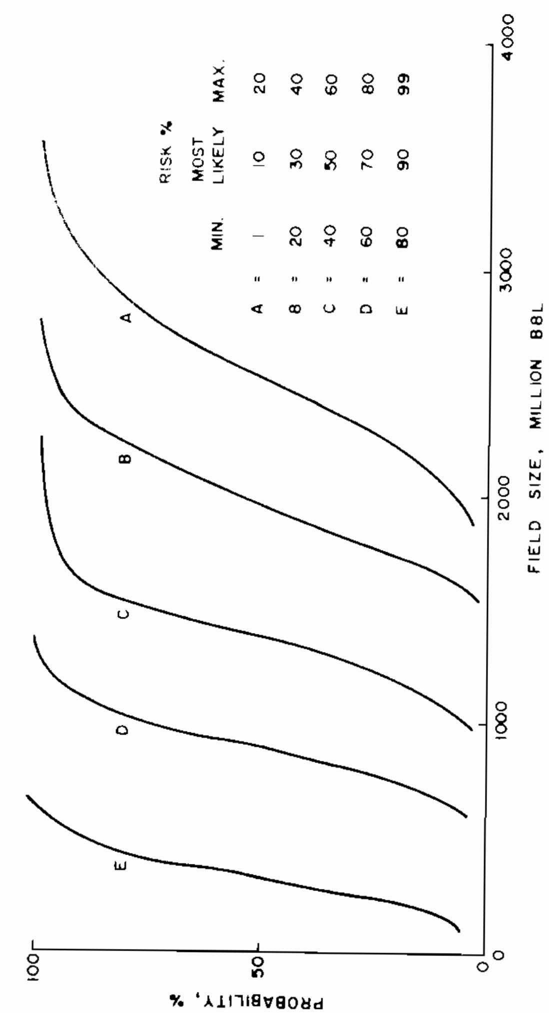

Fig. 105. Summary plots of changing risk factor of organic geochemical simulation (adapted from Huwaidi 1984).

Areal Simulation of Random Drilling

Using the most advanced geological and geophysical techniques, significant petroleum reserves have been discovered in Saudi Arabia. The total ultimate oil recovery of the country is estimated to be about 220 billion bbl (future discoveries are not included in this figure).

What would happen if the entire drilling is made randomly, rather than using the advanced technology? A computer may be used to simulate such random cases.

First of all, the surface areas of the 25 giant oil fields (0.5 billion bbl or more of the recoverable oil) discovered in Saudi Arabia were estimated. These areas were projected on the television screen of the computer, so that the entire screen represents the total original concession area.

The computer then generated a pair of random numbers to determine a set of X and Y values on the screen, and a point was plotted. If this point falls within the known oil field, it is counted as a success, otherwise a failure. The computer repeats the same operation many times and computes the success ratio. The program is shown in Appendix D3.

Following figures show sample computer runs.

Number of sampling	Figure
200	106
400	107
600	108
800	109
1000	110
1200	111
1400	112
1600	113
1800	114

In each computer run, such values as, numbers of success and of failure, discovered oil volume, discovered oil volume/number of sampling (or number of wells), and discovered percentage of the total oil volume are calculated.

Figures 115-117 show the summary plots of these runs.

1. Number of success (Fig. 115)

The average discovery shown by open circles increases with increase of random sampling. Small dots indicate individual computer runs.

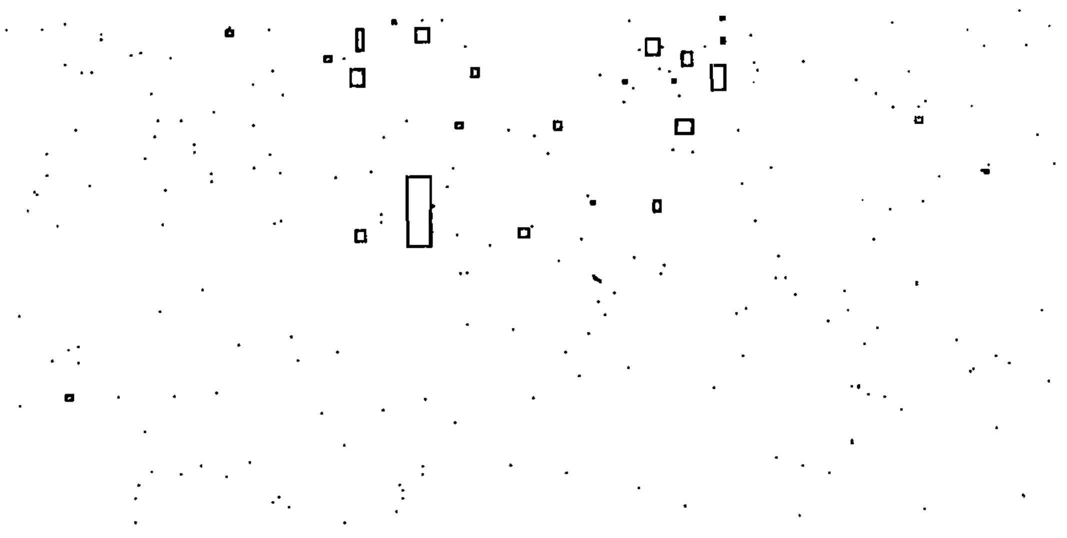

Fig. 106. Sample run of areal random drilling: 200 trials.

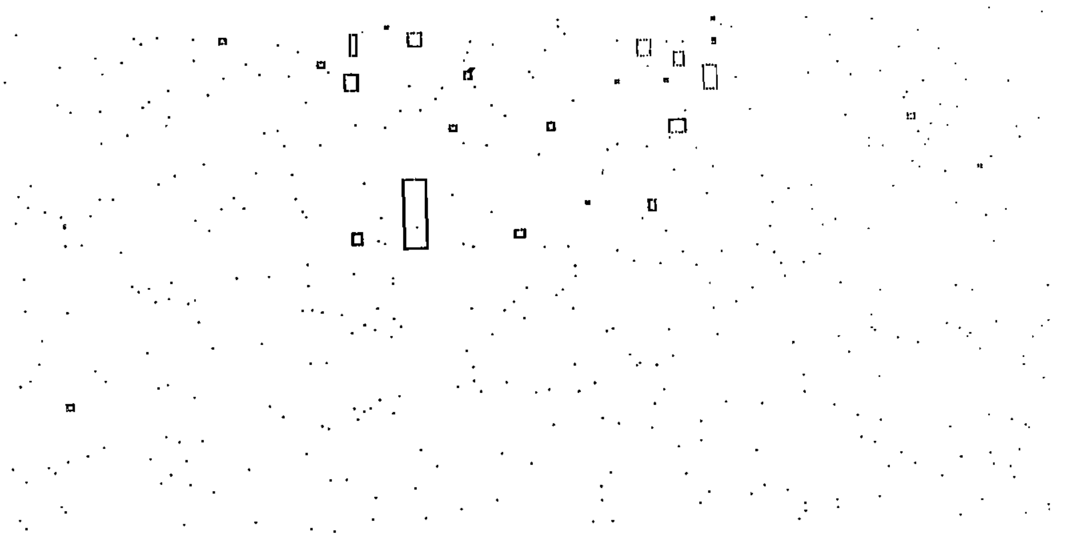

Fig. 107. Sample run of areal random drilling: 400 trials.

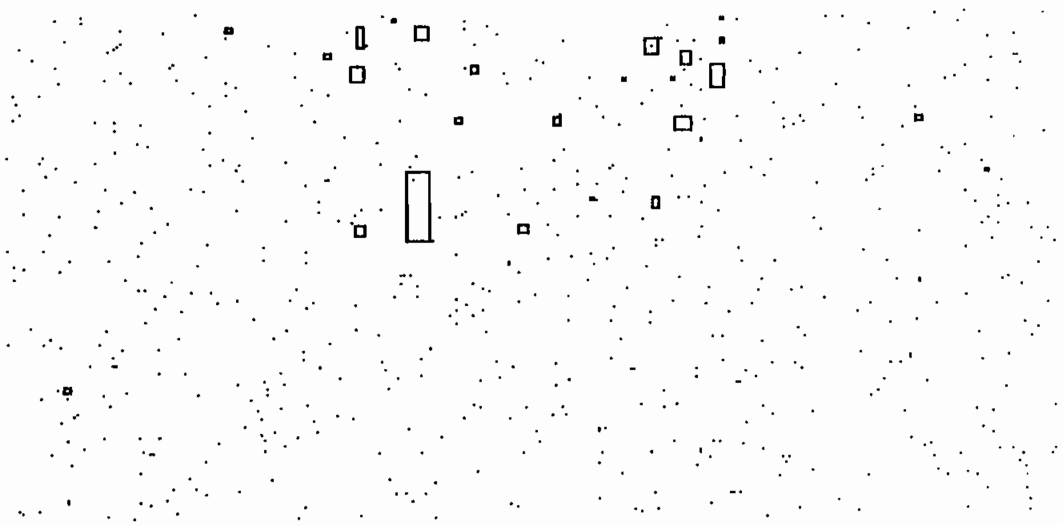

Fig. 108. Sample run of areal random drilling: 600 trials.

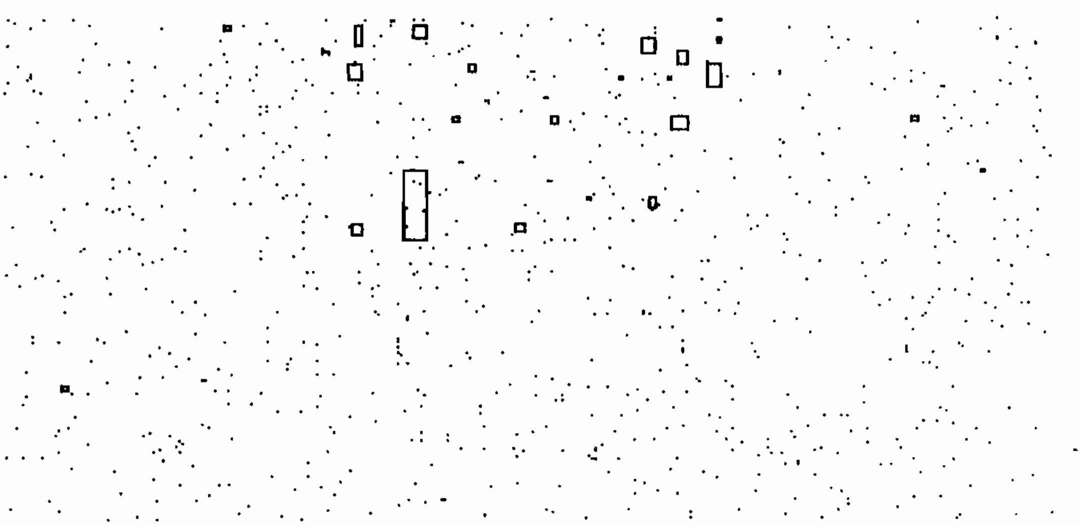

Fig. 109. Sample run of areal random drilling: 800 trials.

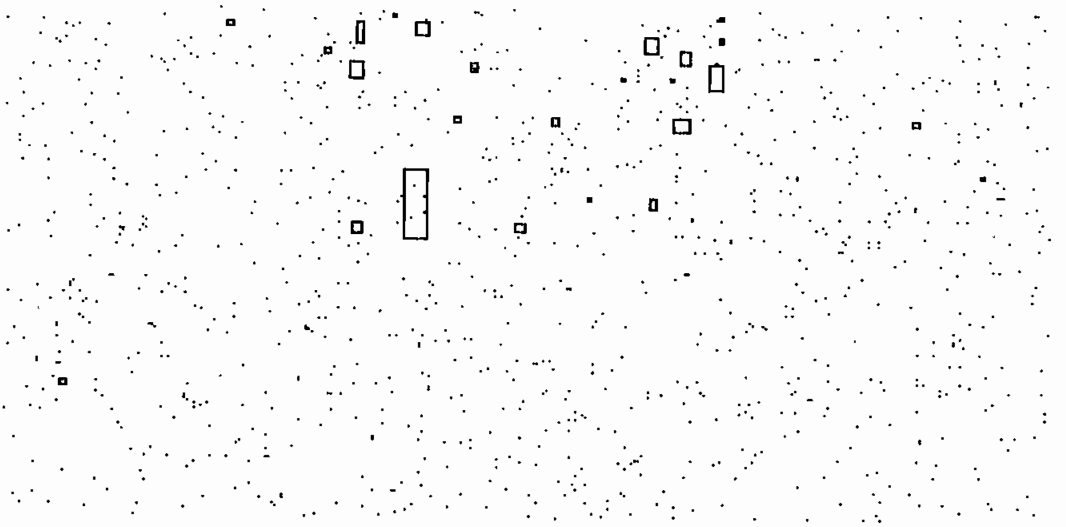

Fig. 110. Sample run of areal random drilling: 1000 trials.

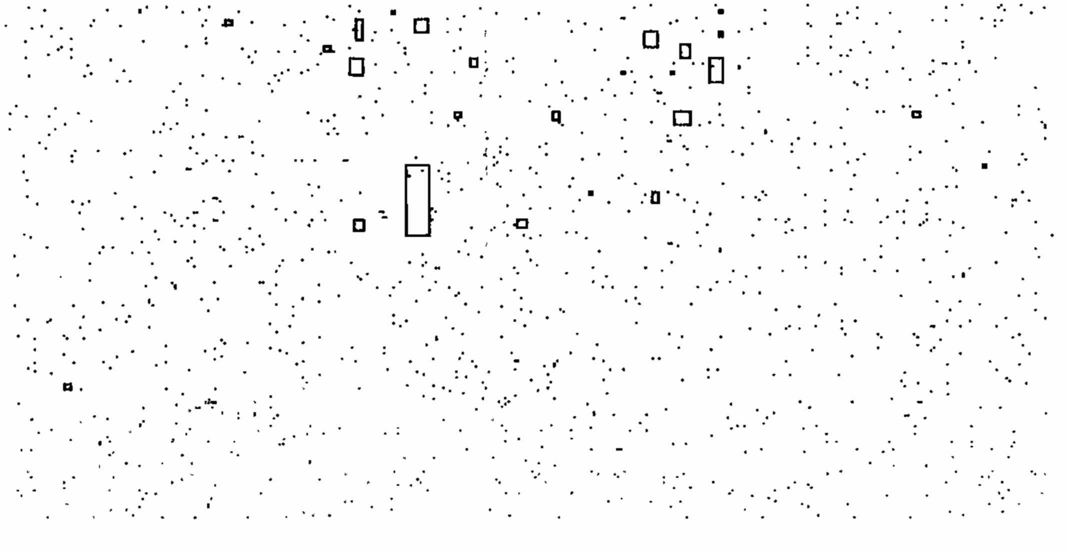

Fig. 111. Sample run of areal random drilling: 1200 trials.

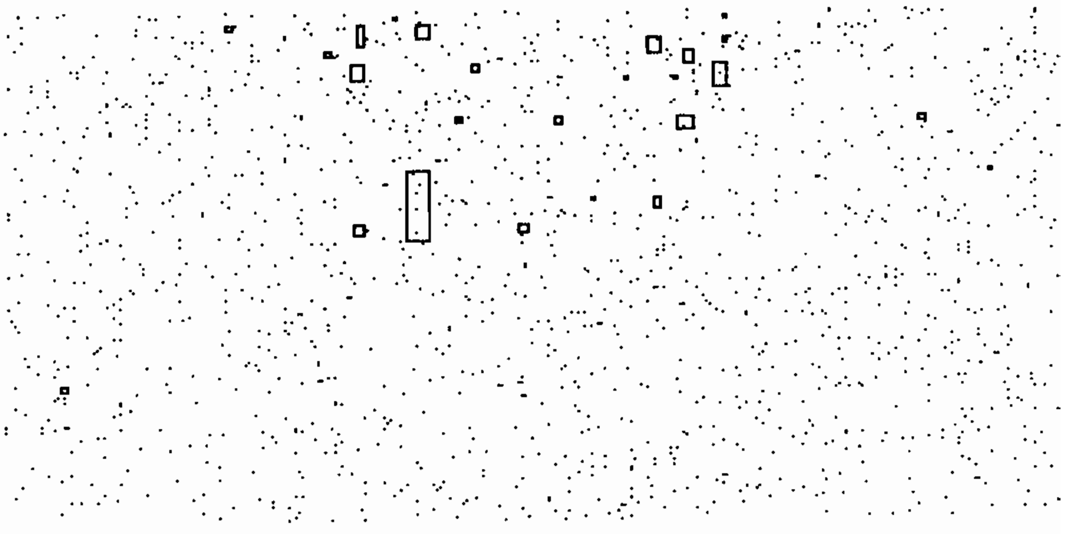

Fig. 112. Sample run of areal random drilling: 1400 trials.

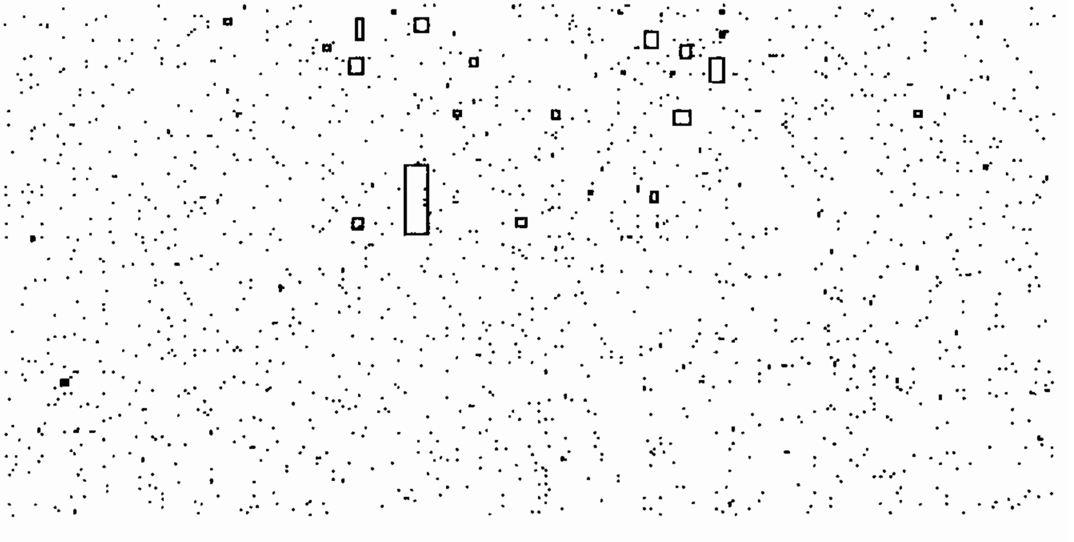

Fig. 113. Sample run of areal random drilling: 1600 trials.

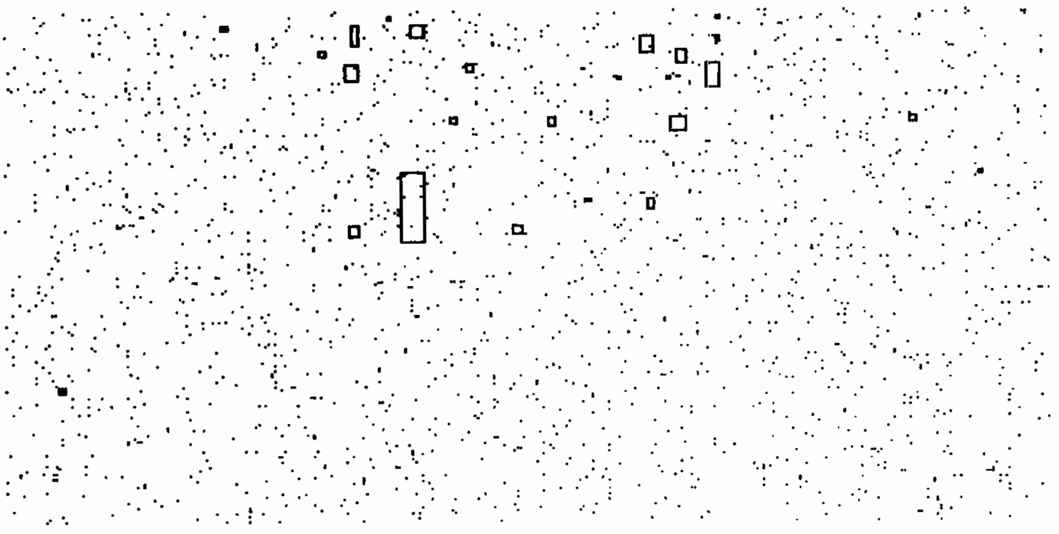

Fig. 114. Sample run of areal random drilling: 1800 trials.

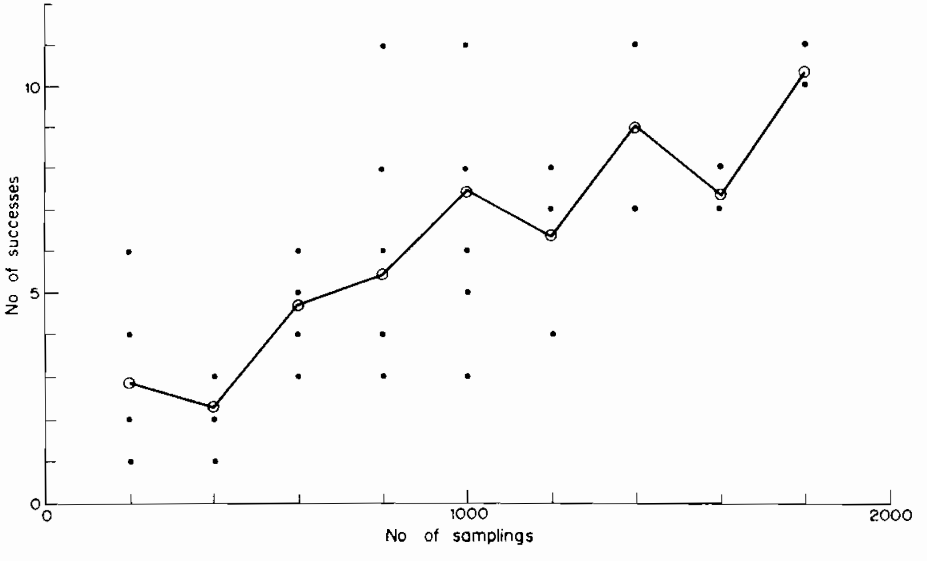

Fig. 115. Summary plot of number of success (adapted from Huwaidi 1984). Small dots indicate individual computer runs and open circles show their averages.

2. Discovered oil volume/number of wells (Fig. 116)

The oil discovery/well drilled generally decreases with increasing number of sampling (drilling).

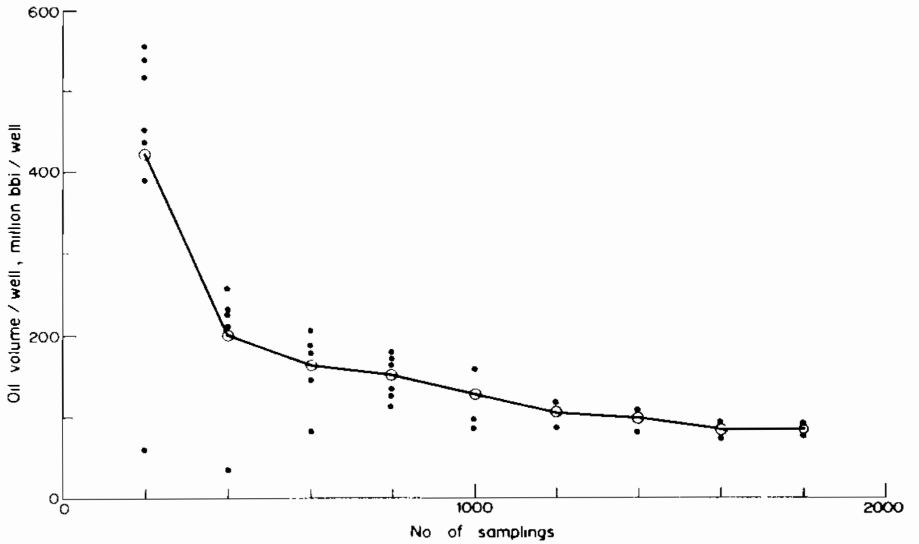

Fig. 116. Summary plot of discovered oil volume/number of wells (adapted from Huwaidi 1984). Small dots indicate individual computer runs and open circles show their averages.

3. % discovery over the total oil volume (Fig. 117)

There is a general increasing trend with increase of number of random sampling or drilling.

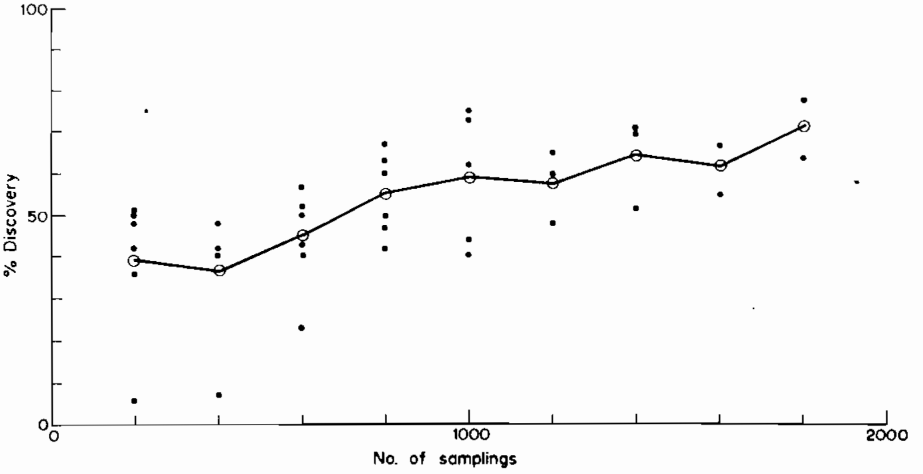

Fig. 117. Summary plot of % discovery of oil volume (adapted from Huwaidi 1984). Small dots indicate individual computer runs and open circles show their averages.

A comparison between the actual discovery history of Saudi Arabia and the result of the computer simulation could not be done, due to lack of data on the number of the exploration drilling. However, the program itself would have potentials for future applications.

Problems

1. Explain the volumetric Monte Carlo simulation.
2. What is the range of the organic carbon per cent of the Callovian-Oxfordian (Jurassic) source rocks in Saudi Arabia?
3. Described about the total number of the giant oil fields and their total recoverable oil volume so far discovered in Saudi Arabia.

Chapter 12

Studying an Applied Science Petroleum Geology

■ Introduction. ■ Three important factors in conducting research. ■ Intellectual curiosity. ■ Unity in science. ■ Scientific honesty. ■ Problem.

Introduction

As in the cases of many other applied sciences, we face a difficult problem in studying petroleum geology: Should we study science or technology at a university?

An applied science is made of two main elements; theory or concept in science, and practical applications or technology. Because it has these two elements, a student must study both together in the classroom. However, an important question is how to study them together.

An instructor may place stress on the theory, based on his belief that learning technology without a sound understanding of the fundamental concepts or theory in science is useless. But if he overdoes it, the subject may become a pure science rather than an applied science. In such a case, the student would not be able to study the practical aspects of the subject.

If, on the contrary, the instructor insists on teaching techniques without explaining the basic scientific concepts, the student would become familiar with, for example, handling machines and equipments without a solid understanding of the scientific concepts. This approach is quite risky, because, with continuous advancements of modern technology, these machines and equipments will be frequently improved or replaced by new ones. With these changes, the student who may already be a company employee at that time must learn many times how to use the new machines without a good understanding of the basic scientific concepts. This approach would thus be quite ineffective.

In summary, for effective teaching and learning of an applied science, it is essential to keep a balance between science and technology or between theories and practical applications. However, this task is not an easy one because the time most university staff members spend with students in the classroom or laboratory is usually quite limited.

Three Important Factors in Conducting Research

In view of the fact that a student spends only several years at a university when he is young and then works for a company or a governmental organization in the following 30 to 40 years of his life, I believe that the university trains him for a good and positive attitude for conducting industrial or scientific work.

According to Hubbert (1974), who is widely known in petroleum industry and academia as the founder of many important concepts and theories, such as hydrofracturing, hydrodynamics, mechanisms of thrust faulting, prediction for future energy supply, ...etc., there are two important factors in conducting effective scientific works. These are (1) intellectual curiosity, and (2) unity in science. A third important factor could be added which is scientific honesty.

Although it is not easy for anyone to behave in the manner Hubbert has suggested, a positive attitude for these goals in scientific works would improve his performance. In addition, the factors suggested by Dr. Hubbert are not only important for scientific works, but also for other industrial works.

1. Intellectual curiosity

In conducting scientific works, it is always essential to ask the reasons of conducting such a research. This attitude will help a person to understand problems deeply, rather than superficially.

Intellectual curiosity is an essential factor in both developing and improving scientific and industrial methods. Many new discoveries and developments have been and will be made by this important character of human being.

In the classroom, when any theory is explained, I think that the instructor must describe why it is important and how to apply it in practice. This is particularly true in teaching applied sciences. *Intellectual curiosity* would also improve his work performance since it is one of the major motivating factors for hard works.

2. Unity in science

A belief in one branch of science may not be accepted in other branches of science. If such is the case, the belief must be corrected or revised to satisfy all the conditions required in the other branches of science.

For example, a method or concept in geology must be examined in the light of physics, chemistry, mineralogy, ...etc., before it is applied to practical works. In applying it, the method would have to be reasonable or acceptable from the engineering stand point, as well.

Although the continuous developments in most branches of science demand many experts in very specialized fields, the results of their work must be examined carefully from a broader view in science which may be called a *"scientific common sense"*. Without a proper control, a highly specialized research could produce very erroneous conclusions.

At universities, I believe that both undergraduate and junior graduate students must be educated for the general and broad knowledge, to avoid risks involved in an over-specialization. In my opinion, a true specialization can start at the Ph.D. level only.

The concept "*unity in science*" can also be applied to works in industries. It may be called "*cooperation*".

In any industry, it is absolutely essential for a professional to understand and communicate with other people working in and out of his organization. As far as the technical expertise is concerned, most modern industries are so diversified in technology that no single person can understand fully. Of course, he does not have to become familiar with all of these techniques. However, he must be able to communicate with other professionals quite freely, if necessary. This will reduce chances of conducting dogmatic or selfish works which could be very hazardous to the entire organization.

3. Scientific honesty

Honesty in science means that conditions and assumptions used must be understood and explained before a main conclusion is drawn. It will eliminate possible exaggerations which could mislead people. When a conclusion is made, we must be aware of the limitation of its reliability and of potential problems involved with this conclusion.

Although it is not an easy matter, I believe that we should always keep these three factors in our mind when we study science or work in an industrial organization. A student who was trained for such a good attitude would perform better than those not trained, and thus would produce more in the future.

Problem

Explain the three important factors in conducting research works.

```
40 CLS
50 KEY OFF
70 REM TRAP
90 DIM D1(20),D2(20),T1(20)
95 DIM Y1(20),Y2(20),X1(20),X2(20)
96 DIM R(20)
100 PRINT "INPUT DEPTH-TIME PAIRS OF ANTICLINE,"
101 PRINT "SHALLOW TO DEEP. TO END, TYPE 9999"
105 D1(0)=D2(0)=T1(0)=0
110 FOR I=1 TO 20
120 INPUT D1(I)
122 IF D1(I)=9999 THEN 190
125 INPUT T1(I)
150 NEXT I
190 I1=I-1
200 PRINT "INPUT CORRESPONDING DEPTHS AT SYNCLINE,"
205 PRINT "SHALLOW TO DEEP"
210 FOR I=1 TO I1
220 INPUT D2(I)
230 NEXT I
231 LPRINT "INPUT DATA":LPRINT:LPRINT "TIME MY","ANT.-FT","SYN.-FT"
234 FOR I=1 TO I1
236 LPRINT T1(I),D1(I),D2(I)
238 NEXT
239 LPRINT:LPRINT:LPRINT
240 CLS:SCREEN 2
250 FOR J=I1-1 TO 0 STEP -1
260 Y1(I1-J)=D1(I1)-D1(J)
270 Y2(I1-J)=D2(I1)-D2(J)
280 X1(I1-J)=T1(I1)-T1(J)
300 NEXT J
310 FOR L=1 TO I1
320 R(L)=((Y1(L)-Y1(L-1))-(Y2(L)-Y2(L-1)))/(X1(L)-X1(L-1))
330 R(L)=-R(L)
340 NEXT L
400 FOR M=1 TO I1
402 X1=X1(M)*2
404 Y1=Y1(M)/125
406 Y2=Y2(M)/125
410 PSET (X1+50 ,Y1+10)
420 PSET (X1+50 ,Y2+10)
430 NEXT M
432 LPRINT "BURIAL DATA":LPRINT
435 LPRINT "TIME-MY","ANT.-FT","SYN.-FT","R-FT/MY"
440 FOR M=1 TO I1
445 LPRINT X1(M),Y1(M),Y2(M),R(M)
446 R(M)=-R(M)
448 NEXT M
450 FOR N=50 TO 639 STEP 50
455 PSET(N,10):NEXT
458 FOR N=10 TO 191 STEP 15
460 PSET(50,N):NEXT N
475 A=0
480 FOR X=6 TO 80 STEP 10
485 LOCATE 1,X
490 PRINT A:A=A+40:NEXT
495 A=0
500 FOR X=2 TO 21 STEP 2
505 LOCATE X,1
510 PRINT USING"#####";A:A=A+2000:NEXT
645 LOCATE 22,1
```

Appendix A. Computer program of burial history and trap formation.

```
647 STOP
650 LINE (0,R(1)/5+85)-(X1(I)*2,R(I)/5+85)
658 CLS: SCREEN 2
659 X=50 :Y=R(1)/6.25 +90
660 FOR I=1 TO I1
665 LINE (X,Y)-(X1(I)*2+50 ,R(I)/6.25 +90)
670 LINE (X1(I)*2+50,R(I)/6.25 +90)-(X1(I)*2+50,R(I+1)/6.25 +90)
680 X=X1(I)*2+50:Y=R(I+1)/6.25 +90
690 NEXT I
700 FOR N=50 TO 639 STEP 20
710 PSET(N,90)
720 NEXT
730 FOR N=10 TO 191 STEP 16
740 PSET(50,N)
750 NEXT
810 A=0
820 FOR X=6 TO 80 STEP 10
830 LOCATE 1,X
840 PRINT A:A=A+40:NEXT
850 A=500
860 FOR Y=2 TO 23 STEP 2
870 LOCATE Y,1
880 PRINT A:A=A-100 :NEXT
1000 END
```

Appendix A. Computer program of burial history and trap formation.

Appendix B.

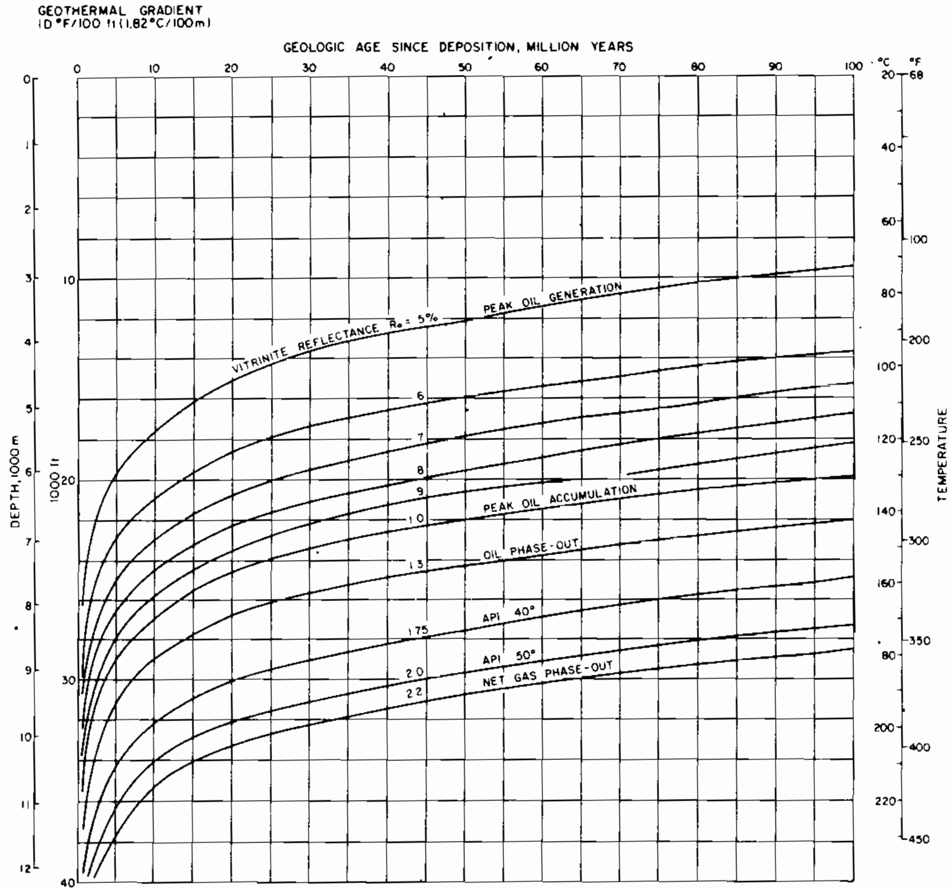

Fig. B-1. Chart for estimation of vitrinite reflectance, 1.0 F/100 ft(0-100 million years).

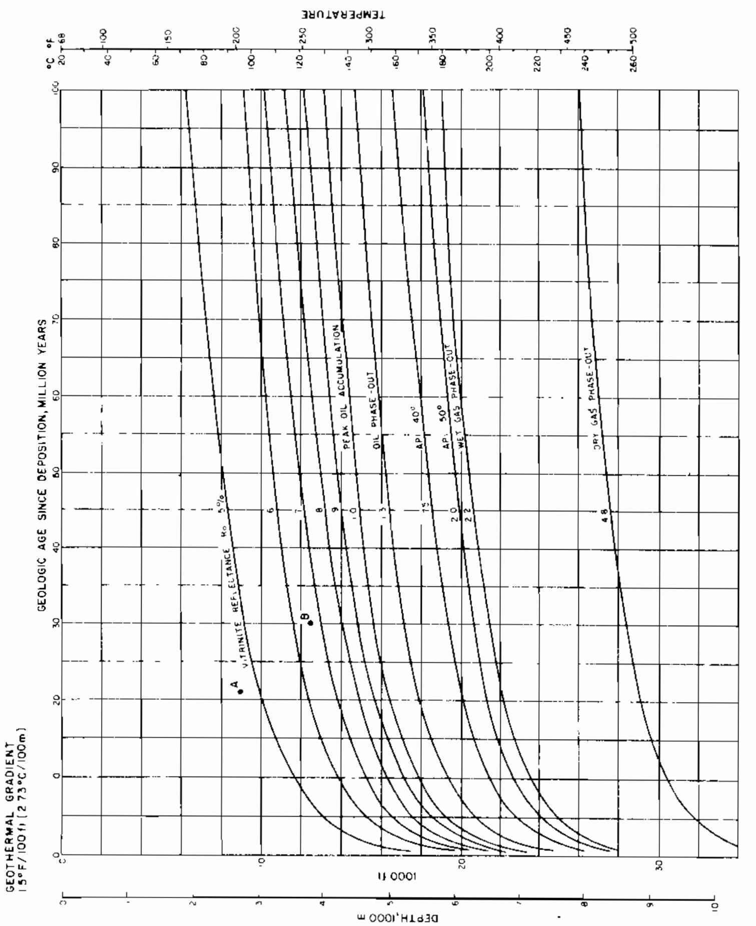

Fig. B-2. Chart for estimation of vitrinite reflectance, 1.5 F/100 ft(0-100 million years).

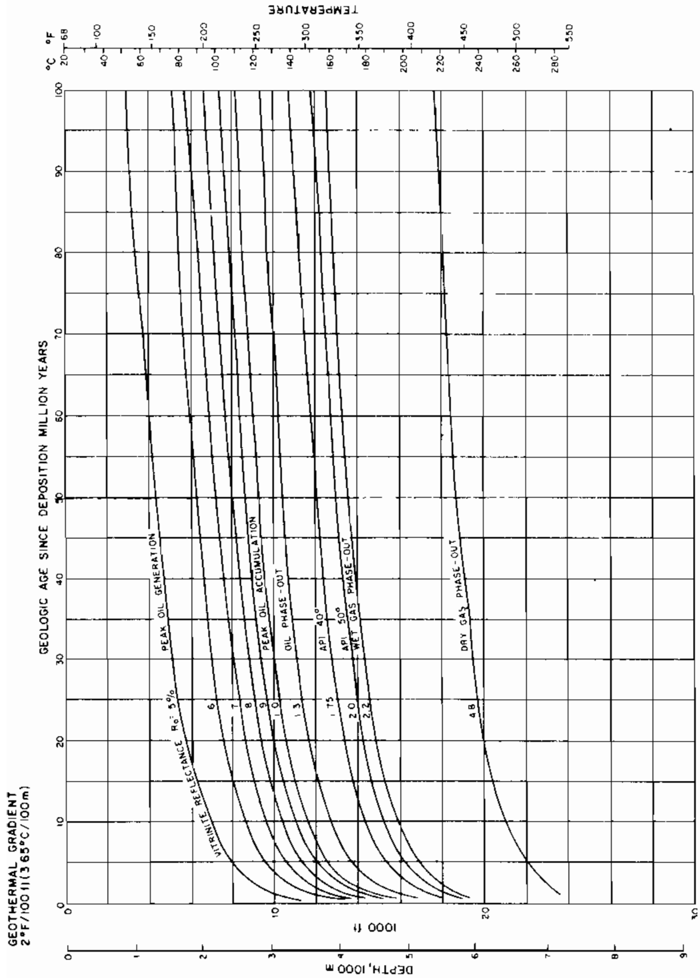

Fig. B-3. Chart for estimation of vitrinite reflectance, 2.0 F/100 ft(0-100 million years).

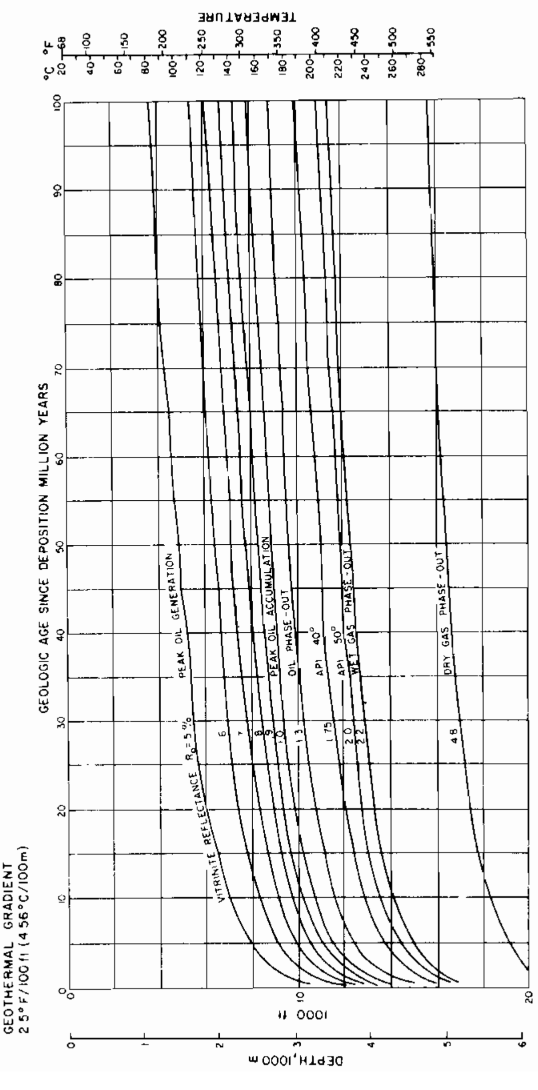

Fig. B-4. Chart for estimation of vitrinite reflectance, 2.5 F/100 ft(0-100 million years).

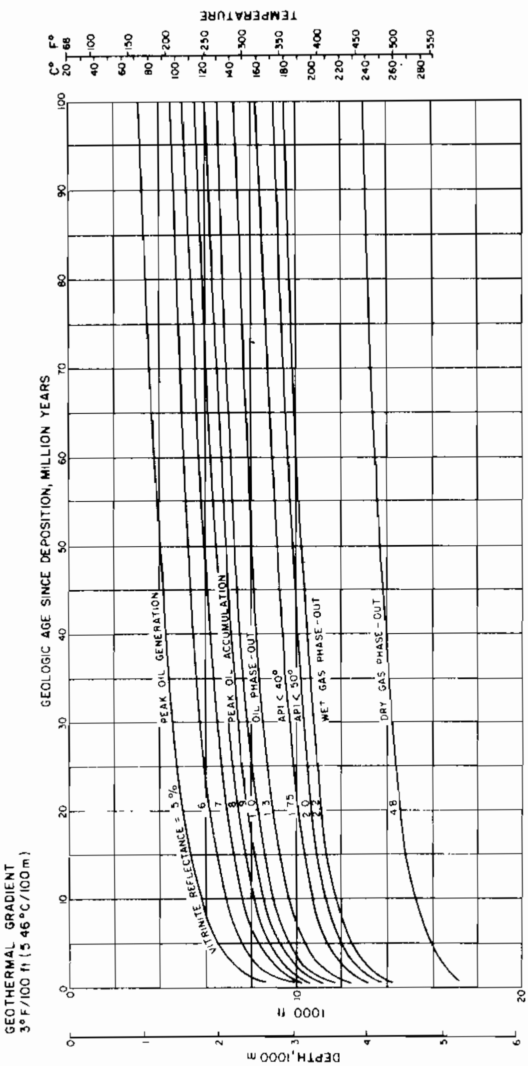

Fig. B-5. Chart for estimation of vitrinite reflectance, 3.0 F/100 ft(0-100 million years).

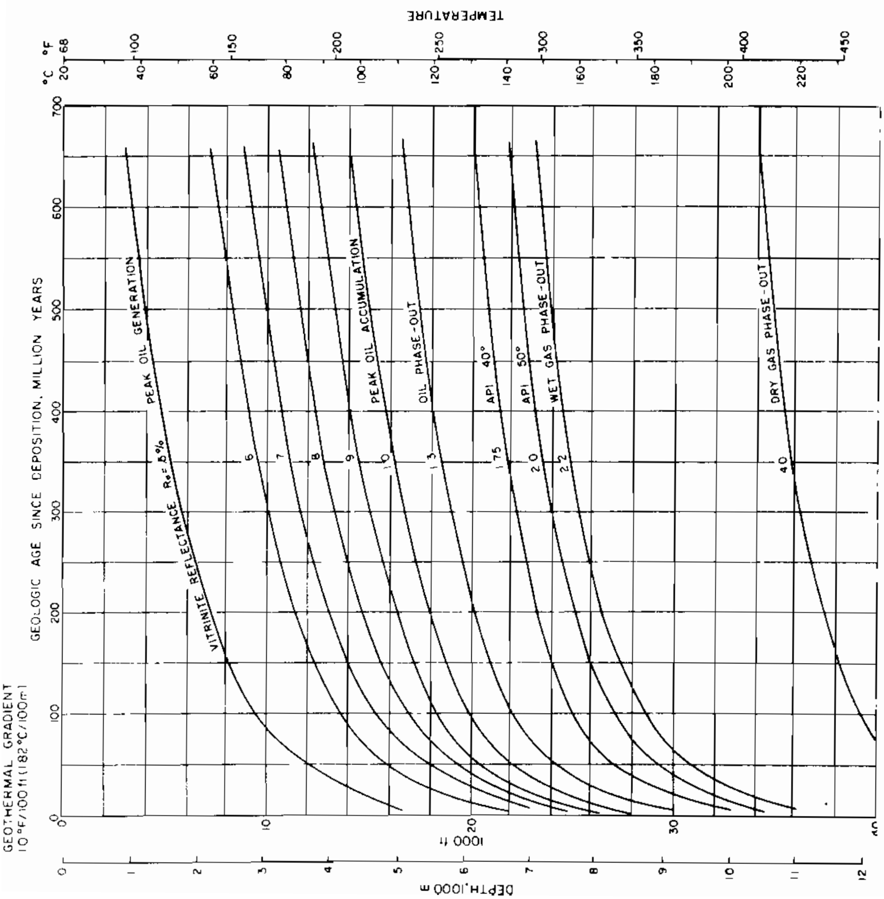

Fig. B-6. Chart for estimation of vitrinite reflectance, 1.0 F/100 ft(0-700 million years).

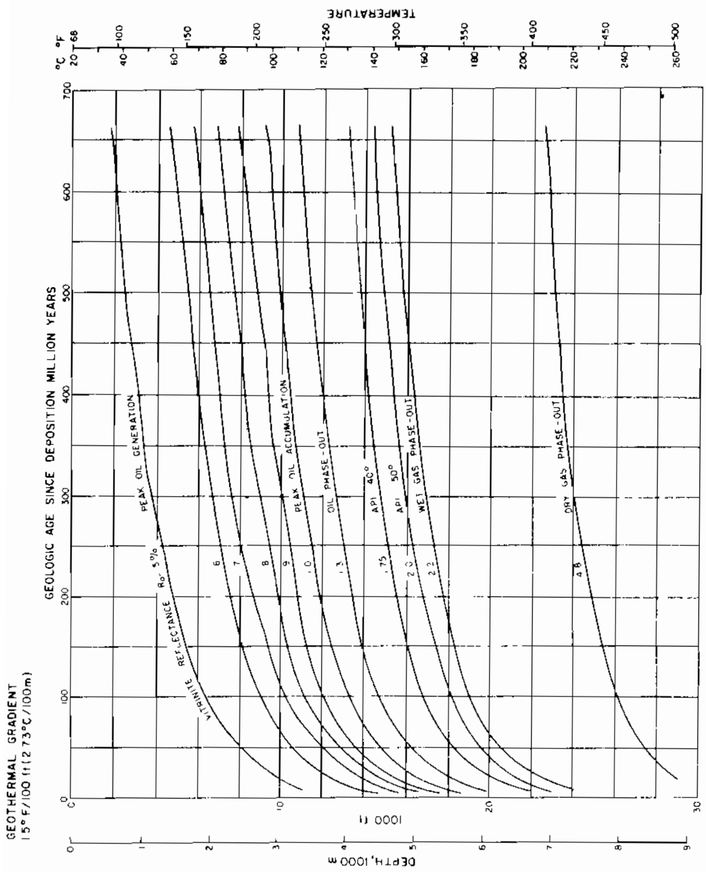

Fig. B-7. Chart for estimation of vitrinite reflectance, 1.5 F/100 ft(0-700 million years).

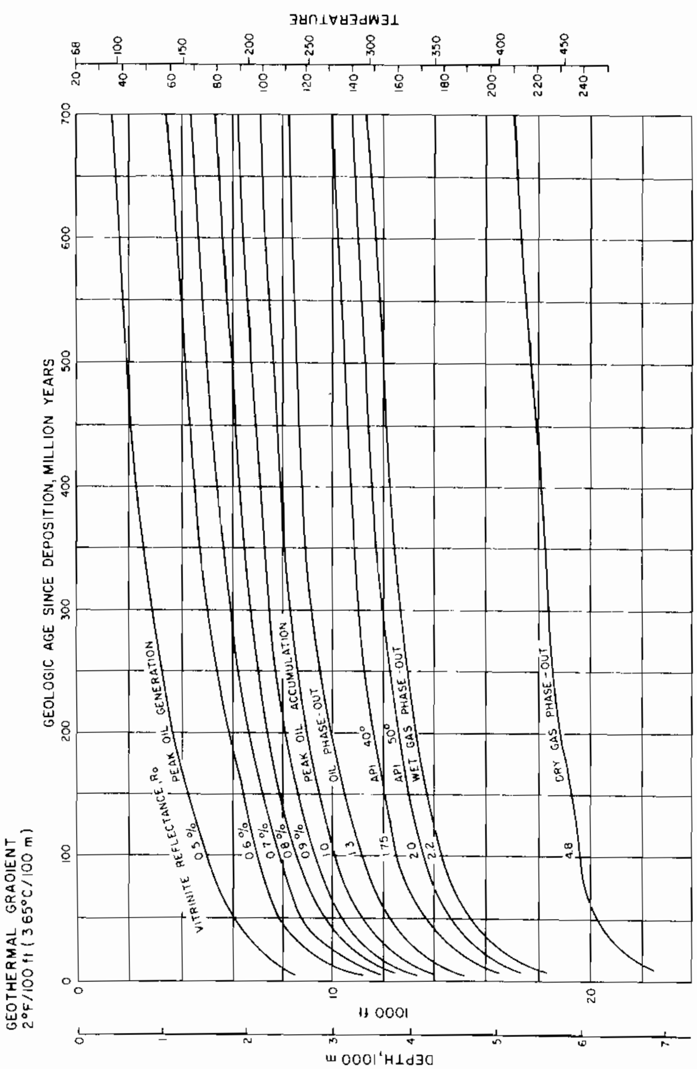

Fig. B-8. Chart for estimation of vitrinite reflectance, 2.0 F/100 ft(0-700 million years).

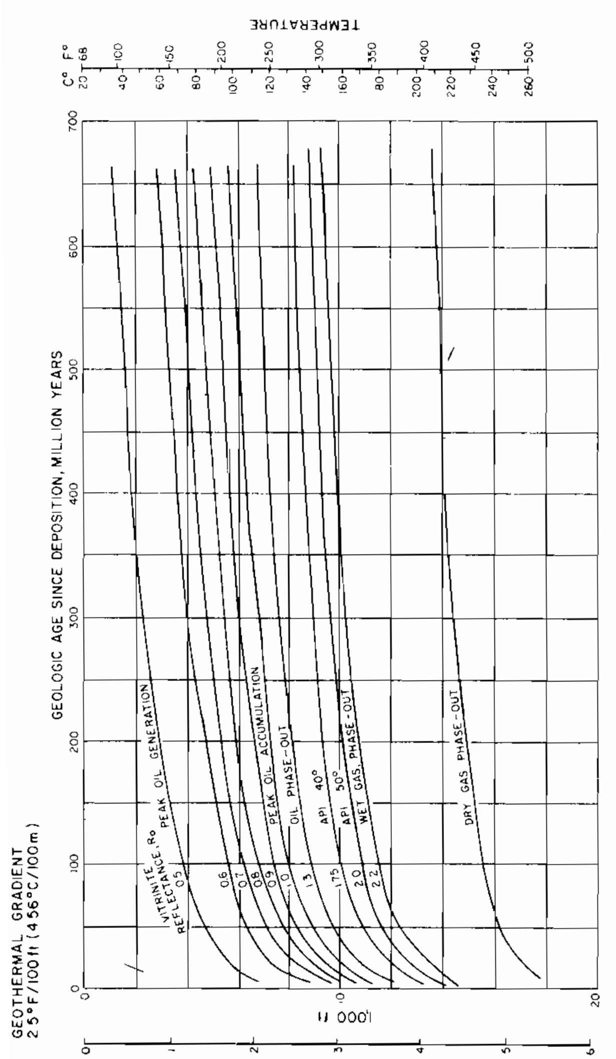

Fig. B-9. Chart for estimation of vitrinite reflectance, 2.5 F/100 ft (0-700 million years).

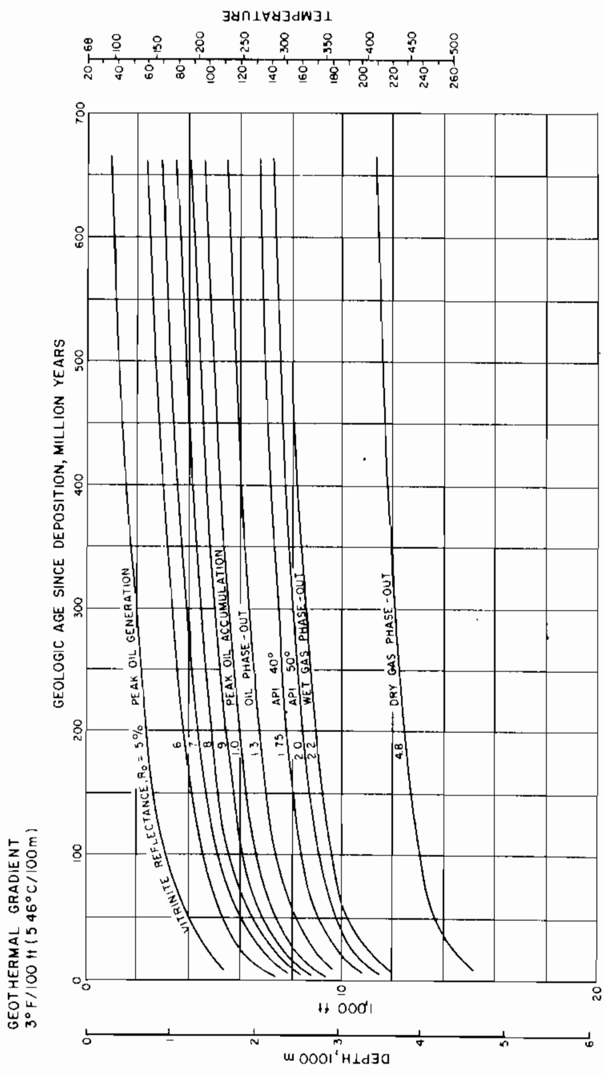

Fig. B-10. Chart for estimation of vitrinite reflectance, 3.0 F/100 ft (0-700 million years).

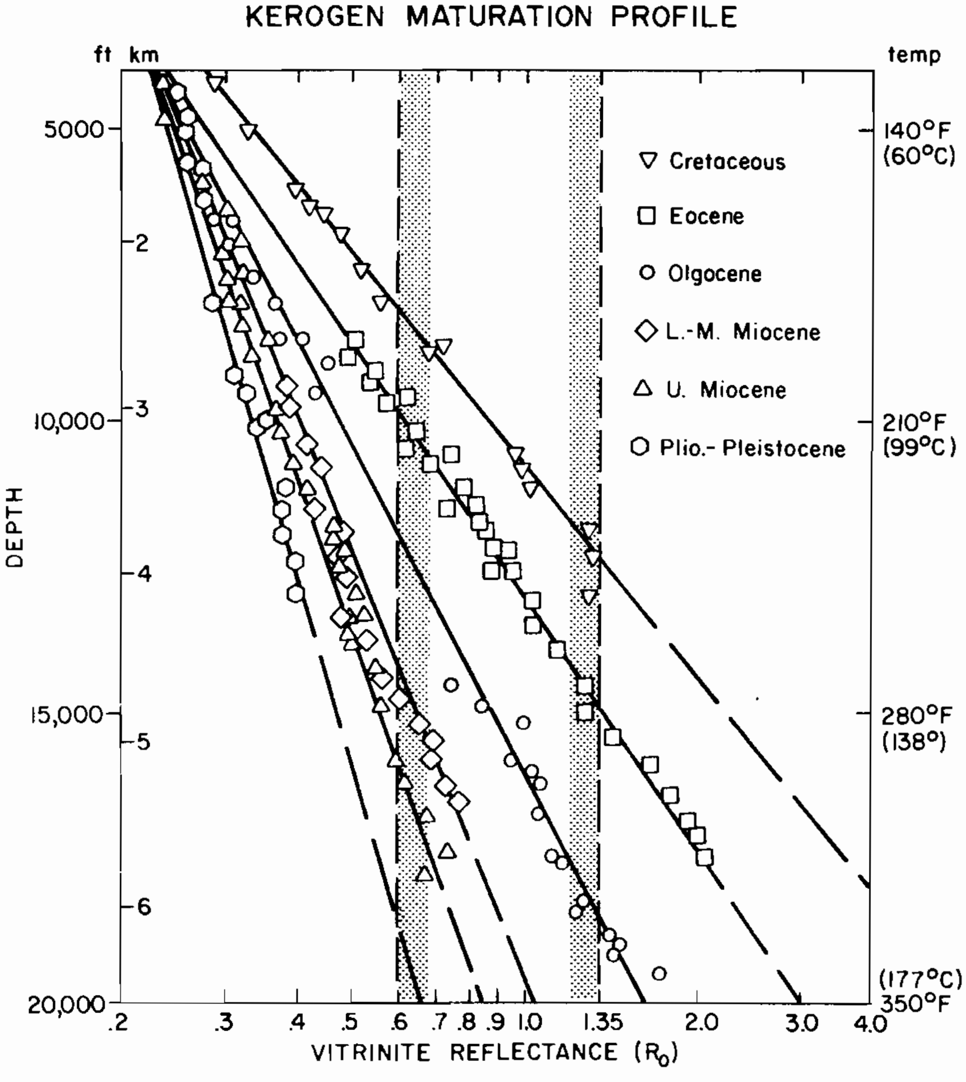

Fig. B-11. Empirical chart relating vitrinite reflectance to depth and to geologic age in the Gulf Coast (from Dow 1978). Courtesy of American Association of Petroleum Geologists.

```
5  REM OPTIMUM RESERVOIR1%
10 DIM N(1000),R(1000)
30 PRINT "TYPE RESERVOIR THICKNÉSS,FT"
35 INPUT T
40 PRINT "TYPE MAXIMUM THICKNESS,FT, OF EFFECTIVE DRAINAGE"
50 INPUT M
60 I1=INT(1000/T)
70 IF I1<=200 THEN 82
75 X=20
78 GOTO 100
82 IF I1 =40 THEN 95
92 X=5
93 GOTO 100
95 IF I1<=20 THEN 99
96 X=2
97 GOTO 100
99 X=1
100 FOR I=1 TO I1 STEP X
110 H=1000-I*T
120 A=H/I
130 IF A M THEN 150
140 A=M
150 N(I)=INT(A*I/40+.5)
155 IF N(I)<35 THEN 160
158 N(I)=35
160 R(I)=INT(T*I/10+.5)
170 NEXT I
180 J=1
185 PRINT " "
190 LPRINT TAB(2);"0   *"
200 FOR L=1 TO 19
205 IF J I1 THEN 400
210 IF L*5<R(J) THEN 285
220 IF L  INT(L/4)*4 THEN 250
230 LPRINT L*5;TAB(5);".";TAB(N(J)+5);"*"
240 GOTO 270
250 LPRINT "    .";TAB(N(J)+5);"*"
270 J=J+X
280 GOTO 200
285 IF L  INT(L/4)*4 THEN 300
290 LPRINT L*5;TAB(5);"."
295 GOTO 350
300 LPRINT "    ."
350 NEXT L
360 LPRINT "100 *"
400 LPRINT "35% I....I....I....I....I....I....I"
410 LPRINT "    0                          1000"
415 LPRINT "       PRODUCT OPEN ";T;" SH ";M;""
```

Appendix C1. Computer program predicting optimum reservoir percentage.

```
5 REM [illegible]
10 CLS
20 [illegible]
30 [illegible]
40 FOR [illegible]
50 READ [illegible]
60 [illegible]
70 [illegible]
80 IF [illegible] THEN [illegible]
90 [illegible]
100 GOTO [illegible]
110 [illegible]
120 NEXT
130 PRINT "LITHOLOGY AND % OF FIRST ROCK TYPE"
140 INPUT A$,A
150 PRINT "LITHOLOGY AND % OF SECOND ROCK TYPE"
160 INPUT B$,B
170 PRINT "LITHOLOGY OF THIRD ROCK TYPE"
180 INPUT C$
190 CLS
200 FOR I=1 TO 16
210 LINE (X(I),Y(I))-(X(I+1),Y(I+1))
220 NEXT I
230 C=100-A-B
240 Y=(2*(100-A)*COS(30/360*2*3.1415))+10
250 IF B=C THEN GOTO 280
260 X=250-A-2*(100-A)*I(B+C)
270 GOTO 290
280 X=250-A
290 PSET (X,Y)
300 LOCATE 2,21:PRINT A$
310 LOCATE 23,5 :PRINT B$
320 LOCATE 23,37:PRINT C$
330 LOCATE 6,27:PRINT "1/4"
340 LOCATE 9,25:PRINT "1/2"
350 LOCATE 12,27:PRINT "1"
360 LOCATE 16,29:PRINT "2"
370 LOCATE 21,32:PRINT "8"
380 LOCATE 2,4:PRINT A$;A;" %"
390 LOCATE 4,4:PRINT B$;B;" %"
400 LOCATE 6,4:PRINT C$;C;" %"
410 E=-1*(A*LOG(A/100)+B*LOG(B/100)+C*LOG(C/100))/(100*1.0986)
420 A1=A:B1=B:C1=C
430 IF A<B THEN A=B1:  B=A1
440 A1=A:B1=B:C1=C
450 IF C<=B AND C<A THEN C=B1:    B=C1
460 A1=A:B1=B:C1=C
470 IF C>=A THEN A=C1:    B=A1  : C=B1
480 B1=B-C:A1=A-B
490 B=B1:A=A1
500 M1=A:M2=B:M3=C
510 IF  A<B THEN  A=M2   :  B=M1
520 M1=A:M2=B:M3=C
530 IF  C<= B AND  C<A  THEN  C=M2   :  B=M3
540 M1=A:M2=B:M3=C
550 IF  C = A THEN  A=M3:     B=M1 :     C=M2
560 M1=A:M2=B:M3=C
570 D=100*(1-(M1-M2)/100)
575 D=INT(D+.5)
580 LOCATE 2,30:PRINT "D= ";D
```

Appendix C2. Computer program plotting lithological composition on triangle graph and calculating D-function and relative entropy function.

```
590 LOCATE 4,30:PRINT "E= ";USING"#.###";E
600 LOCATE 23,1
610 DATA 100,0
620 DATA 0,100
630 DATA 0,0
640 DATA 100,0
650 DATA 80,20
660 DATA 80,0
670 DATA 66.67,0
680 DATA 66.67,33.33
690 DATA 50,50
700 DATA 50,0
710 DATA 50,25
720 DATA 0,50
730 DATA 0,100
740 DATA 11.1,88.9
750 DATA 11.1,0
760 DATA 33.33,0
770 DATA 33.33,33.33
780 FOR I=1 TO 10000:NEXT I
```

Appendix C2. **Computer program plotting lithological composition on triangle graph and calculating D-funetion and relative entropy function.**

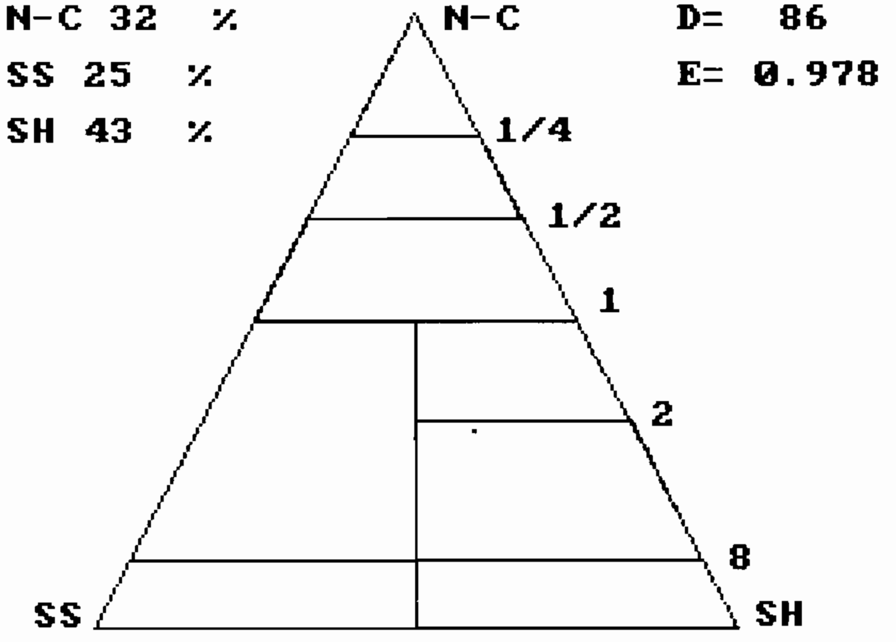

Fig. C-3. Lithological triangle plot of Marrat Formation. Data derived from Powers *et al.* (1966). N-C = non-clastic rocks, SS = sandstone, SH = shale, D = D function, E = relative entropy function.

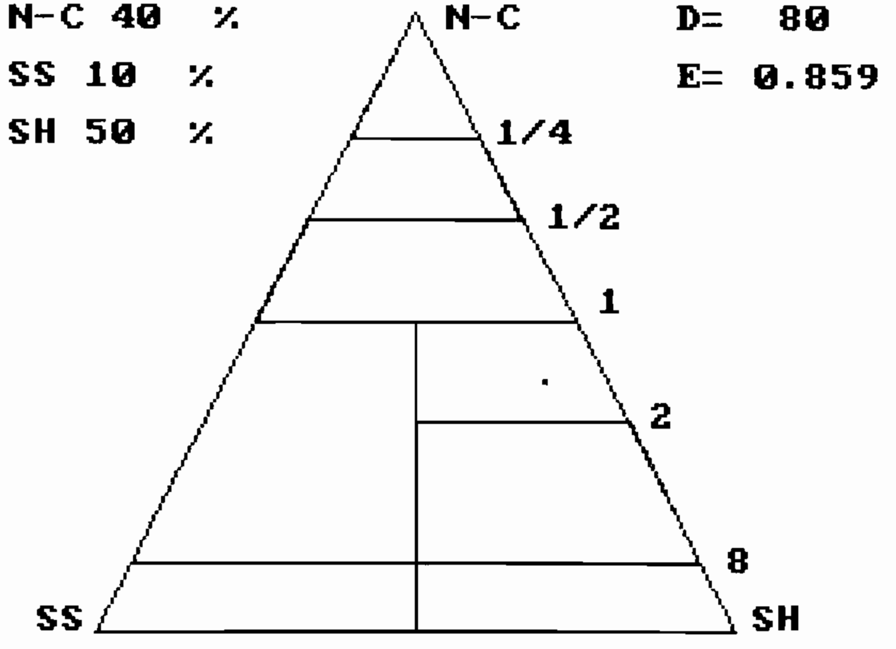

Fig. C-4. Lithological triangle plot of Dhruma Formation. Refer to caption of Fig. C-3. for other explanations.

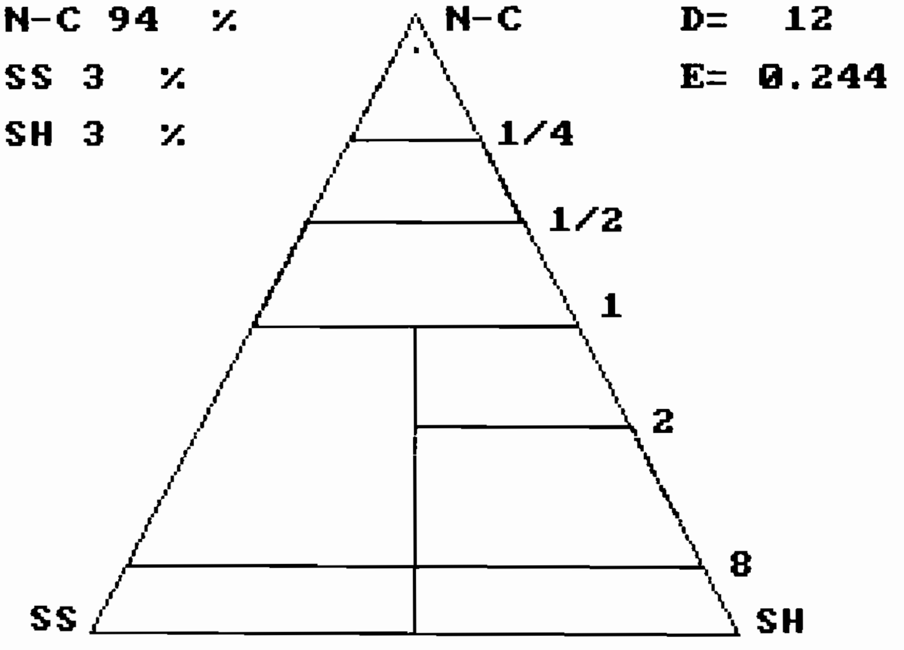

Fig. C-5. Lithological triangle plot of Twaiq Mountain Formation. Refer to caption of Fig. C-3. for other explanations.

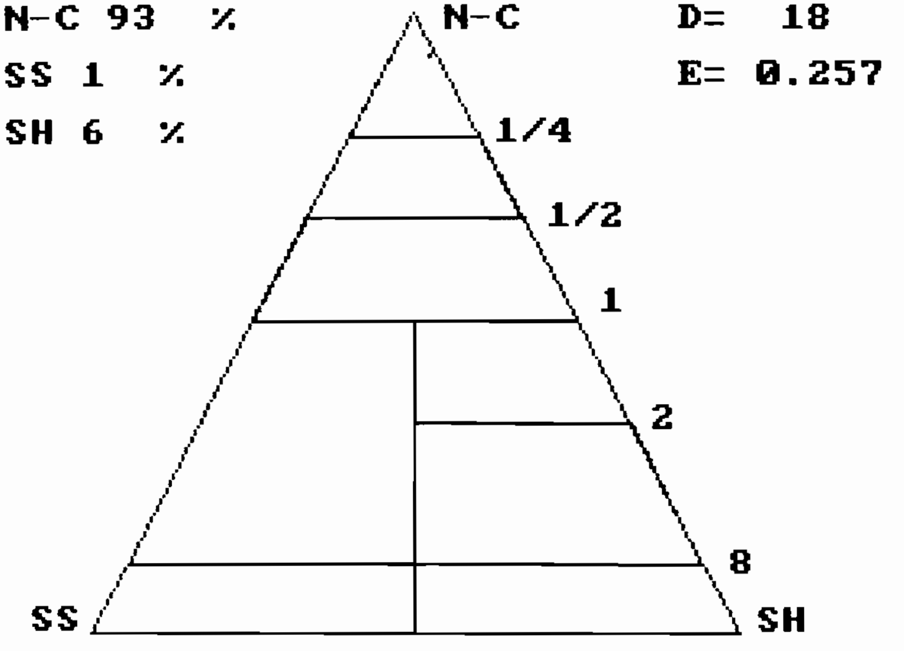

Fig. C-6. Lithological triangle plot of Hanifa Formation. Refer to caption of Fig. C-3. for other explanations.

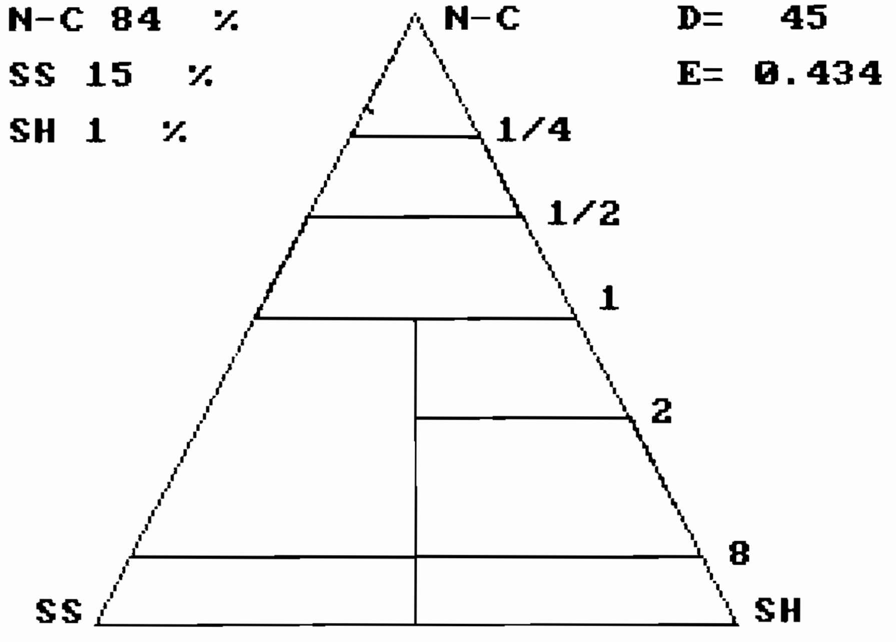

Fig. C-7. Lithological triangle plot of Jubaila Formation. Refer to caption of Fig. C-3. for other explanations.

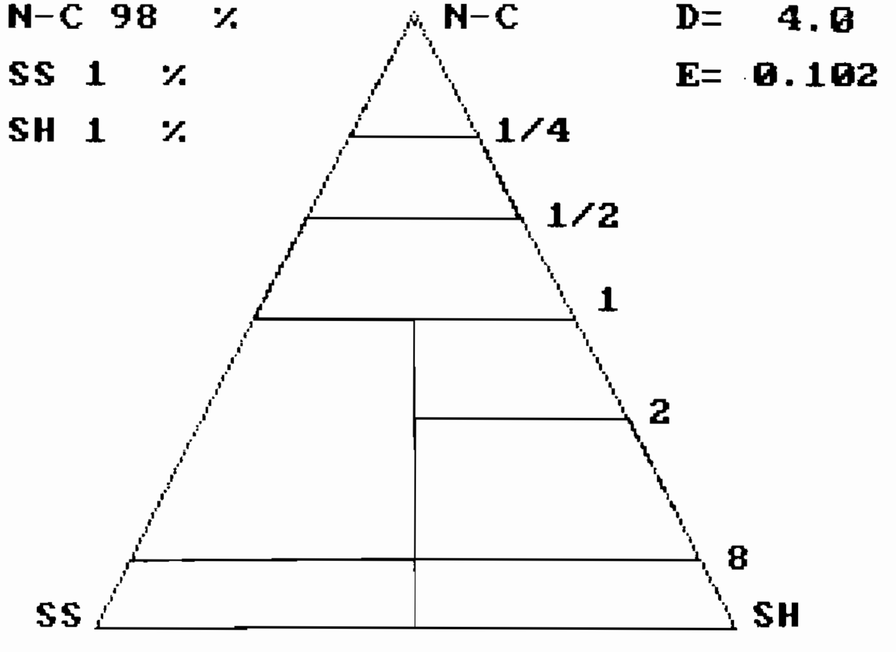

Fig. C-8. Lithological triangle plot of Arab Formation. Refer to caption of Fig. C-3. for other explanations.

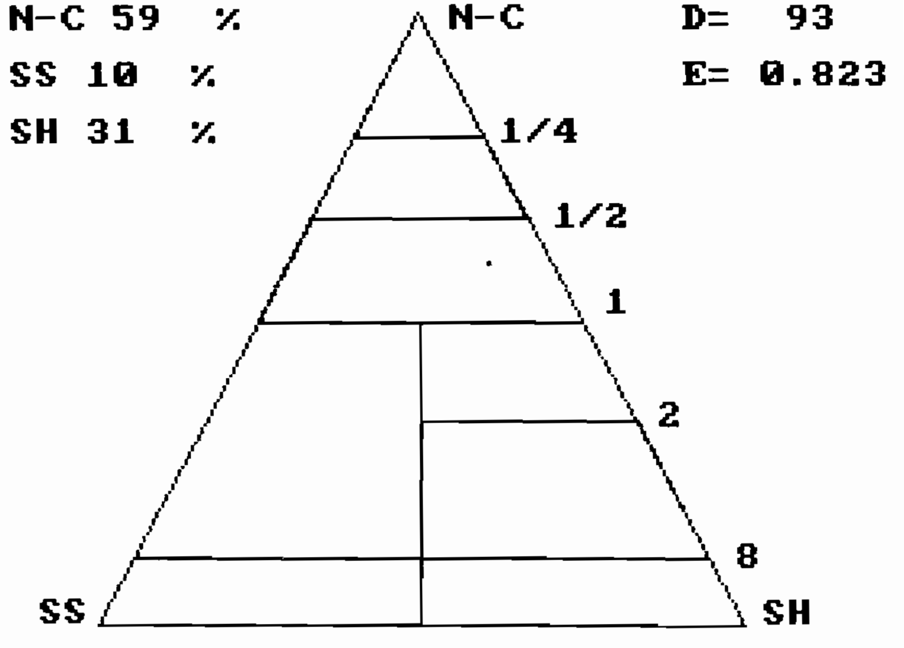

Fig. C-9. Lithological triangle plot of entire Jurassic Formation. Refer to caption of Fig. C-3. for other explanations.

```
90 REM VOL MONTE CARLO
100 DIM A( ,100),R1(100),R2(100)
110 DIM S1(2000),S2(2000),N1(2000),N(2000)
120 LPRINT
180 LPRINT "MONTE CARLO SIMULATION"
182 LPRINT "  VOLUMETRIC METHOD"
185 LPRINT
200 PRINT "INPUT MOST LIKELY [illegible] MINIMUM, MOST LIKELY,"
202 PRINT "MAXIMUM"
205 PRINT
210 PRINT "INPUT AREA IN ACRES"
220 INPUT X1(1),X2(1),X3(1)
230 PRINT "INPUT RESERVOIR THICKNESS IN FEET"
240 INPUT X1(2),X2(2),X3(2)
250 PRINT "INPUT WATER SATURATION IN %"
260 INPUT X1(3),X2(3),X3(3)
270 PRINT "INPUT POROSITY IN %"
280 INPUT X1(4),X2(4),X3(4)
290 PRINT "INPUT RECOVERY EFFICIENCY IN %"
300 INPUT X1(5),X2(5),X3(5)
310 PRINT "INPUT FORMATION VOLUME FACTOR"
320 INPUT X1(6),X2(6),X3(6)
330 PRINT "INPUT RISK FACTOR IN %"
335 PRINT "LARGER NUMBER MEANS HIGHER RISK"
340 INPUT X1(7),X2(7),X3(7)
350 LPRINT " ","MIN","MOST","MAX"
352 LPRINT " "," ","LIKELY"
354 LPRINT "AREA-ACRE",X1(1),X2(1),X3(1)
356 LPRINT "RES.-FT",X1(2),X2(2),X3(2)
358 LPRINT "SW - %",X1(3),X2(3),X3(3)
360 LPRINT "POR. %",X1(4),X2(4),X3(4)
362 LPRINT "R.EFF %",X1(5),X2(5),X3(5)
364 LPRINT "F.VOL.F.",X1(6),X2(6),X3(6)
366 LPRINT "RISK %",X1(7),X2(7),X3(7)
370 FOR I=1 TO 5
380 LPRINT " "
390 NEXT I
400 FOR I=1 TO 7
410 FOR J=1 TO 100
420 A(I,J)=SQR((X3(I)-X1(I))*(X2(I)-X1(I))*RND(0))+X1(I)
440 IF A(I,J)>X2(I) THEN A(I,J)=X3(I)-SQR((1-RND(0))*(X3(I)-X2(I))*(X3(I)-X1(I)
))
460 NEXT J
470 NEXT I
480 R1=0:N1=0:S1=0:[illegible]
490 FOR K=1 TO 100
500 R1(K)=A(1,K)*7758*A(2,K)*(1-A(3,K)/100)*(A(4,K)/100)*(A(5,K)/100)/(5600
000*A(6,K))
510 R2(K)=R1(K)*(1-A(7,K)/100)
520 IF R1(K)>R1 THEN R1=R1(K)
530 NEXT K
600 L=CINT(R1/10+1)*[illegible]
602 FOR I=0 TO L-1
604 S1(I)=0:N1(I)=0:S2(I)=0:N2(I)=0
606 NEXT I
610 FOR I=1 TO 100
620 FOR M=0 TO L-1
625 IF R1(I)>=M*10*[illegible] AND R1(I)<[illegible] THEN S1(M)=S1(M)+R1(I):N1(M)=N1(M)+1:GOTO
670
660 NEXT M
670 S3=S3+R1(I)
```

Appendix D1. Computer program of volumetric Monte Carlo simulation.

```
670 NEXT I
672 FOR I=1 TO 100
675 FOR M=0 TO L-1
680 IF R2(I)<(M+1)*20 AND R2(I)>M*20 THEN S2(M)=S2(M)+R2(I):N2(M)=N2(M)+1:GOTO
690
688 NEXT M
690 S4=S4+R2(I)
692 NEXT I
696 PRINT
697 LPRINT "SIZE,MBL","CASE,%","VOL.,%"
698 LPRINT
699 LPRINT "UNRISKED"
700 FOR M=0 TO L-1
710 N1=N1+N1(M):S1=S1+S1(M)
720 LPRINT (M+1)*20,N1,S1*100/S3
750 NEXT M
760 FOR J=1 TO 5
770 LPRINT
780 NEXT J
790 LPRINT "SIZE,MBL","CASE,%","VOL.,%"
795 LPRINT
796 LPRINT "RISKED"
800 FOR M=0 TO L-1
810 N2=N2+N2(M):S2=S2+S2(M)
820 LPRINT (M+1)*20,N2,S2*100/S4
870 NEXT M
1000 END
```

Appendix D1. Computer program of volumetric Monte Carlo simulation.

```
90 REM VOL MONTE CARLO
100 DIM A(7,100),R1(100),R2(100)
110 DIM S1(200),S2(200),N1(200),N2(200)
120 LPRINT
190 LPRINT "MONTE CARLO SIMULATION"
192 LPRINT "  VOLUMETRIC METHOD"
195 LPRINT
200 PRINT "INPUT MUST BE IN 3 VALUES: MINIMUM, MOST LIKELY,"
202 PRINT "MAXIMUM"
205 PRINT
210 PRINT "INPUT AREA IN SQ KM"
220 INPUT X1(1),X2(1),X3(1)
230 PRINT "INPUT RESERVOIR THICKNESS IN FT"
240 INPUT X1(2),X2(2),X3(2)
250 PRINT "INPUT WATER SATURATION IN %"
260 INPUT X1(3),X2(3),X3(3)
270 PRINT "INPUT POROSITY IN %"
280 INPUT X1(4),X2(4),X3(4)
290 PRINT "INPUT RECOVERY EFFICIENCY IN %"
300 INPUT X1(5),X2(5),X3(5)
310 PRINT "INPUT FORMATION VOLUME FACTOR"
320 INPUT X1(6),X2(6),X3(6)
330 PRINT "INPUT RISK FACTOR IN %"
335 PRINT "LARGER NUMBER MEANS HIGHER RISK"
340 INPUT X1(7),X2(7),X3(7)
350 LPRINT " ","MIN","MOST","MAX"
352 LPRINT " "," ","LIKELY"
354 LPRINT "AREA-SQ KM",X1(1),X2(1),X3(1)
356 LPRINT "RES.-FT"    ,X1(2),X2(2),X3(2)
358 LPRINT "SW  - %"    ,X1(3),X2(3),X3(3)
360 LPRINT "POR.- %"    ,X1(4),X2(4),X3(4)
362 LPRINT "R.EF  %"    ,X1(5),X2(5),X3(5)
364 LPRINT "F.VOL.F."   ,X1(6),X2(6),X3(6)
366 LPRINT "RISK %"    ,X1(7),X2(7),X3(7)
370 FOR I=1 TO 5
380 LPRINT " "
390 NEXT
400 FOR I=1 TO 7
410 FOR J=1 TO 100
420 A(I,J)=SQR((X2(I)-X1(I))*(X3(I)-X1(I))*RND(J))+X1(I)
440 IF A(I,J)>X2(I) THEN A(I,J)=X3(I)-SQR((1-RND(J))*(X3(I)-X2(I))*(X3(I)-X1(I)
))
460 NEXT J
470 NEXT I
480 [illegible]
490 FOR I=1 TO 100
500 R1(I)=[illegible]
[illegible]*A(6,I))
515 R2(I)=R1(I)*(1-A(7,I)/100)
520 IF R1(I)>M1 THEN M1=R1(I)
530 NEXT I
600 [illegible]
602 FOR I=0 TO [illegible]
604 [illegible]
606 NEXT I
610 FOR I=1 TO 100
620 FOR M=0 TO [illegible]
630 IF [illegible]
670
680 NEXT M
690 [illegible]
```

Appendix D2. Computer program of organic geochemical Monte Carlo simulation.

[illegible]

Appendix D2. Computer program of organic geochemical Monte Carlo simulation.

```
60 SCREEN 0
70 CLS
80 KEY OFF
90 REM AREAL MONTE CARLO
100 DIM X(100),Y(100),N(100),R(100),ZZ(100),P(100)
103 N2=0
105 F=0:M=0:P1=0:R=0
107 PRINT "INPUT NUMBER OF SAMPLINGS"
108 INPUT N1
110 SCREEN 1
190 FOR N=0 TO 48 STEP 2
200 READ X(N),X(N+1)
215 IF X(N)=0 THEN 290
220 READ Y(N),Y(N+1)
225 GOSUB 600
230 P=(X(N+1)+1-X(N))*(Y(N+1)+1-Y(N))*20*18
240 P1=P1+P
250 N2=N2+2
280 NEXT N
290 FOR K=0 TO N2*2
292 N(K)=0
294 NEXT K
300 FOR A=1 TO N1*2
310 X1=INT(RND*319)
320 Y1=INT(RND*191)
325 GOSUB 700
330 FOR N=0 TO N2 STEP 2
340 IF X1>=X(N) AND X1<=X(N+1) THEN GOTO 350
345 GOTO 380
350 IF Y1>=Y(N) AND Y1<=Y(N+1) THEN GOTO 367
365 GOTO 380
367 N(N)=N(N)+1
368 IF N(N)=1 THEN GOTO 410
370 GOTO 390
380 NEXT N
390 F=F+1
400 GOTO 430
405 R=R+R(N)
410 R1=(X(N+1)+1-X(N))*(Y(N+1)+1-Y(N))*20*18
415 R=R+RI
420 M=M+1
430 IF F+M=N1 THEN GOTO 450
440 NEXT A
450 LPRINT " "
460 LPRINT "NUMBER OF SAMPLINGS : ";N1;"       UNIT IN M BBL":LPRINT
490 LPRINT "SUCCESS","FAILURE","OIL VOL","TTL OIL"
500 LPRINT M,F,R,P1
502 LPRINT
504 LPRINT "VOL/WELL","% DIS."
510 LPRINT R/(M+F),100*R/P1
530 LOCATE 23,1
540 END
600 LINE (X(N),Y(N))-(X(N+1),Y(N))
610 LINE (X(N+1),Y(N))-(X(N+1),Y(N+1))
620 LINE (X(N+1),Y(N+1))-(X(N),Y(N+1))
630 LINE (X(N),Y(N+1))-(X(N),Y(N))
650 RETURN
700 PSET(X1,Y1)
710 RETURN
1000 DATA 110,115,40,45
```

Appendix D3. Computer program of areal simulation of random drilling.

```
1010 DATA 100,104,20,29
1020 DATA 110,113,15,20
1030 DATA 120,124,10,16
1040 DATA 300,302,140,142
1050 DATA 40,42,40,42
1060 DATA 100,101,10,12
1062 DATA 210,213,80,84
1064 DATA 160,163,80,83
1070 DATA 140,141,70,71
1080 DATA 120,122,70,74
1090 DATA 190,197,60,86
1100 DATA 210,214,20,24
1110 DATA 220,222,15,17
1120 DATA 210,212,5,13
1130 DATA 250,252,5,7
1140 DATA 190,194,5,10
1150 DATA 180,182,40,42
1160 DATA 175,177,20,23
1170 DATA 150,152,40,43
1180 DATA 200,201,2,3
1190 DATA 115,116,25,26
1200 DATA 130,131,25,26
1210 DATA 20,21,60,61
1220 DATA 100,101,2,3
```

Appendix D3. Computer program of areal simulation of random drilling.

References

Archie, G.E. (1950) Introduction to petrophysics of reservoir rocks, *Am. Ass. Petrol. Geologists Bull.* **34**:943-961.

Asakawa, T. and **Fujita, Y.** (1979) Organic metamorphism and hydrocarbon generation in sedimentary basins of Japan, *In: Proceedings of the Seminar on Generation and Maturation of Hydrocarbons in Sedimentary Basins, C.C.O.P.*, pp. 142-162.

Athy, L.F. (1930) Density, porosity and compaction of sedimentary rocks, *Am. Ass. Petrol. Geologists Bull.* **4**:1-24.

Ayres, M.G., Bilal, M., Jones R.W., Slentz, L.W., Tarter, M., and **Wilson, A.O.** (1982) Hydrocarbon habitat in main producing area, Saudi Arabia, *Am. Ass. Petrol. Geologists Bull.* **66**:1-9.

Baker, E.G. (1962) Distribution of hydrocarbons in petroleum, *Am. Ass. Petrol. Geologists Bull.* **46**:76-84.

Barker, C. (1972) Aquathermal pressuring – role of temperature in development of abnormal-pressure zones, *Am. Ass. Petrol. Geologists Bull.* **56**:2068-2071.

Barker, C. (1977) Aqueous solubility of petroleum as applied to its origin and primary migration: *Discussion, Am. Ass. Petrol Geologists Bull.* **61**:2146-2149.

Barker C. and **Dickey, P.A.** (1984) Hydrocarbon habitat in main producing area, Saudi Arabia: Discussion, *Am. Ass. Petrol. Geologists Bull.* **68**:108-109.

Bebout, D.G., Loucks, R.G., and **Gregory, A.R.** (1978) Frio sandstone reservoirs in the deep subsurface along the Texas Gulf Coast, *Bureau of Economic Geology. Univ. of Texas, Report of Investigation no.* **91**, 93 p.

Berg, R.R. (1975) Capillary pressures in stratigraphic traps, *Am. Ass. Petrol. Geologists Bull.* **59**:939-956.

Bonham, L.C. (1978) Solubility of methane in water at elevated temperatures and pressures, *Am. Ass. Petrol. Geologists Bull.* **62**:2478-2481.

Bray, E.E. and **Foster, W.R.** (1980) A process for primary migration of petroleum, *Am. Ass. Petrol. Geologists Bull.* **64**:107-114.

Burst, L.F. (1969) Diagenesis of Gulf Coast clayey sediments and its possible relation to petroleum migration, *Am. Ass. Petrol. Geologists Bull.* **53**:73-93.

Connan, J. (1974) Time-temperature relations in oil genesis, *Am. Ass. Petrol. Geologists Bull.* **58**:2516-2521.

Curtis, B.F. and **Sandstone Reservoir Committee** (1960) Characteristics of sandstone reservoirs in United States, *In:* **Peterson, J.A.** and **Osmond, L.C.** *(ed.) Geometry of Sandstone Bodies, Am. Ass. Petrol. Geologists Bull.* pp. 208-219.

Dickey, P.A. (1975) Possible primary migration of oil from source rock in oil phase, *Am. Ass. Petrol. Geologists Bull.* **59**:337-345.

Dickinson, G. (1953) Geological aspects of abnormal reservoir pressures in Gulf Coast Louisiana, *Am. Ass. Petrol. Geologists Bull.* **37**:410-432.

Dow, W.G. (1978) Petroleum source beds on continental slopes and rises, *Am. Ass. Petrol. Geologists Bull.* **62**:1584-1606.

Dutton, S.P. (1980) Petroleum source rock potential and thermal maturity, Palo Duro Basin, Texas, *Bureau of Economic Geology, Univ. of Texas, Circular.*

Engelhardt, W.V. and **Gaida, K.H.** (1963) Concentration changes of pore solutions during compaction of clay sediments, *J. Sediment. Petrol.* **33**:919-930.

Espitalie, J., Laporte, J.L., Madec, M., Marquis, F., Leplat, P., Paulet, J. and **Boutefeu, A.** (1977) Methode rapide de caracterisation des rouches meres, de leur potentiel petrolier et de leur degre dévolution, *Inst. Francais Petrole, Rev.* **32**:23-42.

Evans, C.R., McIvor, D.K., and **Magara, K.** (1975) Organic matter, compaction history and hydrocarbon occurrence – Mackenzie Delta, Canada, *Proc. 9th World Petrol. Congress, Tokyo*, v. **3**, pp. 149-157.

Forgotson, J.M. Jr. (1960) Review and classification of quantitative mapping techniques, *Am. Ass. Petrol. Geologists Bull.* **44**:83-100.

Foster, J B. and **Whalen, H.E.** (1966) Estimation of formation pressure from electrical surveys – offshore Louisiana, *J. Petrol. Tech.* **18**:165-171.

Galloway, W.E. (1974) Deposition and diagenetic alteration of sandstone in northeast Pacific arc-related basins: Implications for graywacke genesis, *Geol. Soc. Am. Bull.* **85**:379-390.

Gill, D. (1979) Differential entrapment of oil and gas in Niagaram Pinnacle-Reef belt of Northern Michigan, *Am. Ass. Petrol. Geologists Bull.* **63**:608-620.

Graton, L.C. and **Fraser, H.J.** (1935) Systematic packing of spheres with particular relation to porosity and permeability, *J. Geol.* **43**:785-909.

Gussow, W.C. (1954) Differential entrapment of oil and gas: a fundamental principle, *Am. Ass. Petrol. Geologists Bull.* **38**:816-853.

Ham, H.H. (1966) New charts help estimate formation pressures, *Oil Gas J.* **64**:58-64.

Hedberg, H.D. (1936) Gravitational compaction of clays and shales, *Am. J. Sci.* **31**:241-287.

Hedberg, H.D. (1974) Relation of methane generation to undercompacted shales, shale diapirs, and mud volcanoes, *Am. Ass. Petrol. Geologists Bull.* **58**:661-673.

Hedberg, W.H. (1967) *Pore-water chlorinities of subsurface shales,* Univ. Microfilms, Ann Arbor, Michigan (Thesis, Univ. Wisconsin).

Hobson, D.G. (1954) *Some Fundamentals of Petroleum Geology,* Oxford Univ. Press, London, 139p.

Hocott, C.R. (1938) Interfacial tension between water and oil under reservoir conditions, *AIME Petrol. Trans.* **32**:184-190.

Hosoi, H. (1963) First migration of petroleum in Akita and Yamagata Prefectures, Japan. *Assoc. Mineral. Petrol. Econ. Geology J.* **49**:43-55,101-114.

Hubbert, M.K. (1953) Entrapment of petroleum under hydrodynamic conditions, *Am. Ass. Petrol. Geologists Bull.* **37**:1954-2026.

Hubbert, M.K. (1974) Presentation of the Penrose Medal to M. King Hubbert (Response), *Geol. Soc. Am. Bull.* **85** 1341.

Huff, K.F. (1979) Frontiers of world exploration, *In:* **Miall, A.D. (ed.)** *Facts and Principles of World Petroleum Occurrence,* Can. Soc. Petrol. Geologists Memoir **6**, pp. 343-362.

Hunt, J.M. (1974) How deep can we find economic oil and gas accumulations, SPE 5177, *1974 Deep Drilling and Production Symp., Preprint* pp. 103-110.

Hunt, J.M. (1979) *Petroleum Geochemistry and Geology,* W.H. Freeman and Company, San Francisco, 617p.

Huwaidi, I.H. (1984) *Statistical analysis of oil discovery history in Saudi Arabia, a comparative study of the Kingdom with world-wide data,* M.Sc. Thesis, Faculty of Earth Sciences, King Abdulaziz University, 247p.

Ibach, L.E.J. (1982) Relationship between sedimentation rate and total organic carbon content in ancient marine sediments, *Am. Ass. Petrol. Geologists Bull.* **66**:170-188.

Kamen-Kaye, M. (1970) Geology and productivity of Persian Gulf synclinorium, *Am. Ass. Petrol. Geologists Bull.* **54**:2371-2394.

Kennedy, G.C. and **Holser, W.T.** (1966) Pressure-volume-temperature and phase relation of water and carbon dioxide, Section 16 in: *Handbook of Physical Constants, Geol. Soc. Am. Memoir* **97**:371-383.

Kharaka, Y.K., Callender, E., and **Carothers, W.W.** (1977) Geochemistry of geopressured geothermal waters from the Texas Gulf Coast, In: **Meriwether, J. (ed.)** *Proc. 3rd Geopressured Geothermal Energy Conference, Univ. Southwestern Louisiana,* v.1, GI-121–GI-166.

Klemme, H.D. (1980) Petroleum basins – classifications and characteristics, *Petroleum Geology J.* **3**:187-207.

Levorsen, A.I. (1967) *Geology of Petroleum, 2nd Ed.,* W.H. Freeman and Company, San Francisco, 724p.

Lopatin, N.V. (1971) Temperature and geologic time as factors in coalification, *Akad Nauk SSSR, Izv. Ser. Geol.* **3**:95-106.

Loucks, R.G., Dodge, M.M. and **Galloway W.E.** (1979) *Sandstone consolidation analysis to delineate areas of high-quality reservoirs suitable for production of geopressured geothermal energy along the Texas Gulf Coast,* Bureau of Economic Geology, Univ. of Texas, 98p.

Low, P.F. (1976) Viscosity of interlayer water in montmorillonite, *Soil Sci. Soc. Am. Proc.* **40**:500-505.

Magara, K. (1968) Compaction and migration of fluids in Miocene mudstone, Nagaoka Plain, Japan, *Am. Ass. Petrol. Geologists Bull.* **52**:2466-2501.

Magara, K. (1972) Compaction and fluid migration in Cretaceous shales of western Canada, *Geol. Surv. Canada Paper no. 1972-18,* 81p.

Magara, K. (1974a) Compaction, ion-filtration, and osmosis in shales and their significance in primary migration, *Am. Ass. Petrol. Geologists Bull.* **58**:283-290.

Magara, K. (1974b) Aquathermal fluid migration, *Am. Ass. Petrol. Geologists Bull.* **58**:2513-2516.

Magara, K. (1975a) Reevaluation of montmorillonite dehydration as cause of abnormal pressure and hydrocarbon migration, *Am. Ass. Petrol. Geologists Bull.* **59**:292-302.

Magara, K. (1975b) Importance of aquathermal pressuring effect in Gulf Coast, *Am. Ass. Petrol. Geologists Bull.* **59**:2037-2045.

Magara, K. (1976) Water expulsion from clastic sediments during compaction – directions and volumes, *Am. Ass. Petrol. Geologists Bull.* **60**:543-553.

Magara, K. (1977a) Petroleum migration and accumulation, Chapter 3: in **Hobson, G.D. (ed.)** *Developments in Petroleum Geology – 1,* Applied Science Publishers Ltd., London, pp. 83-126.

Magara, K. (1977b) A theory relating isopachs to paleo compaction-water-movement in a sedimentary basin, *Can. Petrol. Geol. Bull.* **25**:195-207.

Magara, K. (1978a) Significanee of the expulsion of water in oil-phase primary migration, *Can. Petrol. Geol. Bull.* **26**:123-131.

Magara, K. (1978b) Geological model predicting optimum sandstone per cent for oil accumulation, *Can. Petrol. Geol. Bull.* **26**:380-388.

Magara, K. (1978c) *Compaction and Fluid Migration – Practical Petroleum Geology,* Elsevier, Amsterdam, 319p.

Magara, K. (1981a) Mechanisms of natural fracturing in a sedimentary basin, *Am. Ass. Petrol. Geologists Bull.* **65**:123-132.

Magara, K. (1981b) Static versus dynamic interpretation in petroleum geology, *Am. Ass. Petrol. Geologists Bull.* **65**:531-539.

Martin, R.T. (1962) Absorbed water on clay: a review, *Clays Clay Miner. 9 (Proc. 9th Natl. Conf. Clays and Clay Minerals, 1960),* Pergamon, New York, pp.28-270.

McAuliffe, C.D. (1978) Chemical and physical constraints on petroleum migration with emphasis on hydrocarbon solubilities in water, in: *Short Course: Physical and Chemical Constraints on Petroleum Migration, Am. Ass. Petrol. Geologists Bull.* **2**:C1-C39.

McAuliffe, C.D. (1979) Oil and gas migration – chemical and physical constraints, *Am. Ass. Petrol. Geologists Bull.* **63**:761-781.

McKelvey, J.G., and **Milne, I.H.** (1962) The flow of salt solutions through compacted clay, Clays Clay Miner., 9 *(Proc. 9th Natl. Conf. Clays and Clay Minerals),* Pergamon, New York, v.11, pp. 248-259.

Meade, R.H. (1966) Factors influencing the early stages of compaction of clays and sands – review, *J. Sediment. Geol.* **36**:1085-1101.

Momper, J.A. (1978) Oil migration limitations suggested by geological and geochemical considerations, In: *Physical and Chemical Constraints on Petroleum Migration, Am. Ass. Petrol. Geologists Bull.* v.1, pp.B1-B60.

Neglia, S. (1979) Migration of fluid in sedimentary basins, *Am. Ass. Petrol. Geologists Bull.* **63**:573-597.

Powell, T.G. (1978) An assessment of the hydrocarbon source rock potential of the Canadian Arctic Islands, *Geol. Surv. Canada, Paper 78-12,* 82p.

Powers, M.C. (1967) Fluid-release mechanism in compacting marine mudrocks and their importance in oil exploration, *Am. Ass. Petrol. Geologists Bull.* **51**:1240-1254.

Powers, R.W., Ramires, L.F., Redmond, C.D., and **Elberg, E.L. Jr.** (1966) Geology of the Arabian Peninsula, sedimentary geology of Saudi Arabia, *U.S.G.S. Professional Paper 560-D,* 147p.

Price, L.C. (1976) Aqueous solubility of petroleum as applied to its origin and primary migration, *Am. Ass. Petrol. Geologists Bull.* **60**:213-244.

Proshlyakov, B.K. (1960) Reservoir properties of rocks as a function of their depth and lithology, *Geol. Neft. Gaza.* **12**:24-29.

Rieke III, H.H. and **Chilingarian, G.V.** (1974) *Compaction of Argillaceous Sediments,* Elsevier, Amsterdam, 424p.

Ryder, H.M. (1948) Permeability, absolute, effective, measured, *World Oil, May:* 173-176.

Sail, I.A.N. and **Magara, K.** (1985) Petroleum generation and maturation of the Arabian Gulf region, *Bulletin, Faculty of Earth Sciences, King Abdulaziz University,* (under publication).

Schmidt, G.W. (1973) Interstitial water composition and geochemistry of deep Gulf Coast shales and sandstone, *Am. Ass. Petrol. Geologists Bull.* **57**:321-337.

Schmidt, V. and **McDonald, D.A.** (1979) The role of secondary porosity in the course of sandstone diagenesis. In Aspects of Diagenesis, *SEPM Spec. Pub.* **26**:175-207.

Schowalter, T.T. (1979) Mechanics of secondary hydrocarbon migration and entrapment, *Am. Ass. Petrol. Geologists Bull.* **63**:723-760.

Smith, J.E., Erdman, J.G., and **Morris, D.A.** (1971) Migration, accumulation and retention of petroleum in the earth, *Proc. 8th World Petrol. Congr. v. 2,* pp. 13-26.

Stephenson, L.P. (1977) Porosity dependence on temperature: Limits on maximum possible effect, *Am. Ass. Petrol. Geologists Bull.* **61**:407-415

Timko, D.J. and **Fertl, W.H.** (1971) Relationship between hydrocarbon accumulation and geopressure and its economic significance, *J. Petrol. Technol.* **22**:923-930

Tissot, B. (1977) The application of the result of organic geochemical studies in oil and gas exploration, Chapter 2 in: **Hobson, G.D. (ed.)** *Developments in Petroleum Geology* – 1, Applied Science Publishers Ltd., London, pp.53-83.

Tissot, B. and **Pelet, R.** (1971) Nouvelles donnees sur les mechanismes de genese et de migration du petrole: simulation mathematique et application a la prospection, *Proc. 8th World Petrol. Congr.*, pp.35-46.

Tissot, B. and **Welte, D.H.** (1978) *Petroleum Formation and Occurrence: A New Approach to Oil and Gas Exploration,* Springer-Verlag, New York, 538p.

Van Olphen, H. (1963) Compaction of clay sediments in the range of molecular particle distance, *Clays and Clay Miner. 11 (Proc. 11th Natl. Conf. Clays and Clay Miner. 1962,* MacMillan, New York, pp. 178-187).

Vyshemirsky, V.S., Trofimuk, A.A., Eontorovich, A.E. and **Neruchev, S.G.** (1973) Bitumoids fractionation in the process of migration, In: **Tissot, B.** and **Rienner, F. (ed.)** *Advances in Organic Geochemistry,* Editions Technip., Paris, pp. 359-365.

Waples, D.W.(1980) Time and temperature in petroleum formation: application of Lopatin's method to petroleum exploration, *Am. Ass. Petrol. Geologists Bull.* **64**:916-926.

Weller, J.M. (1959) Compaction of sediments, *Am. Ass. Petrol. Geologists Bull.* **43**:273-310.

White, I.C. (1885) The geology of natural gas, *Science,* **5**:521-522.

Wilson, H.H. (1975) Time of hydrocarbon expulsion, paradox for geologists and geochemists. *Am. Ass. Petrol. Geologists Bull.* **59**:69-84.

Youn, S.H. (1974) *Comparison of porosity and density values of shale from cores and well logs,* M.A. Thesis, Univ. Tulsa.

Young, A., Monaghan, P.H., and **Schweisberger, R.T.** (1977) Calculation of ages of hydrocarbons in oils, *Am. Ass. Petrol. Geologists Bull.* **61**:573-600.

Index

D

E

F

G

H

I

J

K

L

M

N

O

Printed at King Abdulaziz University Press